

The University of Nottingham

UNITED KINGDOM · CHINA · MALAYSIA

SCHOOL OF LIFE SCIENCES

Title: Cellular and molecular mechanisms underlying extravasation of human Wharton's jelly mesenchymal stem cells across fetal and adult endothelial cell monolayers

By: *Neven Abdelhamid Zaki Ebrahim*

Supervisory Team: Dr. Lopa Leach

Prof. Michael Randall

Thesis submitted to the University of Nottingham for the degree of Doctor of Philosophy

December 2015

Abstract

Introduction

The Wharton's Jelly (WJ) of human umbilical cord (HU) contains multipotent stem cells (WJ-MSC) which express mesenchymal markers but not hematopoietic markers. WJ-MSC are increasingly being tested for use in stem cell therapy, with intravenous delivery being the preferred route. Fetal stem cells from embryonic germ layers are present in maternal blood and can home to damaged maternal tissues. This study investigates how WJ-MSC cross the fetal and adult endothelial barriers; including the cellular and molecular mechanisms employed.

Methods

WJ-MSC were isolated from HU (n=27) which were taken from normal term pregnancies after elective Caesarean section. Flow cytometry and immunofluorescence were used to check presence/absenc of mesenchymal versus haematopoietic markers. Cells were induced to become adipocytes, chondrocytes and osteocytes by using specific induction medium. Isolated WJ-MSC were added after labelling with PKH26 to confluent monolayers of isolated human umbilical vein endothelial cells (HUVEC) or commercially bought human uterine microvascular endothelial cells (HUtMEC) at a 1:5 ratio. Cell-cell interactions were monitored with real time microscopy for 24 to 40h. Fluorescence and confocal scanning microscopy, after vascular endothelial (VE) cadherin immunocytochemistry were used for detailed analysis of VE-cadherin junctional occupancy and spatio-temporal location of stem cells. Tyrosine phosphorylation status of VE-cadherin, whether at Tyr685 or Tyr731, at different time points were investigated by immunoblotting whilst levels of vascular endothelial growth factor (VEGF) in the conditional media (CM) were measured by ELISA. Three different isolates were tested, with 3 experimental repeats for all expermints. Statistical analyses were performed with ANOVA (One or Two way).

Results

Cells (>95%) from each passage were positive for the mesenchymal markers CD 29, CD 105, CD 90, CD 73 and CD 44. <2% cells showed positivity to the haematopoietic markers CD 34, HLA-DR, CD 14, CD 19 and CD 45. WJ-MSC differentiated into adipocytes, osteocytes and chondrocytes. WJ-MSC displayed exploratory behaviour for a minimum of 30 min on HUtMEC or 60 min on HUVEC with interrogation of paracellular openings before crossing rather than replacing endothelial cells. By 2h, half were found at sub-endothelial positions, with a majority reaching this within 16-22h. There was accompanying loss of junctional VE-cadherin (64.9 $\pm$ 3.7 %; $p<0.001$ in HUVEC; 63 $\pm$ 4.6%; $p< 0.001$ in HUtMEC) in the endothelial monolayers followed by a return at 16h and increased continuity by 22h ($p<0.01$ in HUVEC; $p<0.001$ in HUtMEC). Junctional disruptions were found close to overlying or migrating WJ-MSC. Confocal microscopy confirmed paracellular extravasation. VE-cadherin protein levels matched controls in the early hours (0-2h) and increased after 22h co-culture in both fetal and uterine endothelium. VE-cadherin showed a 2-fold increase in phosphorylation at Tyr685 from 30 min to 2h. P-Tyr731 remained unchanged, similar to untreated endothelial layers, then decreased at 2h and 22h. VEGF levels in WJ-MSC – HUtMEC co-culture supernatants was highest at 2h (88 $\pm$ 3 pg/ml) and decreased by 22h, reaching negligible levels by 48h. Anti-VEGF blocked Tyr685 phosphorylation but did not affect the decrease in P-Tyr731; this was accompanied by a 25% decrease in transmigration of cells in the first two hours and a 43% decrease in total by 22h. in WJ-MSC – HUtMEC co-cultures. However, in HUVEC-WJ-MSC co-cultures, no VEGF were detected and anti-VEGF did not block Tyr685 phosphorylation and Tyr731 de-phosphorylation.

Conclusion

WJ-MSC from term umbilical cords can be easily isolated and expanded in culture. They retain mesenchymal stem cell properties for the passages tested (up to P5) making them a

valuable model for studies into mechanisms underlying extravasation. The data obtained suggest that WJ-MSC can influence expression of VE-cadherin, with perturbation during transmigration followed by upregulation and repair once the adlumenal side is reached. There was a similarity in the cellular and molecular mechanisms employed by WJ-MSC in their paracelluar migration across fetal and uterine endothelium, although VEGF may not be the key player in HUVEC interactions. For both endothelial types, WJ-MSC appear to induce phosphorylation events linked with paracellular permeability and de-phosphorylation events normally associated with leukocyte extravasation. The data from the uterine endothelial investigations suggests that fetal stem cells are able to influence paracellular junctional dynamics and strengthens the growing hypothesis that they may also play a role in re-modelling the uterine circulation for fetal advantage. The extra-embryonic WJ-MSC holds the promise of use in restoring junctional maturity and vascular repair in future therapeutic applications.

Thesis related publications and awards

Journal Publications

Neven A. Ebrahim, Lopa Leach

"Temporal Studies into Attachment, VE-cadherin Perturbation and Paracellular Migration of Human Umbilical Mesenchymal Stem Cells Across Umbilical Vein Endothelial Monolayers" *Stem Cells Dev*, vol:24**,** 426-36,2015.

Neven A. Ebrahim, Lopa Leach

Transendothelial migration of Human Wharton Jelly Mesenchymal Stem Cells across Human Uterine Microvascular Endothelial Cell Monolayers: Analysis of Spatio-Temporal Events and Junctional Dynamics
Stem Cells (decision pending)

Peer-Reviewed Abstracts

Neven A. Ebrahim, Lopa Leach

"Isolation and passage of mesenchymal stem cells from human umbilical cords."

Advances in Microcirculation, p31,2013

Neven A. Ebrahim, Jennifer Sedcole, Olivia Volk, Lopa Leach

"Interactions of umbilical mesenchymal stem cells with uterine and umbilical endothelial cells." *Placenta*, vol:35 (9), A92–A93, 2014

Neven A. Ebrahim, Azlina Razak, Jennifer Sedcole, Olivia Volk, Lopa Leach

"Immunolocalisation of cytokeratin 7 in human umbilical mesenchymal stem cells, umbilical vein endothelial cells and human uterine microvascular endothelial cells." *Placenta*, vol:35 (9), A23–A33, 2014

Neven A. Ebrahim, Lopa Leach

"Real time studies of transendothelial migration of human mesenchymal stem cells – junctional disruption and repair." *Microcirculation* ,2014

Neven A. Ebrahim, Lopa Leach

"Effect of the secretome derived from co-cultures of umbilical mesencymal stem cells and endothelial cells on VE-cadherin junctional occupancy. " *Microcirculation*, vol 22 (8), 753, 2015

Neven A. Ebrahim, Lopa Leach

"Putative mechanisms underlying transmigration of human umbilical mesencymal stem cells across uterine microvascular endothelial cells." *Journal of Vascular Research*, 2015

These were presented as posters in BMS, ESM/EVBO, IFPA conferences.

Awards

July 2014	Competitive student assistance sceme award, from the British Microcirculation Society
May 2015	Symington Fund Bequest award from the Anatomical Society

Acknowledgements

"*Praise be to God, Lord of the Universe*"

This study is not the work of one individual alone, but a culmination of efforts by many people, to whom I am immensely grateful. I would first like to thank my supervisor, Dr. Lopa Leach, for patiently guiding me over the last three years while exploring the cutting edge of stem cell research. I am also indebted to Prof. Michael Randall, my second supervisor, for his encouragement and professional support throughout the course of this study. Special thanks and fond remembrance are due my professor, the late Terry Parker, for believing in me; he will never be forgotten. Heartfelt thanks as well to Dr. Vincent Wilson, for his kind support. In addition, I want to express my thanks and gratitude to all those people who volunteered their time and efforts to help me. Thanks also to the Islamic Development Bank (IDB) for funding my PhD studentship.

Thanks are in order for my very good colleagues and friends, who enriched my experience at this notable institution of learning with their exceptional inspiration and support.
Finally, and most importantly, I wish to thank members of my family: first, my wonderful, amazing mother, who literally went out of her way by joining me on this journey; her help and support have been invaluable to me. Also, a special thank-you and remembrance for my late father, who from my earliest years inspired me to seek greater heights. Loving thanks (and hugs) to my two wonderful daughters, for bearing with me in the difficult times, and lifting my spirits. To my uncle, my brothers, and everyone else, thank you so much for being a part of this journey, and for always believing in me. I hope I can always make you proud.

Table of Content

Chapter 1 1
1.1 Stem cell Biology 2
1.1.1 Definition of Stem Cell 2
1.1.2 Categories of Stem Cells 2
1.1.2.1 Embryonic Stem Cells (ESC): 2
1.1.2.2 Adult Stem Cells: 2
1.1.3 Haematopoietic stem cells 4
1.1.4 Endothelial progenitor cells 4
1.1.5 Mesenchymal Stem Cells 5
1.1.5.1 Characterization of MSC 5
1.1.5.2 Morphological characterization 6
1.1.5.3 Immunophenotypic characterization 7
1.1.5.4 Differentiation into different cell types 9
1.1.6 Stem cells and vascular repair 10
1.1.7 Wharton's Jelly of the human umbilical cords as a source of MSC 11
1.1.7.1 Advantages of WJ-MSC over embryonic and adult Stem Cells 11
1.1.7.2 Applications of WJ-MSC in regenerative medicine 12
1.1.8 Stem cells homing mechanisms 14
1.1.9 Stem cell niche 15
1.2. The endothelial barriers: inter-endothelial junction formation and barrier integrity 16
1.2.1 VE-cadherin as the main organizer of endothelial integrity 20
1.2.2 Structure of VE-cadherin 21
1.2.3 Phosphorylation and modulation of VE-cadherin organization 21
1.2.4 VE-cadherin internalization 24
1.3. Vascular Endothelial Growth Factor 26
1.4. Extracellular matrix (ECM) 27
1.4.1 Structure and functional components of ECM 28
1.4.2 ECM dimensions (D) 29
1.4.3 Employment of extracellular matrix in cell migration 30
1.5. Mesenchymal stem cells and pregnancy 31
1.5.1 The placenta 32
1.5.2 Placental barrier 34
1.5.3 Spiral artery remodelling 36
1.6. Thesis Hypothesis 40
1.7. Aims and objectives 40

Chapter 2 42
2.1. Introduction and aims 43
2.1.1. Human umbilical cord Embryology, Function and Anatomy 43
2.1.2. Pre-existing methods of isolation of WJ-MSC 44
2.1.3. Human umbilical vein endothelial cells 45
2.1.4. The aims of this chapter 45
2.2. Material and Methods 46
2.2.1 Isolation of WJ-MSC 47
2.2.2 Proliferation of WJ-MSC 50
2.2.3 Cell counting and freezing 50
2.2.4 Thawing of WJ-MSC 51
2.2.5 Detection of Mesenchymal and haematopoietic markers using Flow Cytometry 51
2.2.6 *In-vitro* Differentiation 51
2.2.6.1 Adipogenic Differentiation 51
2.2.6.2 Chondrogenic Differentiation 52
2.2.6.3 Oestogenic Differentiation 53
2.2.7 WJ-MSC Labelling 53
2.2.8 Isolation of HUVEC 54
2.2.9 Maintaining, harvesting, and subculture of HUVEC 55
2.2.10 Cell counting and freezing 55
2.2.11 Characterization of HUVEC 56
2.2.12 *In situ* localisation of WJ-MSC in HU 57
2.3. Results 57
2.3.1 Isolation and behaviour of WJ-MSC in culture 57
2.3.2 Phenotyping of the WJ-MSC: Flow cytometry 60
2.3.3 Adipogenic Differentiation 63
2.3.4 Chondrogenic Differention 63
2.3.5 Oestogenic Differention 65
2.3.6 WJ-MSC Labelling 66
2.3.7 Isolation and characterisation of HUVEC 67
2.3.8 *In situ* localisation of WJ-MSC in the HU 69
2.4. Discussion 72
Chapter 3 76
3.1. Introduction and aims 77
3.1.1 Clinical applications of mesenchymal stem cells 77
3.1.2 The role of Wharton's Jelly mesenchymal stem cells in gestation 78
3.1.3 Pericyte 78

3.1.4 Stem cell niche 78
3.1.5 Using human umbilical veins endothelial cells as a vascular model 79
3.1.6 Aims of the present chapter 79
3.2. Materials and Methods 79
Materials 79
Methods 81
3.2.1 Effect of mixed media on WJ-MSC and HUVEC 81
3.2.2 Co-culture studies 81
3.2.2.1 Real Time Observations 82
3.2.2.2 Immunohistochemistry of VE cadherin and Systematic Random sampling 82
3.2.2.3 Junctional counts 83
3.2.2.4 Statistical Analysis 83
3.2.2.5 Confocal imaging 84
3.2.2.6 Western Blotting 84
3.3. Results 87
3.3.1 Effect of Mixed media on WJ-MSC and HUVEC 87
3.3.2 Co-culture studies 89
3.3.2.1 Early co-culture interactions 89
3.3.2.2 Transmigration events 93
3.3.2.3 VE-cadherin dynamics 94
3.3.2.4 Western Blotting 98
3.3.2.5 Confocal imaging 100
3.4. Discussion 102
Chapter 4 107
4.1. Introduction 108
4.1.1 Mesenchymal stem cells and pregnancy 108
4.1.2 Cells known to be involved in spiral artery remodelling 109
4.1.3 Mesenchymal stem cells and how it crosses the endothelial barrier 111
4.1.4 Aims of this chapter 111
4.2. Materials & methods 112
4.2.1 Human Uterine Microvascular Endothelial Cells growth and subculture 113
4.2.2 Cell counting and freezing 114
4.2.3 Characterization of Uterine Endothelial Cells and WJ-MSC 114
4.2.4 Co-culture studies of WJ-MSC with HUtMEC 115
4.2.5 Real Time Observations 115
4.2.6 Quantitative analysis of endothelial junctional integrity and migration of WJ-MSC 115

4.2.7 Confocal imaging 116
4.2.8 Expression of CK 7 in WJ-MSC, HUVEC and HUtMEC 116
4.2.9 Co-culture of trophoblast cells with HUtMEC 117
4.3. Results 118
4.3.1 Uterine microvascular endothelial cells and Wharton Jelly mesenchymal cells continue to express endothelial and mesenchymal markers in mixed media 118
4.3.2 Fetal WJ-MSC can interact with maternal (uterine) endothelial cells displaying prolonged exploratory behaviour and paracellular extravasation 119
4.3.3 WJ-MSC can alter VE-cadherin junctional occupancy and display paracellular transendothelial migration 122
4.3.4 Cytokeratin-7 expression in endothelial and mesenchymal stem cells 128
4.3.5 Effect of trophoblast cells on uterine endothelial cells 130
4.4. Discussion 131
Chapter 5 136
5.1. Introduction 137
5.1.1 Migration of WJ-MSC across fetal and adult endothelial monolayers 137
5.1.2 VE-cadherin as a key adhesion molecule 137
5.1.3 Vascular Endothelial Growth Factor 138
5.1.4 Leukocyte transendothelial migration 138
5.1.5 Aims of the chapter 140
5.2. Materials & methods 140
5.2.1 Immunoblot analysis to measure the phosphorylation status of VE-cadherin .. 141
5.2.2 ELISA assay to measure VEGF secretion in different conditioned media 142
5.2.3 Effect of anti-VEGF on the migration of WJ-MSC across HUtMEC monolayers . 143
5.2.4 Effect of secretome derived from co-culture of WJ-MSC and HUVEC on VE-cadherin junctional occupancy 144
5.3. Results 145
5. 3.1 WJ-MSC causes changes in phosphorylation/dephosphorylation of endothelial VE-cadherin at specific tyrosine residues similar to that seen for transmigrating leucocytes 145
5.3.2 VEGF secretion in co-culture condition media 149
3.3 Addition of anti-VEGF attenuated the migration of WJ-MSC across HUtMEC monolayers 150
5.3.4 WJ-MSC-HUVEC co-culture CM alter VE-cadherin junctional occupancy in HUVEC 151
5.4. Discussion 153
Chapter 6 159
6.1. WJ-MSC and their potential role in vascular repair 160
6.2 The basic biology of placental development 164

APPENDIX ..... - 166 -
Antibodies used for the experiments: ..... - 166 -
Reference 167

Table of Figures

Figure 1: Diagram demonstrating classification of stem cells 3
Figure 2: Micrograph (phase contrast) of WJ-MSC 7
Figure 3: Diagram demonstrating the structure of VE-cadherin adherens junction 25
Figure 4: Placental structure (diagrammatic) 35
Figure 5: Diagram illustrating spiral artery remodelling 38
Figure 6: Isolation of WJ-MSC from human umbilical cord 48
Figure 7: Micrograph (phase contrast microscopy) of WJ-MSC 58
Figure 8: Micrograph (phase contrast microscopy) of WJ-MSC 59
Figure 9: Micrograph (phase contrast microscopy) of sub-confluent WJ-MSC 59
Figure 10: Micrograph (phase contrast microscopy) of confluent WJ-MSC 60
Figure 11: Flow cytometric analysis of WJ-MSC (P3) for haematopoietic markers 61
Figure 12: Flow cytometric analysis of WJ-MSC (P3) for mesenchymal stem cell surface markers 62
Figure 13: Micrographs demonstrating adipogenic differention 63
Figure 14: Micrographs demonstrating chondrogenic differention 65
Figure 15: Micrographs demonstrating oestogenic differention 66
Figure 16: Micrographs demonstrating PKH26 Labelled WJ-MSC 67
Figure 17: Micrograph (phase contrast microscopy) of HUVEC 68
Figure 18: Micrographs showing HUVEC immunocytochemistry 69
Figure 19: Micrographs showing histology of the human umbilical cord 70
Figure 20: Micrographs demonstrating immunohistochemistry of the human umbilical cord 71
Figure 21: Micrographs demonstrating HUVEC & WJ-MSC in mixed media 88
Figure 22: HUVEC-WJ-MSC co-culture phase contrast images 89
Figure 23: Micrographs from time lapse microscopy of HUVEC-WJ-MSC co-culture 90
Figure 24: Micrographs from time lapse microscopy of HUVEC-WJ-MSC co-culture 91
Figure 25: Micrographs from time lapse microscopy of HUVEC-WJ-MSC co-culture 92
Figure 26: Histogram illustrating the percentage of sub-endothelial WJ-MSC 93
Figure 27: Micrographs of VE-cadherin immuno-localisation 95
Figure 28: Percentage of VE-cadherin continuous junctions 96
Figure 29: Micrographs of VE-cadherin localisation in HUVEC with or without WJ-MSC 97
Figure 30: Histogram showing the percentage of continuous VE-cadherin junctions 98
Figure 31: Representative Western blot 99
Figure 32: Confocal composite micrographs of HUVEC-WJ-MSC co-culture 100
Figure 33: Micrograph (phase contrast microscopy) of confluent HUtMEC monolayer 118
Figure 34: Micrographs illustrating HUtMEC & WJ-MSC characterization in mixed media 119
Figure 35: Micrographs from Time lapse of HUtMEC-WJ-MSC co-culture 121
Figure 36: Micrograph from Time lapse showing secreted PKH26 labelled exosome 122
Figure 37: Micrographs of VE-cadherin localisation 125
Figure 38: Histograph showing the percentage of continuous VE-Cadherin 125
Figure 39: Histogram showing the percentage of sub-endothelial WJ-MSC 126
Figure 40: Confocal composite micrographs of HUtMEC-WJ-MSC co-culture 127
Figure 41: Micrographs demonstrating cytokeratin 7 localisation 128
Figure 42: Micrographs showing HUtMEC-trophoblast co-culture 130

Figure 43: Mechanisms employed in leukocyte extravasation 139
Figure 44: Representative Immunoblots 146
Figure 45: Tyr685 histogram 146
Figure 46: Tyr731 histogram 147
Figure 47: Representative Immunoblots showing expression and phosphorylation of VE-cadherin 148
Figure 48: Tyr685 histogram 148
Figure 49: Tyr731 histogram 149
Figure 50: Histogram showing VEGF concentrations in CM 150
Figure 51: Micrographs of VE-cadherin localisation in different medium 152
Figure 52: Histograph showing percentage of continuous VE-Cadherin junctions in HUVEC treated with different medium 153

List of abbreviations

AJ	Adherens junctions
AU	Airy unit
BM	Bone marrow
BSA	Bovine serum albumin
CD	Cluster of differentiation
CK7	Cytokeratin 7
CM	Condition media
CO-CM	Co-culture CM
D	Dimensions
DAPI	4’6-diamidino-2-phenyl indole
DMSO	Dimethylsulphoxide
DPBS	Duldecco’s Phosphate Buffered saline
DPX	Di-n-butyl phthalate in xylene
ECGS	Endothelial cell growth supplement
ECM	Extracellular matrix
EDTA	Ethylene tetra acetic acid
EM	Endothelial media
EPCs	Endothelial progenitor cells
ESC	Embryonic stem cells
EVT	extravillous trophoblast
FBS	Fetal Bovine Serum
FITC	Fluorescein isothiocyanate
FSC	Forward scatters

HBSS	Hanks' Balanced Salt Solution
HSCs	Hematopoietic stem cells
HU	Human umbilical cords
HUtMEC	Human Uterine Microvascular Endothelial Cells
HUVEC	Human vein endothelial cells
ICAM-1	Intercellular adhesion molecule-1
IL8	interleukin-8
ISCT	Mesenchymal and Tissue Stem Cell Committee of the International Society for Cellular Therapy
MMP-9	Matrix metallopeptidase 9
MSC	mesenchymal stem cells
OD	Optical densities
PAGE	Polyacrylamide gel electrophoresis
PE	Phycoerythrin
PECAM-1	Platelet endothelial cell adhesion molecule
PI	Propidium iodide
PLGF	Placental growth factor
SDS	Sodium dodecyl sulphate
SSC	Side scatters
TBST	Tris buffer saline with tween 20
TJ	Tight junctions
TNF-α	Tumour necrosis factor –α
TRITC	Tetramethylrhodamine
Unk	Uterine natural killer cells
VCAM-1	Vascular cell adhesion molecule-1

VE-cadherin	Vascular endothelial-cadherin
VEGF	Vascular endothelial growth factor
VE-PTP	Vascular endothelial specific receptor protein tyrosine phosphatase
WJ	Wharton’s Jelly
WJ-MSC	Wharton’s jelly mesenchymal stem cells
ZO	Zonula occludens

Chapter 1

Introduction

1.1 Stem cell Biology

1.1.1 Definition of Stem Cell

Stem cells are undifferentiated cells, with endless self-renewal sustained proliferation *in vitro* and multilineage differentiation capacity. The first stem cell appearance is in the early zygotic cells, which are totipotent and give rise to the blastocyst. They are capable of differentiating into all cell and tissue types. With differentiation, cells become less capable of self-renewal and differentiation into other cell type becomes limited (Triffitt, 2002)

1.1.2 Categories of Stem Cells

Stem cells are broadly classified into two main categories based on their growth behaviour and isolation time during ontogenesis:

1.1.2.1 Embryonic Stem Cells (ESC):

ESC are derived from embryos at the developmental stage before the time of implantation. This developmental stage includes the morula stage, from which the totipotent stem cells are derived and the blastocyst stage, from which pluripotent stem cells can be isolated (Bongso et al., 1994).

1.1.2.2 Adult Stem Cells:

Adult stem cells or somatic stem cells from adult tissues are generally named after the tissue to which they normally give rise, such as neural stem cell and hematopoietic stem cell. They are present throughout the body and are thought to divide to regenerate damaged tissue (Muller et al., 2001). Adult stem cells are multipotent in nature and they have been localized in nearly all human organs (Toma et al., 2001). For instance, the human bone marrow (BM) represents a diverse reservoir for several stem cell types, like hematopoietic stem cells,

endothelial progenitor cells and mesenchymal stem cells (MSC) (Ballas et al., 2002). On the other hand, there are many other sources of MSC which have been discovered including extraembryonic tissue such as human umbilical cord's Wharton's jelly (Fig 1), which contains MSC expressing mesenchymal but not hematopoietic lineage markers (Wang et al., 2004) and fatty and fluid derived from liposuction aspirates (Yoshimura et al., 2006).

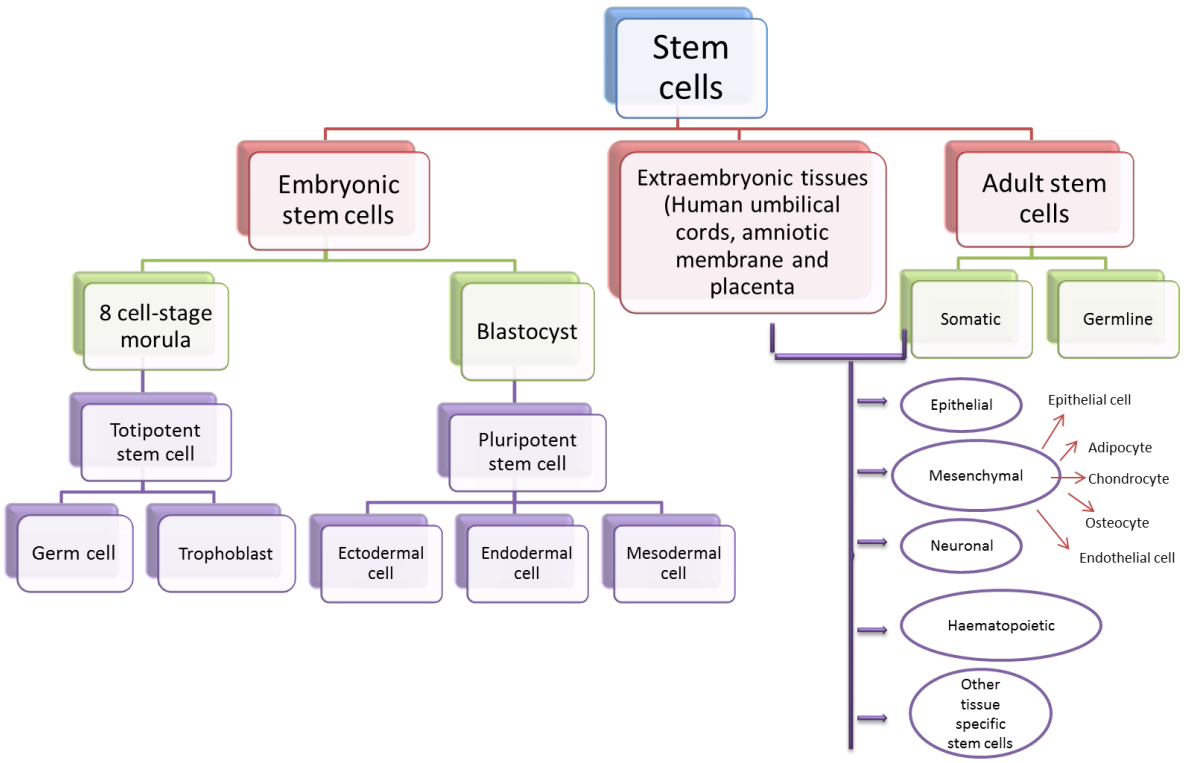


Figure 1: Diagram demonstrating classification of stem cells

Stem cells are embryonic, extra-embryonic and adult stem cells. Embryonic stem cells are originating from morula which gives rise to ecto, endo, mesodermal and trophoblast cells. Blastocyst also is a source of embryonic stem cells and gives rise to all the cells originating from the morula except the trophoblast cells. Extraembryonic stem cells like human umbilical cord, amniotic membrane and placenta. Together with adult embryonic stem cells are giving rise to ecto, endo and mesodermal cells.

1.1.3 Haematopoietic stem cells

Haematopoietic stem cells (HSCs) are the foundation of adult haematopoiesis and give rise to all types of blood cells throughout the lifespan. HSCs are of clinical significance in bone marrow transplantation for the treatment of sickle-cell anemia and leukaemias (Johnson et al., 1984, Johnson et al., 1988). HSCs are defined as multipotent stem cells, which have the capacity to differentiate into a number of cells, including cardiomyocytes, endothelial cells and smooth muscle cells (Yeh et al., 2003). HSCs can be isolated from the bone marrow as well as the peripheral blood (Statkute et al., 2007, Kasow et al., 2007, Bensinger et al., 1990). In response to physiological or pathological stimuli, these stem cells can quickly proliferate and mobilize from their resident bone marrow to peripheral circulation, and then migrate to the site of injury (Borlongan et al., 2011). Human HSCs express surface markers, such as CD34 (Gross et al., 1997, Andrews et al., 1989). By characterization of $CD34^+$ phenotype, it has been found that blood from the human umbilical cord is a relatively abundant source of HSC lineages (Chularojmontri and Wattanapitayakul, 2009).

1.1.4 Endothelial progenitor cells

Endothelial progenitor cells (EPCs) were reported by Asahara *et al* (1997) who showed that purified $CD34^+$ haematopoietic precursor cells from adults can differentiate into endothelial cells and participate in angiogenesis (Asahara et al., 1997). In 2004, Urbich and Dimmeler defined EPCs using three biological parameters: to be non-endothelial cell, but having capacity to give rise to endothelial cells, to show clonal ability to multiply, and have stemness characteristics (Urbich and Dimmeler, 2004). An improvement of neurological functions was reported in chronic cerebral ischaemic rats injected with $CD34^+$ HSC cells, including EPCs (Shyu et al., 2006). Transplantation of EPCs improved coronary endothelial function and wall

motion abnormalities and had a benefit effect on the metabolism in the target area in patients with symptomatic coronary atherosclerosis (Erbs et al., 2005).

1.1.5 Mesenchymal Stem Cells

The concept of MSC, is based on their ability to differentiate into a variety of mesodermal tissues including bone, fat, cartilage, muscle and tendon (Caplan, 1991). Interest in MSC started in 1960s as the result of Friedenstein's observations who reported that the bone marrow stroma can generate bone (Friedenstein et al., 1966). It was later shown that bone marrow stromal cells have chondrogenic and adipogenic properties and a high potential for self-renewal (Owen, 1988). The presence of MSC has been located in many adult and embryonic tissues, such as adipose tissue (Zuk et al., 2001), muscle (Williams et al., 1999), peripheral blood (Kassis et al., 2006), lung (Hennrick et al., 2007), heart (Chong et al., 2011), corneal stroma (Branch et al., 2012), dental pulp (Gronthos et al., 2000), placenta (Fukuchi et al., 2004), endometrium (Cho et al., 2004), amniotic membrane (Alviano et al., 2007), and Wharton's jelly (Wang et al., 2004).

1.1.5.1 Characterization of MSC

The tissue from which MSC are derived may play an important role for surface marker expression. Pluripotency stem cell markers like Oct-4, Nanog, Rex-1, SSEA-3, SSEA-4, Tra-1-60, and Tra-1-81 are expressed on MSC from human first-trimester fetal blood, liver, and BM but not in MSC derived from adult BM (Guillot et al., 2007). MSC expanded under different culture conditions (various types of supplements; fetal bovine serum, human serum, platelet lysate), showed no differences in expression of standard positive mesenchymal markers like CD73, CD90, CD105, CD106, CD146, and HLA-A, B,C or standard negative markers like CD34, CD45, and HLA-DR (Muller et al., 2006, Schallmoser et al., 2007).

According to the Mesenchymal and Tissue Stem Cell Committee of the International Society for Cellular Therapy (ISCT), the minimal criteria to define human MSC are: a) firstly, MSC must be plastic-adherent when maintained in standard culture conditions using tissue culture flasks. b) Secondly, > 95% of the MSC population must express mesenchymal markers; CD105, CD73 and CD90, by flow cytometry and these cells must lack expression (< 2% positive) of haematopoietic markers; CD45, CD34, CD14 or CD11b, CD79a or CD19 and HLA class II. c) Thirdly, the cells must show plasticity which is the ability to develop into other lineages cells and be able to differentiate to osteoblasts, adipocytes and chondroblasts *in vitro* under standard differentiating conditions (Dominici et al., 2006).

1.1.5.2 Morphological characterization

MSC are characterized by the plastic-adherence, spindle-shape, although initially they do show a mixed cellular morphology, from cuboidal to spindle shaped (Fig 2) (Koch et al., 2007). Friedenstein et al. (1976) were the pioneers in the isolation of MSC depending on the ability of those cells to adhere to tissue culture plastic surface.

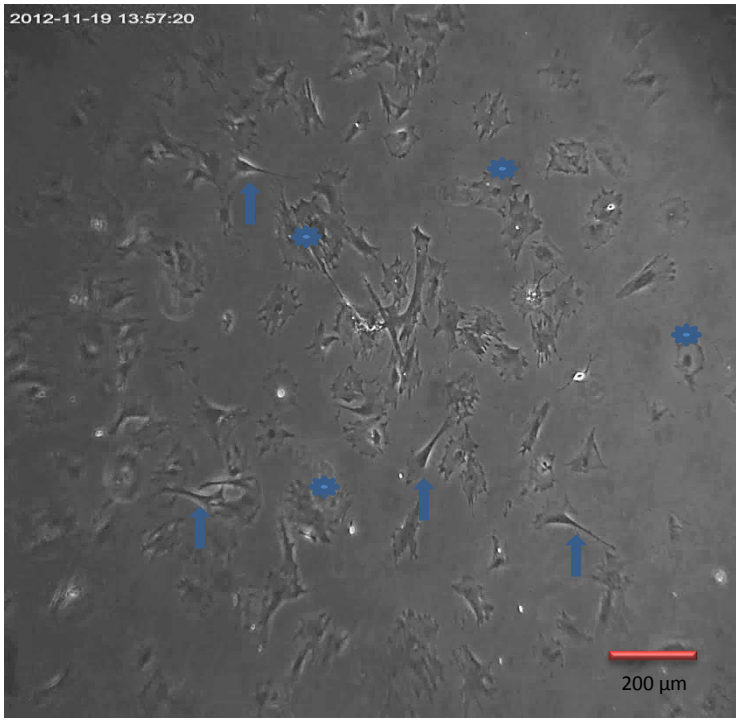


Figure 2: Micrograph (phase contrast) of WJ-MSC

Cells have mixed morphology between cuboidal to spindle shaped at P0.

1.1.5.3 Immunophenotypic characterization

Immunophenotyping is performed by flow cytometry and immuno-fluorescent techniques for rapid identification of the cells. The flow cytometer performs this measurement quickly and reproducibly. Single cells in suspension are presented to a light source through hydrodynamic focusing. The resultant scattered light and fluorescence are collected and converted to electrical pulses, which are digitized for computer analysis. Frequency distributions can be viewed as single- or multiple-variable histograms for evaluating cell measurements. Histograms allow visualization of a single acquired parameter. Mean fluorescence and distributional statistics can be obtained based on markers that the user can graphically set on the plot. Percentages of positively expressing particles relative to a control sample can also obtained in a similar manner.

Multiple histograms can be overlaid on one another to depict qualitative and quantitative differences in two or more markers. Two-parameter data plots are somewhat more complicated than histograms; however, they can yield more information. Two-parameter dot plots of forward scatters (FSC) which correlates with cell volume versus side scatters (SSC) which correlates with inner complexity of the cell (shape of the nucleus, amount, type of cytoplasmic granules and membrane roughness), They are important for identifying populations of interest and differention between living and dead cells (Radcliff and Jaroszeski, 1998).

It is mandatory that cellular protein markers are analysed to assure that the selection of MSC population is not confounded by the presence of other cells, for example haematopoietic stem cells. Multicolour flow cytometer assay should be used to identify that individual cells which are expressing different MSC antigens do not express haematopoietic markers (Dominici et al., 2006).

Cell surface markers belong to the cluster of differentiation (CD) group. The function of CD is based on a protocol used for the identification of surface glycoprotein molecules present on leukocytes (Lunn, 1993). Since 2004, the focus has been extended from leukocytes to other cell types such as endothelial and stromal cells (Zola et al., 2005). The majority of CD molecules function as receptors or ligands or play a role in cell signaling pathways.

Positive markers include β1 integrin (CD29), which are involved in cell adhesion mechanisms. CD44 (hyaluronate receptor), whose is important for the adhesion of various leukocytes to endothelium (Mitchell et al., 2006). CD73 (ecto-5 nucleotidase) is a purine catabolic enzyme. CD90 regulates different biological processes such as cell-cell and cell-

matrix interactions in axon regeneration, apoptosis, adhesion, migration, cancer and fibrosis (Resta and Thompson, 1997). CD105 (endoglin) is a part of the transforming growth factor-β complex (Sanz-Rodriguez et al., 2004).

CD14 protein induces the synthesis of tumour necrosis factor by monocytes. CD19 was the earliest cell surface molecule related to B cell lineage differentiation (Horvath et al., 1998). CD34 protein is L-selectin ligand, which is associated with hematopoietic stem cells (Mitchell et al., 2006). CD45 molecule belongs to the protein tyrosine phosphatase family, its expression is necessary for signal transduction via the B cell antigen-receptor complex (Brown et al., 1994).

1.1.5.4 Differentiation into different cell types

A further way to identify putative MSC is by their capacity to differentiate into various lineages of mesenchymal tissues including bone, fat and cartilage. The classic method for differentiation of MSC to osteoblasts *in vitro* involves incubating a confluent monolayer of MSC with ascorbic acid, β-glycerophosphate, and dexamethasone (Pittenger et al., 1999). The MSC increase their expression of alkaline phosphatase and calcium accumulation can be seen over time.

To promote adipogenic differentiation, MSC are incubated with dexamethasone, insulin, isobutyl methyl xanthine, and indomethacin. Adipogenesis was demonstrated by accumulation of lipid droplets within cells which was assayed histologically by oil red O staining (Pittenger et al., 1999).

For chondrogenic differentiation, MSC are centrifuged to form a pelleted cell aggregation and cultured in the presence of transforming growth factor-β1 (TGF β1), insulin and ascorbic acid. Staining for proteoglycans was carried out using Alcian blue (Santos et al., 2013).

1.1.6 Stem cells and vascular repair

Cardiovascular diseases remain the leading cause of death worldwide (Roger et al., 2012, Lauer, 2012). There are over 5 million patients suffering from chronic heart failure and post-acute myocardial infarction due to inadequate treatment (Roger et al., 2012). Improvement of neovascularization is a therapeutic option to rescue tissue from critical ischaemia (Isner and Asahara, 1999). Because cardiac function depends critically on myocardial perfusion, restoration of cardiac function after myocardial infarction must require not only replacement of lost cardiomyocytes but also revascularization of the injured region.

Stem and progenitor cells isolated from adult tissues have the potential for enhancing neovascularization and regenerating infarcted myocardium (Fuchs et al., 2001, Tomita et al., 1999, Asahara et al., 1997, Al-Khaldi et al., 2003, Kinnaird et al., 2004). In murine model of hind-limb ischemic, circulating stem cells are incorporated into newly formed blood vessels and contribute to increased capillary density and enhanced tissue perfusion (Kalka et al., 2000). BM-MSC mediated improvements in perfusion, may be related to their ability to secrete a variety of angiogenic cytokines, like fibroblast growth factor, vascular endothelial growth factor (VEGF), matrix metalloproteinases, platelet-derived growth factor, TGF-β, interleukin 1, angiopoetin, and others, many of which are upregulated with hypoxia (Kinnaird et al., 2004). The same may be true for fetal mesenchymal stem cells.

1.1.7 Wharton's Jelly of the human umbilical cords as a source of MSC

Wharton's Jelly (WJ) which is the soft, coherent and translucent gelatinous substance of human umbilical cords (HU) formed of mucous connective tissue contains an abundant extracellular matrix composed of collagen fibers, rich in proteoglycans such as hyaluronic acid and contains fibroblast-like cell populations (Parry, 1970, McElreavey et al., 1991, Can and Karahuseyinoglu, 2007) and myofibroblast stromal cells expressing α-actin (Kobayashi et al., 1998, Takechi et al., 1993).

Romanov *et al.* (2003) managed to isolate MSC-like cells from the sub-endothelial layer of HU expressing mesenchymal but not endothelial or leukocyte markers These cells were named HU matrix stromal stem cells to differentiate them from human vein endothelial cells (HUVEC) as well as from MSC isolated from umbilical cord blood (Romanov et al., 2003). Lately, they had been termed Wharton's jelly mesenchymal stem cells (WJ-MSC) which expresses MSC markers, but not haematopoietic markers (Wang et al., 2004).

1.1.7.1 Advantages of WJ-MSC over embryonic and adult Stem Cells

WJ-MSC are important due to their advantages over embryonic and adult stem cells. HU is routinely discarded after delivery, so there is no ethical controversy behind the harvest of the resident stem cells in comparison with the ethical concerns related to the isolation of embryonic stem cells. WJ-MSC can be isolated extracorporeally in contrast to the invasive extraction manoeuvres and patient risks associated with adult stem cell isolation, such as human bone marrow mesenchymal stem cells which is aspirated from the iliac crest, tibia or femur (Hagmann et al., 2013).

The length of the umbilical cord and ease of manipulation increases the number of stem cells that can be harvested. HU developed early in embryogenesis, and represents a source of stem cell populations with advanced potency and less immunogenicity (Fan et al., 2011). WJ-MSC are less immunogenic and escape the host immune response through expressing MHC class I (HLA-ABC) but not class II (HLA-DR) antigens (La Rocca et al., 2009). WJ-MSC had the strongest immunomodulatory and immunosuppressive potential in comparison with BM-MSC, adipose tissue and placental mesenchymal stem cells, thus they are the most efficient cell population for cell therapy when immunosuppressive condition is essential (Li et al., 2014b). Moreover, their transplantation into non-immune-suppressed animals did not produce rejection (Cho et al., 2008, Nagamura-Inoue and He, 2014).

1.1.7.2 Applications of WJ-MSC in regenerative medicine

WJ-MSC thus represent a promising alternative autologous cell source for various tissues and diseases. Direct injection of WJ-MSC into a porcine model of myocardial infarction enhanced cardiac regeneration, through differentiation into cardiomyocytes and endothelial cells within 6 weeks from its transplantation (Zhang et al., 2013). A human trial was recently carried out to demonstrate the feasibility and the procedural safety of using WJ-MSC for cellular therapy in human acute myocardial infarction (Musialek et al., 2015).

WJ-MSC have also been applied in the treatment of type I Diabetes Mellitus or associated pathophysiology. Insulin-producing cells can be generated *in vivo* from transplanted undifferentiated WJ-MSC which its immunomodulatory effects could repair the destroyed NOD mice's islet β-cells (Tsai et al., 2014, Hu et al., 2014, Hu et al., 2015).WJ-MSC and its conditional media accelerated diabetic wound healing in mice (Fong et al., 2012). In a clinical study involved 15 patients with newly onset type 1 diabetes mellitus received 2 doses

of 1.5-3.2 × 10^7 WJ-MSC at 4-week interval by intravenous delivery. Within a period of 24 months, in 3/15 patients insulin supplementation was discontinued and in 8/15 and 3/15 the daily dosage was reduced by more than 50% and 15–50%, respectively. Only 1 patient did not benefit from WJ-MSC treatment. In the control group, not subjected to WJ-MSC treatment, the dose of insulin increased gradually. No adverse reactions or chronic side effects were reported during the follow-up study (Hu et al., 2013).

Recently, human artificial corneal generation took place through differentiation of WJ-MSC *in vitro* into corneal epithelial like cells in a three dimensional model (Garzon et al., 2014b). This could advance the treatment of various corneal diseases including corneal opacity and degenerations which are responsible for the major burden of corneal blindness.

Li *et al.* (2014) demonstrated that WJ-MSC in scaffolds significantly enhanced the recovery of injured liver in mice after 30 days of transplantation (Li et al., 2014a). This also might be the future therapy for patients with liver failure after acute and chronic hepatic diseases.

Regarding the wound healing, after co-transplanted of WJ-MSC and skin microparticles, a new layer of skin and its appendages were developed in murine excisional skin wounds, the healing time was significantly shorter and the healing rate was significantly higher than the control groups (Shi et al., 2014). Intravenous injection of WJ-MSC into artificially severely burned rats also migrated into the wound and promoted healing (Liu et al., 2014). Infiltration of those cells also into a canine chronic skin wound model is associated with decreased extent of ulcerated areas (Ribeiro et al., 2014).

According to Lin *et al.* (2014) WJ-MSC have anti-inflammatory, regulatory effect on intestinal permeability and therefore attenuated ulcerative colitis in a murine model (Lin et al., 2014). Transplantation of WJ-MSC into Parkinsonian rats improved their behavioural deficits (indicated by correction of the rotation induced by amphetamine) through differentiation into efficient dopaminergic cells (Ko et al., 2014). In a human clinical trial, 40 patients with systemic lupus erythematosus received 2 doses of 10^6/kg WJ-MSC at 1-week interval by intravenous delivery. No transplantation's related side effects were observed. During 12 months of follow-up study, 13/40 and 11/40 achieved major or partial clinical response manifested by significant improvement in renal function, decrease in systemic lupus erythematosus disease symptoms. 16/40 patients did not respond to MSC therapy. At 9 months after treatment, 7 patients experienced disease relapse; therefore, the authors concluded that repeated infusion with WJ-MSC is necessary to avoid disease relapse (Wang et al., 2014).

1.1.8 Stem cells homing mechanisms

Stem cell homing is a process which may take hours and no longer than 1-2 days. Circulating haematopoietic cells have been seen to actively cross the blood endothelium barrier and lodge at least transiently, in the BM compartment by activation of adhesion interactions prior to their proliferation (Martin et al., 2003). Stem cells also find their way to other organs, especially in response to stress signals, transmitted in response to alarm situations, for instance; total body irradiation, and can first migrate to the spleen before BM homing (Papayannopoulou, 2003).

The homing ability of stem cells seems to be mediated by the interaction of cytokines/growth factors and their receptors. Since MSC express various cytokine and growth

factor receptors on their membrane surfaces, they are likely to migrate towards cytokine/growth factor production sites by following these cytokine gradients (Park et al., 2011). Tumours secrete stromal cell-derived factor 1 and endothelial growth factor that attract cells from surrounding tissues as well as from the bone marrow to provide support of tumor growth. Due to the over-expression of IL-8 receptor and chemokines, human umbilical cord blood-MSC have a greater capacity to migrate towards glioma than BM-MSC (Kim et al., 2009). Moreover, Xu et al. (2012) stated that N-cadherin overexpression promotes the migration potential of MSC.

Homing to the target tissue is also thought to be modulated by loose adhesion with ligands/receptors that mediate the rolling movement of the blood-borne cells along the endothelial layer. Subsequently, integrins mediate firm adhesion, as well as inducing diapedesis and invasion of the target tissue, via their interaction with endothelial surface molecules and matrix proteins and signal transduction (Avigdor et al., 2004, Dimitroff et al., 2001, Katayama et al., 2003, Papayannopoulou et al., 2001).

1.1.9 Stem cell niche

A niche is described as a subset of tissue cells and extracellular substrates that can indefinitely house one or more exogenous stem cells and control their self-renewal and progeny *in vivo* (Spradling et al., 2001). The microenvironment or niche which consists of signalling molecules, intercellular communication and the interaction between stem cells and their surrounding extracellular matrix, is thought to determine the core properties of the stem cells, such as self-renewal and differentiation to committed cells (Watt and Hogan, 2000, Spradling et al., 2001).

Stem cells may display differentiation potential to various cell types depending on the host microenvironment. For example, when human neuronal stem cells were implanted into different germ layer (skeletal muscle) niche, they were found to produce muscle cells (Galli et al., 2000). Bone marrow cells were also found to differentiate into neuronal cells when they were transplanted into a neural tissue (Zhao et al., 2002).

Bone marrow is the organ with the greatest stem cell niche density. The BM niche is strategically located and organized to support the continuous and balanced production of hematopoietic cells through control of cell survival, self-renewal and differentiation (Calvi et al., 2003, Kiel and Morrison, 2008, Kopp et al., 2005, Zhang et al., 2003). Stem cell niches have also been identified in the heart, the epicardium, the wall of large blood vessels, as well as within adipose tissue, the liver and small intestines (Beltrami et al., 2003, Aicher and Heeschen, 2007, Cai et al., 2008, Campagnolo et al., 2010, Invernici et al., 2007, Zhou et al., 2008, Zengin et al., 2006, Cai et al., 2009).

1.2. The endothelial barriers: inter-endothelial junction formation and barrier integrity

The endothelial barrier is constituted by a monolayer of vascular endothelial cells which forms the intact, innermost layer of the vessel wall and restricts the passage of circulating molecules and inflammatory cells into the underlying tissues forming a physical barrier to maintain cellular function and vascular homeostasis. The endothelium varies from continuous monolayers in microvessels of blood-brain barrier, lung, skin, muscle and placenta to fenestrated vessels in exocrine glands and a discontinuous monolayer in lymphatic vessels and hepatic sinusoids.

Endothelial cells play a key role in controlling the passage of cells, molecules and proteins into the vessel wall and into the target tissues. Endothelial permeability is controlled by trans-endothelial and paracellular pathways (Schnitzer, 1993, Michel, 2012). The transendothelial pathway is formed by fusion of caveolae from luminal and abluminal surfaces to form a transient route for hydrophilic solutes (Michel, 2012).The paracellular pathway is governed by the coordinated opening and closure of endothelial cell-cell junctions. Breakdown of the endothelial barrier whether junctional or increased caveolae, following injury or disease can lead to the unrestricted passage of molecules and inflammatory cells, triggering uncontrolled inflammation and causing further tissue damage.

In general, intercellular junctions maintain adhesion and communication between adjoining endothelial and epithelial cells. In the endothelium where the junctional complexes are the gatekeepers responsible for the integrity of endothelial monolayer, there are two major types of junctions: adherens junctions (AJ) and tight junctions (TJ) (Lampugnani and Dejana, 1997, Dejana, 1996), regulating endothelial monolayers integrity. Gap junctions are another type of junctions which mediate cell to cell communication and allow the passage of small molecular weight solutes between neighboring cells (Simon and Goodenough, 1998). They allow rapid communication between endothelial cells. TJ are the major component providing a strict barrier within the membrane, by controlling both paracellular permeability and maintaining cell polarity. AJ also play an important role in controlling paracellular permeability and are essential for angiogenesis (Bazzoni and Dejana, 2004).

Junctions are better organized in epithelial cells, with a well-defined distribution of TJ and AJ along the intercellular cleft. Zonula occludens (ZO) or TJ are concentrated at the apical side of the cleft, while zonula adherens or AJ are located below the TJ. However, in

endothelial cells, especially non CNS vesseles, the junctional strucutre is less defined and AJ are associated with discontinous TJ along the whole length of the cleft (Stevenson et al., 1986, Li and Poznansky, 1990, Leach and Firth, 1992). In non-brain postcapillary venules, which allow dynamic trafficking of circulating cells and plasma proteins, TJ are poorly organized. In lung, skeletal muscles, mesentry, myocardium and placenta, TJ are not fused. There is a 4 nm gap between the adjoining endothelial cells (Firth et al., 1983, Leach and Firth, 1992, Ward et al., 1988, Adamson and Michel, 1993, Schulze and Firth, 1992). At some areas of discontinuity, the membrane seperation widens up to 18-20 nm of non-junctional parts of paracellular cleft (Adamson and Michel, 1993, Firth, 2002). This allows adhesion molecules in discontinous or wide zones, to play a greater role in controlling paracellular permeability. In contrast, the endothelium of large arteries, which tightly controls permeability, has a well-developed TJ system (Schmelz and Franke, 1993, Schmelz et al., 1994).

The anatomical region can dictate organization of TJ and AJ. Vascular permeability required for tissue/organs perfusion also varies in different parts of the vascular tree depending on the expression and organization of the junctional complexes. In the blood-brain and blood-retinal barrier, where a strict control of permeability is required, junctions are well developed and rich in complex TJ, which are fused for great extents of the intercellular cleft (Rubin and Staddon, 1999, Wolburg and Lippoldt, 2002). In the placental large conduit vesseles have the TJ molecule occludin, whilest capillary exchange vesseles do not (Leach et al., 2000).

The process of paracellular permeability must be strictly regulated to protect the sub-endothelial matrix and maintain vascular integrity (Dejana, 2004). Endothelial cell-cell

junctional complexes transfer intracellular signals, which results in contact inhibition of cells. Perturbations of these complexes results in junctional dissociation, proliferation, angiogenesis, and interactions with smooth muscle cells and pericytes for junctional maturity (Dejana et al., 2009, Grazia Lampugnani et al., 2003). So, the disruption of endothelial junctions not only increases vascular leakiness but also changes the endothelial cell interaction with the surrounding cells and environment.

New blood vessel formation by angiogenesis involves the degradation of the extracellular matrix combined with migration of endothelial cells from pre-existing capillaries (Risau, 1997). One of the initial responses to vascular endothelial growth factor (VEGF) is the loosening of AJ between endothelial cells. This stage is followed by endothelial cells migration to form network-like structures called capillary cords that eventually develop lumens and become functional capillaries (Ausprunk and Folkman, 1977). The molecule primarily responsible for adhesion at endothelial cells AJ is vascular endothelial (VE)-cadherin (Lampugnani and Dejana, 1997), which was discovered by Lampugnani *et al*. 1992 (see later).

Endothelial cells express other adhesive proteins, which are concentrated in the intercellular clefts but are not specifically confined to the AJ or TJ. Platelet endothelial cell adhesion molecule (PECAM-1) or CD31 is one of these molecules, which is a transmembrane immunoglobulin concentrated at intercellular contacts in the endothelium and is also expressed in leukocytes and platelets (DeLisser et al., 1994, Johnson-Leger et al., 2000, Newman, 1997). *In vitro* and *in vivo* studies suggest that PECAM-1 modulate leukocyte infiltration (Muller, 2003, Vestweber and Kemler, 1985). Inactivation of the PECAM-1 gene in mice increases vascular permeability (Graesser et al., 2002). PECAM-1 can modulate cell

adhesion and migration possibly through an interaction with matrix adhesion receptors, such as integrins (Tanaka et al., 1992).

1.2.1 VE-cadherin as the main organizer of endothelial integrity

Adherens junctions are formed by transmembrane adhesion proteins of the cadherin family, which mediate integrity and are able to organize cell-cell adhesions (Angst et al., 2001b, Angst et al., 2001a, Gumbiner, 2000). VE-cadherin is one of the large family of cadherin proteins, and is found almost exclusively in all endothelial cells of all vessel types (Dejana et al., 1995, Lampugnani et al., 1992) and not found in any other type of cells including blood cells and haematopoetic stem cells (Lampugnani et al., 1995). VE-cadherin is a calcium-dependent cell–cell adhesive transmembrane protein, plays a major role in the organization and is considered as the main constituent of intercellular AJ. VE-cadherin is clustered at the junction and mediates cell-cell adhesion through binding to VE-cadherin expressed in neighboring endothelial cell (homotypic binding). These cadherin-cadherin bonds require Ca^{2+} - dependant binding of the projecting extracellular domains which are 20nm long (Dejana et al., 1999).

The role of VE-cadherin in the maintence of vascular integrity *in vivo* was confirmed by development of anti- VE-cadherin blocking monoclonal antibodies (Corada et al., 1999). Early studies using blocking antibodies to VE-cadherin inhibited capillary tube formation of HUVEC in collagen or fibrin gels (Bach et al., 1998), induced monolayer permeability and promoted neutrophils trans-migration (Hordijk et al., 1999). They are thought to promote cell survival, VE-cadherin mutants could not be rescued from apoptosis by VEGF (Corada et al., 2001).

VE-cadherin is not the only cadherin expressed in endothelial cells. N-cadherin is non-specific, can be found in most endothelial cells and other types of cells (Navarro et al., 1998, Salomon et al., 1992, Leach et al., 1993). P-cadherin and T-cadherin expression was also found in the vascular tissue sections (Rubin, 1992, Ivanov et al., 2001). VE-cadherin-2 is another cadherin-like protein in the endothelium, which displays homology with other members of the cadherin family, but has a completely unrelated cytoplasmic tail. For its structural characteristics, it was included in the proto-cadherin family (Telo et al., 1998, Frank and Kemler, 2002).

1.2.2 Structure of VE-cadherin

As stated before, the extracellular domains of VE-cadherin interact with VE-cadherins expressed on neighboring cells. VE-cadherin is linked with their C terminus to specific intracellular partners of AJ catenin proteins; p120, plakoglobin (γ catenin) and β catenin. The latter two proteins bind to α catenin which anchors the complex to the actin cytoskeleton and stabilize the junctions (Fig 3) (Weis and Nelson, 2006, Navarro et al., 1995). All these cytoplasmic linking molecules are signal transduces in their own right, however, p120 binds to a membrane proximal domain of VE-cadherin and does not bind to α catenin or other actin binding proteins (Thoreson et al., 2000). The role of p120 is complicated, in some cell types it induces cadherin-based adhesion, while, the reverse is true (Thoreson et al., 2000, Yap et al., 1998, Aono et al., 1999).

1.2.3 Phosphorylation and modulation of VE-cadherin organization

Tyrosine phosphorylation of components of the cadherin–catenin complexes is associated with cell adhesion perturbation (Yap et al., 2007, Lilien and Balsamo, 2005). Phosphorylation of β-catenin is the most common and sometimes, the phosphorylation of plakoglobin

(Miravet et al., 2003). Tyrosine phosphorylation of VE-cadherin is also associated with p120 (Lampugnani et al., 1997). Phosphorylation of various tyrosine residues on the catenins is associated with the dissociation of the cadherin–catenin complex (Figure 3) (Lilien and Balsamo, 2005).

Histamine, VEGF, thrombin and tumour necrosis factor (TNF)-α were shown to increase tyrosine phosphorylation of different components of the cadherin– catenin complex, disruption of VE-cadherin and enhance permeability of cultured endothelial cell monolayers and perfused human placental microvessels (Bazzoni and Dejana, 2004, Esser et al., 1998, Leach et al., 1995). These inflammatory mediators except TNF-α have a biphasic response with rapid trans-endothelial pore formation (minutes) followed by a paracellular distension after 30 to 60 min (Absi et al., 2014a, Bates, 2010, Wegener and Seebach, 2014b, Esser et al., 1998). However, Tumor necrosis factor alpha takes longer (hours) to phosphorylate, disrupt VE-cadherin and mediate loss of barrier function in endothelial cells (Angelini et al., 2006, Laviola et al., 2013).

The cytoplasmic tail of VE-cadherin harbours phospho-tyrosine sites, like Y645, Y658, Y685, Y731, and Y733 that could be implicated in barrier integrity (Potter et al., 2005, Turowski et al., 2008). VE-cadherin Y685 phosphorylation is induced by VEGF, while Y658 and Y731, which correspond to p120 and β-catenin binding sites, respectively are targeted by leukocytes during transendothelial migration (Wessel et al., 2014, Wallez et al., 2007, Allingham et al., 2007).

Among the permeability enhancing growth factors, VEGF is one of the most potent. It rapidly induces a phosphorylation of VE-cadherin and catenins, which is followed by VE-cadherin redistribution from intercellular junctions and increase in permeability to plasma

proteins (Esser et al., 1998, Wright et al., 2002). This effect may be inhibited by the phosphatase vascular endothelial specific receptor protein tyrosine phosphatase (VE-PTP), which interact with VE-cadherin and strengthens cell to cell adhesion (Nawroth et al., 2002). The non-receptor tyrosine kinase Src was demonstrated to contribute to the phosphorylation of VE-cadherin, catenins and to AJ disassembly (Spring et al., 2012, Gavard et al., 2008). Histamine acted in a way similar to bradykinin by activation of Src which is required for induced permeability (Orsenigo et al., 2012). Thrombin increases phosphorylation by inducing dissociation of the cytosolic non-receptor protein-tyrosine phosphatase Src homology-2 (SHP-2) from the VE-cadherin complex. Thrombin may also change VE-cadherin-catenin organization at junctions and reduce the amount of plakoglobin associated with the complex (Rabiet et al., 1996, Ukropec et al., 2000).

Activation of Rho-associated protein kinase-dependent and increase in intracellular Ca^{2+} levels enhanced actin cytoskeleton contractile activity, VE-cadherin separation, and greater increases in microvascular permeability (Yuan et al., 2014). Other mechanisms for rapid cadherin regulation include digestion by proteases (Ito et al., 1999, Marambaud et al., 2002). VE-cadherin extracellular domain is highly susceptible to lysis (Dejana et al., 1995). Induction of metalloproteases may induce cleavage and promote junction disruption (Noe et al., 2001). Cadherins can be cleaved also at the membrane-cytoplasm interface by proteases activated during apoptosis or Ca^{2+} imbalance (Herren et al., 1998).

Other proteins outside the junctions may contribute to the control of permeability. For example, PECAM-1 can be phosphorylated by permeability-increasing agents, like VEGF, inflammatory cytokines or shear stress (Esser et al., 1998, Nasdala et al., 2002). Intercellular adhesion molecule-1 (ICAM-1) also triggered tyrosine phosphorylation of VE-cadherin, a

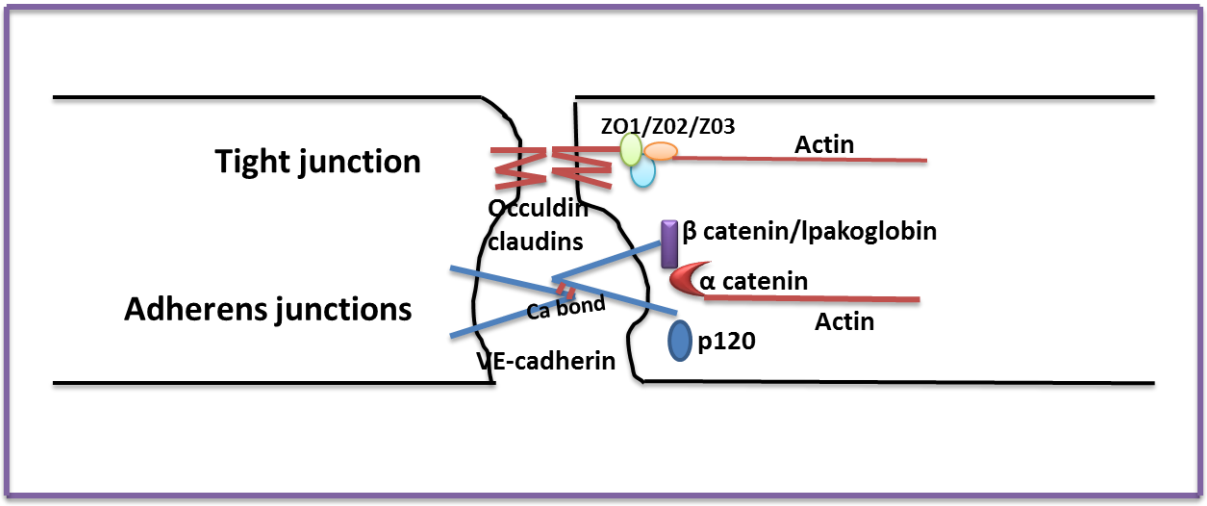
process that required Src and the proline-rich tyrosine kinase 2 which is essential for leukocyte diapedesis (Allingham et al., 2007, Turowski et al., 2008).

1.2.4 VE-cadherin internalization

Regulation of cell–cell adhesion and endothelial barrier function requires availability of VE-cadherin at the plasma membrane (Gaengel et al., 2012, Orsenigo et al., 2012). Internalization of cadherin is associated with cell–cell junction loosening, which could contribute to cell migration and permeability (Gavard and Gutkind, 2006, Yoshioka et al., 2012). VE-cadherin phosphorylation on serine and tyrosine residues has been shown to provoke its internalization both *in vitro* and *in vivo*, leading to cleft disorganization and increase in vascular permeability (Gavard and Gutkind, 2006, Spring et al., 2012, Gavard et al., 2009).

VEGF, chemokines, inflammation and PI3K (transduces TNFα signaling), are involved in VE-cadherin internalization which by turn induce VE-cadherin destabilization and loss of vascular barrier (Dwyer et al., 2011, Yoshioka et al., 2012, Cain et al., 2010). Src kinase also triggers VE-cadherin internalization, directly through its phosphorylation or through the activation of other kinases, such as PAK (Li et al., 2012, Orsenigo et al., 2012). Anti-permeability agents could act through the blockage of VE-cadherin internalization (Gaengel et al., 2012, Gavard et al., 2008). Leukocyte diapedesis required internalisation of VE-cadherin via tyrosine phosphatase SHP-2 with the resultant frank opening necessary for leukocyte paracellular trafficking (Sidibe and Imhof, 2014). Wessel *et al*. (2014) also showed that de-phosphorylation of Tyr731 selectively regulates leukocyte extravasation. siRNA blocked de-phosphorylation of Tyr731 through inhibition of SHP-2 expression which impaired VE-cadherin internalisation and reduced leukocyte migration (Wessel et al., 2014).

A



B

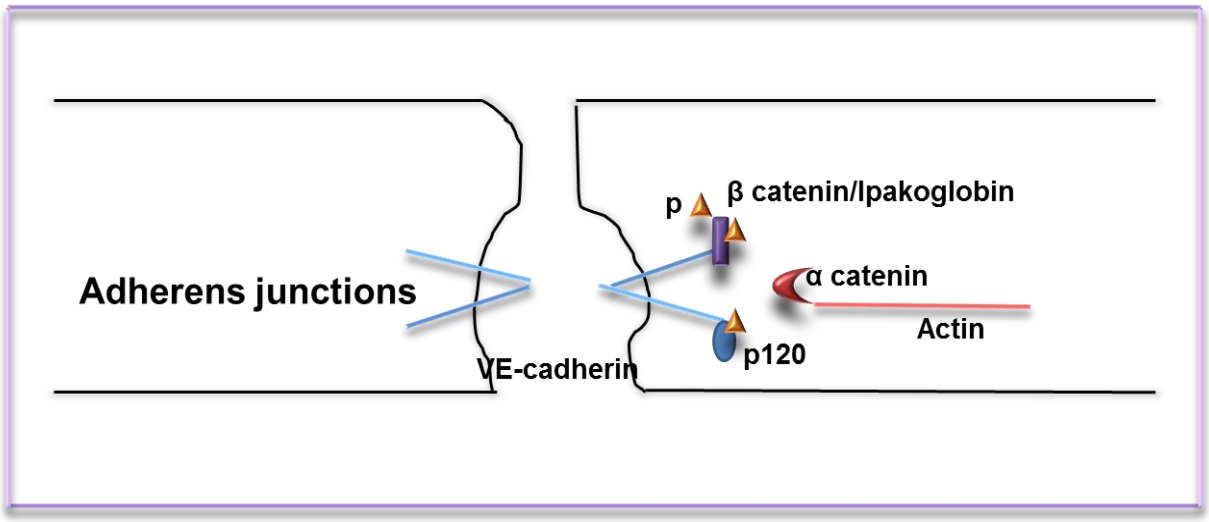


Figure 3: Diagram demonstrating the structure of VE-cadherin adherens junction

(A) Junctional VE-cadherin in resting conditions; p120, β-catenin and plakoglobin bind to VE-cadherin intra-cytoplasmic domains. B-catenin and plakoglobin in turn bind to α-catenin which anchors the complex to the actin cytoskeleton to stabilize the junctions (B) Tyrosine phosphorylation (P) of VE-cadherin, β-catenin, plakoglobin and p120 dissociate AJ. VE-cadherin structure modified from (Leach et al., 2009), with permission.

1.3. Vascular Endothelial Growth Factor

VEGF regulates vasculogenesis, cell proliferation, migration, and integrity of endothelial cells during embryogenesis (Byrne et al., 2005, Robinson and Stringer, 2001). It enhances vascular permeability and thought to contribute to tumor metastasis by promoting cell extravasation and tumor angiogenesis (Weis and Cheresh, 2005, Thurston, 2002). VEGF also enhanced the migration ability of cardiac stem cells in an *in vitro* cellular migration assay (Tang et al., 2009). Whether VEGF has any role in fetal MSC migration into the maternal endothelium remains to be determined.

VEGF is an endothelial-specific cytokine, also known as vascular permeability factor, it is a key mediator of angiogenesis and vasculogenesis (Leung et al., 1989, Keck et al., 1989, Byrne et al., 2005). Its role in increasing vascular permeability is thought to be imperative in opening inter-endothelial cell junctions leading to paracellular transport (Lampugnani et al., 2006, Dejana et al., 2008).

The VEGF family includes: VEGF-A, VEGF-B, VEGF-C, VEGF-D, VEGF-E and PlGF (Eriksson and Alitalo, 1999, Witmer et al., 2003). VEGF-A (generally called VEGF) is expressed in isoforms of 121, 145, 165, 183, 189, and 206 amino acids in length (Robinson and Stringer, 2001). VEGF165 appears to be the most prevalent and the potent isoform (Byrne et al., 2005, Robinson and Stringer, 2001).

VEGF is expressed in multiple cells and tissues including endothelial cells, vascular smooth muscle cells, cardiac muscle, hepatocytes, neutrophils, macrophages, $CD34^{+}$ stem cells, BM-MSC and fibroblasts (Sugishita et al., 2000, Yamane et al., 1994, Gaudry et al., 1997, Bautz et al., 2000, Namiki et al., 1995, Nauck et al., 1997, Beckermann et al., 2008). The expression

VEGF is induced by hypoxia and cytokines like IL-1, IL-6, IL-8 and TNF-α (Gaudry et al., 1997, Angelo and Kurzrock, 2007). Protein array analysis of WJ-MSC after serum starved for 48h found their secretome was enriched with pro-angiogenic growth factors including VEGF (Edwards et al., 2014).

VEGF-A binds to two related receptor tyrosine kinases: VEGF R1 and VEGF R2 (Neufeld et al., 1999). These receptors have seven extracellular immunoglobulin domains, a single hydrophilic transmembrane domain and an intracellular split tyrosine kinase domain (Veikkola et al., 2000, Millauer et al., 1993). They are expressed on vascular endothelial cells and a range of non-endothelial cells (Byrne et al., 2005). VEGF enhanced vascular permeability through binding to VEGF R2 and subsequently Src tyrosine kinase activation (Sun et al., 2012).

1.4. Extracellular matrix (ECM)

Tissues are not composed solely of cells. A network of ECM filling the extracellular space is a substantial part of tissue volume. Coordinated changes between cell-cell adhesion and cell to the ECM are essential for controlling cell growth and tissue homeostasis. Adjustment of cell adhesions is critical for vascular remodeling and angiogenesis (Vestweber, 2000). Dynamic changes in cell-cell as well as in cell-matrix adhesion are responsible for regulating vascular permeability, which allows the diffusion of nutrients, metabolites and hormones from blood to the tissues. Alternation of the permeability due to any factor, affect both types of adhesion complexes (Dudek and Garcia, 2001).

1.4.1 Structure and functional components of ECM

ECM is formed of two main constituents: (1) glycosaminoglycan polysaccharide which is link usually to protein forming proteoglycans. (2) Fibrous proteins of two functional types: structural proteins (collagen and elastin) and adhesive proteins (fibronectin and laminin). The first proteins form a highly hydrated gel like structure in which fibrous proteins are embedded. The adhesive proteins help cells to attach to matrix tissue. Fibronectin promotes attachment of fibroblast and related cells to the matrix connective tissues., while laminin promotes the attachment of epithelial cells to the basal lamina (Hay, 1981).

Collagen forms the main component of EMC. Elastin is also a major component of elastic fibres in matrix where it provides elastic recoil in soft tissues, like arterial wall and ligaments. Elastin has a role in cell adhesion, migration, and cell signaling. Fibronectin plays a role of organization of matrix as it forms a bridge between cell surface receptors, for example: integrins, collagen, proteoglycans and other adhesion molecules. Laminin contributes to the ECM structure and modulate cellular functions such as adhesion, migration, differentiation, phenotype stability, and apoptosis resistance (Halper and Kjaer, 2014).

Integrins are important in cell-matrix adhesion and cell migration. Antibodies against integrins disrupt the endothelial barrier (Lampugnani et al., 1991). Integrins modulate migration by enabling cell adherence to ECM. The activation of integrins allows the functional connection between focal adhesions and actin cytoskeleton that is required to drive cell migration (Klemke et al., 1997, Giancotti, 2000). The process of leukocyte transendothelial migration includes activation of β1 and β2 integrins, which facilitate cell adhesion (Carveth et al., 1989). During adhesion, the endothelial Ig family adhesion molecules vascular cell adhesion molecule (VCAM)-1 and ICAM-1 are engaged by

leukocyte integrins. Engagement of VCAM-1 and ICAM-1 in turn initiates diverse signals within the endothelial cells includes phosphorylation of VE-cadherin, which is required for diapedesis (Cook-Mills and Deem, 2005, Kluger, 2004, Allingham et al., 2007). TNF-α can increase the expression of VCAM-1 on rat BM-MSC and promote its adhesion to endothelial cells and migration to damaged tissue (Xiao et al., 2012).

Several studies demonstrated the importance of integrins in promoting migration of primary cytotrophoblasts through a basement membrane-like matrix (Matrigel) and interstitial collagen (Damsky et al., 1994, Aplin et al., 1999, Zhou et al., 1997b). Application of antibodies against β1 integrins to villous explants, disturb anchorage and reduce cytotrophoblasts column outgrowth (Aplin et al., 1999). Whether other fetal cells including MSC use similar mechanism to migrate into the maternal endothelium and myometrium remains to be shown.

1.4.2 ECM dimensions (D)

When migrating cells encounter ECM, it can be either in the form of 2D flat surface or 3D tissue networks. Cell migrating through 2D sheets in wound healing where there is a unilateral adhesion to the substratum, which provides a transient attachment and a barrier free migration (Farooqui and Fenteany, 2005, Ridley et al., 2003, Keren et al., 2008).

Cells moving across a 3D interstitial network formed of collagen fibrous tissue, leads to limitations counteracting the movement of migratory cells. Therefore, their morphology undergo characteristic changes, from a spread-out morphology to a spindle shaped one to adapt small tissue gaps (Maaser et al., 1999, Wolf et al., 2003).

The migration efficiency depends on pore diameters and it is perfect in gap diameters that match or range slightly below the diameter of migratory cells. If the tissue pores exceed the cell size, migration rates decrease due to the loss of most cell–fibre interactions until only very few or even a single fibre remain engaged with the cell body which is one D migration (Doyle et al., 2009). However, if gaps are less than the cell diameter, cells slow down and may trapped due to the physical resistance (Harley et al., 2008, Haston et al., 1982). Migrating cells underwent elongation, stretching, and changing shape to more spindly to reduce their calibre in response to highly resistant extracellular tissues, while large sized pores tissues allow egress of rounded cells (Lammerding et al., 2006, Dahl et al., 2008).

In addition to changes in shape, cells can cleave ECM structures by cell-surface proteases counteracting physical obstruction by widening gaps and forming routs of variable diameters so they match their own calibres (Wolf et al., 2007). So, in 3D ECM the cell ability to adapt its shape in relation to the available space and to proteolytically remodel tissues detect both the efficiency and mode of migration (Friedl and Wolf, 2010).

1.4.3 Employment of extracellular matrix in cell migration

Dynamic interaction between the cell and the undelaying substratum on which it is attached is mandatory for cell migration (Huttenlocher and Horwitz, 2011). Extracellular matrix provides a molecular and structural frame for the migratory cell; therefore it affects the mode and efficiency of cell migration. Modes of migration are classified based on the morphology of migratory cells, type of cell–matrix interaction and the modification of the tissue structure by migrating cells into two main categories: individually migrated cells (amoeboid or mesenchymal) or grouped (migration of multicellular units) (Friedl and Wolf, 2010, Lammermann and Sixt, 2009). Amoeboid migration is characterized by gliding and rapid migration; it is the main mode of migration for highly motile cells such as neutrophils,

dendritic cells, and lymphocytes. It is commonly referred to as the movement of rounded or ellipsoid cells that lack mature focal adhesions (Lammermann and Sixt, 2009, Friedl et al., 2001).

There are two subtypes of amoeboid movement. The first is the rounded, blebbing migration of cells that do not adhere to substratum but use a pushing, propulsive migration mode (Sanz-Moreno and Marshall, 2009, Fackler and Grosse, 2008). The second occurs in more elongated cells that generate actin-rich pseudopodia at the leading edge that engage in a weak adhesive interaction with the substratum (Yoshida and Soldati, 2006, Smith et al., 2007).

Cells with high levels of attachment develop mesenchymal migration, which involves focal cell–matrix interactions and movement in a fibroblast-like migration, like the fast migration of a single leukocyte or the slow invasion of fibroblasts into wound matrix (Friedl et al., 1998). Collective or grouped cell migration is seen in building and remodeling tissue compartments, such as ducts, glands and vessels. It also demonstrated in cancer progression by local invasion (Alexander et al., 2008, Friedl and Gilmour, 2009). BM-MSC showed blebbing which is thought to be related to low avidity interaction between endothelium and MSC, whilst quenching of blebbing may be promoted by contact with the sub-endothelial matrix after transmigration (Teo et al., 2012).

1.5. Mesenchymal stem cells and pregnancy

The Wharton's jelly of the human umbilical cord is derived from the mesoderm of the primitive streak which invades the connecting stalk and primary chorionic villi and it is a source of MSC (Wang et al., 2004). Whether these cells have a continued role in

placental/umbilical vascular growth and maturity is not known, but they can be formed through out gestation. Their role in influencing maternal physiology is a new topic of interest given that cells from tri- lineages embryonic germ layers; ectoderm, endoderm and mesoderm have been identified in maternal peripheral blood. They have been shown to selectively home to damaged maternal tissues (Seppanen et al., 2013). The mechanism by which fetal cells cross the placental barrier and enter maternal circulation is not known.

MSC from the placenta and other extraembryonic tissue are in close contact with maternal circulation. After invasion of chorionic villi by the mesenchyme, only a thin layer of synctiotrophoblast separates chorionic villi MSC from maternal blood. This may be discontinuous in early gestation or denuded in regions during different trimesters (Nelson, 1996). Denuded regions with fibrin deposition are a feature of normal and pathological placenta (Nelson, 1996, Mayhew and Sampson, 2003). MSC from both the term human placenta or umbilical cord sources have a common origin and share similar surface marker expression and differentiation potential (Kim et al., 2011). Whether MSC have any role in invading or remodelling endometrial spiral arteries to the best of current knowledge, has not been investigated.

1.5.1 The placenta

The placenta is located at the maternal-fetal interface and modulates the intrauterine environment to promote optimal fetal development. The networks of blood vessels within the placenta are responsible for exchanging respiratory gases, nutrients, and wastes between the mother and fetus, which is essential for proper fetal growth throughout gestation. The vasculature of the placenta is continually evolving during pregnancy to accommodate the increasing demands of the fetus.

The establishment of proper placental function first requires successful implantation of the fertilized oocyte followed by the coordinated invasion of trophoblast cells, from the trophoectodermal layer of the blastocyst into the maternal decidua. After invasion, trophoblast cells are thought to remodel the maternal spiral arteries to promote expansion of the maternal vasculature, which is essential for improving uterine blood flow. This facilitates efficient exchange of nutrients from the mother to the fetus and thereby permits exponential fetal growth and development (Reynolds and Redmer, 1995, Pardi et al., 2002).

Abnormal development of the placental vasculature leads to placental insufficiency, which can result in a decrease in the exchange of nutrients and wastes between maternal and fetal circulations. These changes can manifest in adverse uterine conditions leading to various pregnancy complications for both the mother and the fetus including gestational hypertension, intrauterine growth retardation, preeclampsia, stillbirth, preterm delivery and abortion (Pijnenborg et al., 1991, Barut et al., 2010, Jarvenpaa et al., 2007, Pinar and Carpenter, 2010, Kristensen et al., 2005). Therefore, the proper establishment of blood vessels within the placenta is mandatory for fetal growth, survival and may serve as a therapeutic potential for improving clinical conditions that are associated with altered placental vasculature.

Appropriate development of the placental vascular network requires vasculogenesis, angiogenesis, and arterial remodeling. The process of vasculogenesis involves the *de novo* formation of blood vessels from precursor cells, whereas angiogenesis involves the creation of new vessels from already existing ones (Demir et al., 2007, Charnock-Jones et al., 2004, Demir et al., 1989). During vasculogenesis, haemangiogenic stem cells (derived from mesenchymal cells) differentiate to haemangioblastic stem cells, giving rise to angioblastic

cells. These cells in turn differentiate into endothelial cells forming new vascular networks (Charnock-Jones et al., 2004, Hanahan, 1997, Demir et al., 1989, Leach et al., 2002). Endothelial cells organized into tubal networks, and then they become associated with pericytes derived from the mesenchyme surrounding the endothelium. These pericytes then proliferate and migrate, coating the endothelial cell tubes and forming the vessels (Beck and D'Amore, 1997, Sims, 1986, Benjamin et al., 1998).

1.5.2 Placental barrier

In the human placenta, spiral arteries bring blood from uterine artery to the blood lacunae around the placental villi. Chorionic villus contains fetal capillaries that connected to cord vessels, and are covered by endothelium inside and the villous trophoblasts outside facing maternal blood (Fig 4). The placental barrier is consisting of an endothelial cell layer, thin layer of connective tissue and a continuous syncytiotrophoblast (a continuous, uninterrupted, multinucleated epithelial surface layer without separating cell borders, formed from fusion of the villous trophoblasts), with some individual cytotrophoblast underneath (Contractor et al., 1977, Jones and Fox, 1991).

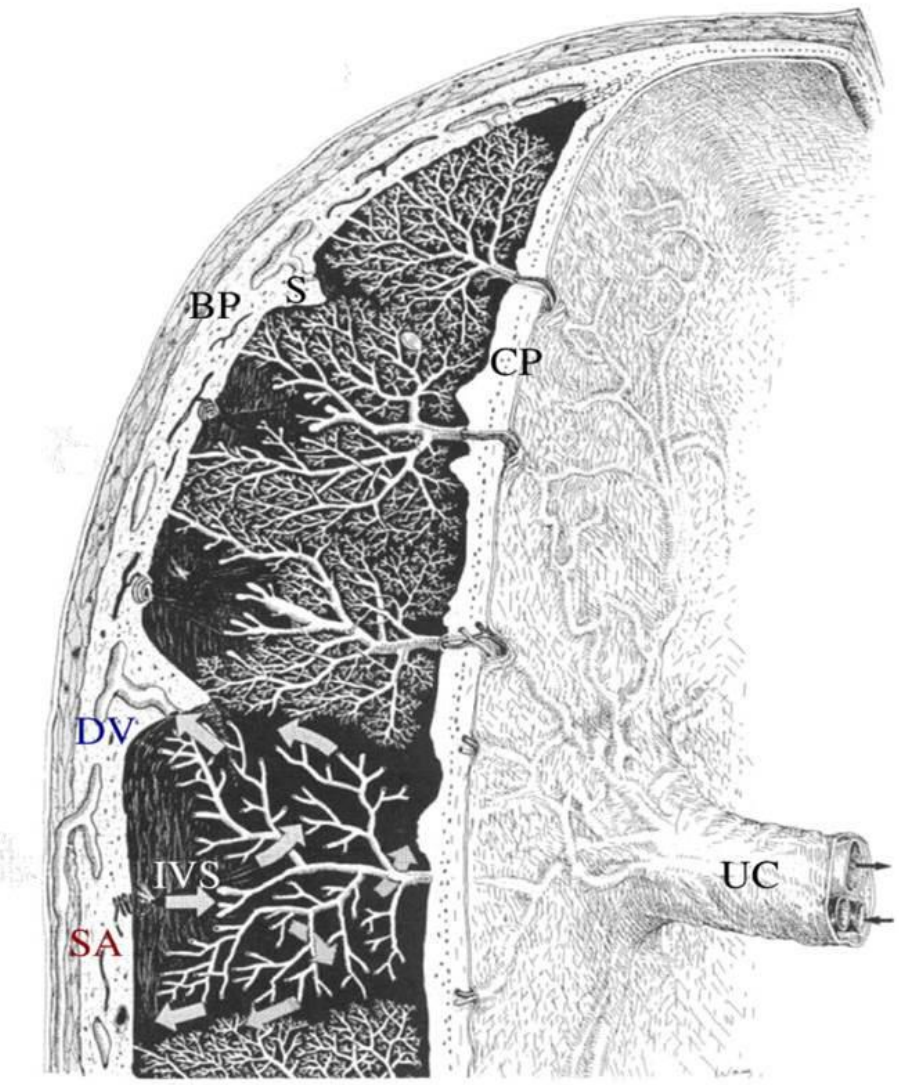


Figure 4: Placental structure (diagrammatic)

The structure of the human placenta contained within and including the chorionic plate (CP) and the basal plate (BP) surrounding the intervillous space (IVS). The villous trees containing fetal vasculature (communicating with the fetus via the umbilical cord, UC) project from the CP into the IVS and are directly surrounded by maternal blood that emerges from spiral arteries (SA) in the BP and circulates to leave the IVS through the decidual veins (DV). The diagram is modified from (Chernyavsky et al., 2011), with (L Leach) permission.

1.5.3 Spiral artery remodelling

It is important to recognise both the maternal and fetal placental circulations in materno-fetal exchange. In the remodelling of placental circulation, the extravillous trophoblasts contribute to the development of the maternal circulation by secreting angiogenic factors (Asan et al., 1999, Harris et al., 2006) and invading the maternal decidua to remodel maternal spiral arteries creating a low resistance, high capacitance vessel, increasing the exchange between maternal and fetal circulations (Cerdeira and Karumanchi, 2012).

During feto-placental circulation development, the fetal component formed of the chorionic plate, which is made up of the inner mesoderm layer from extraembryonic mesoderm and the outer trophoblast layer from tropho-ectoderm. Chorionic villi grow out from the plate and float freely (floating villi) in the maternal lacunae where its blood is coming from spiral arteries, to allow exchange of oxygen, nutrients and waste. Chorionic villi consist of a layer of cytotrophoblast covered by a further layer of syncytiotrophoblast, which is invaded by mesenchymal tissue by the third week of gestation.

The villous cytotrophoblast is the precursor of invasive extravillous trophoblast. At sites of contact with the decidua, the former cells proliferate to form anchoring sites containing cell columns, that eventually break away to infiltrate maternal tissues (Aplin et al., 1998). According to Zhou *et al* (1997), columns of cytotrophoblast cells form the anchoring villi that project into the maternal endometrium, attaching the fetus to the uterus via the placenta. There are two different extravillous trophoblast (EVT) lineages leaving the stem villi; the interstitial and endovascular trophoblasts (Zhou et al., 1997b).

EVT cells invade the uterine decidua (Figure 5) and remodel spiral arteries through retrograde migration (intravasation) of perivascular interstitial trophoblast (Pijnenborg et al., 2006) causing dilatation, decrease arterial resistance and increase oxygen tension (Jauniaux et al., 2000, Burton et al., 1999). After invasion and integration in the wall of spiral arteries, trophoblast started to induce smooth muscle and endothelial cells apoptosis and replace spiral artery endothelial cells (Kam et al., 1999, Pijnenborg et al., 1980). Zhou *et al.* (1997) postulated that trophoblast showed epithelial-endothelial transformation and behaved like endothelial cells through expression of endothelial marker (VE-cadherin) and loss trophoblastic marker (cytokeratin 7) which enhances its invasive capacity (Zhou et al., 1997a). This proposition is now being looked at with new eyes, given the study was observational deduction, not experimental.

It is thought that endovascular trophoblasts migrate through the arterial lumen in large numbers and form trophoblast plugs; they accumulate in the spiral artery lumen and prevent blood flow (Figure 4). This is aid thought to produce of a hypoxic environment, encouraging endovascular trophoblasts proliferation and invasion into the vessel wall followed by endothelial and smooth muscle loss and deposition of fibrinoid material. Moreover, after incorporation in spiral arteries wall, the maternal vascular repair process took place though intimal connective tissue thickening, intramural fibroid embedding and α actin positive cells which may act as a source of smooth muscle replacement (Pijnenborg et al., 2006, Kaufmann et al., 2003).

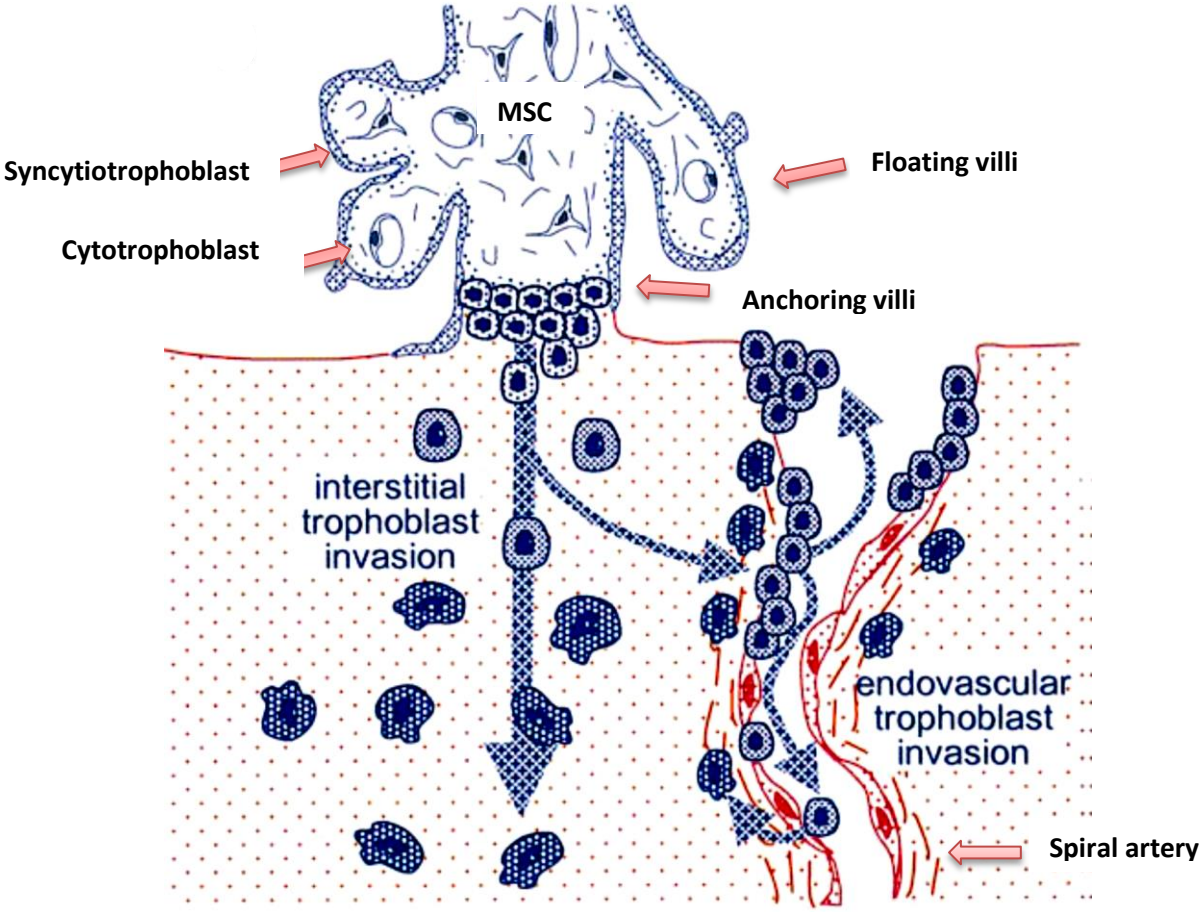


Figure 5: Diagram illustrating spiral artery remodelling

Extravillous trophoblast cells (EVT) showing invasion of the spiral arteries. This was taken and modified from (Kaufmann et al., 2003). Fetal tissues (Blue) include syncytiotrophoblast, cytotrophoblast, MSC, interstitial and endovascular EVT. Maternal tissues (Red) include spiral artery and endometrium. Endovascular and interstitial EVT remodelling the spiral artery is derived from cell columns from the anchoring villi.

There are other types of cells involved in the remodelling process such as uterine natural killer (uNK) cells and macrophages. uNK cells are abundant in the endometrium in early pregnancy and form up to 70 % of the leukocytes in the decidua (Lash et al., 2010) and decrease after 20 weeks of gestation (Bulmer et al., 1991); they surround spiral arteries and secrete a range of angiogenic growth factors. Robson *et al.* (2012) reported that uNK cells initiate spiral artery remodelling through inducing disruption of smooth muscle cells and breakdown of extracellular matrix (Robson et al., 2012). Kaufmann *et al.* (2003) also stated that activated macrophages increase trophoblast apoptosis and reduce its invasion in preeclampsia (Kaufmann et al., 2003).

Remodelling of spiral arteries is an extensively researched area, but controversy has surrounded the part played by fetal trophoblast in the transformation of these spiral arteries over contrasting evidence emerging all the time. For example, Bulmer *et al.* (2012) argued that EVT do not regulate vascular smooth muscle apoptosis but instead regulate its migration away from the spiral arteries (Bulmer et al., 2012). There was also a debate on the chronological order in which different EVT invade, with study suggesting that endovascular trophoblasts begins invasion only after the vessel lumen prepared by interstitial trophoblasts (Kam et al., 1999, Pijnenborg et al., 1983). The exact cellular, molecular mechanisms, the interaction between cells related to the remodelling and the factors controlling this process need further investigations. Whether fetal stem cells, especially those that can influence vascular functions, has any role in this spiral artery remodelling requires investigations.

1.6. Thesis Hypothesis

Laboratory and clinical based research suggests that Wharton's jelly mesenchymal stem cells are a valuable source of cells for regenerative medicine. They are present in vascular regions and are capable of influencing endothelial function and maturity.

Thus this study was performed to isolate, fully characterise WJ-MSC and to investigate their potential role if any in endothelial junctional organization of fetal or uterine endothelium. The cellular and the molecular mechanisms behind the transendothelial migration and the dynamics of cell adhesion molecule VE-cadherin were also investigated.

The **hypothesis** of this thesis is "MSC from the human umbilical cord Wharton's jelly can transmigrate across fetal and maternal endothelial cell monolayers via induced disruption of cell-cell junctions. Furthermore, once perivascular niches are reached, WJ-MSC regulate endothelial junctional maturity".

1.7. Aims and objectives

To test this hypothesis, the aims of this study were:

- To isolate, expand, characterise and label WJ-MSC from the Wharton jelly of term human umbilical cords (Chapter Two).

- To Isolate and charaterise HUVEC from the human cord umbilical veins, use as a fetal endothelial monolayer for co-culture studies (Chapter Two).

- To explore the cellular mechanisms used in attachment and transmigration of WJ-MSC across HUVEC monolayers, the time taken and the associated dynamics of the junctional VE-cadherin (Chapter Three).

- To investigate the events when fetal WJ-MSC encounter confluent maternal endothelial cell monolayers, the chosen transendothelial migration pathway and the VE-cadherin dynamics. To explore the ability of these cells to influence maternal endothelial junctional maturity from sub-endothelial niches (Chapter Four).

- To investigate the molecular mechanisms behind migration of WJ-MSC across fetal and maternal endothelium (Chapter Five).

Chapter 2

Isolation and characterization of Wharton's Jelly mesenchymal stem cells and human umbilical vein endothelial cells from the human umbilical cords

2.1. Introduction and aims

2.1.1. Human umbilical cord Embryology, Function and Anatomy

The human umbilical cord starts to develop around the fifth week of gestation. It is derived from extra-embryonic mesoderm. The latter arises from embryonic mesoderm which is derived from epiblast of the inner cell mass of the blastocyst. During further development the amnion which is derived also from the extra-embryonic mesoderm, forms an outer covering for the HU. The amnion is composed of three layers; inner epithelial layer, an intermediate non cellular basement membrane and outer mesenchymal layer (Pappa and Anagnou, 2009).

Stem cells from HU are derived from several compartments; the vascular compartment (blood lying within the umbilical cord blood vessels), the endothelial compartment, the medial and adventitial compartment of the walls of umbilical cord vessels, the perivascular compartment surrounding the blood vessels, Wharton's jelly compartment, the amniotic compartment (outer epithelial layer and inner sub-amniotic mesenchymal layer) (Kita et al., 2010). Stem cell populations in different compartments have varied stemness (core properties) and the different isolation protocols will result in mixed stem cells populations. Therefore, a standard isolation protocol for MSC from HU is necessary to obtain minimal heterogenic cell population.

HU function as to protect enclosed vessels from compression and torsion while providing a bidirectional, feto-maternal blood circulation. Anatomically, HU contains two umbilical arteries and one umbilical vein; both are embedded in the WJ, which is composed of collagen fibres of Type I and III and a glycosaminoglycan. The collagen forms a three-dimensional network and it is in loose contact with an amorphic intercellular substance which contains

mucopolysaccharids, like hyaluronic acid, and carbohydrates with glycosyl and mannosyl terminals and acid groups (Sobolewski et al., 1997).

The umbilical vein is a source for human vein endothelial cells. HUVEC have played a major role as a vascular model to study of the functional regulation of endothelial cell, the role of the endothelium in response to physiological, pathological factors and in angiogenesis (Park et al., 2006, Hamilton and Leach, 2011, Souadkia et al., 2010).

2.1.2. Pre-existing methods of isolation of WJ-MSC

Several techniques have been devised for the isolation of WJ-MSC for primary culture. These techniques can affect the quantity and quality of the isolated cells (Salehinejad et al., 2012). Choosing the appropriate method for the isolation of human umbilical cord-derived mesenchymal is important. One technique is used in cell isolation is the explant of tissue fragments. This technique is characterized by reducing the tissue size small enough for gases and nutrients to diffuse freely (Liu et al., 2013, Salehinejad et al., 2012).

Another common technique is the use of defined enzyme systems to dissociate tissues. For example; collagenase enzyme, hyaluronidase and trypsin with or without ethylene tetra acetic acid (EDTA), were used in tissue digestion and derivation of WJ-MSC from human umbilical cords (Fong et al., 2010, Montanucci et al., 2011, Tsagias et al., 2011, Liu et al., 2013, Salehinejad et al., 2012). The duration of the enzymatic treatment is critically important, as it may degrade the extracellular matrix and cell membrane, and prevents the cells from adhering to the culture substrate after isolation (Can and Karahuseyinoglu, 2007), so the enzymatic treatment time should be kept to a minimum. Salehinejad *et al.* (2012) postulated that collagenase/trypsin methods of cell isolation yield a higher cell density than the others,

while the explant method of cell isolation resulted in a higher cell proliferation rate and activity compared to the other methods (Salehinejad et al., 2012).

To be able to use the cells in clinics, the isolation procedure ideally has to involve minimal tissue handling and be less time consuming. MSC isolation from the entire cord piece is less time-consuming and less intensive than from WJ part of the cord (Hendijani et al., 2014). For the above stated reasons, the method used by De Bruyn et al. (2011) was chosen to be applied here in this study, it is non enzymatic method to avoid the consequences of using enzymes for prolonged duration, using an entire cord piece to avoid long time tissue handling and to get higher cell density from the longer cord piece with higher proliferation rate,

2.1.3. Human umbilical vein endothelial cells

Endothelial cells from human umbilical vein gained a wide popularity because of their relative ease of isolation and availability. The culture of HUVEC was first reported more than four decades ago (Jaffe et al., 1973). HUVEC are a powerful *in vitro* model system that mimics many endothelial processes that occur *in vivo*. This model system has aided in the identification of adhesion molecules and chemokines critical in the recruitment of many leukocyte subclasses and enabled detailed analysis of how these processes are regulated (Cuvelier and Patel, 2005, Ulfman et al., 2001, Cuvelier et al., 2005, Del Maschio et al., 1996).

2.1.4. The aims of this chapter

This chapter aimed to find the optimum method for isolation, expansion and characterization of WJ-MSC from the Wharton jelly of term human umbilical cords. It also highlighted WJ-MSC labelling with viable fluorescent dye, isoation and charaterization of

HUVEC from umbilical veins in order to use them as a vascular model in co-culture studies. Finally the *in situ* localization of MSC in the umbilical cords, was carried out to domastrate the original site of those WJ-MSC in the umbilical cord specimens.

2.2. Material and Methods

Materials

Chemical and reagents

Duldecco's Phosphate Buffered saline (DPBS); calcium and magnesium free; Hanks' Balanced Salt Solution (HBSS); pencillin – streptomycin (10,000 u/ml pencillin, 10 mg/ml streptomycin in 0.9 % Nacl); trypsin – EDTA solution 1x (0.5 g porcine trypsin and 0.2 g EDTA in 4 Nacl HBSS); dexamethasone; 3-isobutyl-1-methyl-xanthine; recombinant human insulin; indomethacin; β glycophosate; TGF- β1; ascorbate-2- phosphate; Oil Red O; alcian blue 8 GX; BCIP/NBT(5-Bromo-4-chloro-3-indolyl phosphate/Nitro blue tetrazolium) tablets; Tween 20; Fetal Bovine Serum (FBS); Dimethylsulphoxide (DMSO); paraformaldehyde; Bovine serum albumin (BSA); PKH26 red fluorescent stain; heparin sodium salt; Grade 1-A; Endothelial cell growth supplement (ECGS) (30 mg/mL) and gelatin from bovine skin (type B) (Sigma-Aldrich, UK). Antibiotic/antimycotic solution (10,000 u/ml pencillin G, 10,000 µg/ml streptomycin, 25 µg/ml amphotericin B); DMEM/Low Glucose + 4.00 Mm L- Glutamine + 1000 mg/L Glucose + 110 mg/L Sodium Pyruvate (Hyclone, UK). Sodium chloride (Fisher scientific, UK). Medium 199 (1x) + Earle's Balanced salts + L. Glutamine + 25 Mm HEPES + L- Amino Acids and Collagenase type II (Gibco, UK).

Tissue Culture Plastics and Accessories

Tissue culture flasks 25 cm^2 and 75 cm^2; 100 ml Petri dish; 12 and 24 well plates; centrifuge tubes; Cover slips 19 mm, 0.2 mM filters; 10 mL syringes (Life Technologies). Eight well glass chamber slides (Lab- Tek, UK). 3-way stopcocks (Vycon UK Ltd., Gloucester, UK). Vincryl suture (2/0, 75 cm) (Davies and Geck, Gosport, UK). One mL Cryopreservation tubes (Sarstedt, Leicester, UK). Tc 10 counting slides (Bio-Rad, UK). Scissor, forceps, scalpels, Container to incubate umbilical cord and steel trays (Jencons- PLS, Leighton Buzzard, UK).

Antibodies for Immunocytochemistry and Flow Cytometry

Monoclonal antibodies: CD45 – FITC, CD34 – FITC, CD44 – PE and CD29 - FITC (Beckman Coulter, UK); CD105 - FITC, CD73 - APC, CD90 - PE, CD31- FITC, CDHLA-DR - FITC, CD19 - APC, CD14 - PE (ebioscience, UK); Vector: Vectashield mounting medium for fluorescence with or without propidium iodide [PI] (Vector laboratories, Inc Burlingame, CA 94010). Primary antibodies: Purified mouse antihuman vascular endothelial (VE)-cadherin (CD144) (Pharmingen, BD Biosciences, UK). Polyclonal rabbit antihuman Von Willebrand factor (vWF) (Dako, UK). Secondary antibodies: Anti-rabbit IgG (whole molecule FITC); Anti-mouse IgG (whole molecule FITC) (Sigma-Aldrich, UK).

Methods

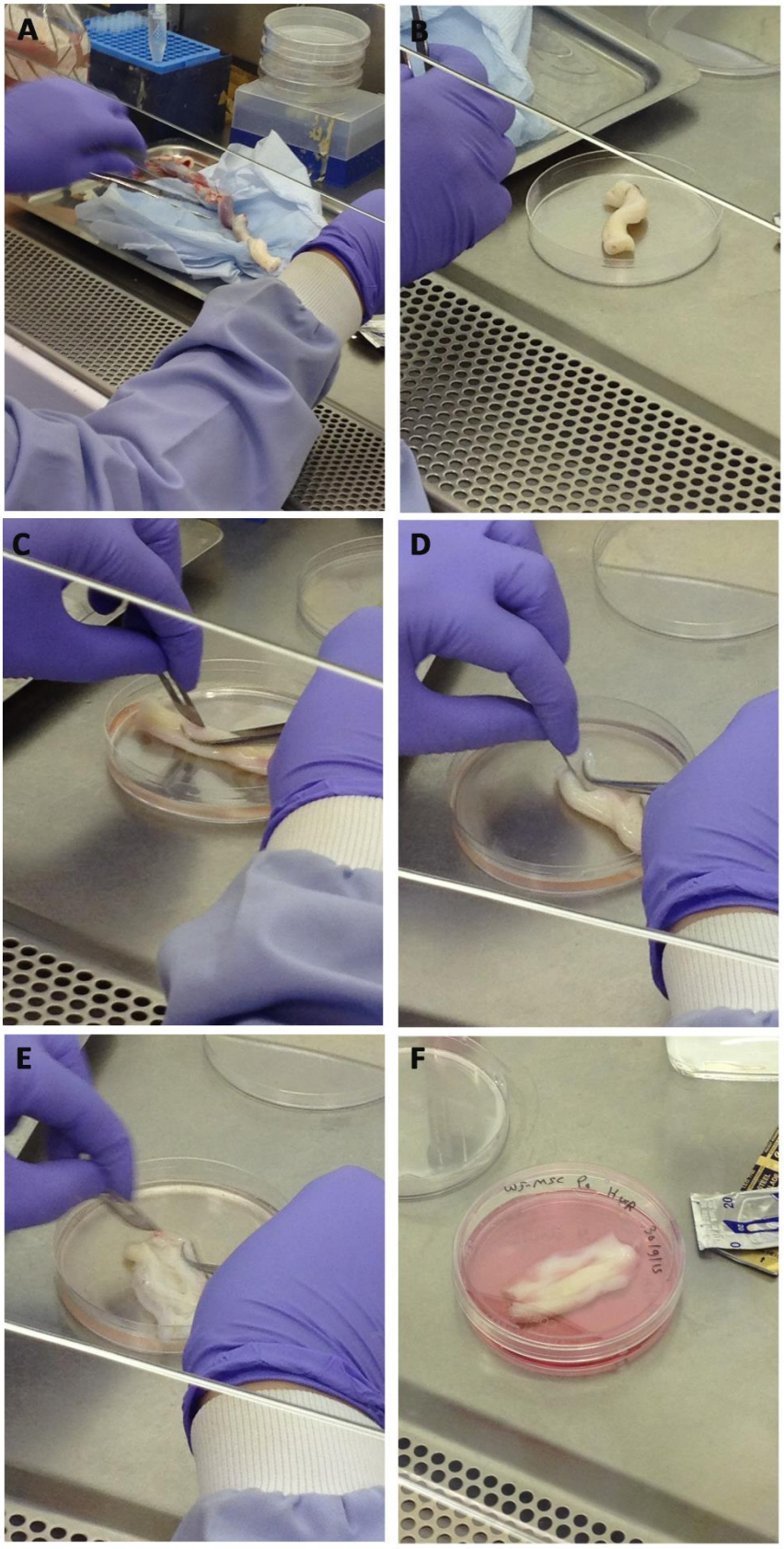
2.2.1 Isolation of WJ-MSC

WJ-MSC were non-enzymatically isolated from freshly collected human umbilical cords (n=27), obtained at elective Caesarean section from normal pregnancies with informed patient consent and full ethical approval (REC Ref 14/SC/1194; NHS Heath Research Authority, UK), and NHS permission from Nottingham University Hospitals, NHS Trust,

UK. This study complied with the legislation contained within the Human Tissue Act. Using the method of De Bruyn et al. (2011). HU was stored in sterile 0.9% (w/v) NaCl saline containing 100 IU/mL penicillin and 100 µg/mL streptomycin at 4˚C, it was used within 24 hours. HU was divided into three parts; each part was about 3 to 5 cm with sterile scalpel. Each piece of the cord was cut longitudinally to expose the WJ and small incisions were done with caution to avoid blood vessel injury and to increase the surface area of the WJ exposed to the plastic surface of the petri dish, washed with pre-warmed sterile saline antibiotic solution to remove any residual blood contents. Each piece of HU was transferred to a $10cm^2$ Petri dish with WJ facing the plastic surface with 20 ml of growth medium (DMED/Low Glucose, 100 IU/mL penicillin, 100 µg/mL streptomycin, 0.25 µg/mL amphotercin B and 15 % FCS) (Figure 6). Petri dishes were incubated at 37˚C and 5% CO_2 in air.

Figure 6: Isolation of WJ-MSC from human umbilical cord

(A &B) HU is divided into three parts; each part is about 3 to 5 cm with sterile scalpel. (C-E) Each piece of the cord is cut longitudinally to expose the WJ and small incisions were done with caution to avoid blood vessel injury and to increase the surface area of the WJ exposed to the plastic surface of the petri dish. (F) Each piece of HU was transferred to a Petri dish with WJ facing the plastic surface with 20 ml of growth medium.


A
B
C
D
E
F

2.2.2 Proliferation of WJ-MSC

WJ-MSCs were allowed to grow at 37˚C and 5% CO_2 in air for five days without any disturbance. HU pieces were removed and the attached cells were fed with pre-warmed growth medium every 5 to 7 days. The migration of cells from HU pieces onto the plastic were monitored daily, using (Olympus inverted microscope). When the cells reached about 80—90% confluence within 25 ± 5 days, the medium was removed, 10ml of DPBS was used to wash any remaining residues of the media from the Petri dish, then the cells were detached by incubation with 2ml of trypsin/ EDTA (0.05 % trypsin and 0.02 % EDTA) for 10 minutes at 37˚C and the reaction was stopped by adding growth medium. WJ-MSC were then collected by centrifugation (1000 rpm for 5 minutes), 1×10^6 cells/ml was seeded on 75 cm^2 culture flask after counting and in the same culture conditions for confluence, the time to reach confluence were halved in the 5 consecutive passages.

2.2.3 Cell counting and freezing

When WJ-MSC in the 75 cm^2 culture flask reached confluence, harvesting of the cells was done as described previously. Then, the pellet was suspended in freezing mixture (10 % DMSO, 90 % full growth media). Cells in the suspension was counted by mixing 10 µl of cell suspension to 10 µl trypan blue, loaded to the counting slide, then using the haemocytometer to measure total number of the cells and the percentage of the viable cells. The suspension was transferred to cryovials (1ml / vial) labelled with cell line, passage number, name and the date. Cryovials were placed in -80°C freezer overnight and transfered into a liquid nitrogen (British oxygen company, UK) Dewar.

2.2.4 Thawing of WJ-MSC

Frozen cells were taken from liquid nitrogen storage and thawed quickly in a warm water bath, gently pipetted into the centrifuge tube with growth medium, centrifuged at 1000 rpm for 5 min, transfered into 75 cm^2 culture flask. The growth medium was changed after approximately 24 hours, and the cells were passaged when confluent.

2.2.5 Detection of Mesenchymal and haematopoietic markers using Flow Cytometry

Cell suspensions were acquired as described previously and 1×10^6 cells were added to a centrifuge tube and incubated for 30 min at room temperature with 5 μL anti-human, either singly or double. Markers used were: haematopoietic markers (CD45 – FITC, CD34 – FITC, HLA-DR - FITC, CD19 – APC and CD14 – PE) and mesenchymal stem cells markers (CD44 – PE, CD29 – FITC, CD105 - FITC, CD73 - APC and CD 90 - PE). One ml of media was added and centrifuged (250 rpm for five minutes) to obtain a loose pellet. Cells only (no added antibody) were used as a negative control. Cells were fixed through adding one ml of 1% paraformaldehyde to each tube for 30 minutes at RT. Positively and negatively stained cells were separated by flow cytometry FC 500 (Beckman Coulter, UK) with 50,000 events captured. Results were analysed using WEASEL v3.0 for Windows (Walter and Eliza Hall Institute, Australia) and presented as histograms.

2.2.6 *In-vitro* Differentiation

2.2.6.1 Adipogenic Differentiation

WJ-MSC differentiation was performed using the method of Pittenger *et al.* (1999) at passage 2 and 4 before and after freezing (Pittenger et al., 1999). Cells were seeded at a density of 60,000 cells per well into 24 well plate and cultured in growth media till

confluence or post confluence. The differention was induced by three cycles of three consecutive inductions and one maintenance using adipogenic induction medium (DMEM-LG, 1 mM dexamethasone, 0.5 mM 3-isobutyl-1-methyl-xanthine, 10 mg/ml recombinant human insulin, 100 µM indomethacin, and 10% FCS) and adipogenic maintenance medium (DMEM-LG, 10 mg/ml recombinant human insulin and 10% FCS). The control cells were fed with growth medium only. Adipogenic differentiation was confirmed by the formation of lipid-droplets with Oil Red O. Cells were fixed with 4% paraformaldehyde for 30 minutes, washed three times with PBS, stained with a working solution (3 Oil Red O: 2 distilled water) of 0.5 % Oil Red O in isopropanol for 30 minutes at RT, washed with PBS and distilled water. The nuclei were counterstained with Mayer's haematoxylin solution for one minute and the cells were washed with distilled water and examined by inverted microscope.

2.2.6.2 Chondrogenic Differentiation

To promote chondrogenic differentiation using the method of Pittenger *et al.* (1999), the cells were harvested as usual in 15 ml conical tube at a density of 10^6 cells per tube, centrifuged at 200 rpm/5 minutes to obtain loose pellet, suspended in 0.5 ml of the chondrogenic differention media (DMEM-LG + 2 mM L- glutamine, 1 % FCS, 6.25 µg/ml insulin, 10 ng/ml TGF – β1 and 50 µM ascorbate-2- phosphate). The cells incubated with loose cap and upright position. The control cells were fed with growth medium. The media were changed every 3 days for 30 days. Differentiation was confirmed by alcian blue stain which stained proteoglycans. Cell pellets were fixed with 4% formalin for 60 minutes at RT, embedded in paraffin, staining on deparaffinised 5 µm sections with 3 % alcian blue over night at RT. Sections were rinsed with distilled water, air dried, immersed in xylene and mounted using DPX (Di-n-butyl phthalate in xylene) before observing under inverted

microscope. The nuclei were counterstained in some slides before mounting through immersing in haematoxylin solution.

2.2.6.3 Oestogenic Differentiation

For oestogenic differentiation using the method of Santos *et al.* (2013), cells were seeded like adipogenic differention and oestrogenic induction medium (DMEM-LG + 2 mM L-glutamine, 100 nM dexamethasone, 10 mM β glycophosphate, 0.2 mM ascorbate-2-phosphate and 10% FCS) was used. The control cells were fed with growth medium. The media were changed every 3 days for 30 days (Santos et al., 2013). Oestogenic differentiation was confirmed by alkaline phosphatase reaction, cells were fixed with 4% formalin for 60 seconds at RT, washed once with washing buffer (0.05 % tween 20 in DPBS), stained with alkaline phosphate solution (one tablet of 5-Bromo-4-chloro-3-indolyl phosphate/Nitro blue tetrazolium dissolved in 10 ml distilled water). This acted as a precipitating substrate for the detection of alkaline phosphatase activity within cells. The enzyme cytochemistry was performed for 15 minutes in the dark, with periodic checking every 2-3 minutes for colour changes. Cells were washed three times with washing buffer, put in PBS and examined under an inverted microscope.

2.2.7 WJ-MSC Labelling

Cell suspensions were acquired as described previously, placed in a conical tube containing 2×10^7 cells and washed once with media without FCS, centrifuged (400 rpm for five minutes) to obtain loose pellet. One ml of diluent C was added to the pellet; another one ml of PKH26 stain (4 µl of the stain to 1 ml of diluent C) was added and incubated at 37˚C for five minutes with periodic mixing. Two ml of FCS was added, incubated at 37˚C for one minute to bind the excess dye and centrifuged (400 rpm for five minutes). The pellet was

suspended in growth media, transferred to fresh tube and centrifuged (400 rpm for five minutes). The pellet was suspended in the growth media and seeded on coverslips in 12 well plates at 37˚C and 5% CO_2 in air. Coverslips were taken, covered with another coverslip and was examined using a Nikon fluorescence microscope. Detection of the dye in the cells was monitored for 10 days.

2.2.8 Isolation of HUVEC

HUVEC were isolated from umbilical cords, obtained at elective Caesarean sections from normal pregnancies with full, informed consent from the mother, using the method of Hamilton and Leach (2011). Umbilical cords were collected in sterile 0.9% (w/v) NaCl saline containing 100 IU/mL penicillin and 100 μg/mL streptomycin and stored at 4˚C for up to 24 hours before use. The vein at each end of the umbilical cord was cannulated with a three-ways stopcock and secured by tying with vincryl suture around the end of the cord. Then, the vein was washed with pre-warmed sterile saline antibiotic solution to remove any residual blood contents and ensure the cord was not damaged at any point.

HUVEC were harvested by collagenase type II digestion, through filling the umbilical vein with 1 mg/mL collagenase type II in 10 ml M0 (medium M199 supplemented with 100 IU/mL penicillin, 100 μg/mL streptomycin, 0.25 μg/mL amphotercin B) until it become firm. Following incubation of the cord for 10 minutes at 37˚C and under 5% CO_2 in a water bath containing the pre-warmed sterile saline antibiotic solution, the collagenase solution was passed back and forth through the vein using 10 mL syringes attached to stopcocks at each end of the cord to ensure that endothelial cells were detached from the vessel wall.

The resulting HUVEC suspension was collected in M20 (M0 and 20% (v/v) heat inactivated FBS), centrifuged three times at 1000 rpm for 5 minutes at RT and re-suspended in growth medium (M20 supplemented with 50 μg/mL ECGS and 50 μg/mL heparin) and allowed to attach to gelatin coated 25 cm^2 tissue culture flask (1% (w/v) gelatin in sterile water, autoclaved and stored at 4°C, 2 mL were used for the 25 cm^2 culture flasks, 5 mL for the 75 cm^2 culture flasks, and 1 mL for each cover slip in an 12-well plate or 8-chamber slide, Incubated at 37°C with 5% (v/v) CO_2 for 90 min, gelatin was removed and air-dried in a laminar flow hood under sterile conditions) at 37˚C and 5% CO_2 in air.

2.2.9 Maintaining, harvesting, and subculture of HUVEC

HUVEC were allowed to grow at 37˚C and 5% CO_2 in air. After 24 hours, unattached cells were removed and the attached cells were fed with pre-warmed growth medium. The cells were re-fed every 2-3 days. When the cells reached about 80—90% confluence, the medium was removed, pre-warmed 5 ml of DPBS was used to wash any remaining residues of the media from the flask, then the cells were detached by incubation with 2ml of trypsin/ EDTA (0.05 % trypsin and 0.02 % EDTA) for 5 minutes at 37˚C and the reaction was stopped by adding 5 ml of growth medium. HUVEC were then collected by centrifugation (1000 rpm for 5 minutes), removed supernatant and the pellet was re-suspended in 3 ml of pre-warmed growth medium. Furthermore, the suspension was seeded on 1% (w/v) gelatin coated 75 cm^2 culture flask (splitting ratio 1:3) and growth medium was refreshed after 24 hours, then every 2 to 3 days.

2.2.10 Cell counting and freezing

When HUVEC in the 75 cm^2 culture flask reached confluence, harvesting of the cells was done as described previously. Then, the pellet was suspended in 3 ml of freezing mixture (50

% growth media, 40 % FCS and 10 % DMSO). The number of the cells in the suspension was counted by mixing 10 µl of cell suspension to 10 µl trypan blue, injected to the counting slide, then using the haemocytometer to measure total number of the cells and the percentage of the living cells. Furthermore, the remaining of the suspension was transferred to cryovials (1ml / vial) labelled with cell line, passage number, name and the date. Cryovials were placed into a Mr Frosty container and placed in - 80°C freezer overnight. This ensures that the cells freeze slowly at an optimum rate of - 1°C/min. Then, transfer the cryovials into the liquid nitrogen containers the next day.

2.2.11 Characterization of HUVEC

HUVEC were seeded on gelatin coated 8 well chamber slides. Upon confluence, HUVEC were fixed with 1% paraformaldehyde at RT for 10 minutes, permeabilized for 10 min with 0.15% Triton X-100, and blocked in 5% goat's serum in PBS for 30 minutes. Cells were exposed overnight at 4 ˚C in a humidified environment to polyclonal rabbit anti-human vWF (1:100 dilutions in PBS/BSA or mouse antihuman CD144 (VE-Cadherin) (1:100 dilutions in PBS/BSA). Control wells were given 5% goat's serum. The wells were washed with 0.1% PBS/BSA three times.

Secondary antibodies were added as follows: the vWF wells and one of the controls were exposed to anti-rabbit IgG (1:50 dilution in PBS/BSA). The VE-Cadherin wells and the other control well were exposed to anti-mouse IgG (1:50 dilution in PBS/BSA) for two hours in the dark at RT. After extensive washing, wells and glue were removed from the chamber slide leaving normal glass slides that were mounted using Vectorshield to preserve the fluorescence of the secondary antibody. It was covered with coverslip, was examined using a Nikon fluorescence microscope with a fluorescence filter of 490nm excitation / 550nm

emission to allow visualisation of FITC (fluorescein isocyanate; green). Finally, it was photographed with a CCD camera (Nikon DS) and was stored (NIS elements F3.0; Nikon).

2.2.12 *In situ* localisation of WJ-MSC in HU

Cryo-sections (5-10 μm thickness) were cut at −20°C and picked on gelatinised slides. Sections were air-dried for 15 minutes, fixed, permeabilized and blocked like WJ-MSC immunocytochemistry. To visualize tissue organization, slides were stained firstly for toluidine blue (histological analysis), endothelial and smooth muscle markers, polyclonal rabbit anti-human vWF (1:100 dilutions in PBS/BSA) and mouse anti-human smooth muscle actin (1:100 dilutions in PBS/BSA). Slides were then washed. The secondary antibodies used were anti-rabbit IgG (1:50 dilution in PBS/BSA) and anti-mouse IgG (1:50 dilution in PBS/BSA). In order to visualise the presence of stem cells, sections were further incubated with undiluted CD105 FITC, CD29 FITC, CD45 FITC or CDHLA-DR FITC. Controls did not have any CD markers. Slides were washed, mounted and examined like HUVEC immunocytochemistry.

2.3. Results

2.3.1 Isolation and behaviour of WJ-MSC in culture

WJ-MSC took 5 days to migrate from HU pieces; about 50 cells from each cord piece (Fig 7), the migrating cells demonstrated a mixed cuboidal to spindle-shaped morphology (Fig 8). These cells underwent proliferation demonstrating the characteristic elongated fibroblast-like morphology (Fig 9) and the cell counts reached to $7 \pm 2 \times 10^5$ cells/ml at confluence in 25 ± 5 days (Fig 10). The cord samples (n=27) showed a very high successful isolation rate (23 out of 27 cords yielded successful isolates), no differences in numbers of cells obtained from the

three parts of the cord, meaning that every cord segment contained WJ-MSC which did not differ in their morphology.

In order to analyse proliferation capacity of WJ-MSC; differences in the time needed to reach confluence or the morphology of the cells in the successive passages was observed. It was observed that passage one took nearly half the duration of passage 0 to reach confluence within roughly 12 ± 3 days with splitting ratio 1:3. The cell count was $1 \pm 0.2 \times 10^6$ cells/ml with 92 ± 4 % viability and it maintained the characteristic fibroblastic morphology of MSC. As regard passage 2 and 3 the cell count was $1.4 \pm 0.3 \times 10^6$ cells/ml with 96 ± 2 % viability within 4± 1 day. As for passage 4 and 5, the cell count was $2.5 \pm 0.5 \times 10^6$ cells/ml with 94 ± 3 % viability within 2± 1 days (n=6).

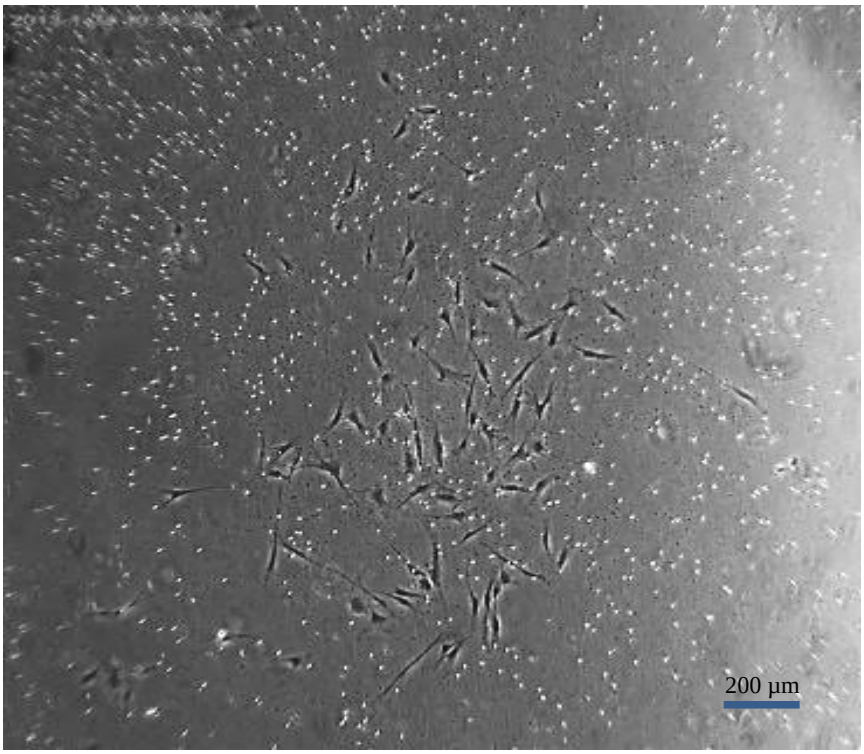


Figure 7: Micrograph (phase contrast microscopy) of WJ-MSC

WJ-MSC P0, 5 days after removal of the cord pieces (about 50 cells from 5cm cord piece).

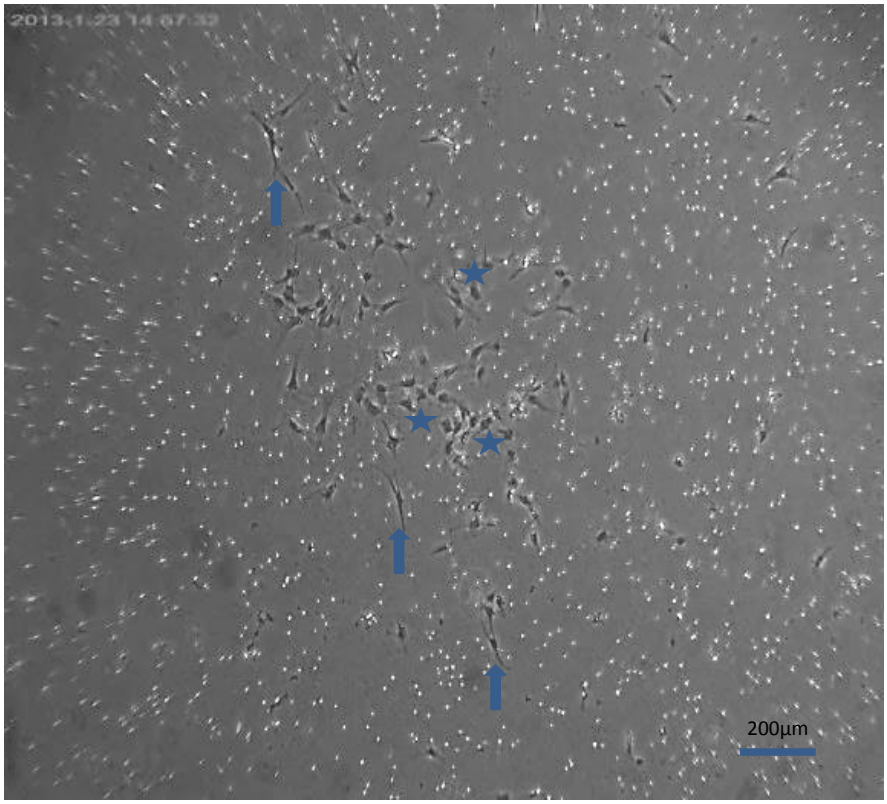


Figure 8: Micrograph (phase contrast microscopy) of WJ-MSC

WJ-MSC with mixed morphology (cuboidal ✦, spindle shaped ⬆)

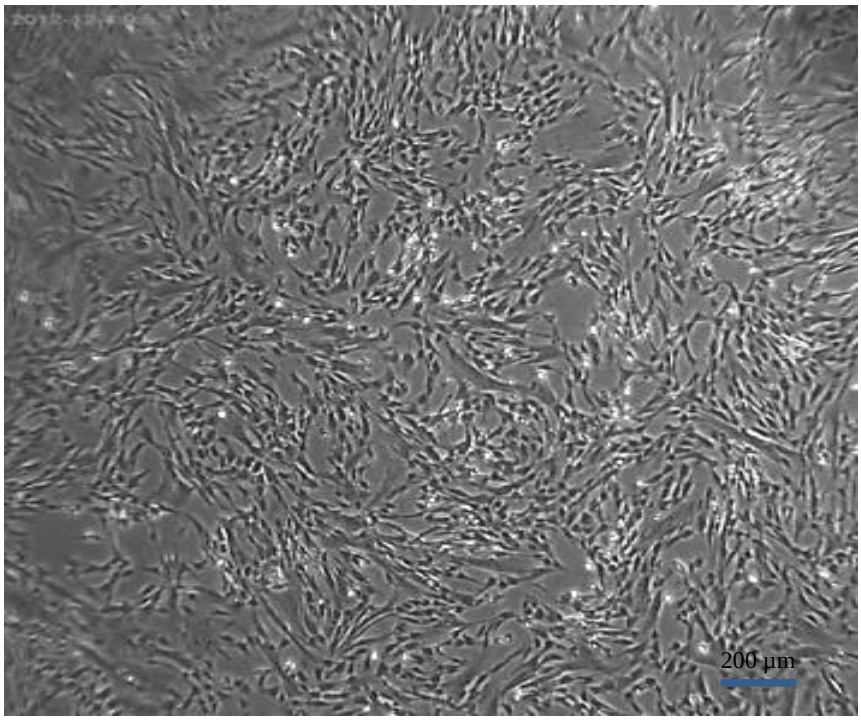


Figure 9: Micrograph (phase contrast microscopy) of sub-confluent WJ-MSC

Cells demonstrating fibroblastic-like morphology of WJ-MSCs at sub-confluence

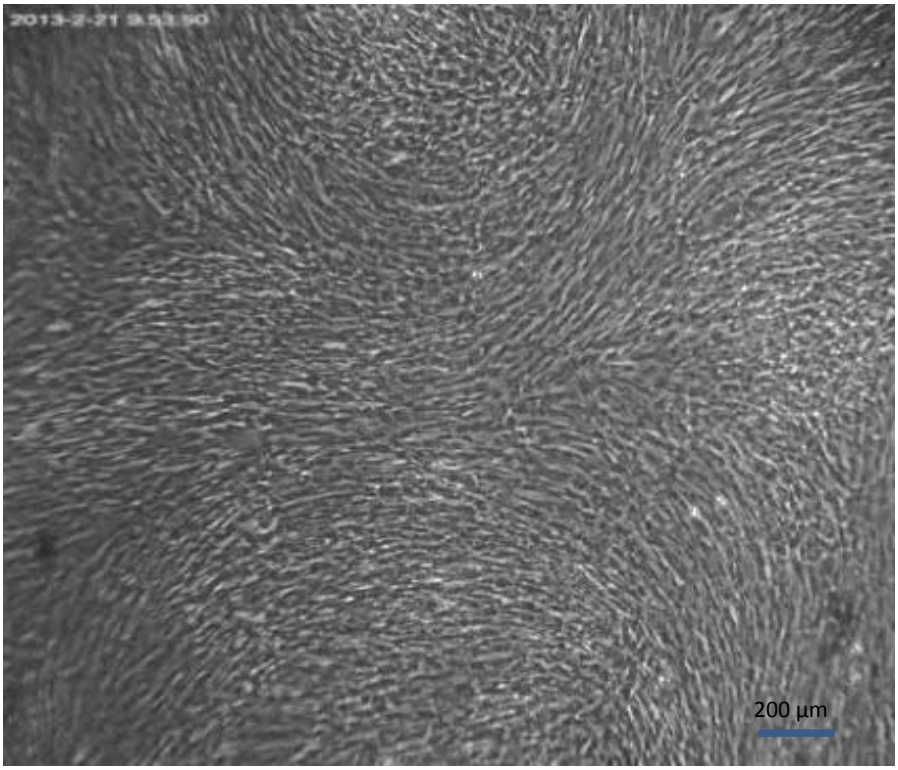


Figure 10: Micrograph (phase contrast microscopy) of confluent WJ-MSC

Cells show swirling manner of the confluent WJ-MSC cells.

2.3.2 Phenotyping of the WJ-MSC: Flow cytometry

Flow cytometry of WJ-MSC (P1, P3, P4 and P5 before and after freezing) revealed < 2% of the cells showed positivity to the haematopoietic markers CD34, CDHLA-DR, CD14, CD19 and CD45 (Fig 11) and (> 95%) from each passage were positive for the mesenchymal markers CD29, CD105, CD90, CD73, whilst 74.9%) were positive for CD44 (Fig 12). Four different isolates were tested, with 3 experimental repeats.

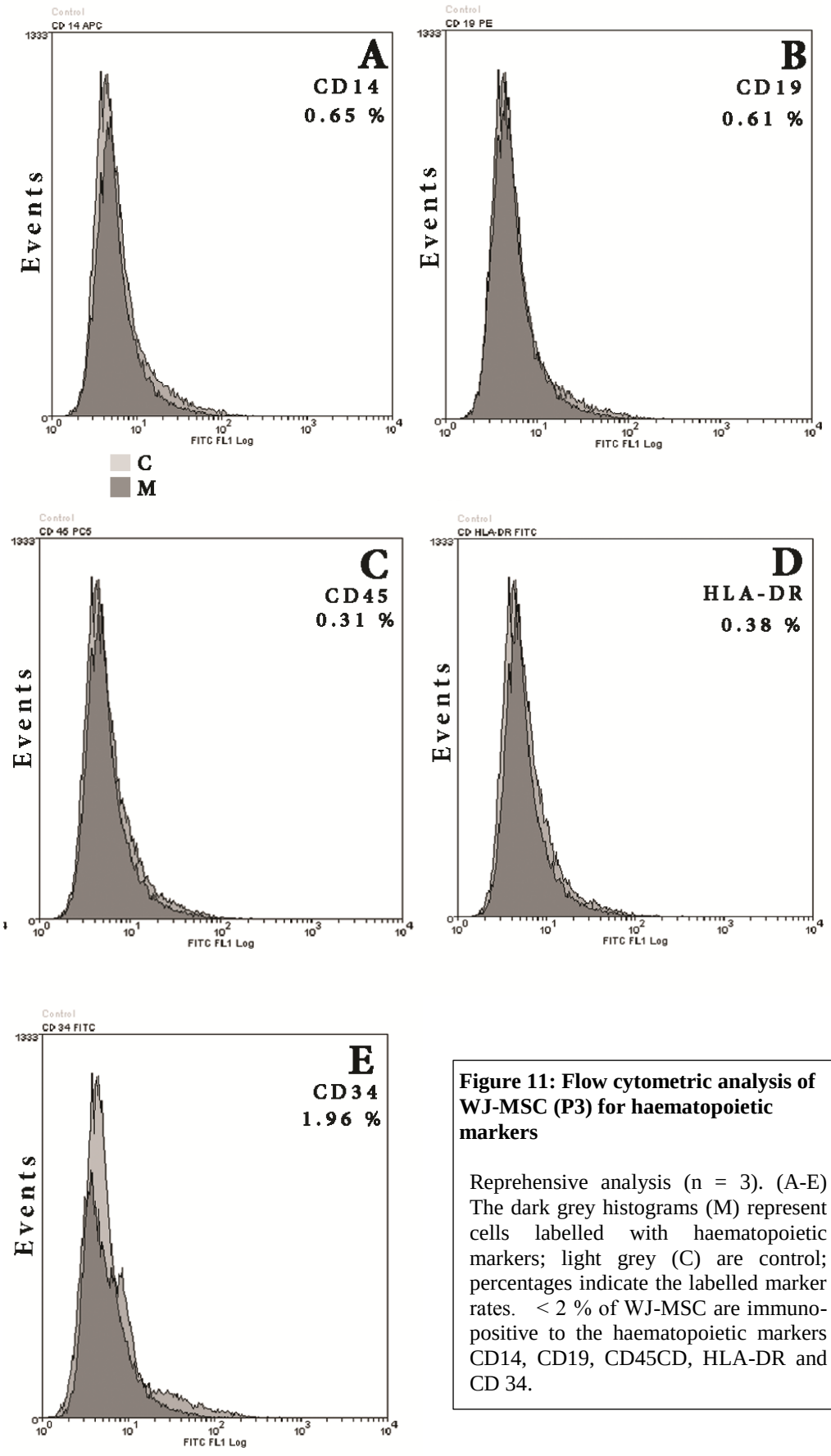


Figure 11: Flow cytometric analysis of WJ-MSC (P3) for haematopoietic markers

Reprehensive analysis (n = 3). (A-E) The dark grey histograms (M) represent cells labelled with haematopoietic markers; light grey (C) are control; percentages indicate the labelled marker rates. < 2 % of WJ-MSC are immuno-positive to the haematopoietic markers CD14, CD19, CD45CD, HLA-DR and CD 34.

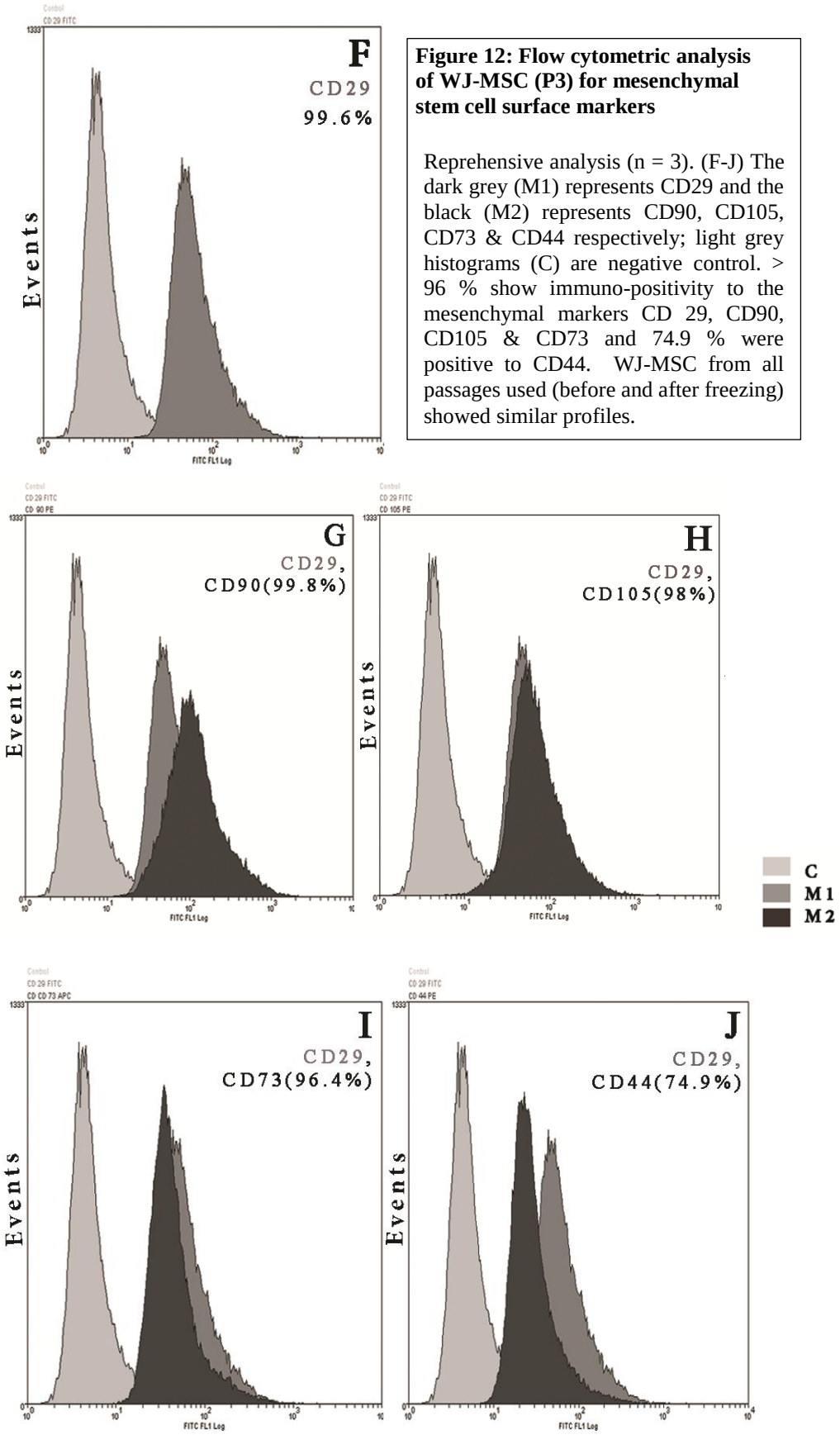


Figure 12: Flow cytometric analysis of WJ-MSC (P3) for mesenchymal stem cell surface markers

Reprehensive analysis (n = 3). (F-J) The dark grey (M1) represents CD29 and the black (M2) represents CD90, CD105, CD73 & CD44 respectively; light grey histograms (C) are negative control. > 96 % show immuno-positivity to the mesenchymal markers CD 29, CD90, CD105 & CD73 and 74.9 % were positive to CD44. WJ-MSC from all passages used (before and after freezing) showed similar profiles.

2.3.3 Adipogenic Differentiation

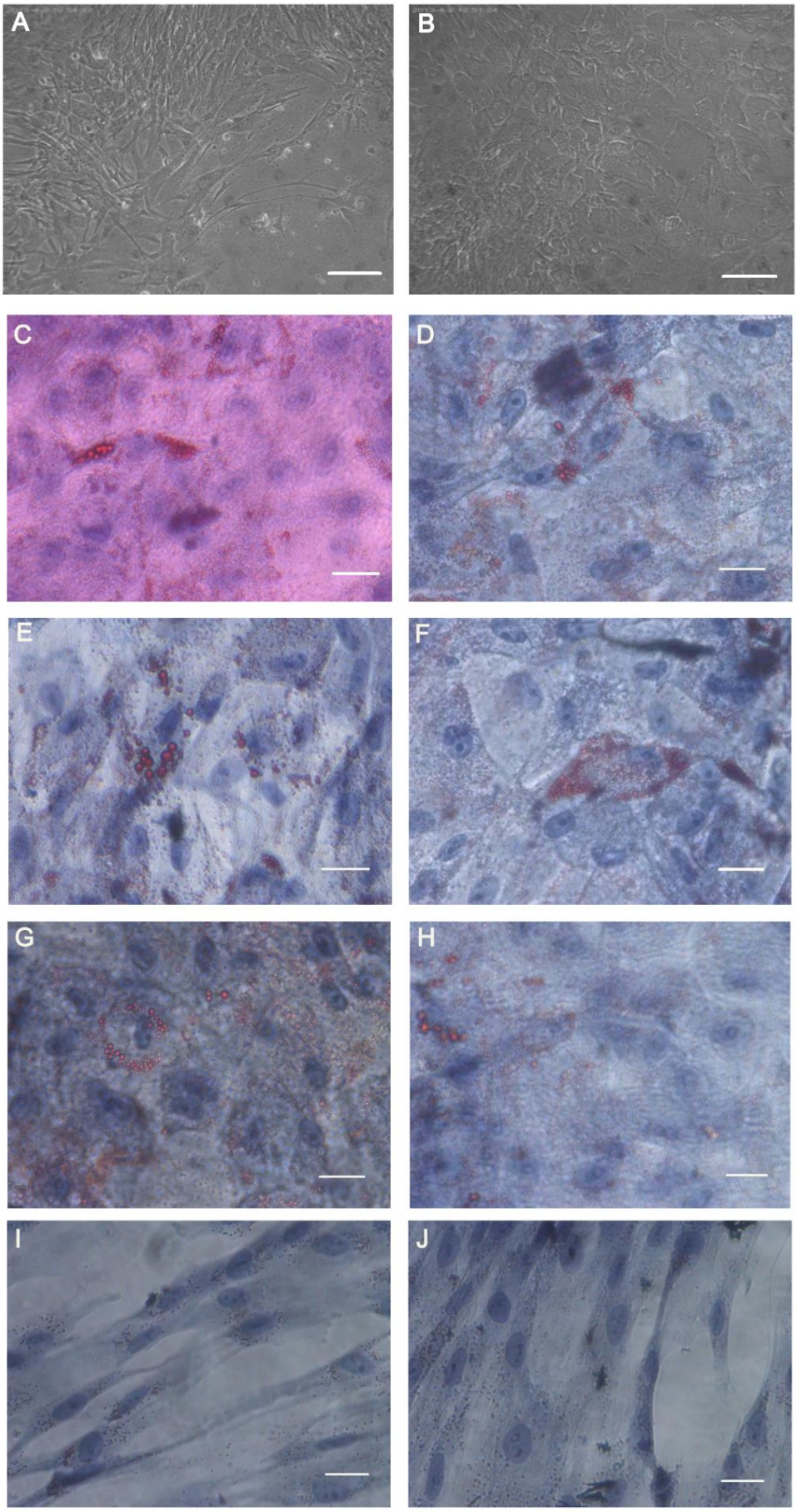
WJ-MSC cultured for 3 weeks in adipogenic medium (or in standard culture medium as control) showed altered morphology from spindle shape to a more rounded shape (Fig 13A, B). The presence of multiple Oil Red O fat droplets, resembling multivacuolar adipocytes was observed (Fig 13C-H). Control cells did not show any change in shape or staining for lipid vacuoles (Fig 13I, J). Three different isolates were tested, with 3 experimental repeats.

2.3.4 Chondrogenic Differention

WJ-MSC (P 2) differentiated into chondrogenic-like cells after 30 days in chondrogenic induction media and formed a firm pellet in comparison to the loose pellet of the control cells. Alcian Blue staining of pelleted cells confirmed chondrocyte differentiation, cells orientated within large whorls (Fig 14a) this whirling effect was not seen in control cells grown for the same period of time (b). Differentiated cells showed clear blue staining of glycosaminoglycan in the extracellular matrix (Fig 14). Three different isolates were tested, with 3 experimental repeats.

Figure 13: Micrographs demonstrating adipogenic differention

Bright field microscopy demonstrating differentiation towards the adipocyte lineage by Oil Red O staining. (A,I & J) WJ-MSC cultured for 3 weeks in stem cell media acted as a control. (B-H)WJ-MSC cultured for 3 weeks in adipogenic medium, showed variations in cellular morphology (became more rounded; B) and accumulation of lipid vacuoles (C-H) (demonstrated by Oil Red O staining) with respect to control cells (I & J) which retained the normal fibroblast-like morphology, without lipid accumulation (I & J); Scale bar A & B =200 µm, C-J =50 µm. Reprehensive sample out of 3 experimental repeats.


A
B
C
D
E
F
G
H
I
J

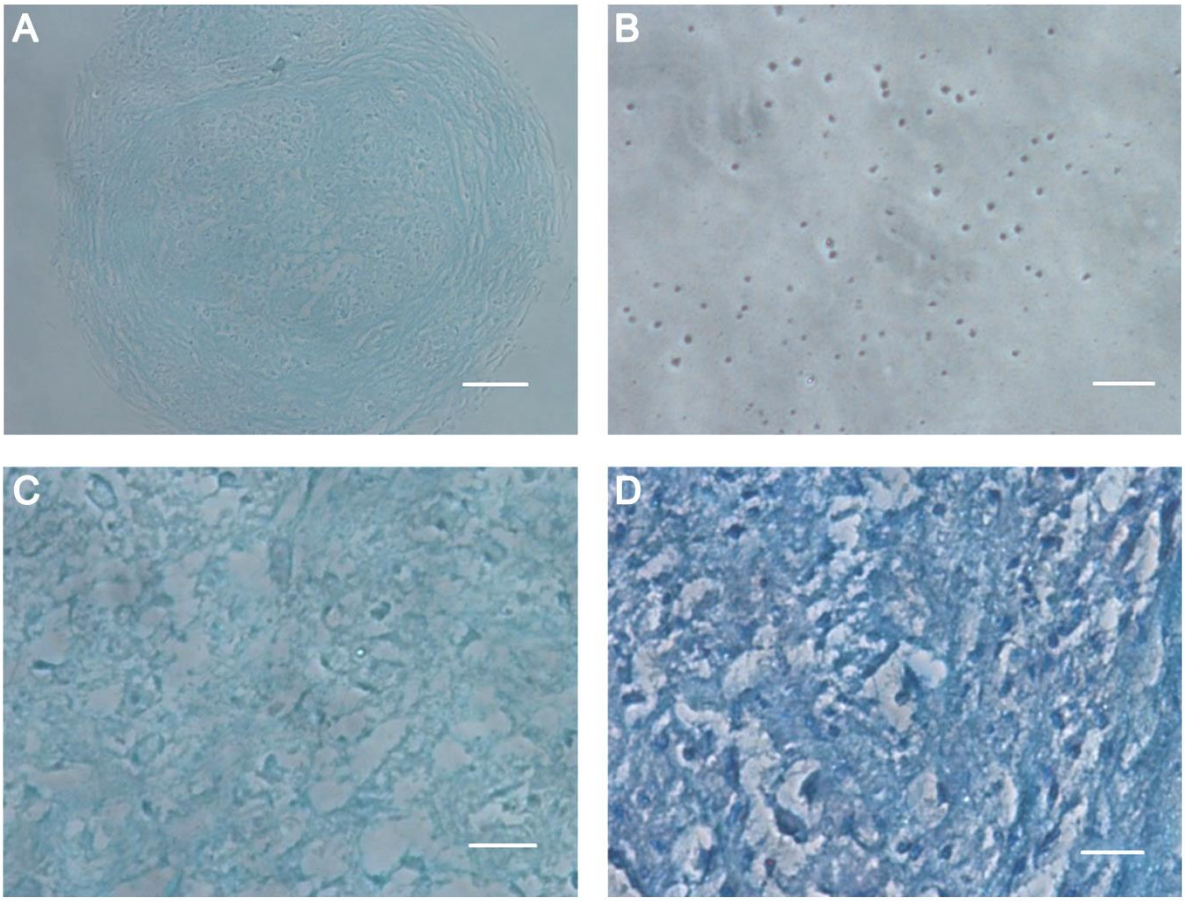


Figure 14: Micrographs demonstrating chondrogenic differention

Cells at passage 2 were cultured as pellets and induced for chondrogenic differention using specific induction media. After 30 days, paraffin sections of the pellets were stained with alcian blue and visualized under microscope. (A, C & D). (A) WJ-MSC showing concentric arrangement. (B) Control WJ-MSC without induction for chondrogenic differention remained scattered. (C) Accumulation of proteoglycans (blue) in extracellular spaces. (D) Cells counter stained with hematoxylin showing dark blue nuclei and lighter blue glycosaminoglycan. A & B; Scale bar=50 µm, C & D; Scale bar=20 µm. Reprehensive sample out of 3 experimental repeats.

2.3.5 Oestogenic Differention

Untreated cells, cultured in standard medium for 30 days, retained the normal fibroblastic morphology, and were negative for alkaline phosphatase activity. However, WJ-MSC cultured in oestogenic induced medium, showed alkaline phosphatase activity, which is an indicator of oestogenic differentiation (Fig 15). Three different isolates were tested, with 3 experimental repeats.

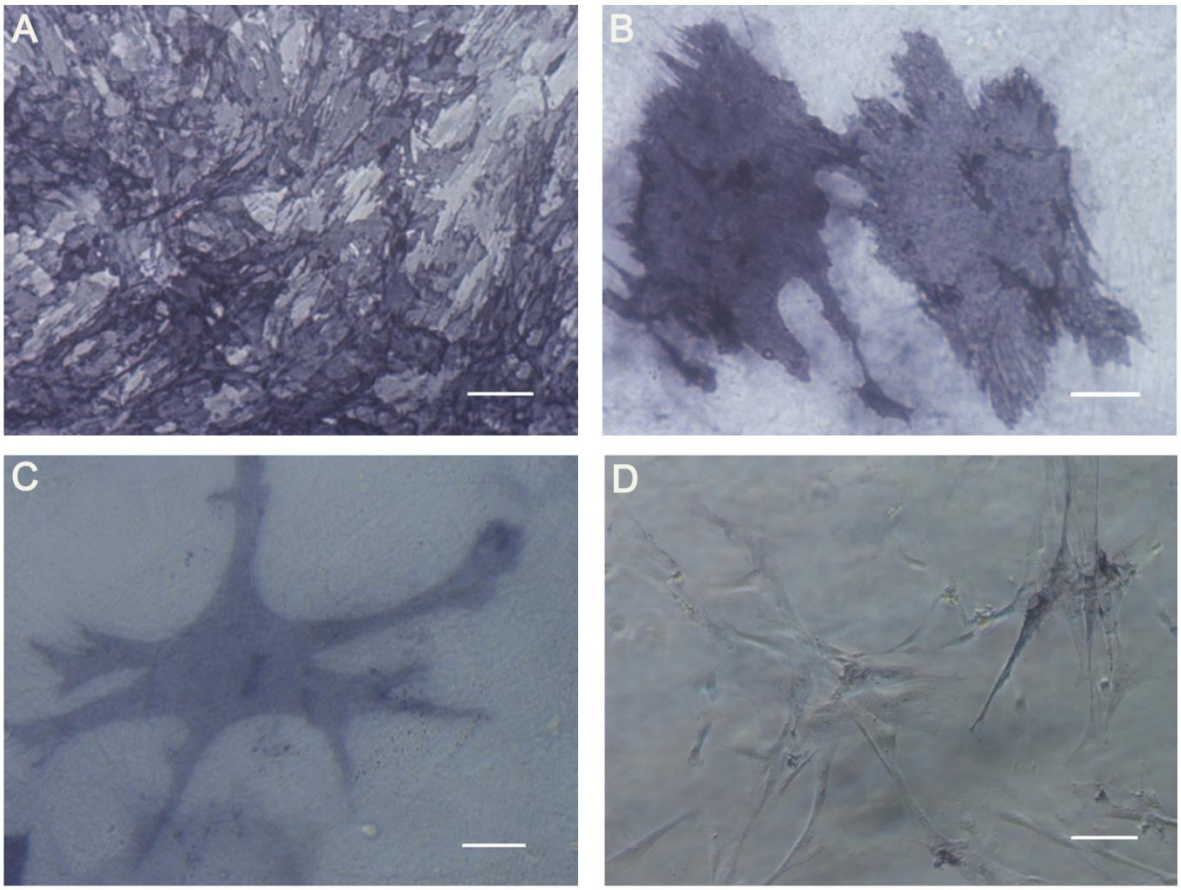


Figure 15: Micrographs demonstrating oestogenic differention

Alkaline phosphatase activity within WJ-MSC after 30 days culture in osteogenesis-inducing media was observed (A, B & C). (A) Low power micrograph showing alkaline phosphatase activity in the majority of cells. (B & C) High power micrographs showing individual cells with a diffuse dark violet colour throughout the cytoplasm; Scale bar=20 µm. (D) No alkaline phosphatase activity can be seen in cells cultured in normal media for 30 days. A & D; Scale bar=50 µm. Reprehensive sample out of 3 experimental repeats.

2.3.6 WJ-MSC Labelling

Fluorescent microscopy revealed cell membrane dye uptake of PKH26, which appeared as discrete puncta. At 1h after seeding, cells were rounded, while by 24h they changed morphology to cuboidal and spindle shaped. Some evidence of mitosis and cell aggregation were demonstrated. The labelled WJ-MSC attached, remained viable, showed unaltered morphology and uncompromised proliferation for the 10 days of observation (Fig16).

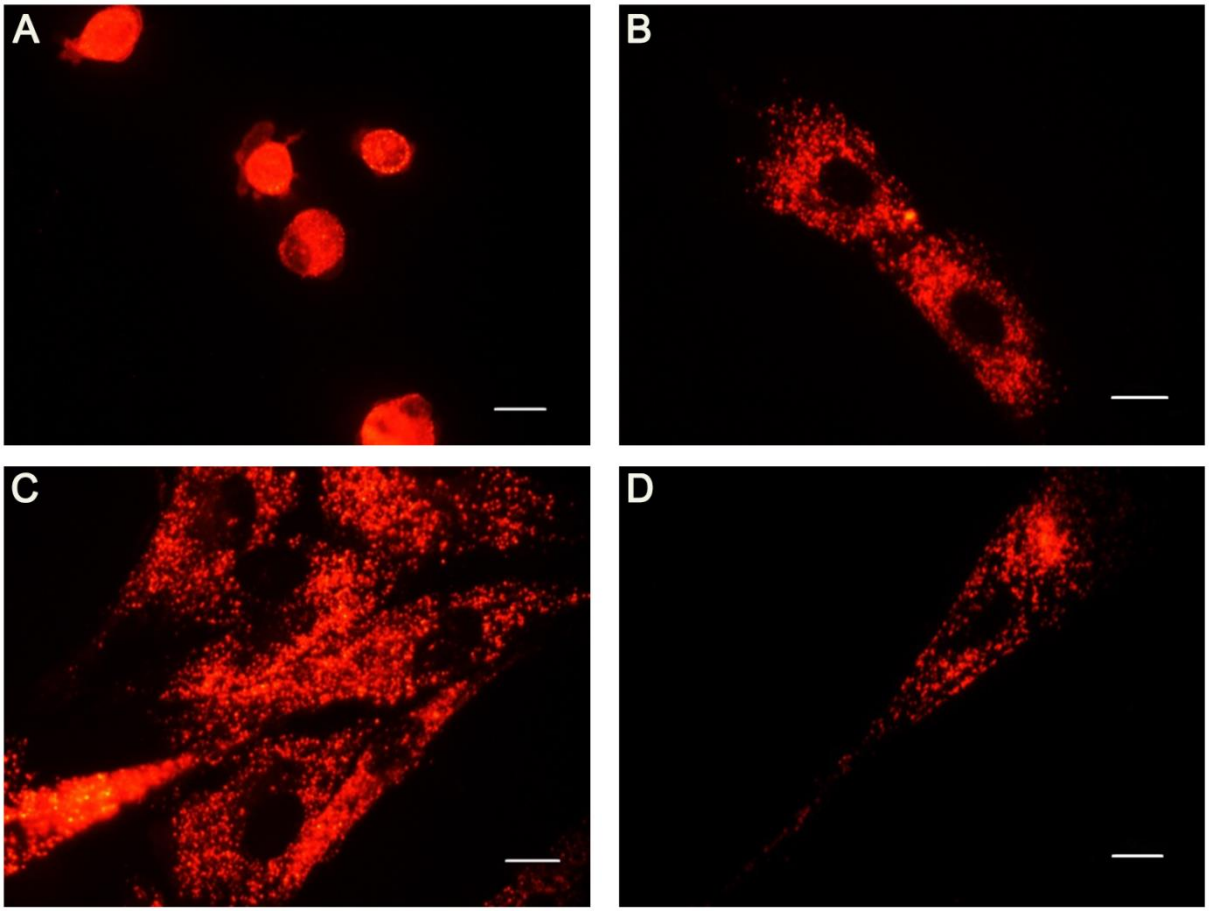


Figure 16: Micrographs demonstrating PKH26 Labelled WJ-MSC

(A). PKH26 labelled WJ-MSC at 1h demonstrating rounded shaped morphology and some pseudopodial extension. **(B).** Labelled cells after 24 hours showing dividing cell in the anaphase, demonstrating cell proliferation whilst the dye inside. **(C).** Labelled WJ-MSC after 6 days revealing the persistent presence of the cell membrane dye and cell aggregations. **(D).** Micrograph showing the normal spindle shaped of MSC after 10 days of labelling with PKH26 dye; Scale bar=20 µm.

2.3.7 Isolation and characterisation of HUVEC

HUVEC were observed with characteristic cobble stone appearance from first day after isolation (Fig 17). The cells took 5 ± 2 days to reach confluence (3 ± 1 x 10^6 cells / ml). Immunocytochemical analysis showed that the cells were positive for vWF and VE-Cadherin. The former localised as punctate distribution in cytoplasm of cells, while the latter was

present in cell-cell junction regions forming well demarked smooth border of cells (Fig 18). Three different isolates were tested, with 3 experimental repeats.

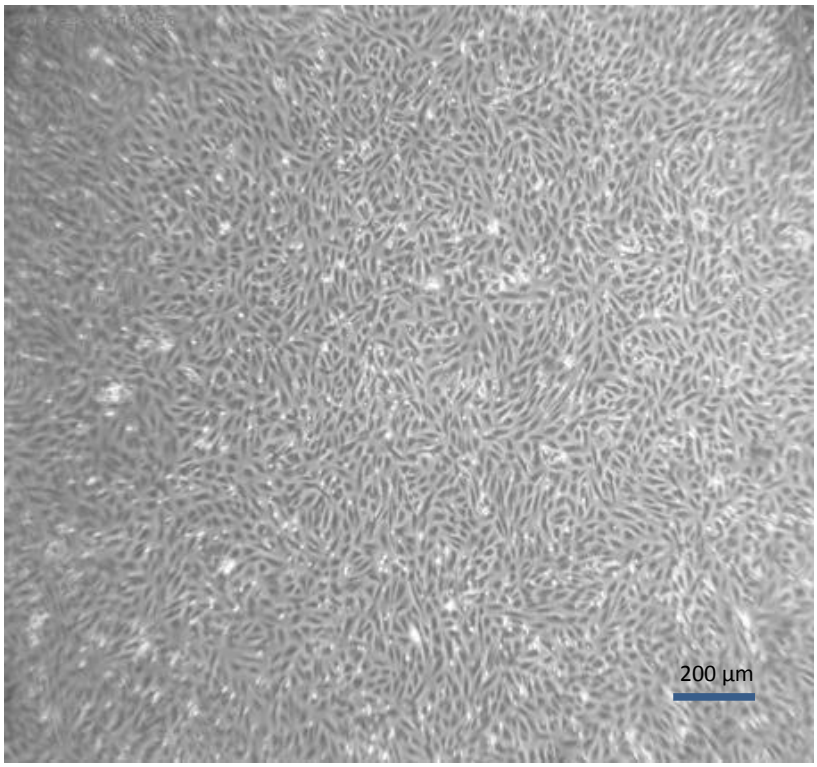


Figure 17: Micrograph (phase contrast microscopy) of HUVEC

Confluent HUVEC monolayer showed cobble stone appearance.

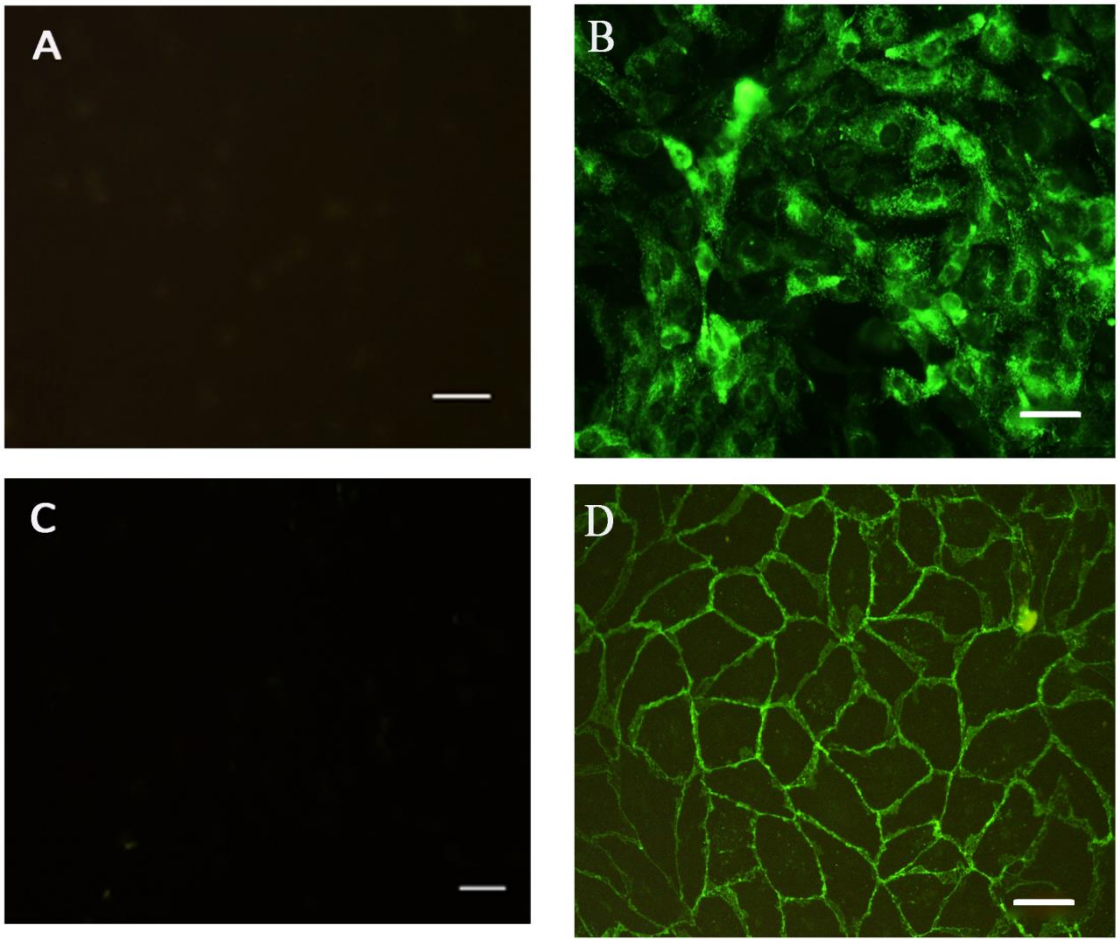


Figure 18: Micrographs showing HUVEC immunocytochemistry

(A) HUVEC without vWF primary antibody acted as control. (B). Micrograph showing cells immunopositive for vWF which appeared punctate in the cytoplasm. (C). Micrograph showing HUVEC without VE-cadherin primary antibody acted as control. (D). Micrograph showing HUVEC are immunopositive for VE-cadherin. It is localised to cell-cell boundaries and displayed a predominantly continuous staining; Scale bar=50 µm. Reprehensive sample out of 3 experimental repeats.

2.3.8 *In situ* localisation of WJ-MSC in the HU

Histological and immunohistochemistry analysis showed a clear demarcation of the vessel lumen, vessels (two arteries and one vein) in the umbilical cross section (Fig 19). Whilst the endothelial cells were positive for vWF, vascular smooth muscles cells were positive for anti-smooth muscle actin (Fig 20). A small number of cells showing immunopositivity for the mesenchymal markers CD29 and CD105 were located around the perivascular region and in

the Wharton's jelly (Fig 20). CDHLA-DR and CD45 cells were not detected in the WJ regions of the cord samples (Fig 20). Three different isolates were tested, with 3 experimental repeats.

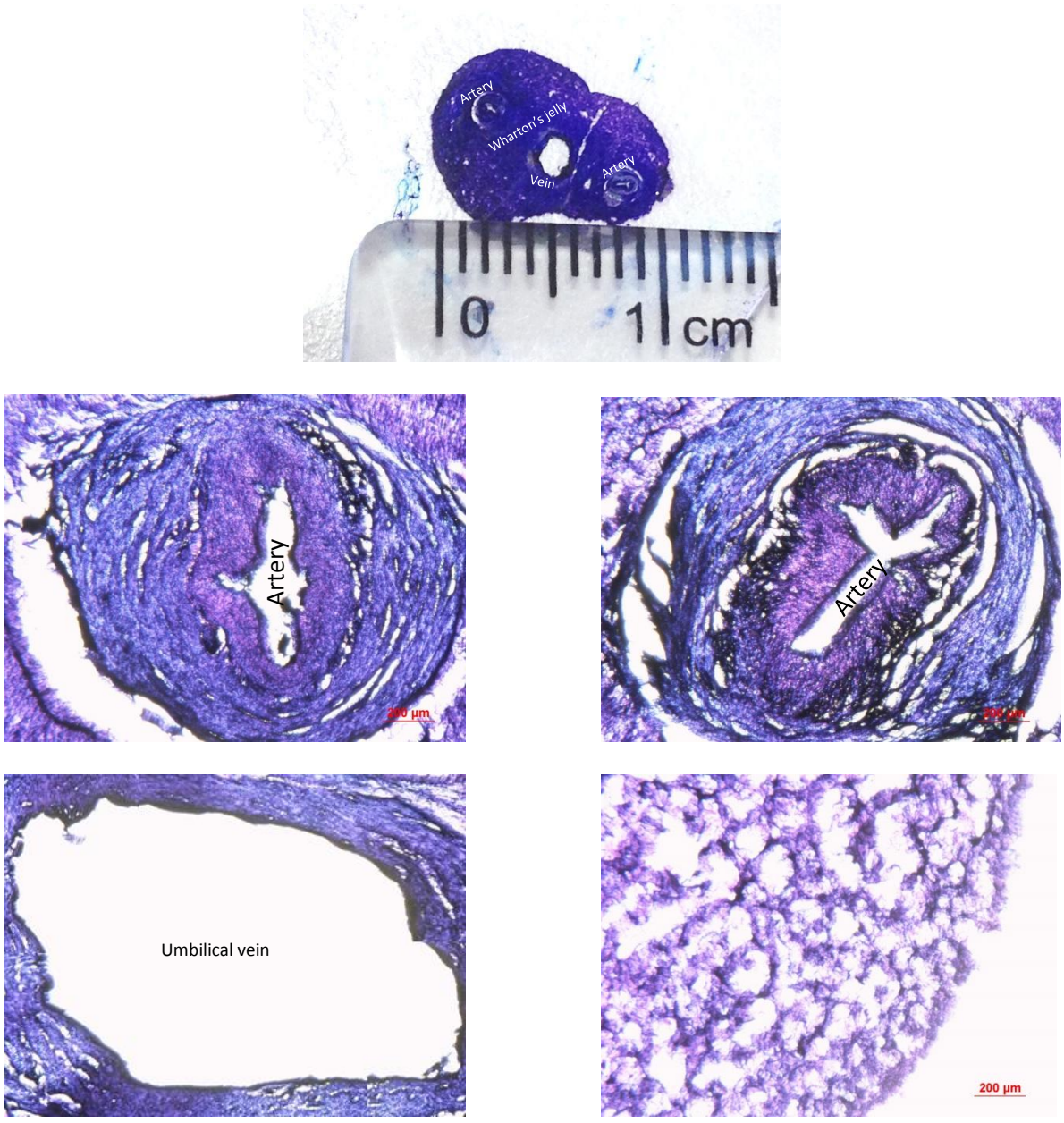


Figure 19: Micrographs showing histology of the human umbilical cord

Human cord section stained with 1 % toluidine blue stain showing two umbilical arteries (A & B) with prominent smooth muscle layer and one umbilical vein (C) with dilated lumen. (D) Shows Wharton's jelly region.

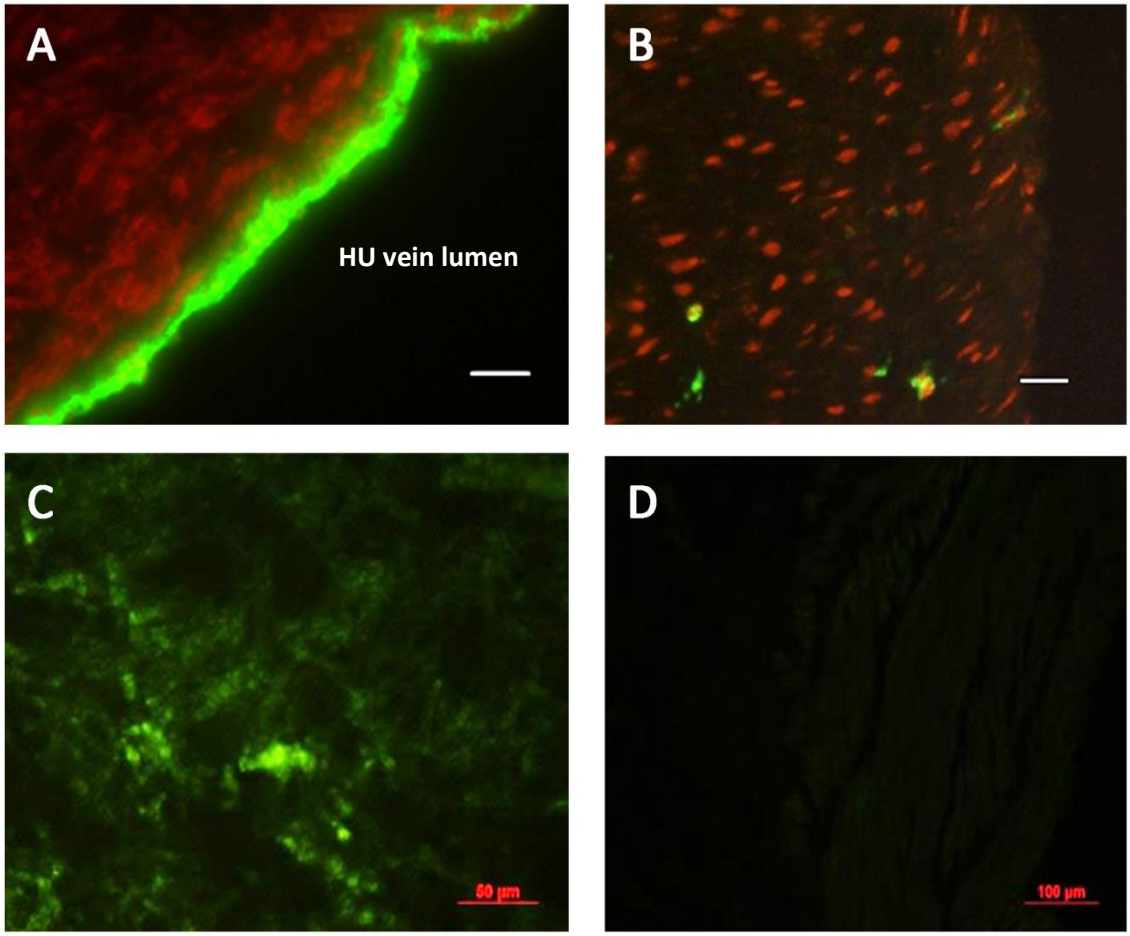


Figure 20: Micrographs demonstrating immunohistochemistry of the human umbilical cord

(A). Micrograph showing endothelial cells positive for vWF (green) and neighbouring cells positive for anti-human smooth muscle actin (red). (B-E). Sections from the umbilical cord Wharton's jelly demonstrating some cells positive for CD29-FITC (green), all nuclei showing PI (red). (C). Cells in similar locations showing positivity for CD105-FITC (green). (D). Cells in WJ showing immunonegativity to CDHLADR-FITC (green). (E). Cells are immunonegative to CD45-FITC(green); Scale bar=50 µm. Reprehensive sample out of 3 experimental repeats.

2.4. Discussion

WJ-MSC can be isolated from full term HU, using the non-enzymatic procedure, and maintained in culture reproducibly. Cells reached numbers needed for differentiation, extravasation and homing studies. Unlike previously reported methodology such as that of De Bruyn et al. (2011), in this study the time to reach confluence were halved in the 5 consecutively passages tested. Data obtained suggest that refinement of the simpler non-enzymatic methods described in this chapter through careful dissection and avoid the injury of cord vessels, may lead to increased numbers and expansion of stem cells necessary for therapeutic treatments through avoidance of contamination with endothelial cells and others.

There were no differences in numbers of cells obtained from the three parts (fetal, middle or maternal side) of the cord samples, meaning that each cord segment contained WJ-MSC which did not differ in their morphology and were equally distributed along the length of the umbilical cord.

Immunocytochemistry and flow cytometry revealed that > 95 % of the isolated WJ-MSC do exhibit MSC markers and < 2 % are positive for hematopoietic markers from passage 1. This is an improvement from previous studies where there was higher contamination with cells positive for haematopoietic markers (2.6 to 13.8%) (De Bruyn et al., 2011) in Passage 1, with subsequent reductions in later passages. In the current study the phenotype was not lost in the passages tested (up to 4) before or after freezing and thawing. Thus WJ-MSC obtained by the method detailed in this chapter are less heterogenic and would allow later passages to be used for stem cell studies.

Differentiation is another key property of stem cells; WJ-MSC can be differentiated into adipocyte like cells and showed accumulation of fat droplets with Oil Red O. In addition, WJ-MSC can also be successfully differentiated towards osteoblasts and chondrocytes phenotype by incubation in appropriate induction media. Adipocytes, osteoblasts and chondrocytes are all mesodermal cells as well as cardiomyocytes which are also obtained from WJ-MSC (Nartprayut et al., 2013, Pereira et al., 2008). Therefore, this is not surprising that these cells have the potential to be used for therapeutic applications of different diseases; for example osteo-chondral defect and inflammatory arthritis (Santos et al., 2013, Dahlin et al., 2014) and myocardial infarction (Zhang et al., 2013). Detailed studies are needed, where the fate of injected stem cells in regions such as cartilage, bone, heart and liver would reveal more clarity about how stem cells intervene therapeutically.

WJ-MSC can be trans-differentiated to other tissue type cells. WJ-MSC can be differentiated into hepatocyte like cells, promote regeneration and restore hepatic functions in rat liver fibrosis (Anzalone et al., 2010, Campard et al., 2008, Tsai et al., 2015). It could also transform into endothelial cells (Alaminos et al., 2010). It is now accepted that the differentiative capacities of such cells span all the mesoderm-derived tissues, extending to neuroectodermal (Mitchell et al., 2003, Tantrawatpan et al., 2013) as well as endodermal lineage. Thus, WJ-MSC are extremely promising for regenerative medicine applications in different pathological settings. Their use in therapeutics also hold promise; WJ-MSC homed to human breast carcinoma cells transplanted into mice lung through the lateral tail vein and attenuated the human mammary tumour size compared to control groups after intravenous injection (Ayuzawa et al., 2009). WJ-MSC induce apoptosis of prostate cancer cells and reduce its proliferation compared to controls without stem cells treatment (Han et al., 2014).

WJ-MSC obtained in this study fulfil the minimum criteria of ISCT, (explained in the Introduction), and proved that they were MSC; they have grown on the plastic surface of Petri dishes, > 95 % showed positivity to MSC markers, < 2 % showed positivity to haematopoietic markers and they could differentiated into tri-lineage cell line. Thus WJ-MSC can be considered as a promising source for stem cell therapy; the high proliferation rate observed in this chapter and other comparative studies with BM-MSC, adipose tissue and placental mesenchymal stem cells demonstrates that WJ-MSC have the highest proliferation potential (Li et al., 2014b). The shorter population doubling time than other cells (Secunda et al., 2014), and the ability to differentiate between three lineages is promising. WJ-MSC, being derived from fetal tissue are of course less immunogenic. They express MHC class I (HLA-ABC) but not class II (HLA-DR) antigens (La Rocca et al., 2009). This was tested to be true in this study. The reduced immunogenicity may allow them to escape the host immune response.

Migration of WJ-MSC from the WJ of the cord in this simple way is exciting and may be related to the media used, as DMED/low glucose is used in this study. It is a stressful environment which stem cells like and is coming out in response to this stress signals.

In situ localization of WJ-MSC in HU revealed that CD29 positive cells can be localised in the cord sections and they were few in numbers (5 - 10 cells), the small numbers seen in 5-10 µm thick sections may be a true reflection of actual numbers *in situ*, given that 50 cells only were obtained from 5 cm cord sections.

WJ-MSC can be effectively labelled with PKH26 red fluorescent cell membrane dye by direct incubation of WJ-MSC to the dye. These labelled cells remain viable for 10 days (with

the dye still visible) thus showing promise for transmigration studies. Many researchers have used this lipophilic, stable, and strong red fluorescent dye during tracing their transplanted cells (Yan et al., 2008, Yoon et al., 2005, Nakajima et al., 2012). PKH26 also showed no toxicity to adipose tissue stem cells and did not inhibit their proliferation. However, cell debris from the labelled cells could transfer to the surrounding unlabelled cells and tissues causing them to emit red fluorescent light (Li et al., 2013). This should be taken in consideration while using this dye in cell tracing.

HU is a rich source for various cell types which are extensively used in research applications. According to Hayward *et al.*, (2013) four types of cells: WJ-MSC, endothelial, epithelial and smooth muscle cells could be isolated from single solid HU tissue (Hayward et al., 2013). Apart from the WJ-MSC already discussed, HUVEC was also easily isolated from term umbilical cords and maintained in culture for up to P3 (later passages were not used as barrier integrity and cell shape can be altered (Galustian et al., 1995). The cells used in this research programme formed the classical cobblestone monolayers and showed full junctional occupancy of VE-cadherin in their bespoke culture medium. The availability of both sources of cells from the umbilical cord enabled the formulation of a successful protocol for WJ-MSC and HUVEC co-culture which will be used to study the interaction between the two cell types (Chapter Three).

Chapter 3

Temporal studies into attachment and paracellular migration of human umbilical mesenchymal stem cells across umbilical vein endothelial cell monolayers

3.1. Introduction and aims

3.1.1 Clinical applications of mesenchymal stem cells

Mesenchymal stem cells from the umbilical cord can be isolated easily after parturition. Their phenotype is similar to adult bone marrow stem cells, but being fetal they have the added advantage of advanced potency and less immunogenicity than adult stem cells (Fan et al., 2011). This makes them an attractive source for future stem cell therapy, although their fundamental biology remains to be fully elucidated.

Currently, a large number of clinical trials are underway evaluating mesenchymal stem cells for the treatment of cardiovascular, inflammatory, autoimmune diseases and cancer. Most involve systemic infusion of MSC into the circulation (Sokolova et al., 2007, Musialek et al., 2015, Ayuzawa et al., 2009) and thus cells have to extravasate to target areas. *In vitro* studies using confocal and dynamic microscopy have shown that BM-MSC transmigrate similar to leukocytes, through predominantly paracellular and also transcellular pathways in the tumour necrosis factor-α activated endothelium (Teo et al., 2012). The authors reported that the initiation of transmigration occurred by 30 min with 50% of stem cells completing transmigration after 120 min. Using a murine isolated heart perfusion system, Schmidt et al. (2006) have shown that MSC transmigrate through the paracellular junctions, with one third of the cells migrating within 30 minutes, consistent with a faster transit time *in vivo* (Schmidt et al., 2006). Whether WJ-MSC use the paracellular route and the duration of attachment and transmigration events is not known and is the central aim of the present chapter.

3.1.2 The role of Wharton's Jelly mesenchymal stem cells in gestation

Wharton's jelly of the umbilical cord is derived from the mesoderm of the primitive streak which invades the connecting stalk and primary chorionic villi early in gestation. Mesenchymal stem cells of the mesoderm differentiate into and participate in neo-vasculogenesis of both the umbilical and placental circulation. They also modify the microenvironment and trigger angiogenesis (Todeschi et al., 2015, Edwards et al., 2014, Santos Nascimento et al., 2014). The Wharton's jelly at term continues to encase the fetal umbilical vein and arteries (two) and still contain multipotent mesenchymal stem cells (Kobayashi et al., 1998). The role of these cells throughout gestation is not known although paracrine cross-talk may be important for vessel growth, maturation and function.

3.1.3 Pericyte

Pericyte is a perivascular cell interacting with the capillary endothelium, capable of tissue regeneration and controlling angiogenesis (Torsney and Xu, 2011, Gerhardt and Betsholtz, 2003). It has also a role in synthesis of matrix proteins, tissue homeostasis, and has macrophage-like properties (Diaz-Flores et al., 2009). Pericytes might be the origin of mesenchymal stem cells, as they expressed MSC markers, and MSC are also located in a perivascular niche (Wu et al., 2010, Zannettino et al., 2008, Caplan, 2008).

3.1.4 Stem cell niche

Stem cell lineage commitment is highly dependent on the stem cells microenvironment or niche which consists of signalling molecules, intercellular communication and the interaction between stem cells and their surrounding extracellular matrix. This 3-dimentional niche is thought to influence and control genes and factors that, determine the core properties of the

stem cells, such as self-renewal and differentiation to committed cells (Watt and Hogan, 2000, Spradling et al., 2001).

3.1.5 Using human umbilical veins endothelial cells as a vascular model

HUVEC are a useful and a favoured *in vitro* model for endothelial barrier studies and are easily isolated from the umbilical cord (Leach et al., 2012, Onat et al., 2011, Kazakoff et al., 1995). The close proximity between the WJ-MSC and the umbilical vein endothelial cells *in situ* and their developmental origins makes the use of HUVEC doubly pertinent for this study.

3.1.6 Aims of the present chapter

Using time lapse fluorescence microscopy and confocal scanning microscopy, the cellular mechanisms used in attachment and transmigration of WJ-MSC across HUVEC monolayers, the time taken and the associated dynamics of the junctional VE-cadherin was therefore investigated. Data obtained may also reveal the importance of paracrine cross talk between umbilical stem cells and blood vessels for continued maintenance of endothelial integrity during gestation.

3.2. Materials and Methods

Materials

Chemical and reagents

DPBS; calcium and magnesium free, HBSS, Pencillin – Streptomycin (10,000 u/ml pencillin, 10 mg/ml streptomycin in 0.9 % Nacl), trypsin – EDTA solution 1x (0.5 g porcine trypsin and 0.2 g EDTA in 4 Nacl HBSS), FBS, BSA, PKH26 red fluorescent stain, heparin sodium salt (Grade 1-A), ECGS (30 mg/mL) and gelatin from bovine skin (type B) [Sigma-

Aldrich, UK]. Antibiotic/antimycotic solution (10,000 u/mL pencillin G, 10,000 µg/mL streptomycin, 25 µg/mL amphotericin B), stem cells media: DMEM/Low Glucose + 4.00 mM L- glutamine + 1000 mg/mL glucose + 110 mg/mL sodium pyruvate [Hyclone, UK]. Endothelial medium: Medium 199 (1x) + Earle's balanced salts + L. glutamine + 25 mM HEPES + L- amino acids (Gibco, UK). Lysis buffer (PH 7.6): 20 mM Tris (Invitrogen) + 320 mM sucrose (BDH) + 0.1% Triton X 100 + 1 mM NaF + 10 mM β glycerophoshate + 1 mM EGTA (Sigma) dissolved in 500 ml distilled water and one protease inhibitor tablet (Sigma) in 10 ml lysis buffer before use. Tris buffer saline with tween 20 (TBST): 25 mM Tris + 125 mM Nacl + 10 ml tween 20 (final concentration of 0.1 %) dissolved in one litre D H2O. Solubilisation buffer (containing 2.5 ml of 0.5 M Tris, 2 ml glycerol, 2 ml 10 % sodium dodecyl sulphate (SDS) 2.5 ml dH_2O, 1 ml β mercaptoethanol and 40 µl of 2.5 % bromophenol blue). Transfer buffer containing 30.3 g Tris, 144 g glycine dissolved in 8 litre dH_2O & 2 litre methanol and kept in cold room. Running buffer is 10 times diluted electrophoresis buffer in MQ H_2O. Electrophoresis buffer containing 30.3 g Tris, 144 g glycine and 10 g SDS dissolved in one litre dH_2O. Lowry solution containing 2 g NaoH, 1 g SDS, 10 g $Naco_3$ dissolved in 500ml dH_2O, then mixed with 1 % $CuSo_4$ and 2 % Nak. Precision plus Protein all blue standards [5~1] (Bio-Rad Laboratories Ltd, UK). Mini protein TGX precast gel (4-20 % gradient) 12 well combs (Bio rad laboratories, Inc). Vectashield mounting medium for fluorescence without propidium iodide (Vector laboratories, Inc Burlingame).

Tissue Culture Plastics and Accessories

Tissue culture flasks 75 cm^2; 12 well plates; Cover slips 19 mm (Life Technologies). Tc 10 counting slides (Bio-Rad, UK). Glass-bottomed tissue culture dishes (Ibidi GmBH, Germany).

Antibodies for Immunocytochemistry and western blotting

Mouse antihuman CD144 and rabbit anti-human VWF (Dako, UK); Rabbit VE-cadherin mAb (Cell Signaling, UK), GAPDH mouse mAb and Anti-mouse IgG- FITC (Sigma-Aldrich, UK), Secondary antibodies conjugated to FITC & TRITC (Santa Cruz Biotechnology, UK) for Western Blotting.

Methods

3.2.1 Effect of mixed media on WJ-MSC and HUVEC

Prior to co-culture study, the ability of HUVECs to attach and grow to confluence in mixed endothelial and stem cell growth media (50% endothelial medium + 50 % stem cell medium) was ascertained by microscopical observations. Changes, if any, of the endothelial markers VE-cadherin and vWF in HUVEC were investigated by immunocytochemistry. WJ-MSC at passage 3, 4 and 5 were labelled with PKH26 fluorescent dye. Similarly, the ability of labelled WJ-MSC to attach, grow and proliferate on 1% gelatin in mixed media was also investigated. WJ-MSC were cultured at an initial cell density of 64 cells/ mm^2 for 22h. The attached cells were photographed and 10 unbiased images were taken for the 2, 16 and 22h groups (3 experimental repeats) using phase contrast microscopy. Every second image was selected from each group and the number of cells counted. The mean number of cells/mm^2 was calculated. The labelled WJ-MSC were also subjected to immunocytochemistry to localise any VE-cadherin expression in mixed media.

3.2.2 Co-culture studies

To obtain co-cultures of HUVEC in contact with WJ-MSC, 100,000 HUVEC were seeded on a 1 % gelatin-coated coverslip (19mm diameter) and incubated in endothelial media (Three different isolates were tested, with 3 experimental repeats). Once 70 ٪ confluence was

reached the media were changed to mixed media. On full confluence (18 -24h later) 20,000 labelled WJ-MSC were seeded on top of the confluent HUVEC monolayer (1: 5 ratio) per coverslip in 1 mL of the mixed media (Pati et al., 2011). HUVEC monolayers without added WJ-MSC in mixed media were used as a control. WJ-MSC - HUVEC interaction was observed at different time intervals (2, 4, 6, 22 and 26 hours) by an inverted phase microscope and photographed.

3.2.2.1 Real Time Observations

Co-cultures of WJ-MSC on HUVEC on glass-bottomed tissue culture dishes (Ibidi GmBH, Germany) were observed with DMIRE2 time-lapse fluorescent microscope with a built-in environmental chamber and a colour CCD camera (Leica DC300FX) and also with a wide field fluorescence microscope (Deltavision Elite; Applied Precision, UK). Cells were observed for 40 hours. All data analysis were carried out using Volocity software (Perkin Elmer, UK).

3.2.2.2 Immunohistochemistry of VE cadherin and Systematic Random sampling

To localise VE-cadherin in HUVEC and monitor the effects of labelled WJ-MSC on VE-cadherin, co-cultured cells were fixed with 1% paraformaldehyde, pH 7.3 at different time intervals (0.5, 1, 1.5, 2, 4, 6, 12, 14, 16, 22 and 26 hours). They were permeabilized for 10 min with 0.15% Triton X-100, blocked in 5% goat's serum in PBS for 30 minutes and incubated overnight at 4 ˚C with mouse antihuman CD144 (VE-cadherin; 5 µg/ml).

Cells were washed with 0.1% PBS/BSA and incubated with FITC conjugated goat anti-mouse IgG for two hours in the dark at RT. The coverslips were mounted using Vectorshield. They were analysed using a Nikon fluorescence microscope with appropriate filters to allow

visualisation of both FITC and PKH26. Localisation and continuous/discontinuous staining pattern of endothelial cell-cell junctions and position of labelled WJ-MSC was photographed with CCD camera (Nikon DS) for the chosen intervals of co-culture and stored (NIS elements F3.0; Nikon). HUVEC alone and labelled WJ-MSC alone for similar durations of culture in mixed media were also subjected to VE-cadherin immunocytochemistry in order to obtain appropriate controls.

3.2.2.3 Junctional counts

Stored Images (duration of co-culture was blinded) were used to count the % of paracellular clefts showing continuous or discontinuous (disrupted) VE-cadherin staining in control and treated HUVEC monolayers. To ensure that all cell-cell junctional regions had an equal chance of being counted, a grid was placed on images and paracellular clefts from every other square were counted and categorised according to staining pattern.

The position and number of the labelled WJ-MSC, apical or sub-endothelial and their proximity to discontinuous junctions were recorded for the co-cultures. The counting method has been used before by many researchers (Budworth et al., 1999, Sharma et al., 2013, Gundersen and Jensen, 1987, Leach et al., 2004).

3.2.2.4 Statistical Analysis

Data were analysed using Two-way ANOVA (Prism 6 software) with Bonferroni's multiple comparison test to compare control versus stem cell treated group at 2, 16 and 22h. Tukey's multiple comparison test was used to compare controls alone and co-cultures alone at the same time intervals. Statistical significance was taken at $p<0.05$.

3.2.2.5 Confocal imaging

Immunocytochemically labelled co-cultures at 2 and 22 hours were further analysed with confocal scanning microscopy (Zeiss Axiovision; Zeiss, Germany) and Zen 2009 software for multi-channel acquisition & image processing. The pinhole diameter used in all confocal imaging was 1 airy unit (AU). Optical slices (0.5 - 0.6 µm intervals) were taken and Z-tilts were obtained to visualise transmigration pathways.

3.2.2.6 Western Blotting

Cell culture and total protein extraction

Confluent HUVEC monolayers were co-cultured with or without WJ-MSC. About 100,000 HUVEC/well were seeded on 1 % gelatin-coated 12 well plates in endothelial growth media (three consecutive experiments). They were allowed to attach and after 18 hours the media was changed to mixed media (0.5 ml WJ-MSC media + 0.5 ml HUVEC media per well).

Once the cells reached confluence, WJ-MSC were seeded on top of the confluent HUVEC monolayer at 20,000 cells (1: 5 ratio) per well in 1 mL of the mixed medium, HUVEC alone in mixed media acted as controls. The cells were cultured up to 22 hours to monitor the effects of WJ-MSC on the HUVEC VE-cadherin protein expression. The early hours of interaction (0, 2 h) and late (22h) were chosen to measure protein levels. WJ-MSC alone was grown in mixed media on gelatin and cells at 0, 2 and 22h were used for immunoblotting to investigate any VE-cadherin expression in mixed media.

To prepare tissue lysate, the media were aspirated and the cells were washed with ice-cold DPBS. The cells were then harvested by scraping and lysed in a 200 µl lysis buffer. After

addition of protease inhibitor, samples were stored at – 80 ˚C in order to avoid protein degradation by endogenous proteases.

Assessment of protein's amount in samples (Lowry test)

A standard curve was prepared using 1mg/ml BSA in dH_2O. 50 µl of tissue lysate were used after defrosting and diluting in dH2O (1:10 dilution). 1ml Lowry solution was added to all samples and standards. After 10 min incubation with Lowry solutions, 100µl of Folin reagent in dH_2O 1:1 was added. 200µl of each sample and BSA standards were pipetted in triplicate in 96 well plates and incubated for 60 min at RT. The plate was read on the revelation programme at 750 nm (it gives the mean values in µg/µl).

Gel electrophoresis

The samples were centrifuged at 6000 rpm/ 5 minutes at 4 ˚C and the remaining 150 µl of cell lysate protein was resolved in 30 µl solubilisation buffer and was heated for 5 minutes 95˚C using a Grant Instruments hot plate for protein denaturation. The samples were then centrifuged at 13,000 rpm force for 1 min. Polyacrylamide gel electrophoresis (PAGE) was prepared according to the manufacturer's instruction for use with a Bio-Rad Mini Protean III apparatus for immunoblotting.

Precision plus Protein all blue standards was used as molecular weight marker. Electrophoresis tanks and modules were cleaned with IMS followed by dH2O. De-natured proteins were separated in a 4-20% gradient polyacrylamide gel after equal loading (15 µl) onto the gel while submerged in running electrophoresis buffer. 1µl of marker was loaded into the first well of the gel and the gel was run for approximately 45 min at 175 V.

Transferring the gel

A tray was cleaned with 70 % ethanol, then with dH_2O and put on ice. The gel was transferred onto a piece of nitrocellulose paper, two pieces of filter papers; two sponges and a cassette were soaked in transfer buffer. After the gel finished running, the gel electrophoresis unit was removed and transfer buffer poured off. The nitrocellulose membrane was placed onto the gel and bubbles removed carefully using a roller. Filter papers and sponges were placed with gently rolling to remove bubbles. The cassette was closed and placed into the transfer module. Then, an ice pack was added and the tank filled with transfer buffer, while making sure that the cassette was completely immersed. The top was fitted and transferring conducted using a Bio-Rad Kit at 100 V constant for 60 min on ice.

Checking protein transfer

The cassette was removed from the tank and the nitrocellulose membrane was placed into a clean glass tray. A few drops of Ponceau S solution was added onto the nitrocellulose, allowing protein bands to appear. Ponceau S solution was later washed with dH2O and TBST buffer.

Blocking

To block nonspecific binding, the nitrocellulose membrane was placed in a clean glass tray and treated with blocking buffer (5% skimmed milk powder in 0.1% TBST) for 60 min at RT with gentle shaking. The blots were later washed twice with TBST buffer.

Primary and secondary antibody

The primary antibody; VE-cadherin and GAPDH were diluted in 6 ml of blocking buffer (1:1000 dilution) and GAPDH (1:3000). The nitrocellulose membrane was incubated with

primary antibodies in a cold room overnight. The membrane was transferred to a glass pot and washed with 20 ml TBST three times every five minutes, ten minutes and 15 minutes. It was then incubated with labelled secondary antibodies (goat anti-rabbit FITC & rabbit anti-mouse TRITC diluted in blocking buffer at a 1:2000 dilution) for 60 min at 37^{o}c. Finally, the blot was washed with TBST buffer as previously and once with dH_2O.

Scanning and data analysis

A Li-cor Odyssey scanner was used, the scanner glass was cleaned with dH_2O. The nitrocellulose blot was placed gently upside down on the scanner, ensuring the blot was moist and bubbles were eliminated. Scanner Odyssey software was opened and the following parameters employed: Resolution for scanning = 169 μm; offset = 0.0; 700-red image 3.0; 800-green image 3.0. Odyssey software (Image Studio Version 3.1.4) was used to measure optical densities (OD). VE-cadherin protein expression (normalized using GAPDH as loading control) for the different durations and study groups were obtained. Data were analysed using Two-way ANOVA and Sidak's multiple comparison test. Statistical significance was taken at $p < 0.05$.

3.3. Results

3.3.1 Effect of Mixed media on WJ-MSC and HUVEC

PKH26 labelled WJ-MSC displayed no alteration in morphology and retained the dye over an observed 10 days. They attached to 1 % gelatin coated coverslips and grew to 70% confluence by 22h in mixed stem cell/endothelial media. The cells displayed proliferation: at 2h, counts revealed a mean cell density of 82 ± 10 cells/mm^2 which increased to 320 ± 45 cells/mm^2 at 16h, whilst at 22h there were on average 487 ± 40 cells per mm^2 (Fig 21 D-F).

The cells displayed the transition of cell shape - from rounded to intermediate to elongated spindle shaped with time over the observation period (Fig 21 D-I). They displayed negative immunoreactivity to anti-VE-cadherin antibodies (Fig 21 G-I). HUVEC also continued to show the typical cobble stone appearance and positivity to the endothelial marker before and after addition of the mixed media for the durations tested (Fig 21 A-C). Continuous VE-cadherin staining was seen in 88 $\pm$ 1.6 (S.D.) % of cell-cell junctions when the cells reached full confluence in mixed media.

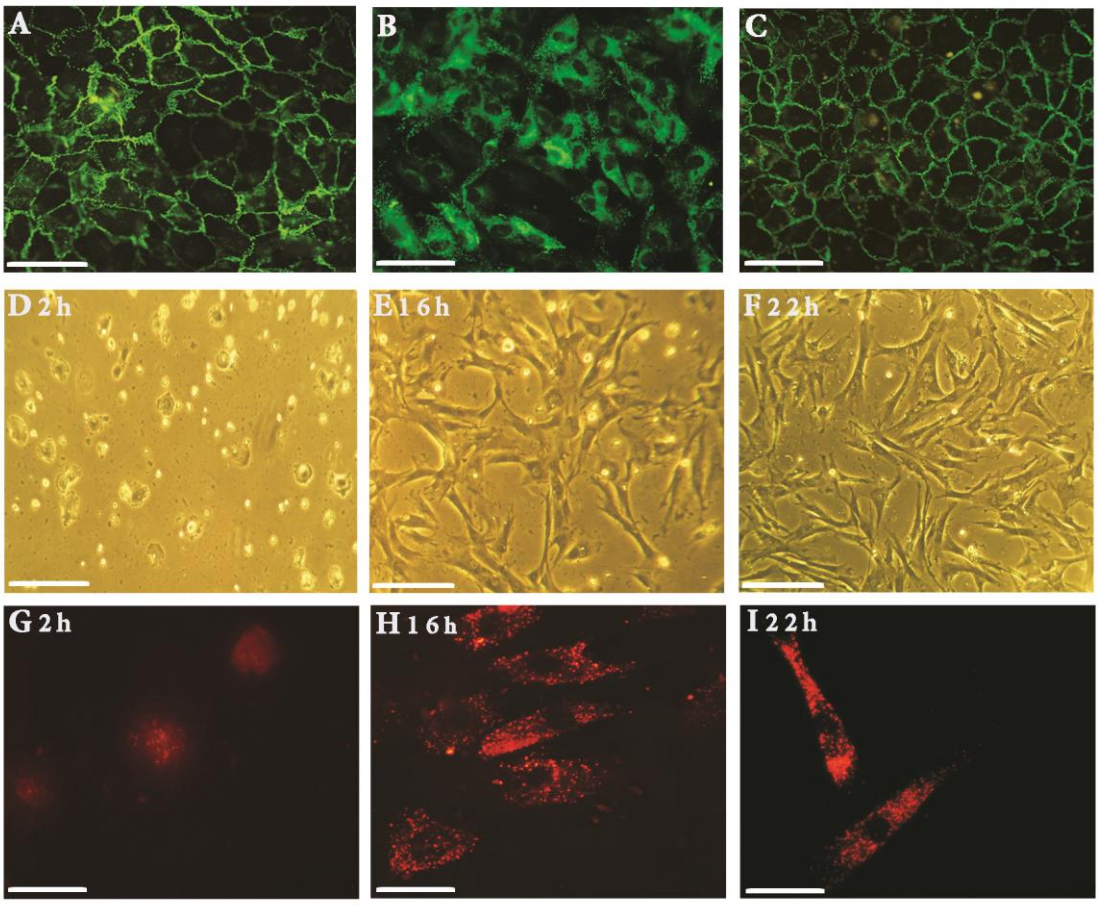


Figure 21: Micrographs demonstrating HUVEC & WJ-MSC in mixed media

(A- C). Immunofluorescence analyses of HUVEC grown in endothelial medium (A,B) versus mixed media (A-C). VE-Cadherin is localised to cell-cell boundaries and display a predominantly continuous staining whilst punctate vWF is found in the cytoplasm. A similar continuous pattern of VE-Cadherin can be seen in mixed media; Bar = 40 µm. (Fig 2 D - I). Images of PKH26 labelled WJ-MSC in mixed media on 1 % gelatin coated coverslips at 2, 16 & 22h. Phase contrast images (D, E, F) show attachment, change in morphology towards the elongated spindle-shape and increasing confluence with time, Bar = 200 µm. Fluorescence micrographs (G-I) of labelled WJ-MSC (red) immuno-stained for VE-cadherin (green). Cells are immuno-negative at each duration; Bar = 40 µm. Reprehensive sample out of 3 experimental repeats.

3.3.2 Co-culture studies

3.3.2.1 Early co-culture interactions

With phase contrast microscopy, WJ-MSC were seen to attach to the HUVEC monolayer within 30 min and appeared to display morphological changes; from rounded to transitional to spindle shaped. The position of these cells in relation to the endothelial layer was difficult to determine (Fig 22).

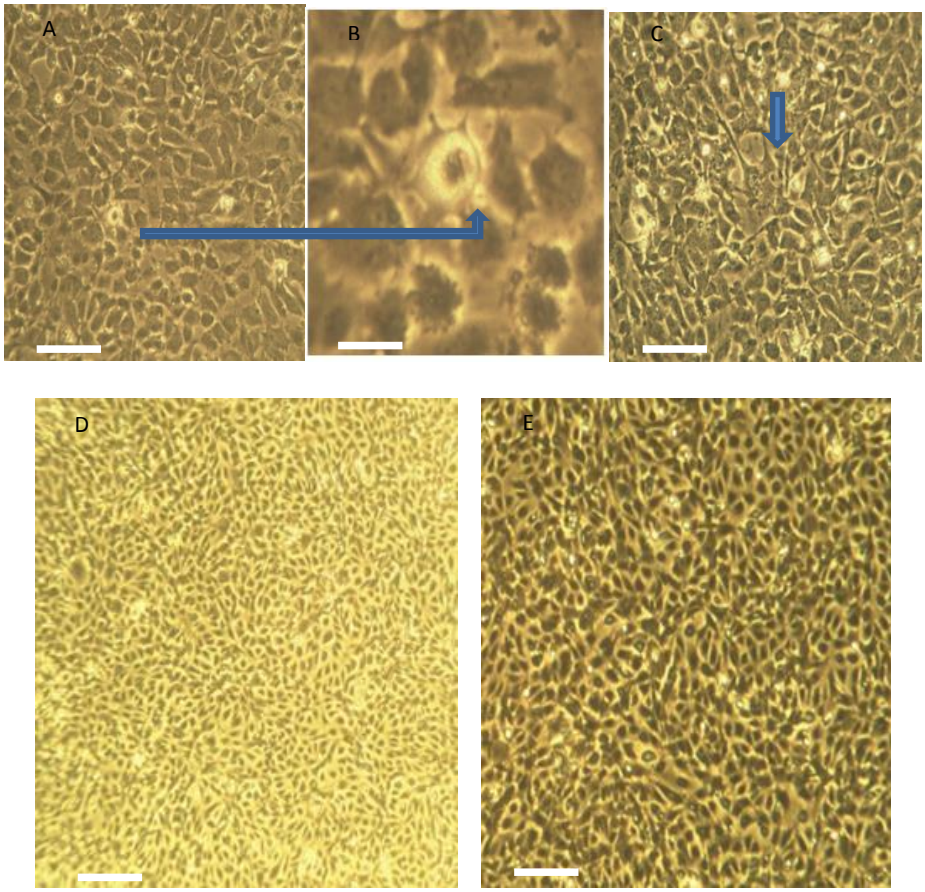


Figure 22: HUVEC-WJ-MSC co-culture phase contrast images

(A). Micrographs from inverted phase contrast microscopy demonstrating attached WJ-MSC on a confluent monolayer of HUVECs after 4h of co-culture. (B). is a higher magnification of A (x2.5) showing one rounded WJ-MSC with multiple cellular processes on its surface (arrow). C is demonstrating two spindle shaped WJ-MSC after 6h co-culture (arrow head). D and E are showing a confluent HUVEC monolayer after 22 and 26h respectively of co-culture with WJ-MSC, Bar = 200 µm. Reprehensive sample out of 3 experimental repeats.

Real time imaging (every 15 min) with a time lapse fluorescence microscope showed that soon after addition of PKH26-labelled WJ-MSC on HUVEC monolayers they displayed membrane blebbing (Fig 23A,B) and shedding of PKH26 filled exosomes (Fig 23C). The blebbing behaviour was followed by pseudopodial extensions and amoeboid movement (Fig 24 and 25) over HUVEC. Cells were then observed to round up and change shape towards the spindle-shaped morphology before migrating paracellularly in an individual migration with no detection of grouped migration (Fig 24 and 25). PKH26 filled exosomes were shed throughout this period.

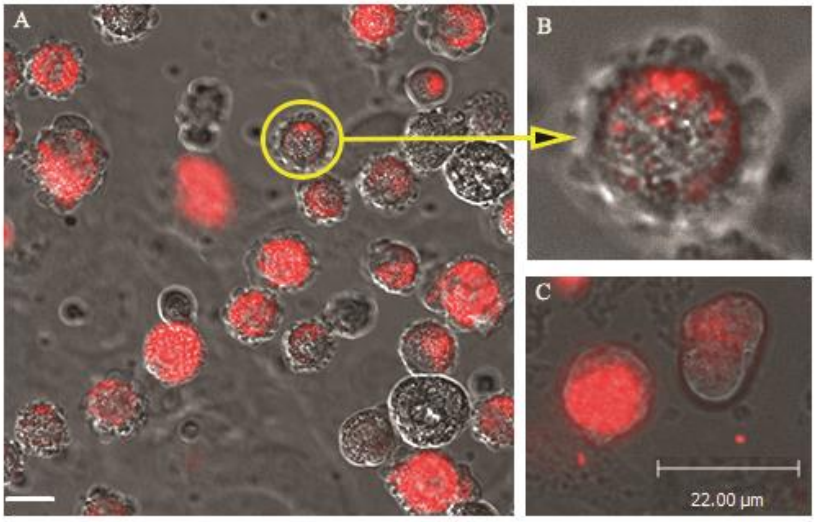


Figure 23: Micrographs from time lapse microscopy of HUVEC-WJ-MSC co-culture

(A, B) Micrographs from time lapse photography (0 - 2h) showing blebbing phenomenon of all PKH26- labelled WJ-MSC when added to HUVEC monolayer. Bar = 6 µm. B is a higher magnification of A (x2.5) of one cell (circle and arrow). (C) Micrograph from time lapse photography showing shedding of PKH26 labelled exosomes from WJ-MSC overlying HUVEC; Bar = 22 µm.

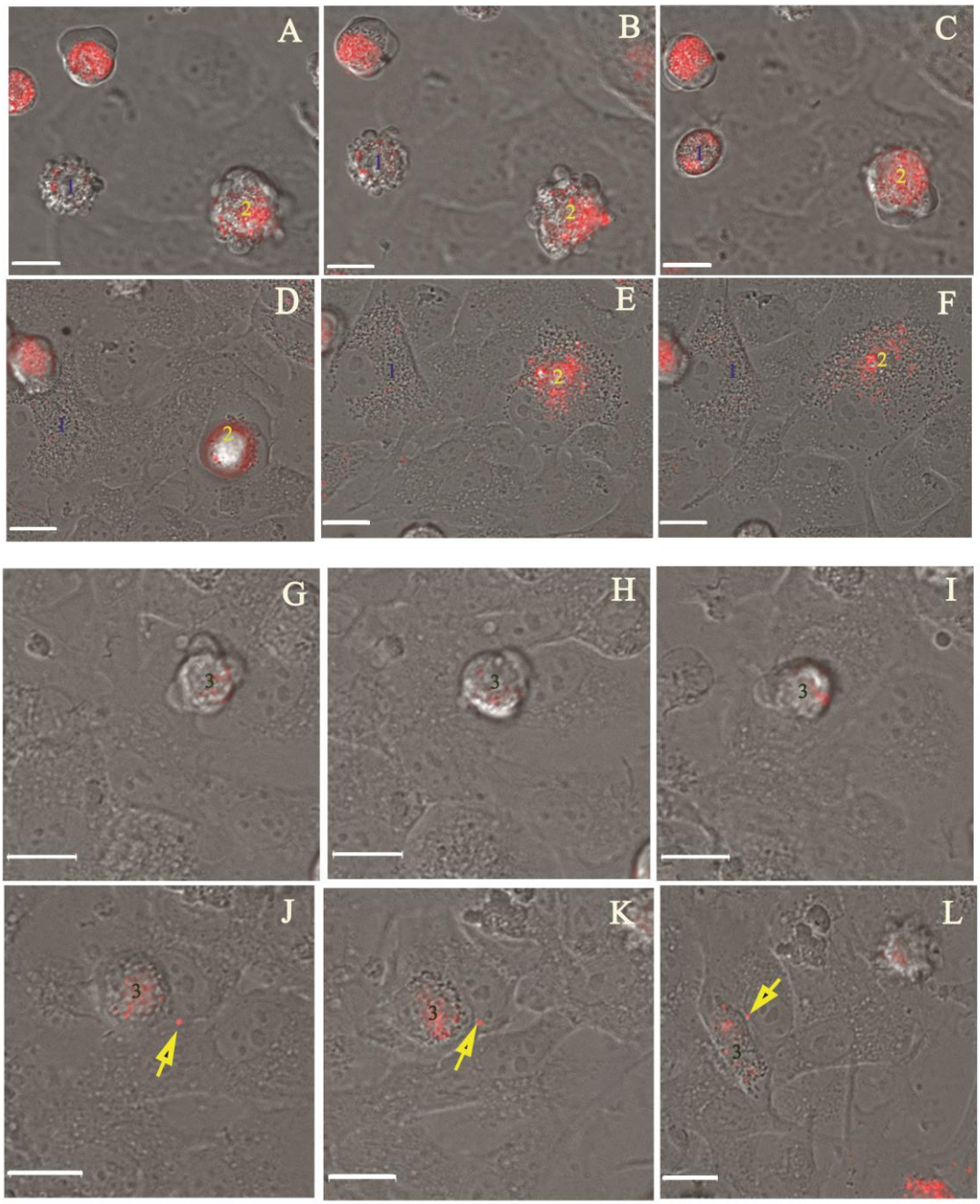


Figure 24: Micrographs from time lapse microscopy of HUVEC-WJ-MSC co-culture

(A-F). Micrographs from time lapse photography (every 15 min for 1.5h) showing behaviour of labelled WJ-MSC over HUVEC monolayers. Cell 1 can be seen displaying blebbing behaviour (A,B) followed by rounding (after 30 minutes; C) and flattening (D, E, F). Cell 2 can be seen blebbing (A,B), crawling (C), rounding (D) and flattening (E,F).

(G-L). Micrographs from a second time lapse movie (every 15 min for 1.5h). Cell 3 can be seen demonstrating pseudopodia and crawling movement over HUVEC monolayer (G,H,I), rounding (J,K) before becoming spindle shaped (L). From A-C micrographs were focused on WJ-MSC, while micrographs from D-L were focused on HUVEC. WJ-MSC have not crossed the HUVEC monolayer in these micrographs of early events. Secreted PKH26 labelled exosome (yellow arrow) can be seen in J, K and L. Bar = 6 µm.

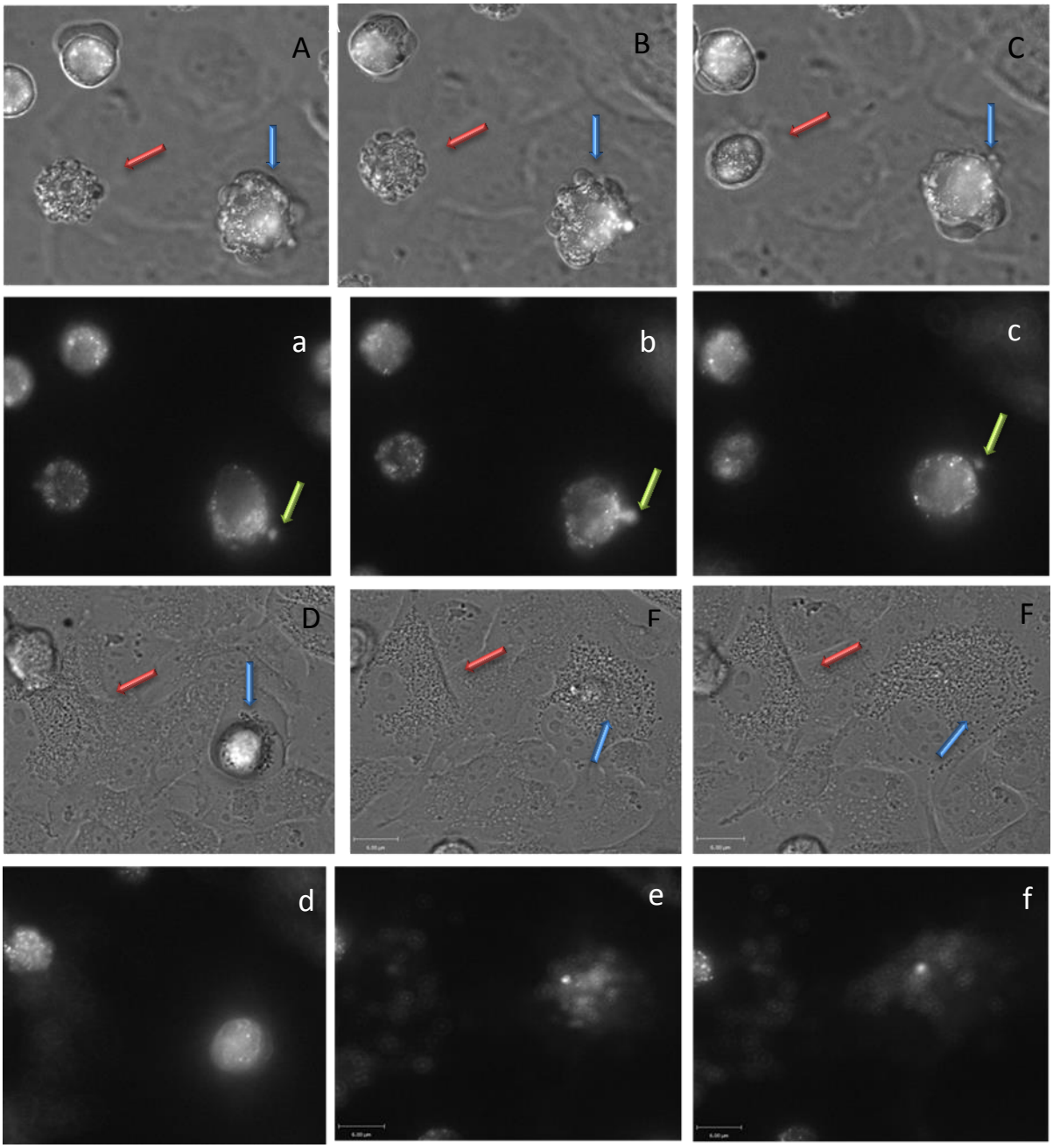


Figure 25: Micrographs from time lapse microscopy of HUVEC-WJ-MSC co-culture

(A, B, C, D, E and F) Micrographs from time lapse photography of the same video above (Fig 4 A-F) using only black and white channel showing behaviour of labelled WJ-MSC over HUVEC monolayers. Cell 1 displays (red arrows) blebbing behaviour followed by rounding (after 30 minutes, C) and flattening (D). Cell 2 (blue arrows) can also be seen demonstrating blebbing, as well as pseudopodial extensions and crawling movement over HUVEC monolayer before becoming spindle shaped with time.

(a,b,c,d, e and f) shows the same cells as above but after closure of bright field channel (HUVEC) to see WJ-MSC only. The green arrows point to Cell 2, which is shedding an exosome (a,b,c) then rounding up with time (d) followed by flattening (e,F).

3.3.2.2 Transmigration events

Fluorescence micrographs of immunostained co-cultures from different durations showed that transmigration of cells from the apical surface to sub-endothelial layers started from 60 minutes onwards. At 2h, 46 ± 11 % of all attached WJ-MSC were found in sub-endothelial locations. At 16h, the majority of WJ-MSC (95± 4%) was found in sub-endothelial position. 96 ± 3% of WJ-MSC were found in sub-endothelial positions at 22h to be completed at 26h (Fig 26).

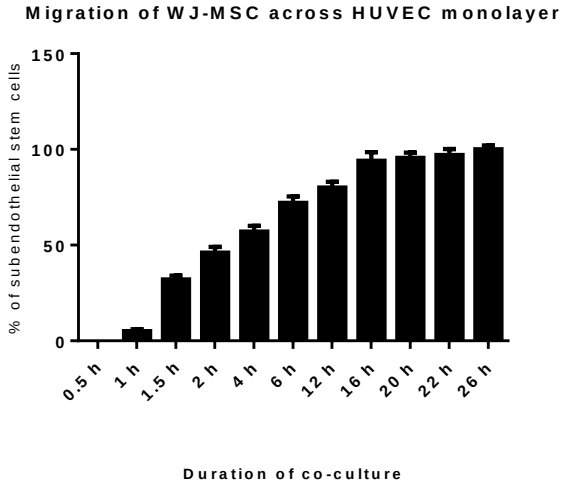


Figure 26: Histogram illustrating the percentage of sub-endothelial WJ-MSC

The percentage of migrating WJ-MSC through HUVEC monolayers at different time intervals is shown here. The migration started at 1h, increased over the time from 1-16h. From16 to 26 h was observed to plateau. (n = 3).

3.3.2.3 VE-cadherin dynamics

The pattern of VE-cadherin localisation showed non-significant changes in HUVEC monolayers with or without added PKH26 labelled WJ-MSC at early hours 0.5, 1 and 1.5 hours (Fig 27 & 28), however it differs at 2, 16 and 22h. Control HUVEC monolayers (no added stem cells) showed the presence of VE-Cadherin at cell-cell boundaries, with a predominant continuous staining pattern at all time-points (Fig 29 and 30).

In co-cultures, attachment and paracellular transmigration across the endothelial layer was observed to peak from 2h and was concomitant with changes in VE-cadherin staining pattern to a discontinuous, stitch-like, or no staining pattern in 35% of all cell-cell junctions. Specifically, HUVEC with overlying or transmigrating labelled WJ-MSC showed junctional disruption (Fig 29B, C) compared with continuous VE-cadherin staining seen in HUVEC cells distant from WJ-MSC.

A similar pattern of disruption related to stem cell proximity was seen in 16h co-cultures. The stem cells overlying HUVEC, traversing inter-cellular gaps and in sub-endothelial positions were all immunonegative to VE-cadherin. At 22h all WJ-MSC were observed in sub-endothelial position with overlying para-cellular clefts showing full occupancy of VE-cadherin (Fig 29 J,K,L).

Quantitative analyses (Fig 30) revealed a statistically significant decrease (64.9 $\pm$ 3.7 %; $p<0.001$) in the % of cell-cell borders showing continuous VE-cadherin staining at 2h compared to control HUVEC (80.9 $\pm$ 2.9%). At 16h both control and treated groups had similar (76.9 $\pm$ 4.6 v 79.2 $\pm$ 3%) continuous junctional profiles. At 22h, the percentage of continuous junctions was statistically higher (93.4 $\pm$ 3.2%) in the WJ-MSC treated samples

versus the control (78.8% ±3.4%; $p<0.01$). Intra-specific comparisons of groups showed that junctional staining pattern in control HUVEC monolayers were not significantly different at 2, 16 and 22h whilst in treated groups the % of continuous junctions differed at each time point of co-culture ($p<0.01$).

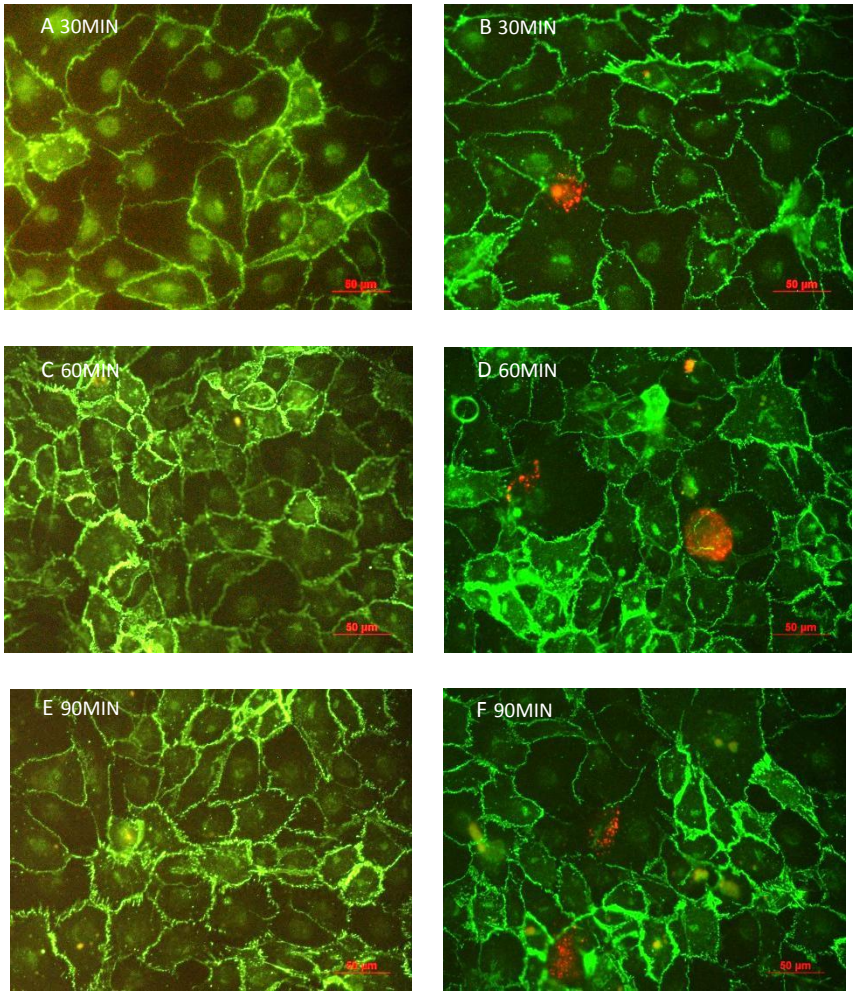


Figure 27: Micrographs of VE-cadherin immuno-localisation

(A-F). Micrographs showing localisation of VE-cadherin (green) in HUVEC monolayers without (A,C,E) or with added PKH26 labelled WJ-MSC (red) at 30, 60 and 90MIN (B,D and F). (A, C and E). Control HUVEC monolayers show presence of VE-Cadherin at cell-cell boundaries, with a predominant continuous staining pattern at all time-points. (B,D and F). Image of co-culture showing VE-cadherin localisation in HUVEC at cell-cell junctions with a predominant continuous VE-Cadherin pattern as well at the different time points. Reprehensive sample out of 3 experimental repeats.

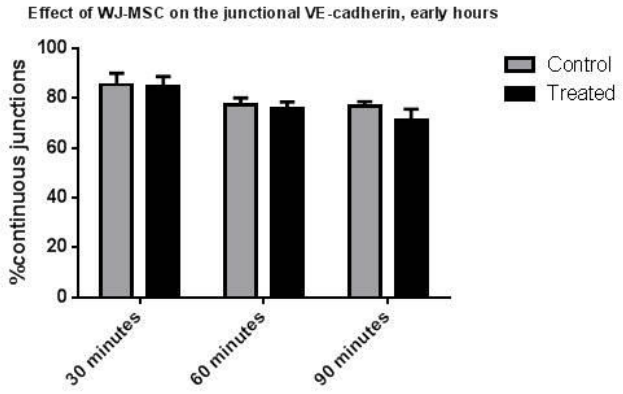


Figure 28: Percentage of VE-cadherin continuous junctions

Histogram of percentage of continuous VE-cadherin junctions at different time intervals for control and co-cultured cells.

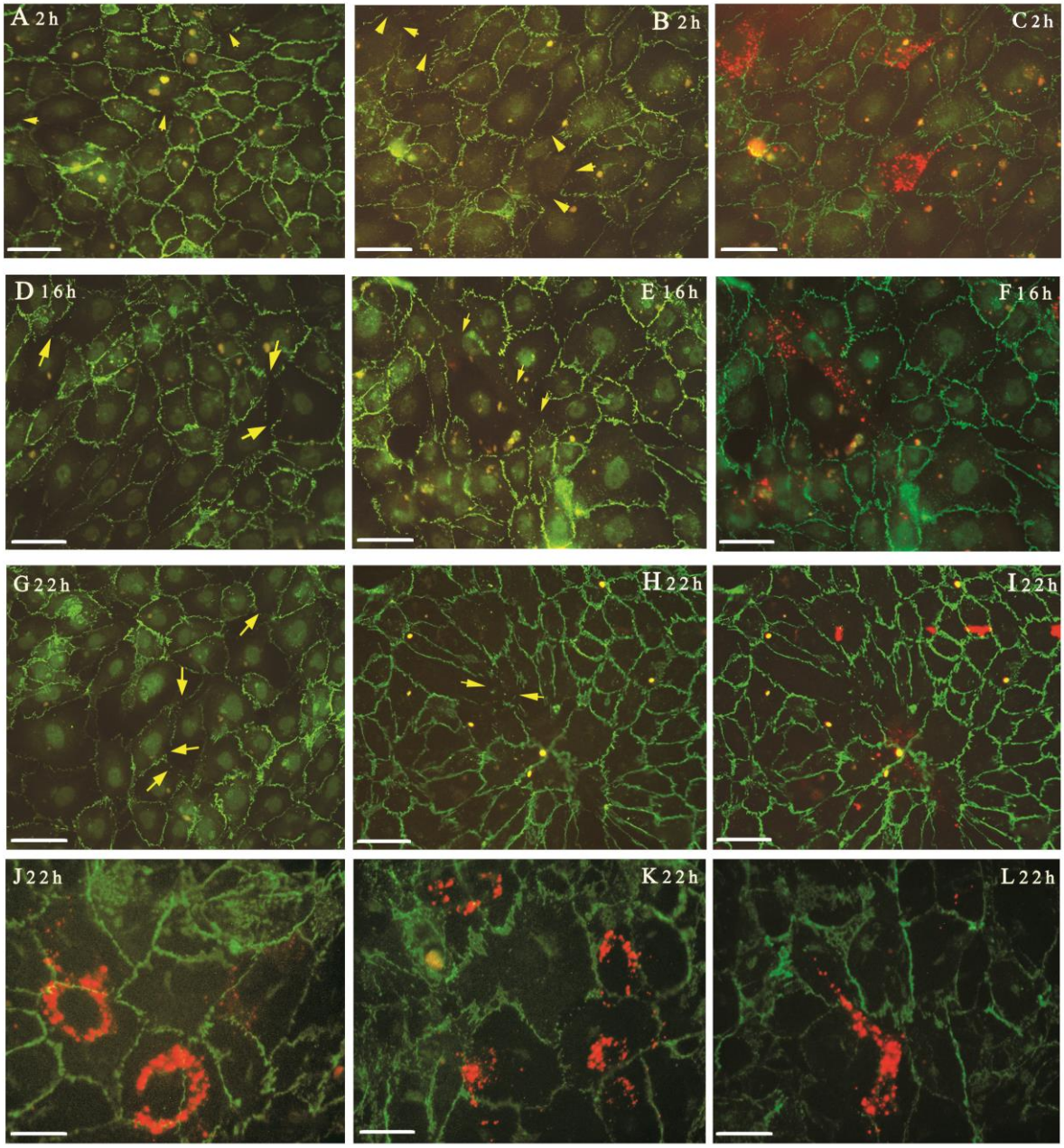


Figure 29: Micrographs of VE-cadherin localisation in HUVEC with or without WJ-MSC

(A-L). Micrographs showing localisation of VE-cadherin (green) in HUVEC monolayers without (A,D,G) or with added PKH26 labelled WJ-MSC (red) at 2, 16 and 22h (B,C,E,F,H,I,J,K,L). (A, D and G). Control HUVEC monolayers show presence of VE-Cadherin at cell-cell boundaries, with a predominant continuous staining pattern at all time-points. (B). Image of co-culture with FITC filter only showing VE-cadherin localisation in HUVEC after 2 hours of co-culture with WJ-MSC. Cell-cell junctions with discontinuous VE-Cadherin pattern or loss of staining (arrow) can be seen. (C). Superimposed images (FITC/TRITC filters) of same area showing position of WJ-MSC (red) to the discontinuous cell - cell junctions. They can be seen overlying or in close association with the disrupted cell-cell borders.

(E,F); Similar dual images at 16h of co-culture show co-localisation of WJ-MSC at disrupted cell-cell junctions. (H and I). At 22h of co-culture, increased numbers of cell-cell borders contain a continuous VE-Cadherin staining. In the merged image (I) WJ-MSC can be seen underlying the HUVEC monolayer. Bar = 40 µm for images A-I.

(J-L). Merged images at higher magnification at 22h co-culture from different experimental repeats, Bar = 20 µm. Full junctional occupancy of VE-cadherin can be seen in cell-cell boundaries overlying WJ-MSC (J). Sub-endothelial position of WJ-MSC can be seen in K and L. Again overlying junctions show full VE-cadherin occupancy. Note discreet shed exosomes can be seen in co-culture images. Reprehensive sample out of 3 experimental repeats.

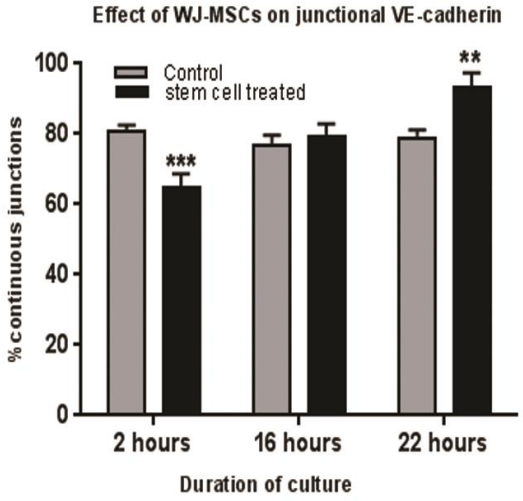


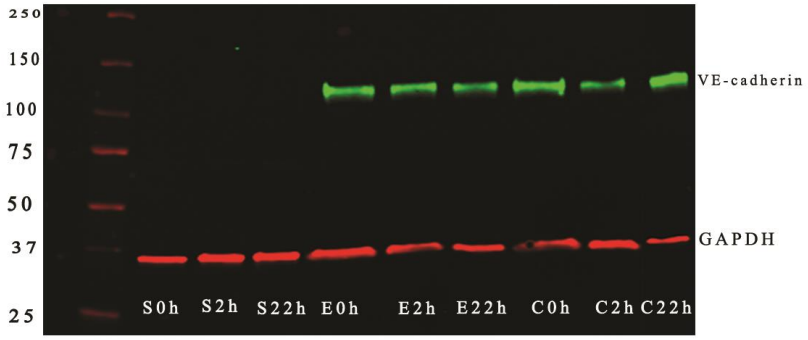
Figure 30: Histogram showing the percentage of continuous VE-cadherin junctions

Histogram of percentage of continuous VE-cadherin junctions at different time points for control and co-cultured cells. Two-way ANOVA revealed a significant decrease at 2 hours ($p<0.001$) and significant increase at 22 hours ($p<0.01$) in the co-cultures compared to control indicating maturity in stem cell treated groups. Junctional continuity was also statistically significant at each duration of co-culture ($p<0.01$). ($n = 3$).

3.3.2.4 Western Blotting

Western blot analysis (n=3) of co-cultures and control monolayers at 2 and 22h showed that that WJ-MSC did not express VE-cadherin, whilst HUVEC showed differential expression dependent on treatment and duration of stem cell interaction (Fig 31A). Statistical analysis revealed no significant change in VE cadherin values (normalized against GAPDH) in the control groups from 2 to 22h, while the co-cultures showed significant up-regulation of VE cadherin protein in the same time interval ($p<0.1$; Fig 31B). This intra-specific difference corresponded with junctional changes seen by immuno-fluorescence analyses.

A



B

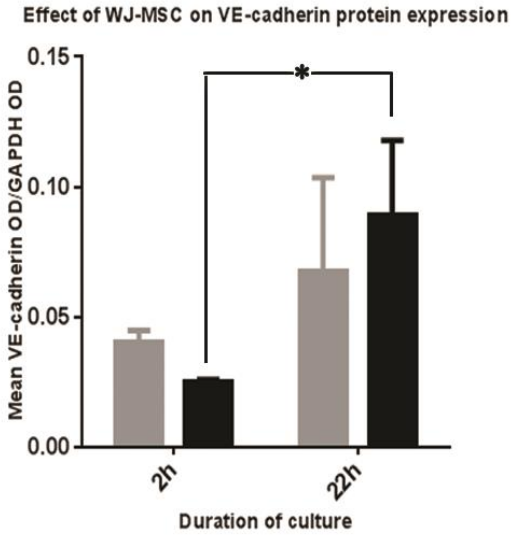


Figure 31: Representative Western blot

(A). Representative Western blot (n = 3) showing expression of VE-cadherin. WJ-MSC show negative expression (S0h,S2h,S22h) for each duration, HUVEC without WJ-MSC (E0h,E2h,E22h) show no change in expression with duration of culture whilst an upregulation of VE-cadherin can be seen in at 22h in HUVEC co-cultured with WJ-MSC (C0h,C2h,C22h). GAPDH acted as loading control. (B). Histogram showing mean optical density (OD) + S.E.M of normalised VE-cadherin expression from three different blots of control HUVEC and co-cultures at 2h and 22h. No significant changes were seen in the control groups. There was a significant upregulation of VE-cadherin expression at 22h in the co-culture group ($p < 0.05$).

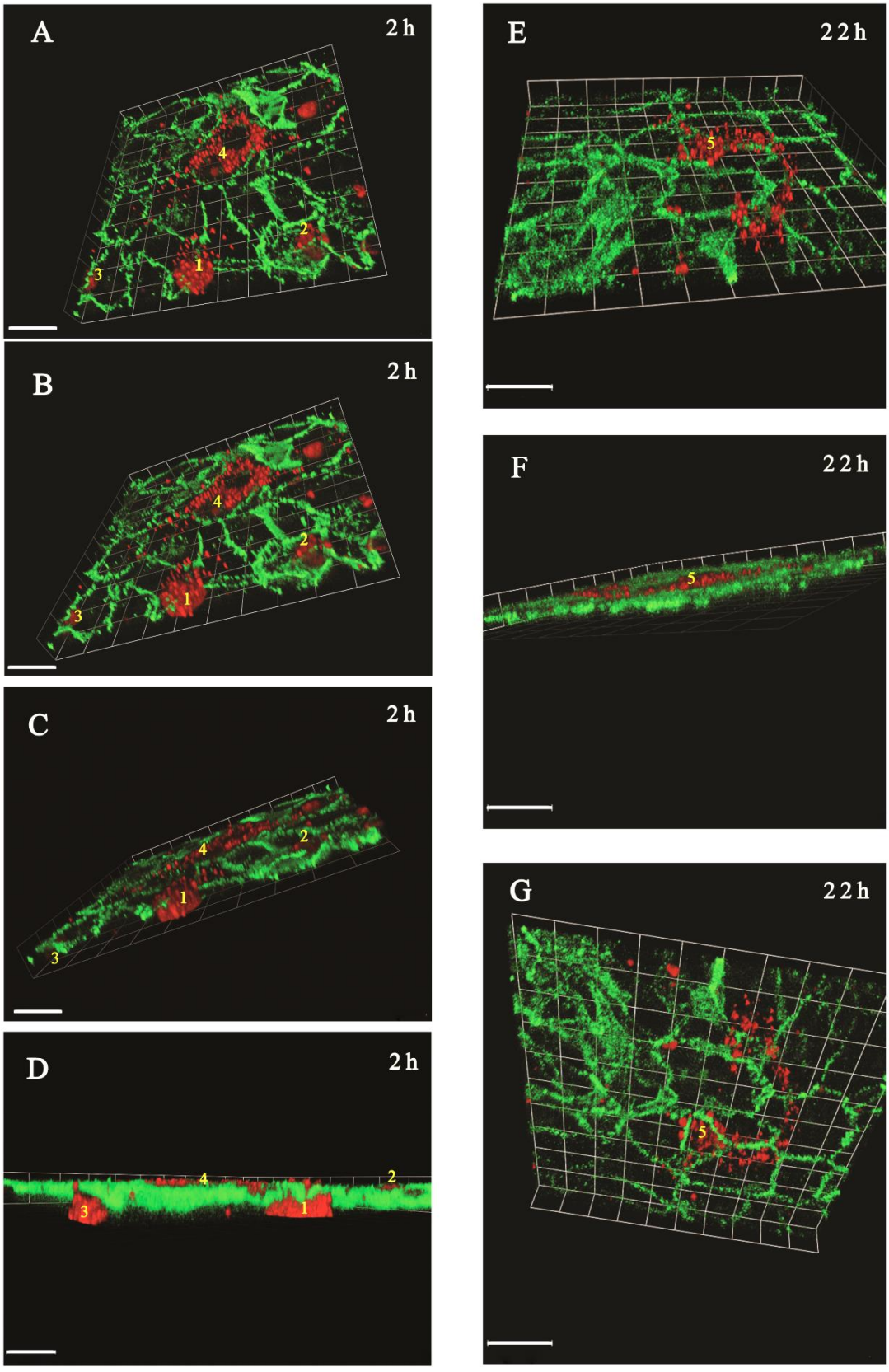
3.3.2.5 Confocal imaging

Confocal microscopy of co-cultures, immunostained with VE-cadherin and tilting at the Z axis confirmed attachment and paracellular transmigration of WJ-MSC across the endothelial layer at 2h, (Fig 32A-D). Furthermore, Z-tilts confirmed basal position of all stem cells at 22h (Fig 32E-G). The endothelial cell-cell junctions showed the continuous VE-cadherin pattern above the transmigrated stem cells.

Figure 32: Confocal composite micrographs of HUVEC-WJ-MSC co-culture

(A-G) Confocal composite micrographs of optical sections. (A-D; 22 slices at 0.5µm intervals and E-G; 10 slices at 0.6µm intervals) of PKH26 (red) labelled WJ-MSC co-cultured with VE-cadherin (green) labelled HUVEC, where VE-cadherin clearly demarcates cell-cell contact regions of the monolayer. Images were tilted on the Z-axis at varying angles with Volocity Software, starting from the sub-endothelial position. (A, B) At 2h co-culture, 3 WJ-MSC (1,2,3) can be seen traversing at cell-cell borders, where VE-cadherin staining is disrupted or absent. Cell 4 is seen fully attached and spread under the HUVEC monolayer. (C & D) confirms the paracellular transmigrating of cells 1-3. Bar = 120 µm.

FIG.12. (E, F and G). Confocal micrographs of optical sections of co-cultures at 22 hours, tilted with Volocity software, starting from a sub-endothelial position; Bar = 100 µm (E, F). Elongated spindle-shaped WJ-MSC (5) can be seen under the HUVEC monolayer traversing over several cells. Tilting to the apical surface of the monolayer (G) demonstrates repair of the junctional regions with full occupancy of VE-cadherin (continuous staining) in paracellular clefts overlying the stem cell (5).


A
2 h
4
2
1
3
B
2 h
4
2
1
3
C
2 h
4
2
1
3
D
2 h
4
2
3
1
E
22 h
5
F
22 h
5
G
22 h
5

3.4. Discussion

Data obtained in the present chapter showed that human mesenchymal stem cells isolated from the umbilical cord can cross HUVEC endothelial barrier without causing endothelial damage. The transmigration appeared to be similar to that shown for bone marrow stem cell migration (Teo et al., 2012), taking a period of hours rather than minutes.

WJ-MSC demonstrated non-apoptotic blebbing upon addition, amoeboid motility, changes in cell shape toward spindle shaped morphology and paracellular transmigration to the sub-endothelial layer. This mode of migration is matching with the individual category of cellular migration discussed in the Introduction and it is related to cell–matrix interactions. The data also suggest that WJ-MSC can influence junctional expression of the paracellular adhesion molecule VE-cadherin, with VE-cadherin perturbation as an early event followed by transmigration and a full return of VE-cadherin to junctional domains. Indeed, once WJ-MSC were in the sub-endothelial niche they appeared to upregulate both VE-cadherin protein expression and their occupancy at HUVEC cell-cell borders.

Exposure of PH26-labelled WJ-MSC to 50% endothelial media did not alter their ability to attach, proliferate, grow to confluence and retain the dye. They did not demonstrate phenotypic alteration towards the endothelial lineage; they continued to be negative for VE-cadherin when grown in mixed media or when co-cultured with HUVEC. Addition of 50% stem cell media to HUVEC at near confluence did not alter its ability to reach full confluence within 24h. Junctional maturity (as evidenced by continuous VE-cadherin staining) and vWF expression was similar to that seen in HUVEC grown in 100% endothelial medium.

There were no statistically significant differences in the percentage of junctions showing continuous VE-cadherin at 0.5, 1, 1.5, 2, 16 or 22h in mixed media alone (control). In co-cultures there was a significant upregulation of total protein in HUVEC after 96% of WJ-MSC had transmigrated to the ablumenal (sub-endothelial) position. This increase was due to changes in HUVEC since WJ-MSC remains immunonegative for VE-cadherin at all durations of co-culture. However, where VE-cadherin resides, junctional occupancy rather than cytoplasmic location, dictates barrier integrity (Dejana et al., 2008). Thus the observed changes in junctional VE-cadherin staining with duration of co-culture were revealing. The statistically significant increase in disruption of the VE- cadherin adherens junctions in the HUVEC monolayer was an early event and peaked at 2h after introduction of WJ-MSC.

Trans-endothelial migration of WJ-MSC started from 60 min and a 46% of cells had transmigrated by 2h. Return of VE-cadherin and full junctional occupancy was a post-migratory event, starting around 16 h and reaching higher % continuous than control HUVEC monolayers at 22 hours. VE-cadherin protein expression was at its highest here.

The discreet but significant perturbations of HUVEC cell-cell borders which started after 60 min are reminiscent of that seen for vasoactive agents such as VEGF and histamine (Esser et al., 1998, Leach et al., 1995). These inflammatory mediators have a biphasic response with rapid trans-endothelial pore formation (minutes) followed by a paracellular distension after 30 to 60 min (Absi et al., 2014b, Bates, 2010, Wegener and Seebach, 2014a). The delayed interaction we observed argues towards VE-cadherin re-location to facilitate transmigration.

Bone marrow derived mesenchymal stem cells have been shown to migrate through the paracellular pathway of human brain micro-vascular endothelial cell monolayers, via

disruption of ZO-1 and occludin and alteration of tight junction integrity (Lin et al., 2013). The post migratory return of VE-cadherin in co-cultures agrees with other studies. Pati *et al*. (2011) showed that BM-MSC can reduce HUVEC monolayers permeability *in vitro* after 24 hours with enhanced VE-cadherin / β- catenin interactions (Pati et al., 2011). Menge *et al*. (2013) showed that BM-MSC inhibit HUVEC proliferation and angiogenesis after two days of co-culture through modulation of VE- cadherin / β- catenin signalling pathway (Menge et al., 2013). These studies showed that umbilical mesenchymal cells have a similar ability; moreover this is preceded by paracellular VE-cadherin disruption during transmigration.

The return of VE- cadherin and HUVEC confluence seems to be related to a paracrine conversation between WJ-MSC and HUVEC. According to Choi *et al.* (2013) WJ-MSC can stimulate neovascularization by secreting paracrine factors and by acting as perivascular precursor cells (Choi et al., 2013). The observed shedding of exosomes prior to transmigration suggests exosomal signalling may also be an early event. Uptake of MSC exosomes by HUVEC increases the tube formation by endothelial cells, induces proliferation and migration of fibroblasts to mediate wound healing (Shabbir et al., 2015). Confirmation the existence of exosomes, excluding that it is not cell debris from the labelled WJ-MSC and whether exosomal signalling can induce WJ-MSC migration across HUVEC monolayer requires investigation and is a future aim.

The real-time studies revealed that transmigration is not an all or nothing event, with all added cells transmigrating soon after addition. Increasing number of WJ-MSC crossed the endothelial barriers over the 24h observation period, with migration starting around 60 min. 46% of attached cells crossed in the first 2h and the remainder continued crossing up to 24h in an individual migration of cells with no detection of grouped migration. The initial lag

phase and prolonged duration is similar to an *in vivo* study of the perfused mouse heart, where Schmidt *et al.* (2006) reported that 50% of introduced bone marrow stem cells migrated through the endothelial barrier within 60 minutes perfusion (Schmidt et al., 2006). No reverse trafficking of migrated cells was observed. Once the sub-endothelial position was reached, cells attached and became quiescent. This may be the consequence of improved adhesion of WJ-MSC on gelatin.

In this study isolated mesenchymal stem cells from the incised umbilical cord were used. These cells showed essential mesenchymal stem cell characteristics such as plastic adherence, tri-potency and expression of CD29, CD105, CD90, CD73 and CD44. However, heterogeneous populations of mesenchymal stem cells, both in origin (pericytic or fibroblastic) and differentiation potency is now a hotly discussed topic (Lv et al., 2014) and may explain the reported vascular repair potential of mesenchymal stem cells. Of the 20,000 WJ-MSC added to each endothelial- lined well and grown in mixed media, only a proportion (50%) of the added stem cells crossed the endothelial barrier. The ability of this cohort to survive (adapt) in 50% endothelial media and their preference for the sub-endothelial niche is suggestive of the existence of cells with different lineage potential in the > 96% pure characterised mesenchymal stem cells. Thus these stem cells may be more amenable to peri-vascular lineage commitment. Indeed the subsequent maturation of endothelial VE-cadherin junctions seen in HUVEC at 22 h co-culture mimics an endothelial-pericyte cross talk and gives credence to this hypothesis.

The blebbing behaviour of the WJ-MSC upon introduction was observed not to be an apoptotic phenomenon. The very same cells were then seen to display amoeboid movement and change shape. This type of membrane changes after trypsinisation of adhered cells and

addition to new extra-cellular matrix has been shown for cells; indeed bleb-mediated migration for navigation and mechanical homeostasis is a critical cellular activity (Norman et al., 2010). Teo *et al.* (2012) also attributed blebbing of bone marrow stem cells to low avidity interaction between endothelium and MSC, whilst quenching of blebbing may be promoted by contact with the sub-endothelial matrix after transmigration (Teo et al., 2012). In the present chapter WJ-MSC showed exactly the same response in their search for new optimal attachment sites at the sub-endothelial niches. As stated before, in this study, confocal microscopy and Z-tilting indicate that emigration sites for WJ-MSC were at cell-cell contact regions. Transcellular migration was not observed but cannot be excluded. The time taken to transmigrate was similar to that seen for bone marrow stem cells rather than leucocytes (Stock and Riethmuller, 2011).

In conclusion, the data obtained in this chapter are the first to show the early events of transmigration of WJ-MSC isolated from the human umbilical cord through HUVEC, adding strength to the observations that alteration in VE-cadherin localisation at junctional domains accompanies mesenchymal stem cell migration to perivascular regions. The traffic to sub-endothelial regions and influence on HUVEC endothelial integrity and VE-cadherin occupancy suggest that WJ-MSC have an important perivascular/pericytic function in general and throughout gestation in particular. These interactions were demonstrated in fetal endothelial cells, whether the same mechanisms take place in adult endothelium requires further studies (Chapter Four). The molecular mechanisms behind transmigration of WJ-MSC across HUVEC monolayer also need more investigations (Chapter Five).

Chapter 4

Temporal studies into attachment and paracellular migration of human umbilical mesenchymal stem cells across human uterine microvascular endothelial cell monolayers

4.1. Introduction

4.1.1 Mesenchymal stem cells and pregnancy

The presence of pregnancy-associated fetal progenitor cells in the maternal circulation is well documented. Fetal cells have been detected in the mother's peripheral blood from the first trimester and the numbers raised as pregnancy progressed through checking the presence of XY cells in women with male pregnancies for ease of discrimination (Dawe et al., 2007, O'Donoghue et al., 2003). Long-term fetal cells with self-renewal capability and multipotency have been named pregnancy-associated progenitor cells were found in the maternal circulation (Bianchi, 2004).

Fetal cells have also been demonstrated at sites of maternal injury and may have an active role in the repair of maternal tissues. They can be detected in the mother's peripheral blood from the first trimester of pregnancy, with numbers increasing as pregnancy progresses; indeed persistent microchimeric fetal cells can remain in the maternal circulation decades after birth (Dawe et al., 2007, O'Donoghue et al., 2003, Bianchi, 2004). The maternal blood in placental intervillous spaces has been shown to contain fetal cells even at term, strengthening the observation that these cells continue to cross the placental barrier throughout gestation (Parant et al., 2009). Cells from all three embryonic germ layers; ectoderm, endoderm and mesoderm have been identified in maternal peripheral blood and damaged maternal tissues such as brain, kidney and heart (Seppanen et al., 2013, Seppanen et al., 2012, Zeng et al., 2010, Cha et al., 2003, Roy et al., 2014). They are thought to play an active role in the repair of maternal tissues; *CDX2* cells of fetal/placental origin have been shown to home into injured endocardium in mice and undergo differentiation into diverse cardiac lineages (Kara et al., 2012). Fetal stem cells have also been detected in the livers of females with hepatitis C, in the thyroid of those with Hashimoto's disease and different

organs of women with a severe form of systemic lupus erythematosus, suggesting their presence was part of the maternal immune response (Boyon et al., 2011).

The exact process by which fetal cells cross the placental barrier and enter maternal circulation is still unclear. The mechanism by which fetal MSC migrated and homed into maternal tissue requires more investigations. To date, there are no studies on the interactions of MSC with normal human uterine spiral artery endothelium. Only Yang *et al.* suggested that WJ-MSC is a good source of repair the damaged human endometrial stromal cells. Through promotion of VEGF secretion and reducing apoptosis induced by mifepristone in endothelial stromal cells (Yang et al., 2011).

4.1.2 Cells known to be involved in spiral artery remodelling

Uterine spiral arteries play a critical role in providing the fetus with essential nutrition and oxygen vital for its growth and maturation through a constant and uninterrupted blood flow to the placenta. Spiral arteries remodelling is essential for a normal pregnancy and impairment of its transformation is associated with pregnancy complications, such as preeclampsia, and in uterine fetal growth retardation (Ball et al., 2006, Pijnenborg et al., 2006, Lyall, 2002).

The remodelling of uterine spiral arteries by placental derived extra-villous trophoblast cells in order to ensure high flow, low resistance conduits of maternal blood flow to the placenta is well documented (Pijnenborg et al., 2011). Whether fetal mesenchymal stem cells play a part in this is not known. Fetal endothelial colony forming cells isolated from human cord blood and injected into the fetal heart have been shown to transmigrate from the fetus to the uterus and home into and aid expansion of mouse uterine vessels in pregnancy (Sipos et al., 2013). These authors also located endothelial-associated fetal cells in the human myometrial

microvessels at term and hypothesised that fetal stem cells play a role in influencing expansion of maternal vascular supply to the placenta. How fetal cells, whether endothelial colony forming or mesenchymal stem cells, cross the maternal endothelial barrier is not known. On the other hand, there are other types of cells involved in the remodelling process such as maternal uterine natural killer cells and macrophages (Lash et al., 2010, Bulmer et al., 1991, Robson et al., 2012, Kaufmann et al., 2003).

Remodelling of spiral arteries is an extensively researched area, with much controversy surrounding the role played by fetal trophoblast in the transformation of these spiral arteries over contrasting evidence emerging all the time. For example, Bulmer *et al.* argued that EVT do not regulate vascular smooth muscle apoptosis, but instead regulate smooth muscle migration away from the spiral arteries into the decidual stroma or rarely migrating between two endothelial cells into the lumen of the vessel (Bulmer et al., 2012). There is also debate on the chronological order in which different EVT invade, with studies suggesting that endovascular trophoblasts begins invasion only after vessel lumen prepared by interstitial trophoblasts (Kam et al., 1999). In summary, the exact cellular and molecular mechanisms and the interaction between cells related to remodelling are still vague and in need of further investigations.

Cytokeratin 7 (CK7) is extensively used as a marker of invasive extra-villous trophoblast cells from long time ago and still being used (Dunk et al., 2003, Demir et al., 2002, Zhou et al., 1997a). CK7 is an intermediate filament cytokeratin (54 kDa) expressed in the glandular epithelium, transitional epithelium and transitional carcinoma. CK7 was observed to be expressed in the trophoblast of human blastocyst from day six post-fertilization prior to implantation (Niakan and Eggan, 2013). Unek *et al*. used it also as a marker for trophoblasts

to study the expression of certain proteins in normal and preeclampsia complicated human placenta (Unek et al., 2014). Moreover, Telugu *et al*. postulated that trophoblasts derived from human embryonic stem cells are similar in their invasive properties and genetic profile to that of the first trimetric placental cells using CK7 as a trophoblastic marker (Telugu et al., 2013).

However, the specificity of CK7 as a marker of trophoblast needs revaluation. Recently CK7 was seen to be expressed in cells other than trophoblast. For instance, human amniotic mesenchymal stromal cells have been shown to express CK7 (Konig et al., 2014). It might be related to some mesenchymal – epithelial transition or that mesenchymal cells originally have population of cells which are already directed to epithelial cells.

4.1.3 Mesenchymal stem cells and how it crosses the endothelial barrier

In the previous chapter, it has been shown that WJ-MSC isolated from term umbilical cords can cross the fetal human umbilical vein endothelial monolayers using a paracellular route, with full repair of VE-cadherin junctions once a sub-endothelial niche has been reached (Ebrahim and Leach, 2015). Whether a similar non-destructive mechanism is employed by these fetal stem cells to cross the maternal endothelium, including the uterine microvascular endothelium, important for utero-placental circulation requires elucidation.

4.1.4 Aims of this chapter

Using real time, confocal microscopy and protein expression analyses, this study specifically investigated the spatio-temporal events when fetal WJ-MSC encounter confluent maternal endothelial cell monolayers, the chosen transendothelial migration pathway and the VE-cadherin dynamics which would allow physiological paracellular extravasation. The

ability of these cells to influence maternal endothelial junctional maturity from sub-endothelial niches was also investigated. The use of uterine microvascular cells allowed insights to fetal and maternal interactions as well as a possible role of fetal mesenchymal stem cells in mature functioning of the uterine vasculature to ensure optimal utero-placental perfusion.

4.2. Materials & methods

Materials

Chemical and reagents

DPBS, calcium and magnesium free, trypsin – EDTA solution 1x (0.5 g porcine trypsin and 0.2 g EDTA in 4 Nacl HBSS), FBS, red fluorescent dye PKH26, were all purchased from Sigma-Aldrich, UK. Basal endothelial cell growth medium MV with its growth supplement (Promocell, UK). Stem cell growth medium (DMEM/Low Glucose), antibiotic/antimycotic solution 100x (10,000 µg /ml pencillin G, 10,000 µg/ml streptomycin, 25 µg/ml amphotercin B) (Hyclone, UK). DMSO, paraformaldehyde, BSA and Gelatin from bovine skin (type B), Ham F10 medium and L-glutamine (Sigma- Aldrich, UK).

Tissue Culture Plastics and Accessories

Tissue culture flasks 75 cm^2, 12 wells plates and cover slips 19 mm (Life Technologies). Cryopreservation tubes (1 mL) (Sarstedt, UK). Tc 10 counting slides (Bio- Rad, UK). Glass-bottomed tissue culture dishes (Ibidi GmBH, Germany).

Antibodies and kits

Purified mouse antihuman CD144 or VE-cadherin (Pharmingen, BD Biosciences, UK), CD31 (R&D Systems, UK), Cytokeratin 7 (Dako, UK), Rabbit-anti human VE-cadherin (Cell

Signalling, UK). CD29-FITC (Beckman Coulter). Secondary antibodies: Anti-rabbit IgG (whole molecule TRITC, developed in Goat affinity isolated antigen specific antibody); Anti-mouse IgG (whole molecule FITC produced in goat affinity isolated antibody) (Sigma-Aldrich, UK). Vector: Vectashield mounting medium for fluorescence (Vector Lab Inc, Burlingame, CA, USA) with or without propidium Iodide (PI).

Methods

4.2.1 Human Uterine Microvascular Endothelial Cells growth and subculture

HUtMEC (5×10^5 cells/ml) were commercially bought from Promocell, UK. They were grown to confluence on 1% gelatin coated T75 flasks with endothelial cell growth medium MV with added growth supplement and 100 IU/mL penicillin, 100 μg/mL streptomycin, 0.25 μg/mL amphotercin B. They were allowed to grow at 37˚C and 5% CO_2 in air. After 24 hours, unattached cells were removed and the attached cells were fed with pre-warmed growth medium. HUtMEC cells were re-fed every 2-3 days.

When the cells reached about 80—90% confluence, the media was removed, pre-warmed 10 ml of DPBS was used to wash any remaining residues of the media from the flask, then the cells were detached by incubation with 2ml of trypsin/ EDTA (0.05 % trypsin and 0.02 % EDTA) for maximum three minutes at 37˚C and the reaction was stopped by adding 7 ml of growth medium and 3 ml FCS. HUtMEC were then collected by centrifugation (700 rpm for 5 minutes), supernatant was removed and the pellet was re-suspended in 3 ml of pre-warmed growth medium. Furthermore, the suspension was seeded on 1% (w/v) gelatin coated 75 cm^2 culture flask (splitting ratio 1:3) and growth medium was refreshed after 24 hours, then every 2 to 3 days.

4.2.2 Cell counting and freezing

Once HUtMEC in the T75 cm^2 culture flask reached confluence, harvesting of the cells was carried out as described previously. The pellet was suspended in 3 ml of freezing mixture (70 % growth media, 20 % FCS and 10 % DMSO). The number of the cells in the suspension was counted by mixing 10 µl of cell suspension to 10 µl trypan blue, loaded to a counting slide, then using the haemocytometer to measure total number of the cells and the percentage of the living cells. Furthermore, the remaining of the suspension was transferred to cryovials (1ml / vial) labelled with cell line, passage number, name and the date. Cryovials were placed into a Mr Frosty container and placed in - 80°C freezer overnight. This ensures that the cells freeze slowly at an optimum rate of - 1°C/min. Then, transfer the cryovials into the liquid nitrogen containers the next day.

4.2.3 Characterization of Uterine Endothelial Cells and WJ-MSC

HUtMEC and WJ-MSC monolayers (grown on uncoated coverslips) were further characterized by direct and in-direct immunocytochemistry with antibodies against the endothelial markers VE-cadherin and CD31; mesenchymal markers CD105-FITC and CD29-FITC and the epithelial marker cytokeratin 7. Rabbit-anti human VE-cadherin was used for the double immuno-labelling of HUtMEC. For immunofluorescence imaging confluent monolayers were fixed, permeabilized, blocked and incubated overnight at 4 ˚C with the primary antibodies as previously described in Chapter Three. Appropriate TRITC or FITC conjugated secondary antibodies were added. Coverslips were mounted using Vectorshield. Propidium iodide (PI; 1.5µg/ml) or 4’6-diamidino-2-phenyl indole (DAPI; 1µg/ml) was used to counterstain nuclei. Cells were visualised with a Nikon fluorescence microscope and images acquired (CCD camera; Nikon DS, Kingston-upon-Thames, UK) and stored (NIS elements F3.0; Nikon, Kingston-upon-Thames, UK).

4.2.4 Co-culture studies of WJ-MSC with HUtMEC

To obtain co-cultures of HUtMEC in contact with WJ-MSC, 100,000 HUtMEC were seeded on a 1 % gelatin-coated coverslip (19mm diameter) and incubated in endothelial media (3 experimental repeats). Once 70 ٪ confluence was reached the media was changed to mixed media. On full confluence (18 -24h later) 20,000 isolated PKH26 labelled WJ-MSC were seeded on top of the confluent HUtMEC monolayer (1: 5 ratio) per coverslip in 1 mL of the mixed media (Pati et al., 2011, Ebrahim and Leach, 2015). HUtMEC monolayers without added WJ-MSC in mixed media were used as a control. All experiments were repeated 3 times.

4.2.5 Real Time Observations

Co-cultures of WJ-MSC with HUtMEC on gelatinized glass-bottomed tissue culture were observed for 24 hours with Deltavision Elite Imaging system (Applied Precision, Issaquah, WA, USA). Images were acquired every 15 min. All data analysis was carried out using Volocity software (Perkin Elmer, Coventry, UK). Duration of exploratory behaviour and chosen transendothelial pathway to sub-endothelial niches was recorded.

4.2.6 Quantitative analysis of endothelial junctional integrity and migration of WJ-MSC

Confluent monolayers of HUtMEC with/without added PKH26-labelled WJ-MSC for 2, 16 and 22 hours (informed by the real time experiments) were fixed and immune-labelled for VE-cadherin as previously described. Systematic random sampling was used to acquire 10 images per coverslip for the chosen durations. After blinding, the percentage of paracellular clefts in each image was categorised according to VE-cadherin staining pattern: continuous or discontinuous staining. The latter category included total loss of VE-cadherin immunoreactivity. To ensure that all cell-cell junctional regions had an equal chance of

being counted, a grid was placed on images and paracellular clefts from every other square which did not cross the "forbidden line" (Gundersen and Jensen, 1987, Leach et al., 2004) were counted and categorised according to staining pattern. Data were analysed using Two-way ANOVA (Prism 6 software) and with Bonferroni's multiple comparison test to compare control versus stem cell treated group at 2, 16 and 22h. Statistical significance was taken at $p<0.05$.

The position and number (% of total cells in field of view) of the labelled WJ-MSC, apical or sub-endothelial and their proximity to discontinuous junctions were also recorded for the co-cultures at early durations (30, 60, 90 min) as well as 2, 16 and 22h, using the same unbiased systematic sampling method.

4.2.7 Confocal imaging

VE-cadherin labelled cells from co-cultures at 2 and 22h were further analysed with confocal scanning microscopy (Zeiss Axiovision; Zeiss, Goettingen, Germany) and Zen 2009 software for multi-channel acquisition & image processing. The pinhole diameter used in all confocal imaging was 1 AU. Optical slices (0.5 - 0.6 µm intervals) were taken and Z-tilts were obtained to visualise transmigration pathways, position of stem cells and VE-cadherin staining pattern using the same parameters used previously in Chapter three.

4.2.8 Expression of CK 7 in WJ-MSC, HUVEC and HUtMEC

Isolated WJ-MSC (P2, 3 and 5) and HUVEC (P2 - 5) and commercially bought HUtMEC (P 4 and 5) were grown to confluence, double labelled with epithelial marker; anti-CK 7 monoclonal antibody (12.4 µg/ml) and mesenchymal marker (CD29-FITC) or endothelial marker (VE-cadherin) and underwent the same protocol for immunohistochemistry as

previously described. Briefly, confluent monolayers of WJ-MSC, HUVEC and HUtMEC or WJ-MSC-HUtMEC co-cultures at set durations were fixed with 1% paraformaldehyde at RT for 10 min, permeabilized for 10 min with 0.15% Triton X-100, blocked in 5% goat serum in PBS/BSA for 30 min at RT and incubated overnight at 4 ˚C with the primary antibodies. Appropriate TRITC or FITC conjugated secondary antibodies were added for two hours in the dark at RT after washing. Coverslips were mounted using Vectorshield. Propidium iodide (PI; 1.5µg/ml) or 4'6-diamidino-2-phenyl indole (DAPI; 1µg/ml) was used to counterstain nuclei. Cells were visualised with a Nikon fluorescence microscope and images acquired (CCD camera; Nikon DS, Kingston-upon-Thames, UK) and stored (NIS elements F3.0; Nikon, Kingston-upon-Thames, UK).

4.2.9 Co-culture of trophoblast cells with HUtMEC

Trophoblast cell line; SGHPL-4 are a human first-trimester extravillous trophoblast-derived cells used extensively as an extravillous trophoblast model. The trophoblast cell line was a kind gift from Professor Guy S. Whitley (St. George's Medical School, University of London, London, UK). Trophoblast cells were cultured in Ham F10 containing 10 ٪ FCS, 2mM L-glutamine, 50 U/Ml penicillin and 50 µl streptomycin. In order to determine the effect of trophoblast on uterine endothelial cells, 100,000 HUtMEC were seeded on a 1 % gelatin-coated coverslip (19mm diameter) and incubated in endothelial media as previously described in co-culture of WJ-MSC with HUtMEC. Once 70 ٪ confluence was reached the media was changed to mixed media (endothelial and trophoblast media). On full confluence 20,000 PKH26 labelled SGHPL-4 P19 (labelled using the same protocol of WJ-MSC labelling as previously described in Chapter two), were seeded on top of the confluent HUtMEC monolayer (1: 5 ratio) per coverslip in 1 mL of the mixed media (Pati et al., 2011, Ebrahim and Leach, 2015). HUtMEC monolayers without added SGHPL-4 in mixed media

were used as a control. Confluent monolayers of HUtMEC with/without added PKH26-labelled SGHPL-4 for 2 and 24 hours were fixed and immune-labelled for VE-cadherin as previously described.

4.3. Results

4.3.1 Uterine microvascular endothelial cells and Wharton Jelly mesenchymal cells continue to express endothelial and mesenchymal markers in mixed media

HUtMEC were observed with characteristic cobblestone appearance after seeding (Fig. 33). The cells took 4 ± 1 days to reach confluence (1 ± 0.2 x 10^6 cells / ml) in 75 cm^2 flask.

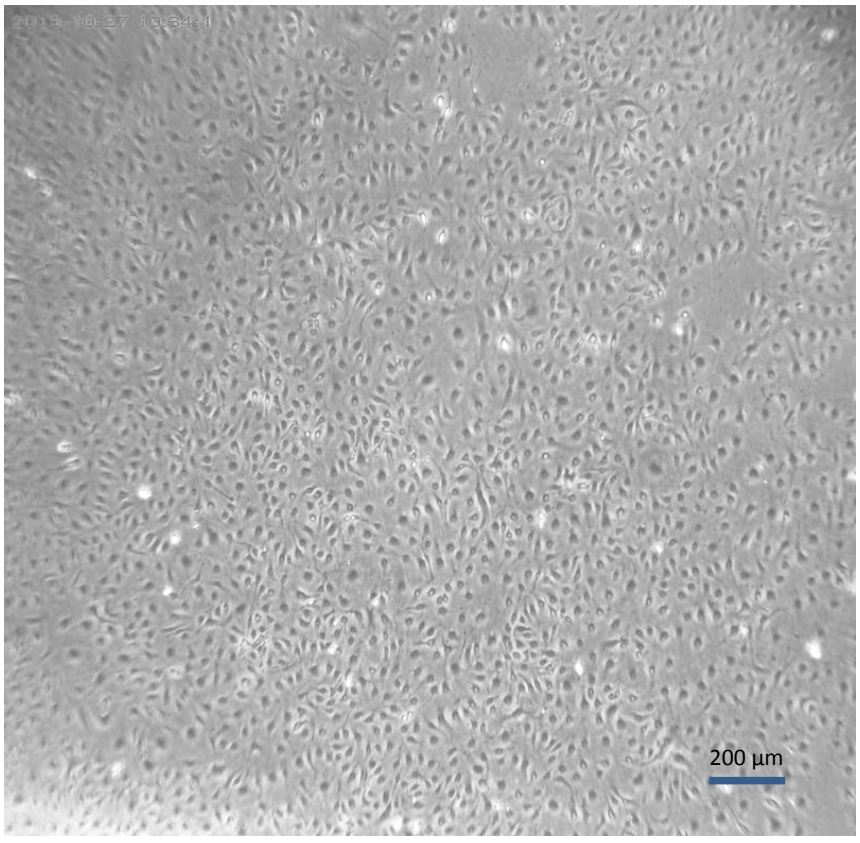


Figure 33: Micrograph (phase contrast microscopy) of confluent HUtMEC monolayer

Micrograph showing confluent HUtMEC cells with cobblestone appearance.

Human uterine myometrial microvascular endothelial cells showed immunopositivity to the endothelial markers VE-cadherin and CD31 (Fig. 34A, B) with strong continuous staining at cell-cell contact regions of confluent monolayers. This phenotype was maintained in mixed media.

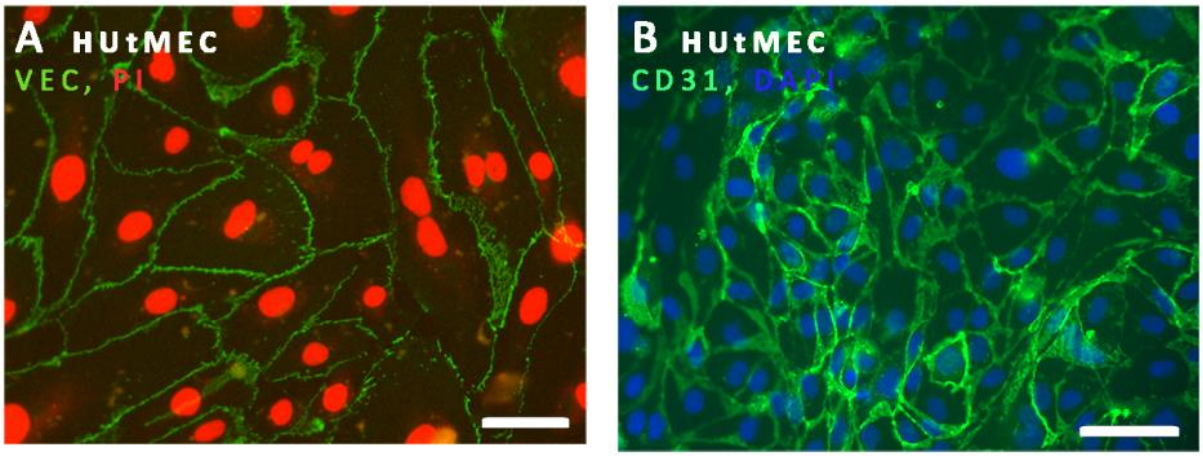


Figure 34: Micrographs illustrating HUtMEC & WJ-MSC characterization in mixed media

(A). Micrograph showing HUtMEC cells immunopositivity for VE-cadherin (green) which was localised to continuous staining of cell-cell boundaries; nuclei stained with PI. (B). Micrograph of HUtMEC showing immunolocalisation of CD31 at cell-cell boundaries (green); nuclei stained with DAPI; Scale bar = 50 µm. Reprehensive sample out of 3 experimental repeats.

4.3.2 Fetal WJ-MSC can interact with maternal (uterine) endothelial cells displaying prolonged exploratory behaviour and paracellular extravasation

Real time microscopy revealed that the two cell types can co-exist with no observed apoptosis or detachment of the uterine endothelial cells, which remained as a monolayer throughout the 24h observation period. Upon addition the PKH26-labelled WJ-MSC displayed a prolonged exploratory behaviour, with classical membrane blebbing, psuedopodic extension and amoeboid movement (Fig. 35A-C) over the uterine (maternal) endothelial monolayer, similar to that reported for behaviour over fetal endothelial

monolayers in Chapter Three (Ebrahim and Leach, 2015). Within 24h observation period and after a 30 min lag phase, cells were observed to change shape towards the spindle-shaped morphology (Fig. 35 D-I), interrogate widened endothelial paracellular clefts and migrate to sub-endothelial positions (Fig. 35G-L). Shedding of PKH26 filled exosomes were observed throughout the early interaction period (Fig 36). A percentage of stem cells showed exploratory behaviour but did not cross the endothelial layer within the 24h duration of observation.

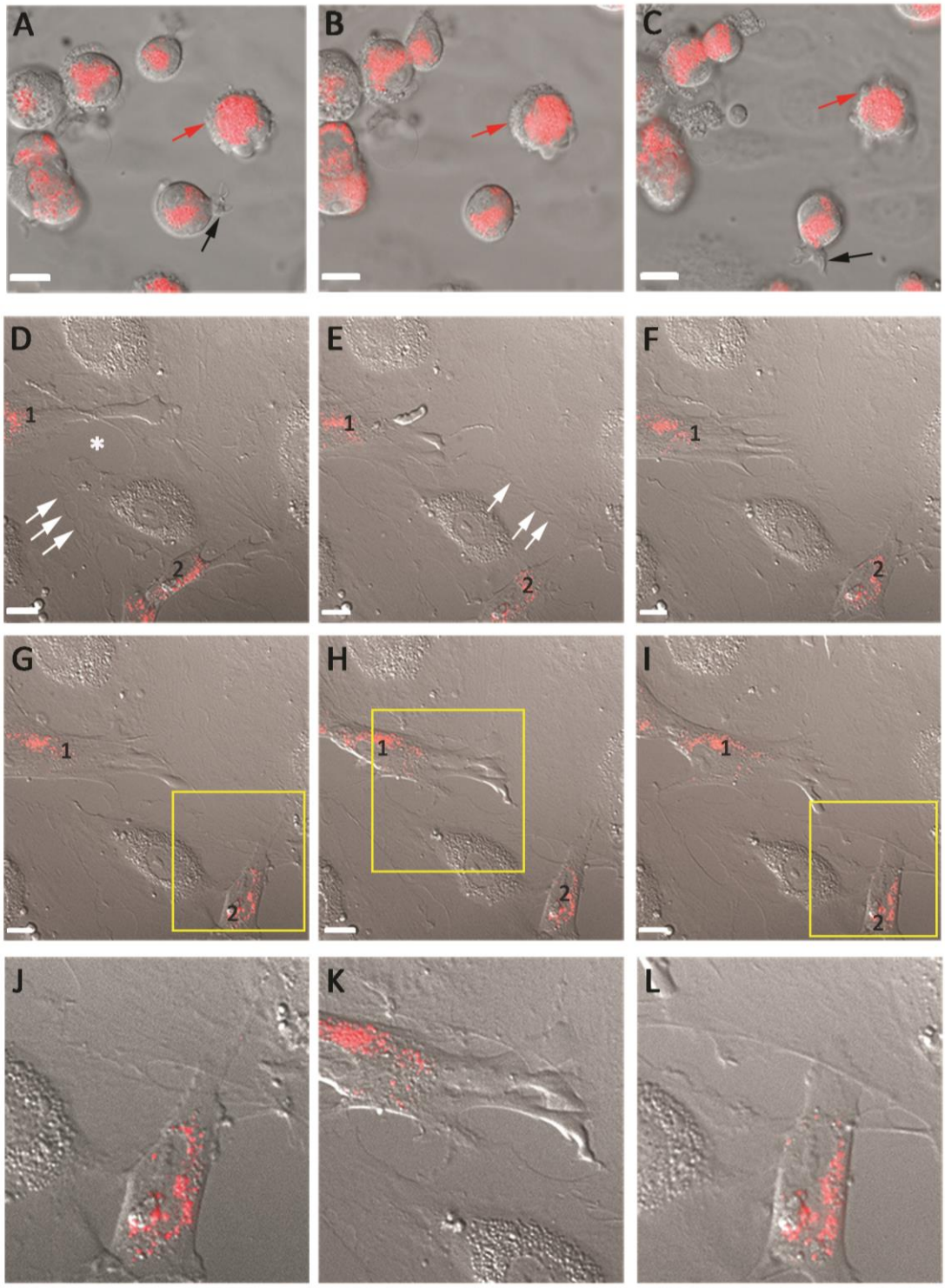


Figure 35: Micrographs from Time lapse of HUtMEC-WJ-MSC co-culture

Time lapse observations of WJ-MSC on HUtMEC monolayers. (A-C) Micrographs showing three sequential (15') time lapse acquisitions focusing on WJ-MSC labelled with PKH26 (red) 30 min after addition to HUtMEC monolayers. Rounded stem cells can be seen displaying blebbing behaviour (red arrow) and pseudopodial extensions (black arrow). (D-I). Co-culture at 16h. Six sequential images over 90 min with focus on endothelial plane. HUtMEC cells are showing flattened cytoplasm, prominent nuclei and cell-cell borders with intermittent gaps (arrows) or larger separations (star). In D, labelled WJ-MSC (cell 1 and 2) are spindle shaped, with cell 1 showing partial egress into a large gap (star), whilst cell 2 remain overlying HUtMEC. In (E) cell 2 can be seen in association with cell-cell border which display gaps (arrows). In F, cell 1 shows further sub-endothelial interrogation whilst cell 2 is closer to paracellular cleft. (G, H, I). After 45 min, cell 1 occupies the paracellular space and continues to probe sub-endothelial location, whilst cell 2 shows spreading of psuedopodial extension into a now more enlarged paracellular cleft (yellow squares); J,K, L are 2.5 times higher magnifications of squares in G, H, I. Bar = 14 µm. Reprehensive sample out of 3 experimental repeats.

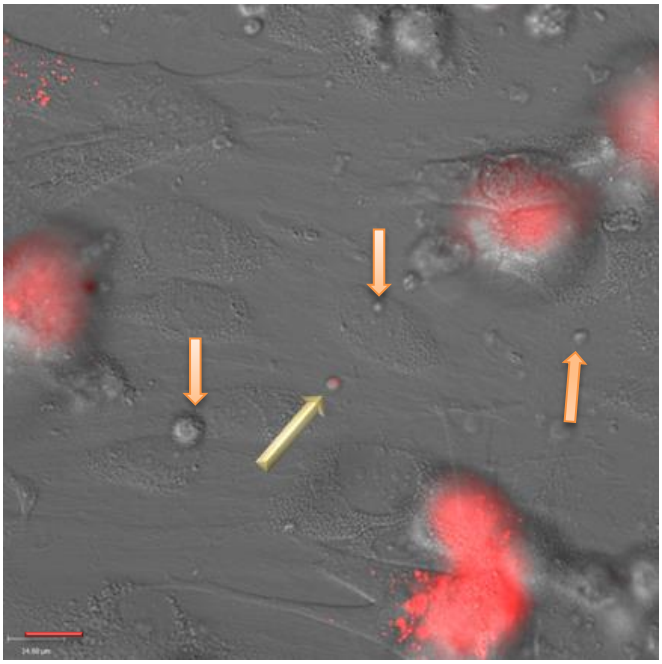


Figure 36: Micrograph from Time lapse showing secreted PKH26 labelled exosome

Secreted PKH26 labelled exosome **(yellow arrows)** can be seen on top of a confluent monolayer of HUtMEC; Scale bar = 14 µm.

4.3.3 WJ-MSC can alter VE-cadherin junctional occupancy and display paracellular transendothelial migration

Addition of 50% stem cell media to the uterine endothelial cells did not affect their ability to form VE-cadherin junctions and reach full confluence. The pattern of VE-cadherin staining at cell-cell boundaries was continuous and similar to that seen for HUtMEC grown in endothelial medium alone, suggestive of minimal disruption. Moreover, the control group for co-culture studies, HUtMEC monolayers without added WJ-MSC for all durations studied (0.5 to 22h) also showed continuous VE-cadherin staining at cell-cell junctions (Fig. 37A-D).

However, in the presence of WJ-MSC (1:5 ratio), the endothelial VE-cadherin at cell-cell boundaries changed to a discontinuous pattern/complete loss of VE-cadherin staining from 30 min to 2h (Fig. 37E, F). There was a statistically significant reduction in % of clefts with

continuous staining at 2h of co-cultures (63 ± 4.6%; $P < 0.001$) compared to controls (83.5 ± 3.5 %). These disrupted clefts/junctions were associated with overlying or transmigrating WJ-MSC (Fig. 37F, Fig38).

A similar pattern of disruption related to stem cell proximity was also seen in 16h co-cultures. At this duration there was evidence of junctional repair in the endothelial monolayer with an increase in the percentage of junctions now showing continuous VE-cadherin (79 ± 1.7 %) which approached that of control values (83.6 ± 2.8 %; Fig. 38G; Fig. 39).

At 22h all WJ-MSC were found in sub-endothelial position. There was a statistically significant increase in number of overlying paracellular clefts showing continuous VE-cadherin staining (94 ± 2.7 %) when compared to 22h control HUtMEC without stem cells (82.2 ± 2.5 %; $p < 0.001$; Fig. 37H; Fig. 38).

Counts of PKH26 labelled WJ-MSC at specific locations- apical transmigrating or sub-endothelial for the different durations of co-culture confirmed that transmigration of cells from the apical surface to sub-endothelial layers started from 30 minutes onwards (5% of cells) with the number of extravasating cells increasing with time. 48 ± 15 % of total cells in field of view were found in sub-endothelial locations at 2h. By 16h, the majority of WJ-MSC (88± 10%) was found in sub-endothelial position. 98 ± 2% of WJ-MSC were found in sub-endothelial positions at 22h. Of the initial 20,000 cells placed on confluent HUtMEC layers over a surface area of 19 mm^2, 62 ± 18% of cells crossed the endothelial layer within 22h (Figure 39).

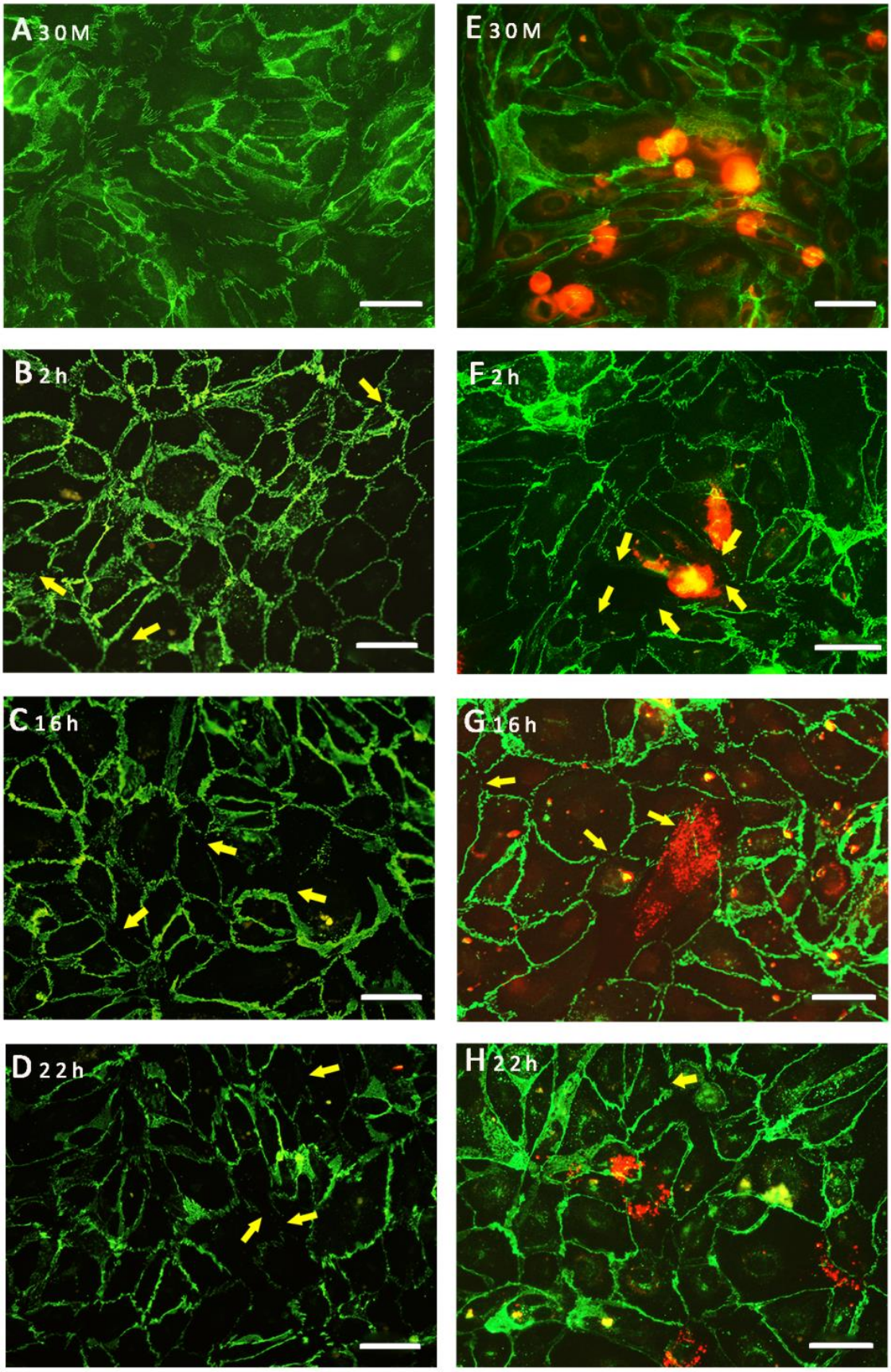

A 30M
E 30M
B 2h
F 2h
C 16h
G 16h
D 22h
H 22h

Figure 37: Micrographs of VE-cadherin localisation

WJ-MSC can alter VE-cadherin junctional occupancy. (A, B, C & D). Control HUtMEC at 0.5, 2, 16 & 22 hours showing similar predominantly continuous pattern of VE- Cadherin immunofluorescence at cell-cell boundaries. (E). PKH26 labelled WJ-MSC added to HUtMEC monolayers showing rounded morphology at 30 minutes. (F). HUtMEC after 2 hours of co-culture with WJ-MSC show increased number of cell-cell junctions with VE-Cadherin discontinuity. Labelled WJ-MSC are in close association with these disrupted regions (arrow), they now demonstrate a change in morphology towards spindle shaped. (G). At 16h of co-culture, the VE-Cadherin continuous/discontinuous pattern is similar to control. A central more spindle-shaped PKH26 labelled WJ-MSC can be seen. (H). At 22h of co-culture, higher numbers of junctions with continuous VE-Cadherin staining can be seen; junctions overlying WJ-MSC show full VE-cadherin occupancy; Bar = 50 µm. Reprehensive sample out of 3 experimental repeats.

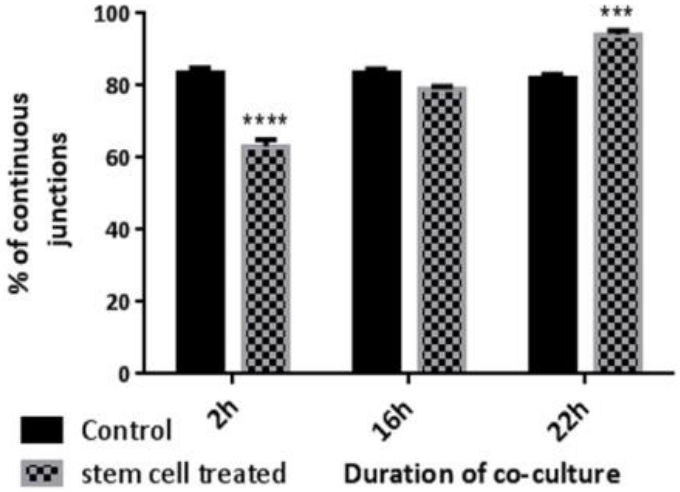


Figure 38: Histograph showing the percentage of continuous VE-Cadherin

The percentage of continuous VE-Cadherin junctions at different time points for control and co-cultured cells. Two-way ANOVA revealed a significant decrease at 2 hours ($P < 0.0001$) and significant increase at 22 hours in the co-cultures junctional counts ($P < 0.001$). ($n = 3$).

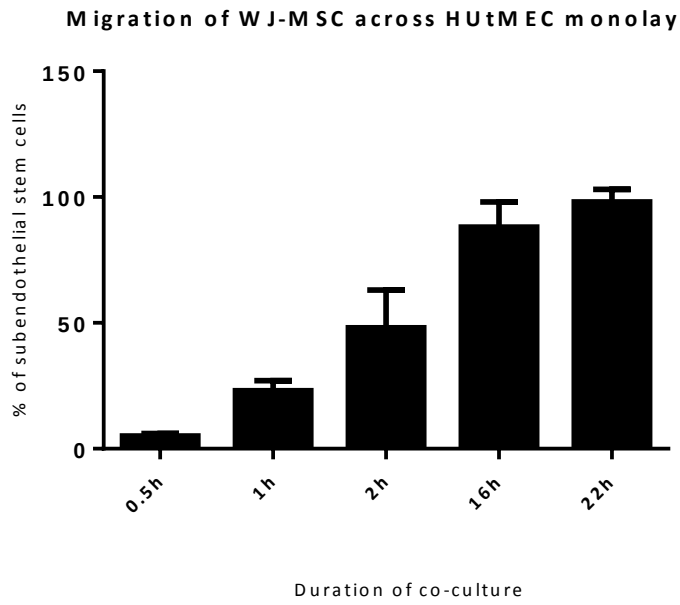


Figure 39: Histogram showing the percentage of sub-endothelial WJ-MSC
Histograph demonstrating the percentage of WJ-MSC found in the Sub-endothelial position of WJ-MSC at different durations of co-culture. (n = 3).

VE-cadherin immunostained co-cultures were further analysed with confocal microscopy to allow tilting of images at the Z axis. This confirmed attachment and paracellular transmigration of WJ-MSC across the endothelial layer at 2h through disrupted junctions and sub-endothelial position of all stem cells at 22h (Fig 40).

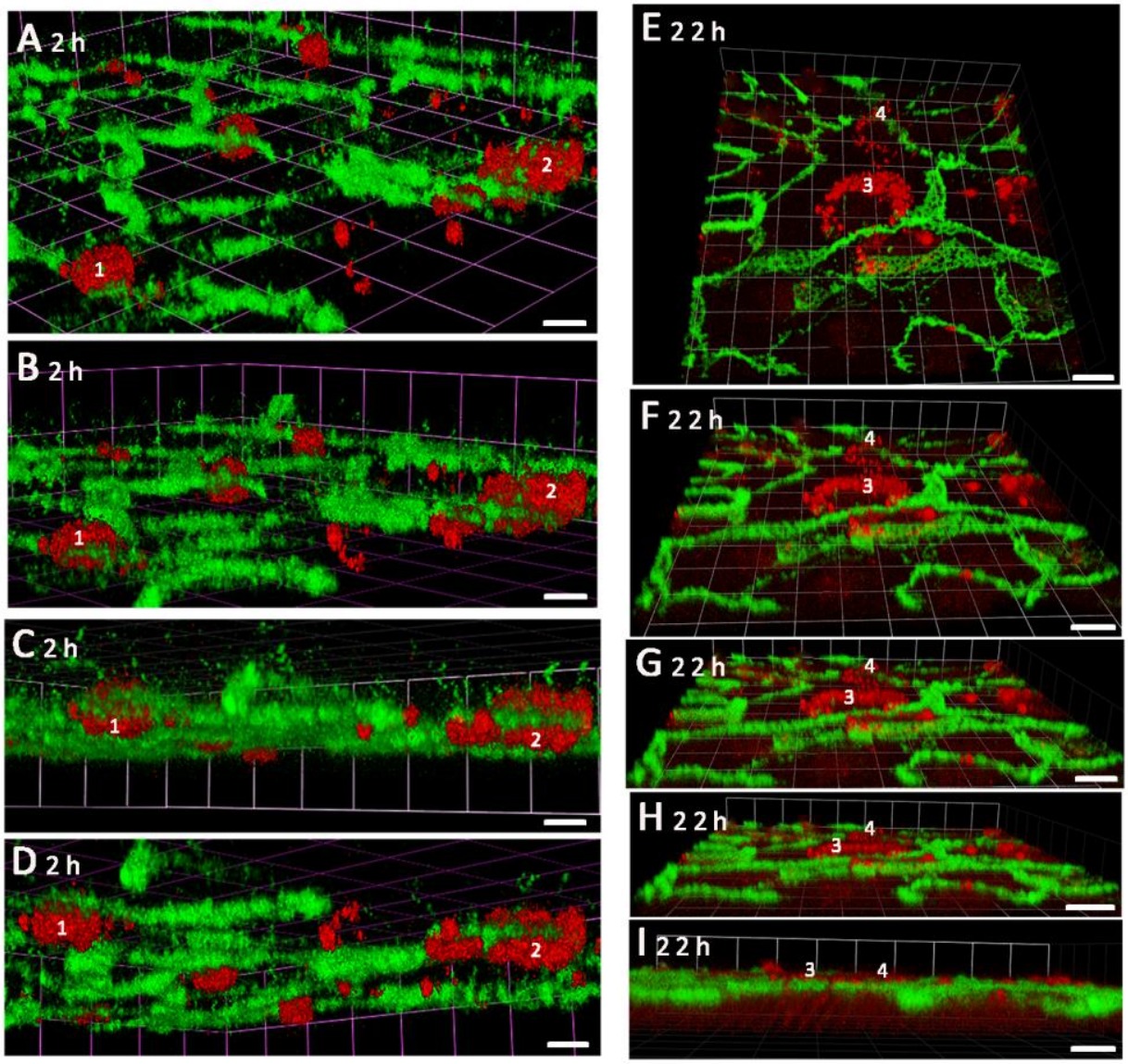


Figure 40: Confocal composite micrographs of HUtMEC-WJ-MSC co-culture

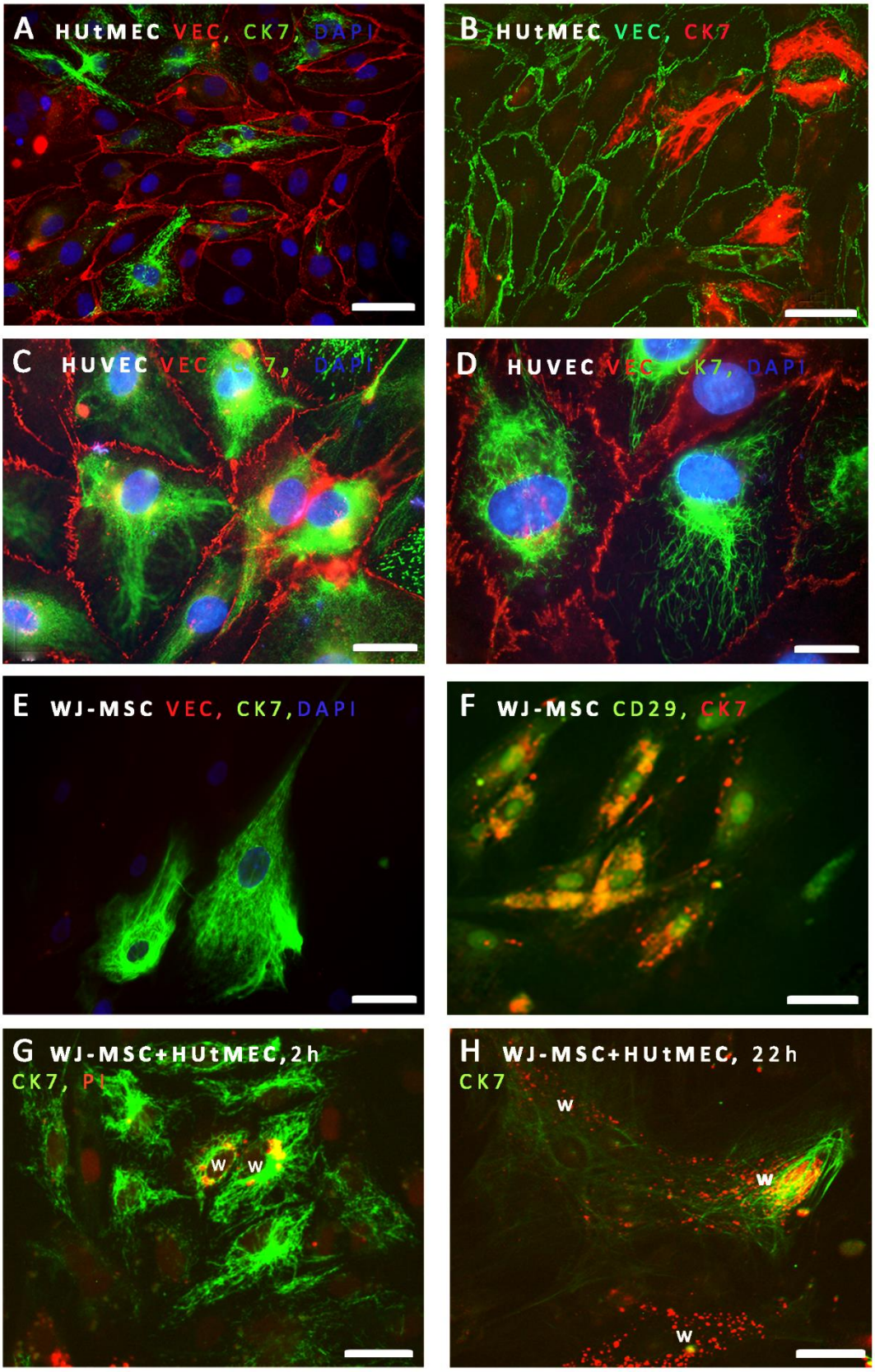
Confocal microscopy reveals sub-endothelial location by 22h. Confocal composite micrographs of optical sections of PKH26 labelled WJ-MSC co-cultured with HUtMEC (immunostained with VE-cadherin). Images were tilted on the Z-axis with Volocity Software, starting from the sub-endothelial position. (A-D) At 2h co-culture, WJ-MSC can be seen located to cell-cell boundaries. Tilts reveal WJ-MSC (cell 1 & 2) are traversing cell-cell borders where VE-cadherin staining is disrupted or absent. (E-I) 22h co-culture. Tilts reveal sub-endothelial location of WJ-MSC (cell 3 & 4). Bar = 100 µm.

4.3.4 Cytokeratin-7 expression in endothelial and mesenchymal stem cells

Double-immunolabelling revealed that 29 ± 4% of HUtMEC in the monolayers were immunopositive to CK7, a marker used extensively as an epithelial and a trophoblast marker for both villous and extra-villous trophoblast cells (Fig. 41A, B). Interestingly, human umbilical vein cells were also found to contain a high percentage (81 ± 6) of CK-7 expressing cells (Fig 41C, D). A percentage of the mesenchymal stem cells (30 ± 3%) were positive to CK7 (but negative to VE-cadherin) in monocultures (Fig 41E). These cells were still positive to CD29 (Fig 41F). In the co-culture studies, no increase was seen in the percentage of CK7+ cells in either cell type (Fig. 41G, H). CK7+ WJ-MSC were found in both apical and sub-endothelial positions of HUtMEC monolayers along with CK-7 negative WJ-MSC over the different durations of co-culture (Fig 41).

Figure 41: Micrographs demonstrating cytokeratin 7 localisation

Endothelial cells and mesenchymal cells can express cytokeratin 7. (A) VE-cadherin (red) positive HUtMEC monolayer showing CK-7 intermediate filaments (green) in a proportion of cells. (B) A second source of HUtMEC showing the presence of VE-cadherin + (green) and CK-7+ (red) cells. Nuclei - blue (C & D) HUVEC cells isolated from umbilical cords labelled with VE-cadherin and CK-7 showing a majority of cells contained CK-7. (E) WJ-MSC monoculture showing immunonegativity to VE-cadherin with a few cells demonstrating filamentous CK-7 staining. (F) WJ-MSC monolayers immunolabelled with CK-7 (green) & CD29 (red). A cohort of CD29+ cells show co-localisation with CK-7. (G & H) In co-cultures (at 2 & 22h) of PKH26 labelled WJ-MSC (red) and HUtMEC, a proportion of cells continued to express CK-7 (green). Bar = 50 µm. Reprehensive sample out of 3 experimental repeats.


A HUtMEC VEC, CK7, DAPI
B HUtMEC VEC, CK7
C HUVEC VEC, CK7, DAPI
D HUVEC VEC, CK7, DAPI
E WJ-MSC VEC, CK7,DAPI
F WJ-MSC CD29, CK7
G WJ-MSC+HUtMEC,2h
CK7, PI
W
W
H WJ-MSC+HUtMEC, 22h
CK7
W
W
W

4.3.5 Effect of trophoblast cells on uterine endothelial cells

Trophoblast cells did not cause any injury to uterine endothelial monolayers within 24h, the time frame of co-culture experiments. PKH26 labelled SGHPL-4 remained rounded and did not change its shape after 2 or 24h co-culture with HUtMEC, moreover the trophoblast cells attached to each other and showed clusters on top of a confluent monolayer of HUtMEC (Fig 42).

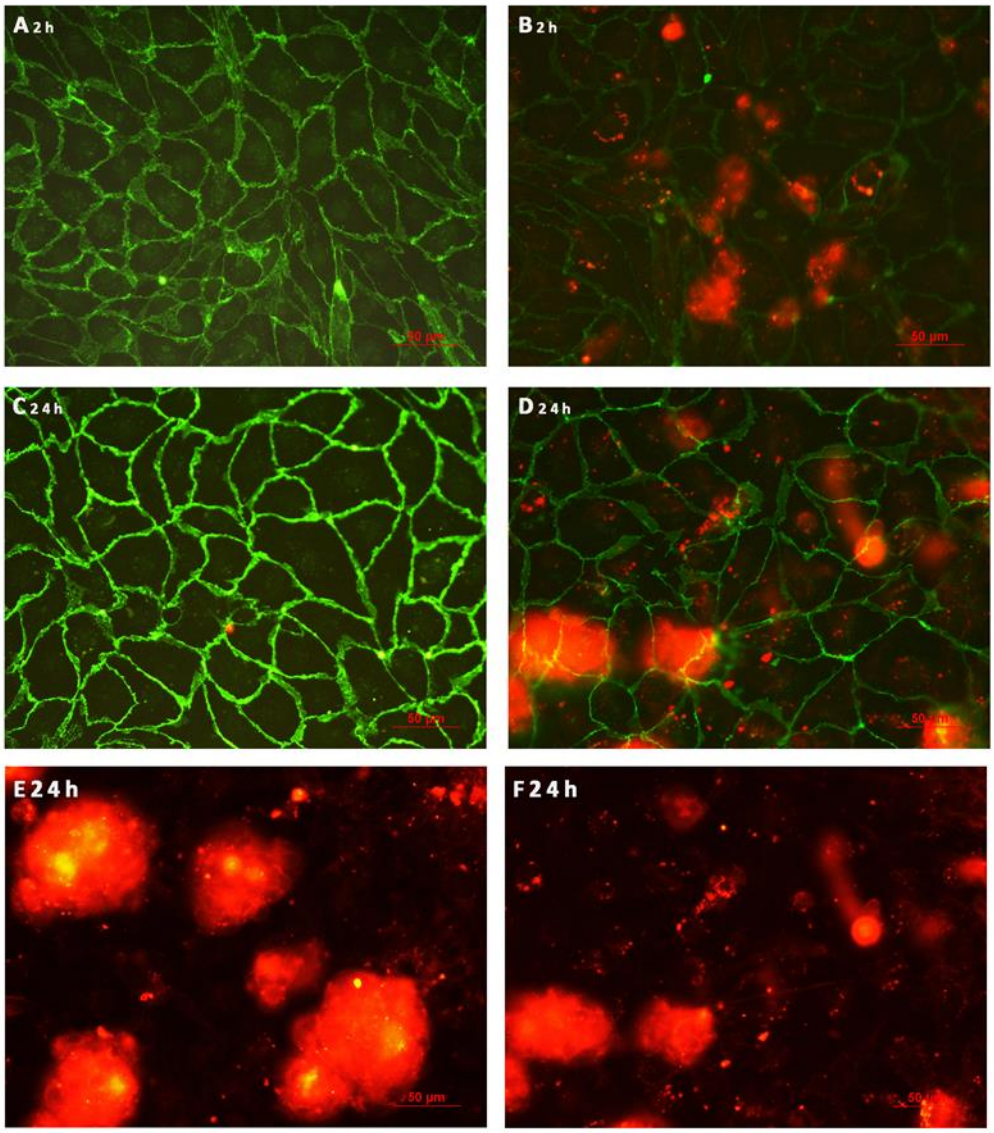


Figure 42: Micrographs showing HUtMEC-trophoblast co-culture

(A & C) Control HUtMEC at 2 & 24 h in mixed endothelial and trophoblast media showing continues staining pattern of VE- Cadherin at cell-cell boundaries. (B). PKH26 labelled SGHPL-4 co-cultured with HUtMEC at 2h, showing rounded shaped morphology of the trophoblast cells. (D). HUtMEC at 24 h of co-culture with SGHPL-4 showing VE-Cadherin continuity at cell - cell junction. Rounded labelled SGHPL-4 can be localised on top of these continues junctions. (E & F) PKH26 labelled SGHPL-4 co-cultured with HUtMEC at 24h, showing aggregations or islands of the trophoblast cells.

4.4. Discussion

This *in vitro* study is the first to show that fetal mesenchymal stem cells derived from the Wharton's jelly of term human umbilical cords can cross monolayers of microvascular endothelial cells derived from the human myometrium in a non-destructive manner without detaching the endothelial cells of the monolayer. Moreover, these fetal mesenchymal cells demonstrated a paracellular egress to sub-endothelial niches with disruption of VE-cadherin junctions followed by repair. Sipos *et al.* 2013 demonstrated that human fetal endothelial colony forming cells can cross the placental feto-maternal barrier and transmigrate to the maternal uterine vasculature in mice. These cells exhibited mesenchymal markers (CD105 & CD 146), expressed the endothelial marker (CD 31) and VEGFR-2, but did not express haematopoietic markers (CD14, CD45 or CD133) (Sipos et al., 2013). This study demonstrated that WJ-MSC can also traverse maternal endothelial cells and influence their junctional integrity as measured by significant increase in VE-cadherin junctional counts after transendothelial migration to sub-endothelial location.

WJ-MSC displayed non-apoptotic blebbing, amoeboid movement and interrogation of intercellular openings as early events in their exploration of the uterine endothelial monolayer, similar to what observed in WJ-MSC interaction with fetal endothelial monolayers (Chapter Three). There was a minimum time lag of 30 min before WJ-MSC transmigration was observed with a higher rate of migration between 30 min to 2h. The highest percentage of junctional disruption, defined by loss or discontinuous VE-cadherin localisation was also recorded at 2h. Junctional VE-cadherin profiles returned to normal from 16h when a majority of WJ-MSC were resident underneath the endothelial monolayers. Indeed, at 22h of co-culture there was a higher percentage of paracellular clefts with continuous VE-cadherin labelling than controls, indicative of induced increased junctional

maturity similar to the interaction with HUVEC monolayers (Chapter Three, (Ebrahim and Leach, 2014). The observed prolonged exploration time suggest a paracrine conversation between WJ-MSC and the endothelial cells.

Studies into the re-modelling of uterine spiral arteries have used cytokeratin-7 and karyotyping to conclude that placenta derived extra-villous trophoblast cells invade and modify these maternal vessels. However, in the current study CK7 displayed an ubiquitous localisation in endothelial and human umbilical mesenchymal stem cells [29 $\pm$ 4% of adult endothelium (HUtMEC), 81 $\pm$ 6 % of fetal endothelium (HUVEC) and 30 $\pm$ 3% of WJ-MSC which co-expressed the mesenchymal marker CD29]. The percentage of WJ-MSC showing positivity to CK 7 may be related to a specific cohort in the isolated stem cells or to a mesenchymal-epithelial transition of these cells in culture. The cells co-expressing cytokeratin still maintain a typical MSC phenotype, which includes the expression of CD90, CD105, CD73, CD44, CD29, lack of expression of CD14, CD19, CD34, CD45 and HLA-DR and a differentiation potential towards the adipogenic, chondrogenic and osteogenic lineages (Chapter Two). Indeed this was confirmed by a recent study demonstrating the heterogeneity and intrinsic potential of WJ-MSC to express epithelial markers including CK 7 *in situ* and in culture conditions. CK7 mRNA microarray analysis revealed positivity of 33.3 % of cultured WJ-MSC (Garzon et al., 2014a).

Konig *et al.* also demonstrated that, one day after isolation of human amniotic mesenchymal stem cells (hAMSC), 92 ± 7% expressed the mesenchymal marker vimentin, 2 ±1% stained for the epithelial marker cytokeratin-7 and 5 ± 4 % co-expressed these markers. After 5 days, the double positive cells slightly increased to 7 ± 3 %, while exclusive expression of cytokeratin-7 or vimentin remained unchanged. After the first passage till the

third passage, all attached cells were vimentin-positive, while about 50 % co-expressed cytokeratin-7 and vimentin. Culture of hAMSC in a medium optimized for the growth of endothelial cells, led to the same results as in amnion mesenchymal stem cells. Thus, under culture, hAMSC adopt mesenchymal–epithelial phenotype (Konig et al., 2014).

The endothelial localisation found here was curious, the co- expression of cytokeratin 7 and VE-cadherin confirmed their endothelial phenotype but suggested a de-differentiation capability of fetal endothelial in conditions that favour proliferation and migration. The persistence of CK7 positive cells in the HUtMEC cell line in culture suggests this is not just a fetal trait. Moster *et al.* (2011) suggested that anti-CK-7 alone is not adequate as a marker for invasive trophoblast and additional staining with a more specific marker such as human leukocyte antigen-G (HLA-G) is essential to distinguish between different trophoblast subtypes (Moser et al., 2011). The current study strength this suggestion. The specificity of CK 7 as a trophoblastic marker needs a re-evaluation and it is more accurate to use multiple markers instead of one to characterize cells. The Heterogeneity of isolated stem cells and de-differentiation property of endothelial cells did not necessarily promote transmigration of stem cells. Under *in vitro* conditions, the same ratio of WJ-MSC and HUtMEC cells remained positive for CK7 after 22h of co-culture. Further studies are necessary and it is beyond the remit of this thesis.

Trophoblast cells did not cause any apoptosis to HUtMEC monolayers within 24h, the duration of co-culture. Furthermore, SGHPL-4 did not cross or interact with the uterine endothelial monolayer, kept the rounded morphology and clumped with each other on top of HUtMEC monolayer. Ashton *et al.* postulated that trophoblast cells induced endothelial apoptosis after *in vitro* co-culture using time lapse microscopy starting beyond 10h in HUVEC and 21h in decidual endothelial cells. Moreover, SGHPL-4 cells induce also

apoptosis of endothelium from the lumen of spiral artery by 96h after vessel perfusion with trophoblast cells (Ashton et al., 2005). Using ordinary inverted fluorescence microscopy every 15 min which entails repeated exposure to high heat from the fluorescent lamp may have caused injury and damage to the cells, this should be excluded as an artificial cause of apoptosis. Furthermore, the longer duration of contact between the trophoblast cells and the endothelial cells seem to have more apoptotic effect, so 24h used in this chapter for co-culture of trophoblast cells with HUtMEC might be insufficient to demonstrate the exact effect of SGHPL-4 on HUtMEC monolayer. An experimental design with longer duration might be a valuable future work. HUVEC cells might be more vulnerable and using HUtMEC cells is more suitable to test the effect of trophoblast on myometrial spiral arteries endothelium. However, Human uterine myometrial microvascular endothelial cells have been used previously to investigate trophoblast invasion and integration into the endothelial layers (Bainbridge et al., 2009). Trophoblast cells, albeit added at a high number (2:1rather than the 1:5 ratio used in this study) were shown to actively displace endothelial cells and form trophoblast islands in the same plane as the endothelial cells. Trophoblasts appeared here with 1:5 ratio used, not to displace HUtMEC but rather formed trophoblast islands on top of the endothelial monolayer.

Robson *et al.* (2012) postulated that uterine natural killer cells contribute to early spiral artery remodelling through secretion of a range of angiogenic growth factors found in uNK condition media (CM) not in uNK/EVT co-culture CM. This indicates sequential remodeling events where uNK initiate remodelling of spiral arteries and make it more penetrable to EVT which colonize the wall and cause more disruption in vascular smooth muscles (Robson et al., 2012). The possibility of MSC role may come after uNK and EVT, migrating to and supporting spiral artery endothelial cells and it is interesting possibility. This route would also

allow homing to maternal blood and distribution to different maternal organs specially the damaged one.

The dynamics (disruption then maturation and full occupancy) of VE- cadherin in HUtMEC after addition of umbilical stem cells seems to be related to a paracrine conversation between WJ-MSC and the adult endothelial monolayer. Choi *et al.* (2013) postulated that WJ-MSC can stimulate neovascularization by secreting paracrine factors, such as IL8, angiogenin and by acting as perivascular precursor cells (Choi et al., 2013). The observed shedding of exosomes from WJ-MSC on top adult endothelial monolayers prior to transmigration, suggests a role of exosomal signalling in the cross talk between MSC and uterine microvascular endothelial cells. Released exosomes from placental mesenchymal cells have been shown to have a dose-dependent effect on migration and tube formation of placental microvascular endothelial cells (Salomon et al., 2013). Whether exosomal signalling has a role in junctional disruption and or repair require investigation and is a future aim. The exact molecular mechanism behind transmigration of WJ-MSC across HUtMEC monolayer requires further investigations (Chapter Five).

Chapter 5

Molecular mechanisms underlying the transmigration of human umbilical mesenchymal stem cells across fetal and adult endothelial cell monolayers

5.1. Introduction

5.1.1 Migration of WJ-MSC across fetal and adult endothelial monolayers

WJ-MSC in the previous chapters, crossed fetal endothelial barrier; HUVEC and adult HUtMEC monolayers via the paracellular pathway, with maximal disruption of junctional VE-cadherin occurring at 2h after addition of the stem cells to confluent endothelial monolayers (Ebrahim and Leach, 2015). Whether this disruption is due to the physical interaction of the two cell types or whether it is induced by the secretome of WJ-MSC requires investigation. Protein array analysis of WJ-MSC (serum starved for 48h) found their secretome was enriched with pro-angiogenic growth factors including VEGF, placental growth factor (PLGF), Matrix metallopeptidase 9 (MMP-9), angiopoitein-1 and interleukin-8 (IL8) (Edwards et al., 2014).

5.1.2 VE-cadherin as a key adhesion molecule

Permeability across the endothelial barrier in non-CNS vascular beds is regulated in a dynamic manner by adherens junctions, which are composed of VE-cadherins molecule, that restrict paracellular permeability (Dejana et al., 2008). The endothelial paracellular pathway, and the adhesion molecules present therein respond to physiological and pathological factors including inflammatory mediators and permeability increasing agents such as VEGF and histamine (Esser et al., 1998, Wessel et al., 2014, Dejana et al., 2008). Activation of Src family kinases and tyrosine phosphorylation of VE-cadherin has been associated with a loss of barrier function. VEGF has been shown to increase phosphorylation of Tyr-685 in human umbilical vein cells (Wessel et al., 2014, Wallez et al., 2007). However controversy exists in the literature, with Adam *et al.* 2009 showing that Src-induced tyrosine phosphorylation of VE-cadherin is not sufficient to promote an increase in monolayer permeability in human dermal microvascular cells (Adam et al., 2010). This may be a cell specific response. A

recent *in vivo* study suggests that the opening of endothelial junctions for the passage of plasma proteins or leukocytes depends on two different tyrosine residues of VE-cadherin where phosphorylation is regulated in opposite ways. Using knock-in mice expressing a Y685 mutant of VE-cadherin or a Y731F mutant, the authors demonstrated phosphorylation and de-phosphorylation of VE-cadherin at Tyr685 and Tyr731 governs induction of vascular permeability or leukocyte diapedesis leukocyte diapedesis (Sidibe and Imhof, 2014). The latter required internalisation of VE-cadherin via tyrosine phosphatase SHP-2 with the resultant frank opening necessary for leukocyte paracellular trafficking.

5.1.3 Vascular Endothelial Growth Factor

VEGF has long been known to increase vascular permeability (Senger et al., 1983). In HUVEC, it stimulated VE-cadherin–catenin complex tyrosine phosphorylation within 15 min and exaggerated cellular permeability significantly after more than one hours delay from the beginning of stimulation (Esser et al., 1998). This delay might be as a result of pre-treatment of the cells with vanadate (protein tyrosine phosphatase inhibitor) for biochemical analysis (Vestweber et al., 2009).

5.1.4 Leukocyte transendothelial migration

Leukocyte extravasation is a complex multistep process that requires activation of various adhesion molecules and signaling pathways in both leukocytes and endothelial cells. Induction of endothelial permeability is dependent on the phosphorylation of only VE-cadherin Tyr685, but not Tyr731, by vascular permeability inducing factors such as VEGF or histamine. However, leukocytes extravasation relies exclusively on the de-phosphorylation of Tyr731, which by turn stimulate endocytosis of VE-cadherin (Figure 43) (Wessel et al., 2014, Vestweber et al., 2014).

This chapter therefore will address whether WJ-MSC transmigrating across fetal or adult endothelial monolayers employ a strategy similar to leukocytes. Mesenchymal stem cells derived from bone marrow and WJ-MSC have been shown to cross primary human lung and heart microvascular endothelial monolayers (Teo et al., 2012) and HUVEC (Ebrahim and Leach, 2015) in a fashion similar to leukocytes, although the duration of the process: from encounter to sub-endothelial destination, took longer than that for leukocytes crossing at sites of inflammation (Ebrahim and Leach, 2015, Teo et al., 2012, Wessel et al., 2014, Stock and Riethmuller, 2011).

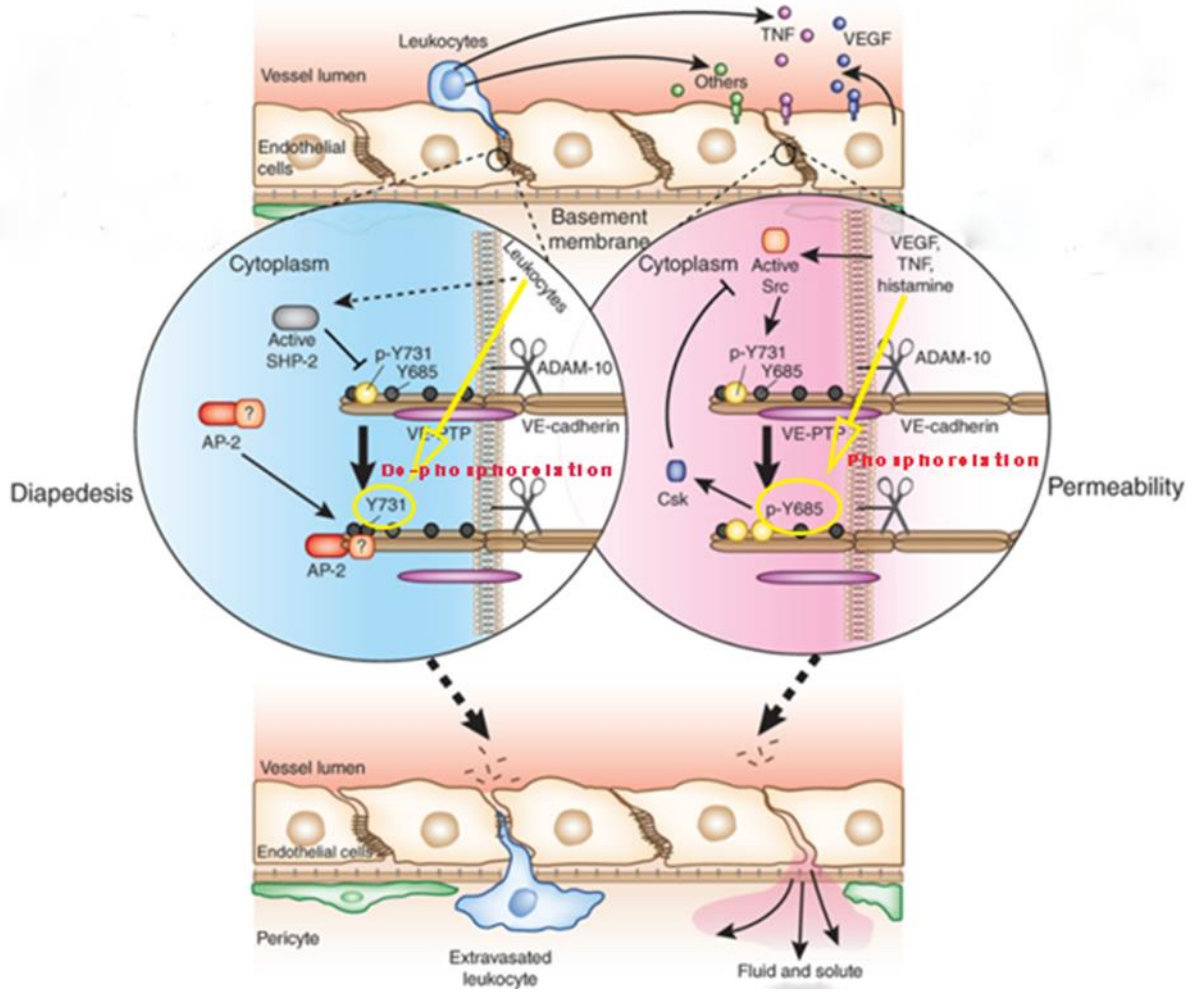


Figure 43: Mechanisms employed in leukocyte extravasation

A diagram demonstrating the mechanisms controlling leukocyte transendothelial migration was taken and modified from (Sidibe and Imhof, 2014). When the leukocytes come to contact with inflamed endothelium, it secretes inflammatory agents like TNF-α and induce the endothelial cells to secrete VEGF, which by turn phosphorylate Tyr685 and increase vascular permeability. During leukocyte extravasation process, Tyr731 underwent de-phosphorylation, this induces internalization of VE-cadherin away from the cell membrane and open the junctions more for the leukocytes to cross the endothelium.

5.1.5 Aims of the chapter

The aims of this chapter are to investigate the mechanisms behind paracellular migration of WJ-MSC across HUVEC or HUtMEC cells and the effect of WJ-MSC on VE-cadherin integrity in both fetal and adult endothelial monolayers. Using ELISA and protein expression analyses this chapter specifically investigated the phosphorylation events which would allow physiological paracellular extravasation and the secretion of VEGF in the condition media after co-culture of WJ-MSC with both HUVEC and HUtMEC monolayers.

5.2. Materials & methods

Materials

Chemical and reagents

DPBS, calcium and magnesium free, trypsin – EDTA solution 1x (0.5 g porcine trypsin and 0.2 g EDTA in 4 Nacl HBSS), FBS, all were purchased from Sigma-Aldrich, UK. Basal endothelial cell growth medium MV with its growth supplement (Promocell, UK). Antibiotic/antimycotic solution (10,000 u/mL pencillin G, 10,000 µg/mL streptomycin, 25 µg/mL amphotercin B) (Hyclone, UK). DMSO, paraformaldehyde, BSA and gelatin from bovine skin (type B) (Sigma- Aldrich). Lysis buffer (20 mM Tris (Invitrogen) + 320 mM sucrose (BDH) + 0.1% Triton X 100 + 1 mM NaF + 10 mM β glycophosphate + 1 mM EGTA + 300 µM Sodium Orthovanadate and protease inhibitor; pH 7.6).

Tissue Culture Plastics and Accessories

Tissue culture flasks 75 cm^2, 12 wells plates and Cover slips 19 mm (Life Technologies). Cryopreservation tubes (1 mL) (Sarstedt, Leicester, UK). Tc 10 counting slides (Bio- Rad, UK).

Antibodies for Immunocytochemistry

Polyclonal antibody to VE-cadherin p-Tyr 685(ECM Biosciences, UK), polyclonal antibody to VE-cadherin p-Tyr731(abcam, UK) and β-Actin (Sigma-Aldrich, UK). Rabbit-anti human VE-cadherin (Cell Signalling, UK). Purified mouse antihuman CD144 (Pharmingen, BD Biosciences, UK). Secondary antibodies: IgG secondary antibodies for Western blotting were purchased from Li-Cor Bioscience. Anti-mouse IgG (whole molecule FITC produced in goat affinity isolated antibody) (Sigma-Aldrich, UK), Vector: Vectashield mounting medium for fluorescence (Vector laboratories, Inc Burlingame, CA 94010). ELISA kit and human anti-VEGF-A (R&D Systems, UK).

Methods

5.2.1 Immunoblot analysis to measure the phosphorylation status of VE-cadherin

The early hours of WJ-MSC interactions with either HUVEC or HUtMEC monolayers (0, 0.5, 1 & 2 h) and the late hours (22 & 48h) were chosen to measure the phosphorylation status of VE-cadherin at Tyr685 or Tyr731 tyrosine residues by Western blotting in controls (HUVEC or HUtMEC in 50:50 endothelial/stem cell media) and stem cell treated groups. A third study group, included stem cell treated groups cultured in the presence of anti-VEGF (2µg/ml) and analysed at 2 and 22h (n = 3).

HUVEC and HUtMEC cells were grown to 70% confluence on gelatin-coated 6 well plates in endothelial media (EM) and then grown to full confluence in mixed culture media (50% EM: 50% stem cell media) before addition of WJ-MSC (20,000 WJ-MSC: 100,000 endothelial cells).

Briefly, cells were scraped and lysed in 200 µl Lysis buffer. De-natured proteins were separated in a 4-20% gradient polyacrylamide gel after equal loading (15 µl) and transferred to a nitrocellulose membrane. After blocking with 5% skimmed milk powder in 0.1% Tris buffered saline with Tween 20 for 60 min at RT, the membranes were incubated with the antibodies against VE-cadherin, phosho Tyr685, phosho Tyr731 (1:1000 dilution) and β-Actin (1:3000). A Li-cor Odyssey scanner and Odyssey software (Image Studio Version 3.1.4) were used to measure OD. P-Tyr 685, p-Tyr731 and VE-cadherin protein expressions for the different durations and study groups were obtained. P-Tyr 685, p-Tyr731 protein expression (normalized against VE-cadherin) were analysed using Two-way ANOVA (Prism 6 software) and Sidak's multiple comparison test to compare controls versus stem cell treated groups. Statistical significance was taken at $p<0.05$.

5.2.2 ELISA assay to measure VEGF secretion in different conditioned media

Levels of VEGF in the different conditioned media (CM); WJ-MSC CM, HUVEC CM, HUtMEC CM and HUVEC or HUtMEC co-cultured with or without (in 50:50 endothelial/stem cell media) WJ-MSC at 2, 22 & 48h and co-cultured groups at 2, 22h after neutralisation with anti-VEGF antibody were measured by ELISA (Human VEGF Immunoassay designed to measure VEGF165 and 121 levels in cell culture supernates, serum, and plasma).

WJ-MSC, HUVEC and HUtMEC were grown to confluence separately in 75 cm^2 flasks and the different CM were collected. HUVEC and HUtMEC were again seeded, co-cultured with or without WJ-MSC and with WJ-MSC after addition of anti-VEGF antibody (2µg/ml) as described previously in western blotting section. The control groups; mono-culture CM (in

50:50 endothelial/stem cell media), co-culture CM (CO-CM) and CO-CM neutralized with anti-VEGF antibody were collected.

Assays were conducted according to the manufacturer's instructions. Briefly, reagents were brought to room temperature. Standards and samples (200µl/well) were pipetted in duplicate. After 2 h incubation, the plate was washed three times, and then 200µl of VEGF Conjugate was added to all wells. After 2 h incubation, the plate was washed again and 200µl of substrate solution was added to each well. The reaction was stopped after 20 min by adding the stop solution. The optical absorbance of the wells was read at 450 nm (Infinite F50 absorbance microplate readers, & Magellan Tracker software, TECAN, Switzerland).

Sample concentrations are expressed as pg/ml based on standard curves plotted using protein standards supplies with the kits. Statistical analysis was performed using GraphPad Prism software (Version 6, GraphPad Prism Software Inc.). Data were analysed using One-way ANOVA and Sidak's multiple comparisons test. Statistical significance was taken at $p < 0.05$, presented as mean ± SEM. Internal repeats (x3) from three different isolates were compared.

5.2.3 Effect of anti-VEGF on the migration of WJ-MSC across HUtMEC monolayers

To obtain co-cultures of HUtMEC in contact with WJ-MSC, 100,000 HUtMEC were seeded on a 1 % gelatin-coated coverslip (19mm diameter) and incubated in endothelial media. Once 70 ٪ confluence was reached the media was changed to mixed media. On full confluence, 20,000 isolated PKH26 labelled WJ-MSC were seeded on top of the confluent HUtMEC monolayer (1: 5 ratio) per coverslip in 1 mL of the mixed media with or without (controls) anti-VEGF (2µg/ml).

Confluent monolayers of HUtMEC with added PKH26-labelled WJ-MSC for 2 and 22 hours with or without anti-VEGF, were fixed and immune-labelled for VE-cadherin as previously described in the previous chapters. Systematic random sampling was used to acquire 10 images per coverslip for the chosen durations. After blinding, the position and number of the labelled WJ-MSC, apical or sub-endothelial were recorded for the co-cultures with or without anti-VEGF.

5.2.4 Effect of secretome derived from co-culture of WJ-MSC and HUVEC on VE-cadherin junctional occupancy

WJ-MSC cultures alone were grown to confluence (1 x 10^6 cells) in 75 cm^2 tissue culture flasks in 100% stem cell media alone (with added 15% fetal calf serum). Conditioned media (WJMSC-CM; 1ml) were collected 24h after confluence was reached. Collected media were centrifuged at 1000 rpm for 5 minutes and stored at -80^0C.

Freshly isolated HUVEC (P2-4) were grown on gelatin-coated 19mm coverslips in 12 well plates and incubated at 37^{o}C, 5% CO2 in one ml of endothelial growth medium in each well. Again, once 70% confluence was reached, they were grown to full confluence in mixed culture media. They were then treated with 1 ml of Co-CM or WJMSC-CM. Unstimulated HUVEC in mixed culture media and stem cell media (100%) acted as controls.

After 2h incubation, VE-cadherin dynamics were analysed. Samples were fixed (1% p-formaldehyde), permeabilized, blocked in non-immune goat serum (5%) and incubated overnight with mouse anti-human VE-cadherin (5µg/ml). They were then incubated with goat anti-mouse FITC conjugated secondary antibody. Cells were viewed with a Nikon

fluorescence microscope with the suitable fluorescence filter to visualise FITC, was photographed with CCD camera (Nikon DS) and was stored (NIS elements F3.0; Nikon).

Images were taken in a systematic fashion (10 per coverslip). Acquired images were anonymised and the percentage of paracellular clefts showing continuous immunostaining of VE-cadherin was counted using a grid overlay and the forbidden line principle. Three different isolates were tested, with 3 experimental repeats. Data were analysed using One-way ANOVA (Prism 6 software) and Sidak's multiple comparison test to compare controls versus CM groups. Statistical significance was taken at $p<0.05$.

5.3. Results

5. 3.1 WJ-MSC causes changes in phosphorylation/dephosphorylation of endothelial VE-cadherin at specific tyrosine residues similar to that seen for transmigrating leucocytes

Immunoblot studies showed that protein expression of VE-cadherin in HUVEC was similar to controls in the early hours of co-culture. Increased expression of VE-cadherin was seen at 22 and 48h co-culture (Figure 44). This is indicative of increased junctional maturity after transmigration of stem cells to sub-endothelial niche. Upon addition of WJ-MSC, a significant up-regulation in phosphorylation of Tyr685 was seen as an early event - from 60 min onwards compared to controls (Figure 44, 45). However, Tyr731 showed basal level of phosphorylation similar to the controls at 0 and 0.5 h, followed by decrease in p-Tyr731 expression at 1-2h, however it failed to reach statistical significance (Figure 44, 46). By 48h, both phosphorylation and de-phosphorylation status of VE-cadherin returned to normal. Adding anti-VEGF did not block the phosphorylation of Tyr685 and did not affect Tyr731 de-phosphorylation (Figure 44).

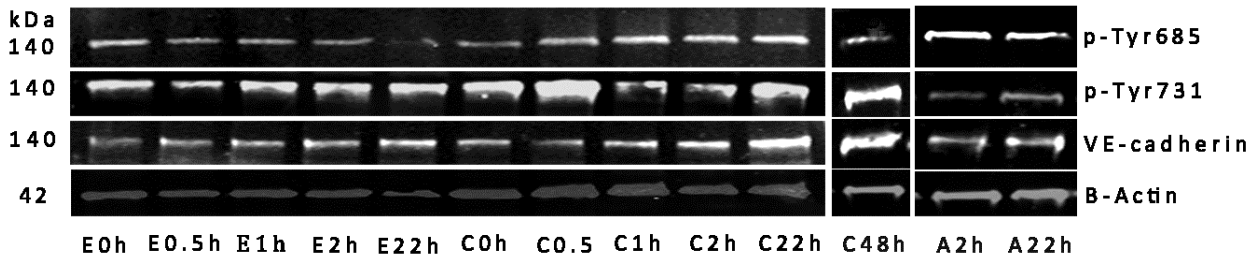


Figure 44: Representative Immunoblots

Representative Immunoblots (n = 3) HUVEC with (co-cultured groups; C0h-C48h) or without WJ-MSC (endothelial groups; E0h-E22h) and co-cultured group at 2, 22h after neutralisation with anti-VEGF antibody (A2h & A22h). VE-cadherin, p-Tyr685 and p-Tyr731 expressions at different durations are shown. B-actin was used as a loading control. HUVEC treated with WJ-MSC showed increase in phosphorylation of Tyr685 at early hours (1- 2h) compared to controls. However, Tyr731 showed basal level of phosphorylation similar to the controls at 0 and 0.5 h, followed by decrease in p-Tyr731 expression at 1 and 2h. By 48h, both phosphorylation and de- phosphorylation status of VE-cadherin returned to normal. Adding anti-VEGF did not block the phosphorylation of Tyr685 and did not affect Tyr731 de- phosphorylation at 2 and 22h.

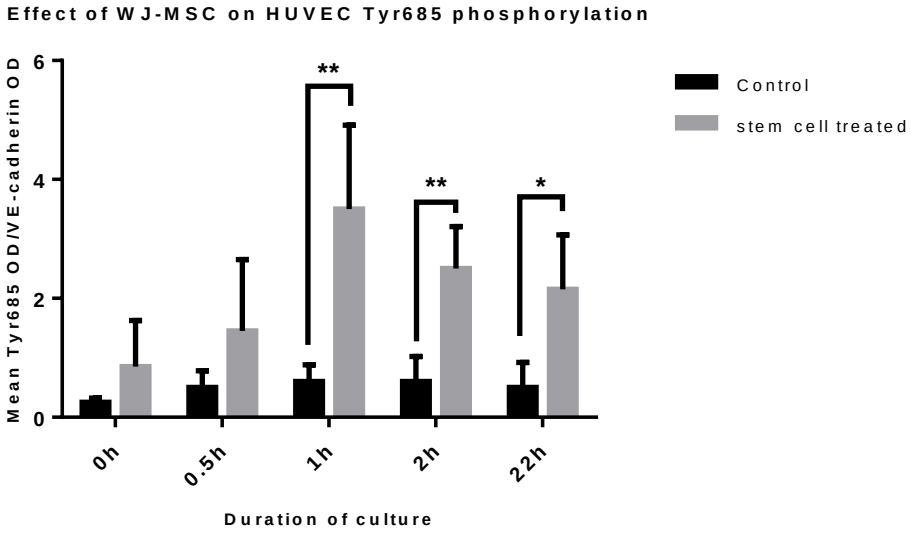


Figure 45: Tyr685 histogram

Histogram showing mean optical density (OD) + S.E.M of normalised Tyr685 expression against VE-cadherin from three different blots of control HUVEC and co-cultures with WJ-MSC from0h to 22h. There was a significant upregulation of Tyr685 expression at 1-2h ($p < 0.01$) and 22h ($p < 0.05$) in the co-culture groups. (n = 3).

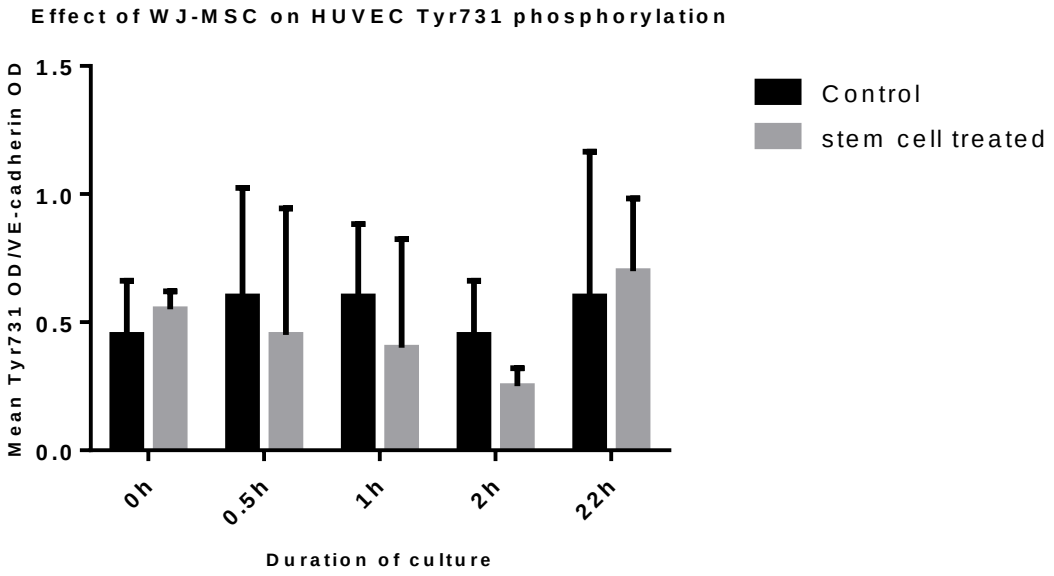


Figure 46: Tyr731 histogram

Histogram showing mean optical density (OD) + S.E.M of normalised Tyr731 expression against VE-cadherin from three different blots of control HUVEC and stem cell treated from0h to 22h. There was down regulation of Tyr731 expression at 2h in the co-culture group, however it failed to reach to significant value ($p < 0.05$). ($n = 3$).

HUtMEC treated with WJ-MSC showed a 2-fold significant ($p< 0.01$) increase in phosphorylation of Tyr685 at early hours compared to controls (Fig 47, 48). Tyr731 showed basal level of phosphorylation similar to the controls, followed by a significant decrease in p-Tyr731 expression at 2 and 22h (Figure 47, 49). By 48h, both phosphorylation and de-phosphorylation status of VE-cadherin returned to normal. Adding anti-VEGF blocked the phosphorylation of Tyr685 at, but did not affect Tyr731 de-phosphorylation (Figure 47). Protein expression of VE-cadherin was highest at 22 and 48h, indicative of increased endothelial junctional maturity after transmigration of WJ-MSC and residence in sub-endothelial niche similar to HUVEC (Figure 47).

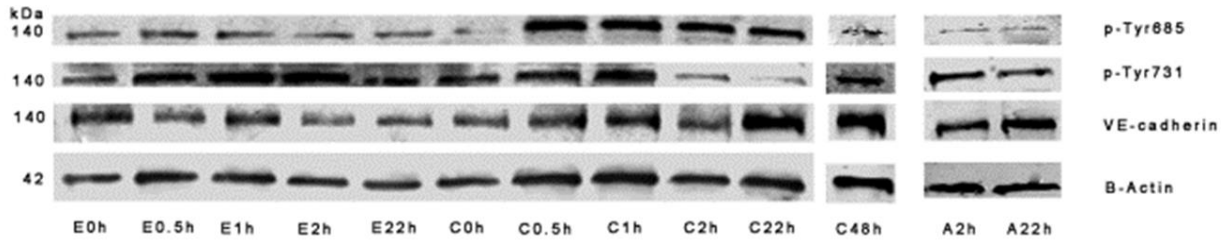


Figure 47: Representative Immunoblots showing expression and phosphorylation of VE-cadherin

Representative Immunoblots (n = 3) showing expression and phosphorylation of VE-cadherin at different durations of co-culture. Representative Immunoblots of HUtMEC co-cultured with (C0-C48h) or without WJ-MSC (E0-E22h) and co-cultured group at 2, 22h after neutralisation with anti-VEGF antibody (A2h & A22h). VE-cadherin, p-Tyr685 and p-Tyr731 expressions at different durations are shown. B-actin was used as a loading control. HUtMEC treated with WJ-MSC show a 2-fold increase in phosphorylation of Tyr685 at the early hours (0.5, 1 and 2h) compared to controls. Tyr731 shows a basal level of phosphorylation similar to the controls at 0, 0.5 and 1h, followed by a dramatic decrease in p-Tyr731 expression at 2 and 22h. By 48h, both phosphorylation and de- phosphorylation status of VE-cadherin returned to normal. Adding anti-VEGF blocked the phosphorylation of Tyr685 at 2 & 22h, but did not affect the later Tyr731 de- phosphorylation.

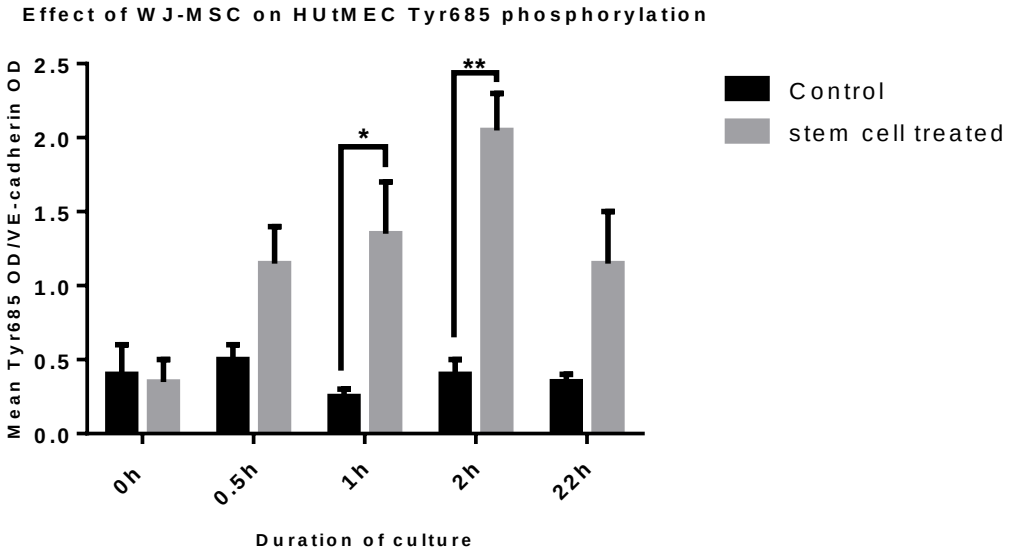


Figure 48: Tyr685 histogram

Histogram showing mean optical density (OD) + S.E.M of normalised Tyr685 expression of control HUtMEC and co-cultures with WJ-MSC from 0h to 22h. One-way ANOVA revealed a significant upregulation of Tyr685 expression at 1h ($p < 0.05$) and 2h in the co-culture groups ($p < 0.01$). (n = 3).

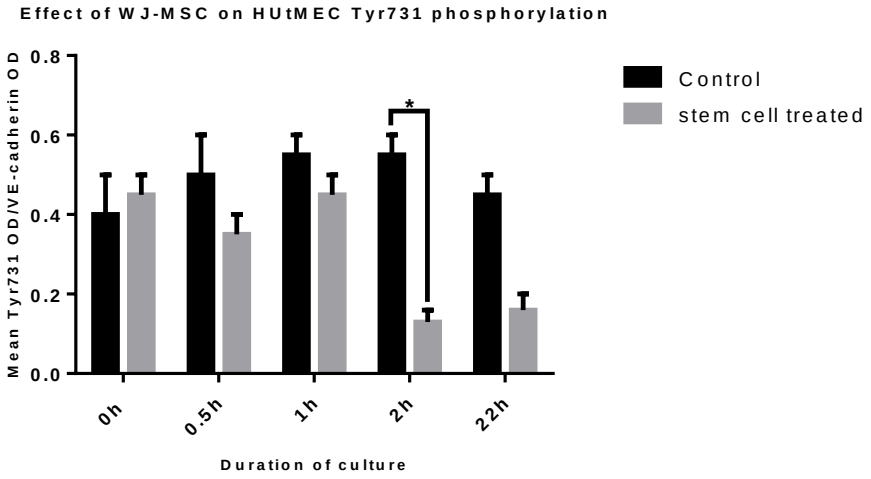


Figure 49: Tyr731 histogram

Histogram showing mean optical density (OD) + S.E.M of normalised Tyr731 expression of control HUtMEC and stem cell treated from 0h to 22h. One-way ANOVA revealed a significant down regulation of Tyr731 expression at 2h in the co-culture group, $p < 0.05$. ($n = 3$).

5.3.2 VEGF secretion in co-culture condition media

ELISA revealed negligible concentrations of VEGF in WJ-MSC and HUVEC conditioned media. Moreover, HUVEC co-cultured with WJ-MSC showed no VEGF secretion at 2h and 22h. In comparison, HUtMEC CM contained 0-40 pg/ml of VEGF. When HUtMEC cultured in mixed media VEGF level was between 0-10 pg/ml at 2h and reduced to an undetected value by 22 and 48h. Treatment of HUtMEC with WJ-MSC induced a significant increase in VEGF at 2h followed by a significant decrease at 22h. No VEGF was detected by 48h like control HUtMEC in mixed media. Presence of anti-VEGF in the co-cultures blocked VEGF secretion (detection) at 2 and 22h (Figure 50).

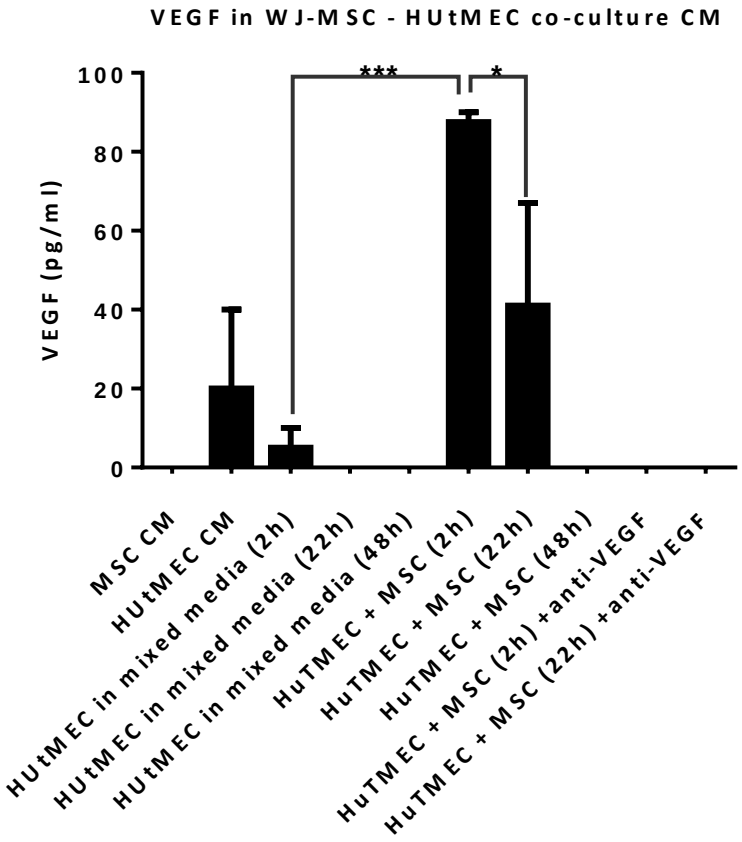


Figure 50: Histogram showing VEGF concentrations in CM

VEGF concentrations in conditioned media/supernatants at different durations (n = 3). ELISA studies (n=3) revealed negligible concentrations of VEGF in WJ-MSC CM, whilst levels in HUtMEC CM ranged from 0 - 40 pg/ml. HUtMEC in mixed media (Stem cell: endothelial media) revealed an initial VEGF secretion that became undetectable at 22 and 48h. In supernatants from HUtMEC treated with WJ-MSC, there was a statistically significant increase in VEGF at 2h (One-way ANOVA $p < 0.001$) compared to HUtMEC in mixed media at 2h, followed by a decrease ($p < 0.05$) at 22h. No VEGF was detected by 48h. The increase in VEGF at 2 and 22h was not seen in the supernatant of co-cultures grown in the presence of VEGF neutralising antibodies.

Addition of anti-VEGF to WJ-MSC-HUtMEC co-cultures reduces the migration of fetal stem cells from 52 $\pm$ 3% (control groups without adding anti-VEGF) to 27 $\pm$ 2 % at 2h interactions. By 22h, migrations in control groups were 90 $\pm$ 8 %, while in anti-VEGF treated groups were 47 $\pm$ 6 %.

5.3.4 WJ-MSC-HUVEC co-culture CM alter VE-cadherin junctional occupancy in HUVEC

In control experiments, VE-cadherin was localised to paracellular junctional regions in HUVEC (Fig 51). The percentage of paracellular clefts showing junctional disruption was not statistically significant whether grown in mixed media (21.4 $\pm$ 3.8%) or stem cell media (26.2 $\pm$ 8.5%).

When HUVEC monolayers were subjected to the co-culture conditioned media (Co-CM) for 2h, there was an increase in percentage of paracellular clefts (36.6 $\pm$ 7.3%) showing discontinuous (stitch- like to complete loss) VE-Cadherin staining (Fig 51). Frank gaps between cells were also present. This junctional disruption was significantly different ($p < 0.001$) from that counted in mixed media only control (Fig 51; Fig 52).

Conditioned media from 24h stem cell cultures alone (WJMSC-CM) also caused a statistically significant disruption of VE-cadherin junctions (43.9 % $\pm$ 10.9; Fig 52). This was similar to that seen for the co-culture secretome. No statistically significant difference was found between these two experimental groups (Fig 52).

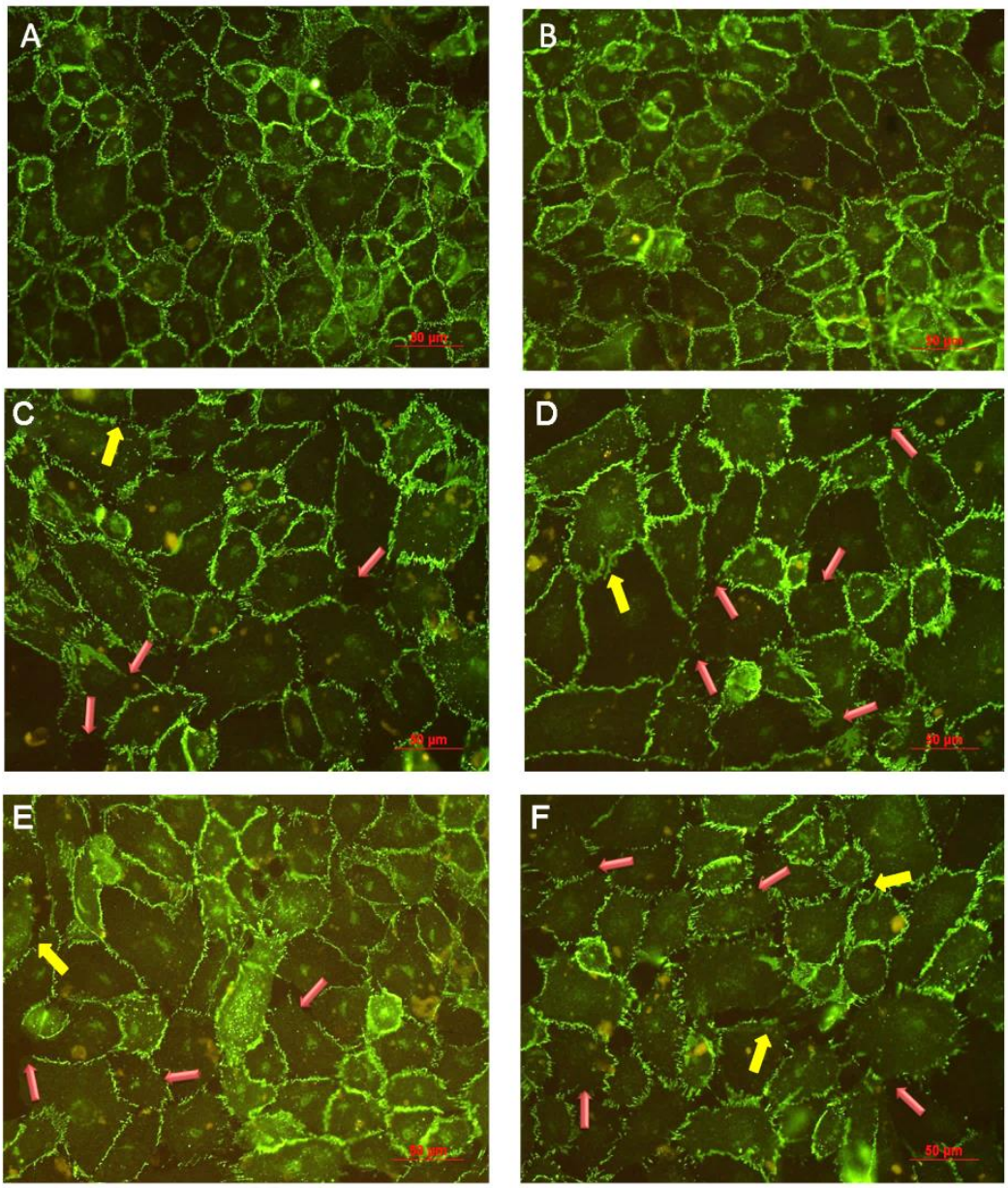


Figure 51: Micrographs of VE-cadherin localisation in different medium

(A & B) Micrographs of HUVEC grown in mixed media & stem cell media respectively (Controls). VE-Cadherin is localised to cell-cell boundaries and display a predominantly continuous staining. (C & D) Micrographs of HUVEC grown in in co-culture condition media showing increased numbers of paracellular clefts with discontinuous VE-Cadherin. (E & F) Micrographs of HUVEC grown in WJ-MSC condition media showing increased numbers of paracellular clefts with discontinuous VE-Cadherin. Yellow arrow = stitch-like; pink arrow = complete loss. Representative sample out of 3 experimental repeats

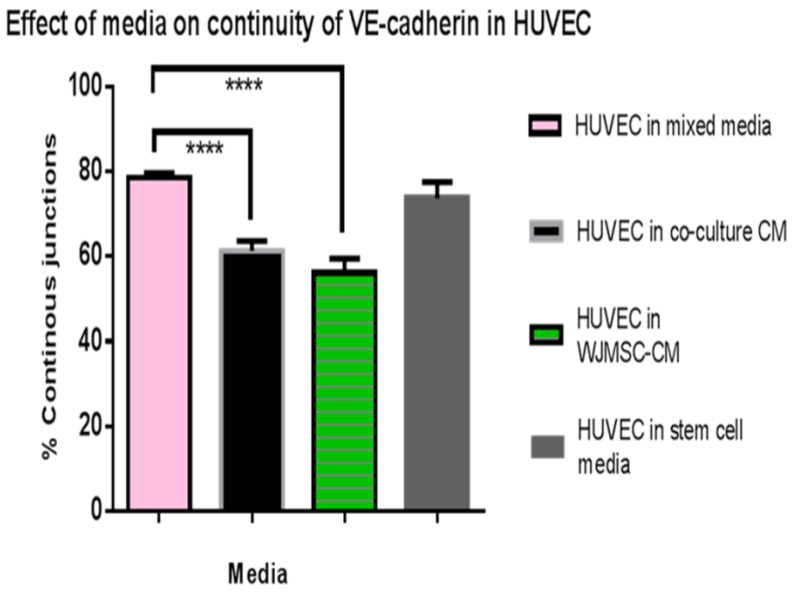


Figure 52: Histograph showing percentage of continuous VE-Cadherin junctions in HUVEC treated with different medium

One-way ANOVA revealed a significant decrease in the percentage of continuous VE-Cadherin junctions ($p < 0.0001$). HUVEC treated with co-culture CM compared to control and significant decrease also in the group treated with WJ-MSC CM ($p < 0.0001$). While the group treated with stem cell media showed no significant change from control. ($n = 3$).

5.4. Discussion

The data obtained in the previous chapters suggests that WJ-MSC can traverse confluent intact fetal and maternal endothelial monolayers via paracellular junctions, through disruption of junctional molecule VE-cadherin. This chapter showed the molecular mechanisms behind this endothelial VE-cadherin disruption, the paracellular migration of WJ-MSC and whether the mechanism employed here is similar to leukocytes extravasation.

Addition of WJ-MSC induced a significant Tyr685 phosphorylation of VE-cadherin and junctional discontinuity in early interactions (1-2h). This was followed by Tyr731 de-

phosphorylation during the period of maximum stem cell extravasation in both HUVEC and HUtMEC endothelial cell monolayers. The de-phosphorylation of Tyr731 was significant in HUtMEC, while it failed to reach to significant levels in HUVEC. VEGF levels were highest in supernatants from co-cultures at 2h in HUtMEC co-cultured with WJ-MSC, suggestive of its role in early interactions, while no VEGF levels were detected in HUVEC co-cultures. Addition of anti-VEGF antibody also did block Tyr685 phosphorylation, but did not affect the VEGF-independent Tyr731 de-phosphorylation in HUtMEC co-cultured with WJ-MSC. However in HUVEC co-culture with WJ-MSC, anti-VEGF did not block the phosphorylation of Tyr685 or the de-phosphorylation of Tyr731.

The molecular mechanism utilised by the fetal stem cells to cross the uterine endothelial barrier, appeared to involve the initial phosphorylation of VE-cadherin at its Tyr685 residue from 30 min onwards followed by return to normal by 48h. Enhanced de- phosphorylation of Try731 tyrosine residue was also seen at 2h which coincided with maximum extravasation time of WJ-MSC. Given the accepted role of VEGF in increasing vascular permeability (Leung et al., 1989, Keck et al., 1989, Byrne et al., 2005) and its ability to induce opening of inter-endothelial cell junctions, including VE-cadherin junctions (Lampugnani et al., 2006, Dejana et al., 2008). VEGF level was highest at 2h, suggestive of its role in early interactions. VEGF have been shown to target the Y685 residue of VE-cadherin (Wallez et al., 2007), thus a similar phosphorylation in this study may be partly induced by VEGF in the early hours of co-culture. The resultant transmembrane redistribution of VE-cadherin from junctional regions favours egress of the spindle-shaped WJ-MSC, blocking of this by VEGF neutralising antibodies reduced the number of cells transmigrating in the early hours by a quarter. VEGF may only be one contributory secretory factor, given WJ-MSC can secrete a repertoire of permeability enhancing factors and cytokines which are also able to induce Src-

mediated VE-cadherin changes. Wessel *et al* (2014) showed that whilst Tyr685 phosphorylation induces vascular permeability, de-phosphorylation of Tyr731 selectively regulates leukocyte extravasation (Wessel et al., 2014). The authors used siRNA to block de-phosphorylation of Tyr731 through inhibition of SHP-2 expression. This impaired VE-cadherin internalisation and reduced leukocyte migration by 36 %. In this co-culture study, VE-cadherin showed a similar Tyr731 de-phosphorylation at 2 and 22h – a period of continued trans-endothelial migration. Addition of anti-VEGF antibody did not affect the de-phosphorylation. There was a continued egress of WJ-MSC between 2-22h, suggestive that these cells may also be inducing the SHP-2 associated de-phosphorylation and internalisation of VE-cadherin in HUtMEC.

Several observations support the hypothesis of involvement of VEGF in transendothelial migration of stem cells across adult endothelium, VEGF secretion was significantly induced in CM after addition of WJ-MSC. Neutralizing antibody blocked VEGF dependant Tyr-685 phosphorylation. Finally, Antibody that block VEGF receptor interaction partially attenuated the paracellular trafficking of MSC across maternal endothelium. This observation was supported by the report that bone marrow derived endothelial progenitor cells migration and proliferation *in vitro*, were significantly increased in response to treatment with VEGF and could be also partly attenuated by anti-VEGF (Fu et al., 2006). Human MSC trans-endothelial migration *in vitro* or across the placenta to the fetal side in pregnant rat model was also induced by VEGF-A and integrins which mediated MSC adhesion to the endothelium. VEGF-A neutralizing antibody or antibodies against VEGFR-1 or integrin inhibited the migration (Chen et al., 2008).

However in HUVEC, VEGF seems not to be the key player. No VEGF was detected in co-culture CM. Moreover, addition of anti-VEGF did not block the phosphorylation of Tyr-685. In the meantime, addition of stem cells induced a significant Tyr685 phosphorylation in the early hours of interaction of WJ-MSC with fetal endothelial cells. Moreover, Interaction of WJ-MSC (20,000 cells) with HUVEC (100,000 cells) for 2h leads to secretion of other growth factors that can disrupt VE-cadherin localisation. The potency of this is similar to that obtained from WJ-MSC (1 x 10^6 cells) grown for 24h. Time constraints did not allow analysis of the growth factors/cytokines which may have been at play here.

Protein array analysis of WJ-MSC (serum starved for 48h) found their secretome was enriched with pro-angiogenic growth factors including VEGF, PLGF, Matrix metallopeptidase (MMP)-9, angiopoitein-1 and interleukin-8 (IL-8) (Edwards et al., 2014). On the other hand, WJ-MSC supernatant was quantified for different cytokines and growth factors after cell proliferation in full growth media supplemented with 10% FBS for 8 days. The data obtained was compared to BM-MSC and adipose tissue MSC supernatants grown in the same condition. WJ-MSC did not produce any detectable amount of VEGF, however, it was the highest in secretion of IL 6 and 8 compared to BM-MSC or adipose tissue MSC (Amable et al., 2014). VEGF secreted by WJ-MSC seems to be detected under stressful conditions like serum starvation not in basal condition.

VEGF takes up to 30min to phosphorylate VE-cadherin (Esser et al., 1998), however, TNF-α takes longer (hours) to phosphorylate, disrupt VE-cadherin, mediate loss of barrier function and induce leukocyte transmigration *in vitro* across HUVEC (Angelini et al., 2006, Laviola et al., 2013). Treatment of endothelial cell with TNF-α for 1h enhanced MSC-endothelial cells interactions and increased the numbers of migrating BM-MSC across the endothelium by 2–3

folds. Demonstrating that TNF-α endothelial activation promotes both adhesion and transmigration of MSC (Teo et al., 2012). TNF-α can also increase the expression of VCAM-1 on rat BM-MSC and promote its adhesion to endothelial cells and migration to damaged tissue (Xiao et al., 2012).TNF-α and or other factor of the previous agents such as IL6 or 8, might be behind phosphorylation and dislocation of VE-cadherin adherens junction in HUVEC monolayers. Thus, stem cell and HUVEC interactions results in an enrichment of pro-angiogenic growth factor secretions other than VEGF into the medium which induces VE-cadherin translocation from adherens junctions. The accompanying early phosphorylation of VE-cadherin at Tyr-685, failure of anti-VEGF to block this phosphorylation and the longer time lag (60 min) than in HUtMEC transmigration (30 min), strengthens this hypothesis. Histamine was observed to induce Tyr685 phosphorylation in venules rather than arterioles, VEGF was even more selective and induced phosphorylation of Tyr685 only on small sub-population of capillaries (Wessel et al., 2014). Histamine was demonstrated to open up junctions in the entire placental microcirculation (Leach et al., 1995). Tyr685 in various types of endothelial cells seems to be phosphorylated by different triggers. This was matching the observation in the current study, where Tyr685 phosphorylation in HUtMEC not in HUVEC may be induced by VEFG.

These data also demonstrates that pro-angiogenic secretions that can alter fetal endothelial junctional integrity are a feature of stem cell conditioned media from WJ-MSC monocultures; this adds to the growing literature that suggests that cell-free conditioned media may be of use in stem cell therapy (Edwards et al., 2014, Todeschi et al., 2015). Use of neutralising antibodies to identify the specific growth factors involved would be valuable future work.

WJ-MSC appears to utilise similar molecular mechanisms employed by leukocytes migrating through endothelial monolayers. However, WJ-MSC transmigration events to reach the sub-endothelial niches, takes hours, rather than minutes and might be a consequence of transmigration across non-stimulated or non-inflamed endothelium. The post migration upregulation of VE-cadherin in both fetal and adult endothelial cells monolayers is exciting and holds the promise of the usefulness of WJ-MSC in vascular repair and junctional maturation.

Chapter 6

General discussion and future work

6.1. WJ-MSC and their potential role in vascular repair

In this study, WJ-MSC migrated to their perivascular niches across fetal and adult endothelial cell monolayers and induced endothelial repair and junctional maturity once the adlumenal surface is reached. This suggests that these cells can play a pericytic role in the vascular system and strengthen the hypothesis that pericytes may be derived from MSC. Pericytes are cells that reside on the wall of the blood vessels and their primary function is to maintain the vessel integrity. Pericytes have an essential role in the development and formation of a vascular network (Yancopoulos et al., 2000). Indeed pericytes have been shown to have stem cell-like properties, being able to differentiate into adipocytes, chondrocytes and osteoblasts, leading them to be regarded as mesenchymal stem cells (Richardson et al., 1982, Caplan, 2008, Paquet-Fifield et al., 2009, Hirschi and D'Amore, 1996). Understanding the role of WJ-MSC in the vascular system and the migration to their perivascular niches rather than integration into the endothelial monolayers provide new insight and may benefit stem cell cytotherapy studies. It may lead to better monitoring of WJ-MSC applied in experimental and clinical studies. WJ-MSC could be also used in treatment of vascular diseases where repair of the vascular endothelium is necessary.

After migration to sub-endothelial niches, WJ-MSC maintained their spindle shaped morphology and showed negativity to VE-cadherin. However, it is important to flow up those cells to investigate their ability to maintain the mesenchymal and the pluripotent properties after migration through fetal or adult endothelial monolayers. For example, using transwell plates may be a valuable future work, to seed fetal or adult endothelial cells on the membrane of the upper chambers till sub-confluence in endothelial media then to full confluence in mixed media. WJ-MSC should be seeded on top of endothelial cells, then after 24h, mesenchymal stem cells could be collected from the bottom of the upper chambers.

Characterization of WJ-MSC could be carried out by flow cytometry to check presence or absence of mesenchymal or pluripotent markers.

The data obtained in this study are the first to show the early events of transmigration of WJ-MSC isolated from the human umbilical cord through fetal and adult endothelial cell monolayers. WJ-MSC displayed non-apoptotic blebbing, amoeboid movement and interrogation of intercellular openings as early events in their exploration of the fetal and the uterine endothelial monolayer. The changes in morphology to a more spindle shaped phenotype may aid the egress of WJ-MSC though paracellular pathways.

WJ-MSC preferred the paracellular pathway taking hours rather than minutes to reach their sub-endothelial niches; this would help in better monitoring of stem cells after intravenous injection in human stem cell therapy applications. Many clinical trials are currently evaluating WJ-MSC for treatment of diverse cardiovascular, inflammatory and autoimmune diseases (Wang et al., 2014, Musialek et al., 2015). Most of the clinical trials involve the systemic infusion of WJ-MSC into the vascular circulation (Wang et al., 2014, Musialek et al., 2015, Hu et al., 2013). Moreover, physiological homing ability of endogenous MSC is supported by studies reporting that endogenous MSC can be mobilized from the bone marrow and recruited into the site of injury in acute myocardial infarction (Kawada et al., 2004). A critical step in such recruitment and engraftment is the exit of MSC from the vascular circulation (extravasation), which requires crossing the endothelial cell barrier that lines blood vessels. For WJ-MSC, this process of extravasation was studied in this project.

This study (although it is *in vitro*) provides some understanding of the cellular and molecular mechanisms used by WJ-MSC to cross the endothelial monolayers; this has

implications on stem cell therapy. Moreover, continued work into elucidation of the mechanisms used in WJ-MSC diapedesis in normal and inflamed (induced first with inflammatory mediators) would help understand WJ-MSC recruitment to the sites of inflammation in physiological, pathological and clinical settings.

The molecular mechanisms utilised by the fetal stem cells to cross the endothelial barriers, appeared to involve transmembrane redistribution of VE-cadherin from junctional regions which might be a resultant from the initial phosphorylation of VE-cadherin at its Tyr685 residue from 30 min onwards followed by return to normal by 48h. Enhanced de-phosphorylation of Try731 tyrosine residue was also seen at 2h which coincided with maximum extravasation time of WJ-MSC and persist to 22h – a period of continued egress of WJ-MSC. Blocking phosphorylation of Tyr685 and de-phosphorylation of Tyr731 using siRNAs would allow a valuable insight into the importance of either or both mechanisms in stem cell extravasation.

The role of adhesion receptors, such as ICAM-1 or VCAM used in leukocyte extravasation, in transendothelial migration of WJ-MSC is an essential extension of this study. Initiation of the Src pathway induced by ICAM-1 binding or SHP-2 required for internalisation of VE-cadherin and leukocyte diapedesis, needs to be monitored in WJ-MSC extravasation across HUVEC or HUtMEC. ICAM-1 has been found to be expressed in MSC from bone marrow (Fu et al., 2009). The role of cytokines or pro-angiogenetic factors other than VEGF, such as TNF-α, IL6 or 8 (Edwards et al., 2014) in migration of WJ-MSC across HUVEC and also across HUtMEC monolayers, need further studies given that VEGF neutralising antibody only caused partial inhibition of cell extravasation across uterine endothelium. Using ELISA kits or microarray analysis to measure the secretion of various cytokines and angiogenetic

factors in WJ-MSC-HUVEC co-culture condition media or using also blocking antibodies would be a valuable future work.

Placental or umbilical cord perfusion with PKH26 labelled WJ-MSC would be also a valuable future work to compare the cellular and molecular mechanisms employed by WJ-MSC to extravaste across the endothelial barriers *in vivo*, under flow.

The observed shedding of microvesicles from WJ-MSC on top of both HUVEC and HUtMEC monolayers might play a role in either VE-cadherin disruption or repair or both. The role of exosomes or microRNAs contained within them in endothelial disruption and or repair is an important future work. Wang *et al.* 2010 suggested that serum level of microRNAs correlated with the severity of heart injury and may represent as a good biomarker of myocardial infarction in human (Wang et al., 2010). Great interest focuses on exploiting exosomes as therapeutic targets for vascular diseases and as clinical biomarkers. As biomarkers, circulating miRNAs offer a great potential for the diagnosis and prognosis of different diseases. The mechanism by which exosomes are released into the condition media and whether these microparticles have any functional capabilities, need further investigations using the models tested in this study.

More than 95 % of WJ-MSC used express β1 integrin (CD29), which are involved in cell adhesion mechanisms. CD44 (hyaluronate receptor) is important for the adhesion of various leukocytes to endothelium (Mitchell et al., 2006) and it is also expressed on WJ-MSC. CD90 regulates different biological processes like cell-cell and cell-matrix interactions in axon regeneration, apoptosis, adhesion, migration, cancer and fibrosis (Resta and Thompson, 1997), this marker is expressed on the surface of WJ-MSC. The role of Integrins in cellular

migration would be a valuable future work. Integrins are known to mediate the adhesion of various cells including hematopoietic stem cells and leukocytes to extracellular matrix proteins and to endothelial cells (Springer, 1994, Muller, 2002). Integrins and VEGFR-1 were involved in BM-MSC trafficking through the placenta endothelial barrier (Chen et al., 2008). Adhesion to endothelial cells and transmigration events are involved in the *in vivo* homing of stem cells to tissues with active angiogenesis (Vajkoczy et al., 2003). Studying the expression of VEGFR-1, integrins and other adhesion molecules before and after co-culture of WJ-MSC with both fetal and adult endothelial monolayers would benefit in understanding their role in cell adhesion and transendothelial migration.

6.2 The basic biology of placental development

Abnormal development of the placental vasculature, both utero-placental and feto-placental leads to placental insufficiency, which can result in a decrease in the exchange of nutrients and wastes between maternal and fetal circulations. Such changes can lead to various pregnancy complications for both the mother and the fetus including gestational hypertension, pre-eclampsia and fetal growth retardation and morbidity (Pijnenborg et al., 1991). Improving the current knowledge regarding the spiral artery remodelling process, would lead to both preventive and therapeutic interventions with lifelong impact, not only for the health of a woman and her fetus during pregnancy but also for the lifelong health of both.

The general consensus is that EVT are the cells which replace the endothelial and smooth muscle lining of the spiral arteries. However, in this study the data shows that WJ-MSC can interact with myometrial endothelial cells, including junctional disruption followed by a repair attempt. As discussed in Chapter 4 (Discussion), EVT co-culture studies used a 2:1 ratio (Bainbridge et al., 2009), far higher than those used in MSC studies (Ebrahim and Leach, 2015, Pati et al., 2011). Alterations in the ratio of stem cells to endothelial cells should

be considered in *in vitro* spiral artery remodelling studies. Most of the EVT studies used CK-7 as the definitive marker for identification of trophoblast. 30 % of WJ-MSC, in this study culture conditions demonstrated expression of CK7, thus the use of CK7 as a specific (and only) trophoblast cell marker should be re-considered in spiral artery remodelling studies. Spiral artery from uterine biopsies should be used and manipulated according to the methods demonstrated by Cartwright *et al.* (2002) and interacted with PKH26 labelled WJ-MSC or trophoblast or both cell types with different fluorescent tags. They can be perfused through the lumen of the arteries to study endovascular invasion, or seeded on top of artery segments embedded in fibrin gels to study interstitial invasion (Cartwright et al., 2002).

In summary, the data obtained in this study addresses an important question as to how fetal stem cells cross the fetal and maternal endothelium. Moreover, the transit times for MSC transendothelial migration and the mechanisms employed may be valuable for stem cell cytotherapy. The data here also opens a debate into how spiral arteries are remodelled and whether fetal stem cells, especially ones which can display non-destructive transendothelial migration and endothelial junctional repair may be involved. Finally, the interaction of fetal MSC with adult endothelial cells without causing apoptosis increases the potential usefulness of these extra-embryonic stem cells which are not subject to a maternal immune response.

APPENDIX

Antibodies used for the experiments:

Antibody	Species	Source	Patch number	Concentration used
CD45 – FITC	Monoclonal mouse anti-human	Beckman Coulter, UK	IM2078U	0.25 µg/ml
CD34 – FITC	Monoclonal mouse anti-human	Beckman Coulter, UK	A86354	0.25 µg/ml
CD44 – PE	Monoclonal mouse anti-human	Beckman Coulter, UK	IM0845	0.25 µg/ml
CD29 – FITC	Monoclonal mouse anti-human	Beckman Coulter, UK	PN IM0791U	0.25 µg/ml
CD105 – FITC	Monoclonal mouse anti-human	ebioscience, UK	323203	0.25 µg/ml
CD73 – APC	Monoclonal mouse anti-human	ebioscience, UK	17-0739	0.125 µg/ml
CD90 – PE	Monoclonal mouse anti-human	ebioscience, UK	12-0909	0.25 µg/ml
CDHLA-DR – FITC	Monoclonal mouse anti-human	ebioscience, UK	307603	0.25 µg/ml
CD19 – APC	Monoclonal mouse anti-human	ebioscience, UK	12-0199	0.25 µg/ml
CD14 – PE	Monoclonal mouse anti-human	ebioscience, UK	17-0149	0.25 µg/ml
VE-cadherin (CD144)	Rabbit antihuman	Cell Signaling, UK	2500	5 µg/ml
CD144	Mouse antihuman	Pharmingen, BD Biosciences, UK	55-7H1	6 µg/ml
Vwf	Rabbit antihuman	Dako, UK	IS527	5 µg/ml
CD31	Monoclonal mouse anti-human	R&D Systems, UK	BBA7	5 µg/ml
Cytokeratin 7	Monoclonal mouse anti-human	Dako, UK	M7018	12.4 µg/ml
VE-cadherin p-Tyr 685	Polyclonal rabbit anti-human	ECM Biosciences, UK	CP1981	2 µg/ml
VE-cadherin p-Tyr731	Polyclonal rabbit anti-human	abcam, UK	Ab27776	2 µg/ml
β-Actin	Monoclonal mouse anti-human	Sigma-Aldrich, UK	A5316	0.4 µg/ml
GAPDH	Monoclonal mouse anti-human	Sigma-Aldrich, UK	G8795	0.3 µg/ml
Anti-human VEGF	Monoclonal mouse anti-human	R&D Systems, UK	MAB293	2 µg/ml

Reference

ABSI, M., BRUCE, J. I. & WARD, D. T. 2014a. The inhibitory effect of simvastatin and aspirin on histamine responsiveness in human vascular endothelial cells. *Am J Physiol Cell Physiol,* 306**,** C679-86.

ADAM, A. P., SHARENKO, A. L., PUMIGLIA, K. & VINCENT, P. A. 2010. Src-induced tyrosine phosphorylation of VE-cadherin is not sufficient to decrease barrier function of endothelial monolayers. *J Biol Chem,* 285**,** 7045-55.

ADAMSON, R. H. & MICHEL, C. C. 1993. Pathways through the intercellular clefts of frog mesenteric capillaries. *J Physiol,* 466**,** 303-27.

AICHER, A. & HEESCHEN, C. 2007. Nonbone marrow-derived endothelial progenitor cells: what is their exact location? *Circ Res,* 101**,** e102.

AL-KHALDI, A., AL-SABTI, H., GALIPEAU, J. & LACHAPELLE, K. 2003. Therapeutic angiogenesis using autologous bone marrow stromal cells: improved blood flow in a chronic limb ischemia model. *Ann Thorac Surg,* 75**,** 204-9.

ALAMINOS, M., PEREZ-KOHLER, B., GARZON, I., GARCIA-HONDUVILLA, N., ROMERO, B., CAMPOS, A. & BUJAN, J. 2010. Transdifferentiation potentiality of human Wharton's jelly stem cells towards vascular endothelial cells. *J Cell Physiol,* 223**,** 640-7.

ALEXANDER, S., KOEHL, G. E., HIRSCHBERG, M., GEISSLER, E. K. & FRIEDL, P. 2008. Dynamic imaging of cancer growth and invasion: a modified skin-fold chamber model. *Histochem Cell Biol,* 130**,** 1147-54.

ALLINGHAM, M. J., VAN BUUL, J. D. & BURRIDGE, K. 2007. ICAM-1-mediated, Src- and Pyk2-dependent vascular endothelial cadherin tyrosine phosphorylation is required for leukocyte transendothelial migration. *J Immunol,* 179**,** 4053-64.

ALVIANO, F., FOSSATI, V., MARCHIONNI, C., ARPINATI, M., BONSI, L., FRANCHINA, M., LANZONI, G., CANTONI, S., CAVALLINI, C., BIANCHI, F., TAZZARI, P. L., PASQUINELLI, G., FORONI, L., VENTURA, C., GROSSI, A. & BAGNARA, G. P. 2007. Term Amniotic membrane is a high throughput source for multipotent Mesenchymal Stem Cells with the ability to differentiate into endothelial cells in vitro. *BMC Dev Biol,* 7**,** 11.

AMABLE, P. R., TEIXEIRA, M. V., CARIAS, R. B., GRANJEIRO, J. M. & BOROJEVIC, R. 2014. Protein synthesis and secretion in human mesenchymal cells derived from bone marrow, adipose tissue and Wharton's jelly. *Stem Cell Res Ther,* 5**,** 53.

ANDREWS, R. G., SINGER, J. W. & BERNSTEIN, I. D. 1989. Precursors of colony-forming cells in humans can be distinguished from colony-forming cells by expression of the CD33 and CD34 antigens and light scatter properties. *J Exp Med,* 169**,** 1721-31.

ANGELINI, D. J., HYUN, S. W., GRIGORYEV, D. N., GARG, P., GONG, P., SINGH, I. S., PASSANITI, A., HASDAY, J. D. & GOLDBLUM, S. E. 2006. TNF-alpha increases tyrosine phosphorylation of vascular endothelial cadherin and opens the paracellular pathway through fyn activation in human lung endothelia. *Am J Physiol Lung Cell Mol Physiol,* 291**,** L1232-45.

ANGELO, L. S. & KURZROCK, R. 2007. Vascular endothelial growth factor and its relationship to inflammatory mediators. *Clin Cancer Res,* 13**,** 2825-30.

ANGST, B. D., MARCOZZI, C. & MAGEE, A. I. 2001a. The cadherin superfamily. *J Cell Sci,* 114**,** 625-6.

ANGST, B. D., MARCOZZI, C. & MAGEE, A. I. 2001b. The cadherin superfamily: diversity in form and function. *J Cell Sci,* 114**,** 629-41.

ANZALONE, R., LO IACONO, M., CORRAO, S., MAGNO, F., LORIA, T., CAPPELLO, F., ZUMMO, G., FARINA, F. & LA ROCCA, G. 2010. New emerging potentials for

human Wharton's jelly mesenchymal stem cells: immunological features and hepatocyte-like differentiative capacity. *Stem Cells Dev,* 19**,** 423-38.

AONO, S., NAKAGAWA, S., REYNOLDS, A. B. & TAKEICHI, M. 1999. p120(ctn) acts as an inhibitory regulator of cadherin function in colon carcinoma cells. *J Cell Biol,* 145**,** 551-62.

APLIN, J. D., HAIGH, T., JONES, C. J., CHURCH, H. J. & VICOVAC, L. 1999. Development of cytotrophoblast columns from explanted first-trimester human placental villi: role of fibronectin and integrin alpha5beta1. *Biol Reprod,* 60**,** 828-38.

APLIN, J. D., HAIGH, T., VICOVAC, L., CHURCH, H. J. & JONES, C. J. 1998. Anchorage in the developing placenta: an overlooked determinant of pregnancy outcome? *Hum Fertil (Camb),* 1**,** 75-79.

ASAHARA, T., MUROHARA, T., SULLIVAN, A., SILVER, M., VAN DER ZEE, R., LI, T., WITZENBICHLER, B., SCHATTEMAN, G. & ISNER, J. M. 1997. Isolation of putative progenitor endothelial cells for angiogenesis. *Science,* 275**,** 964-7.

ASAN, E., KAYMAZ, F. F., CAKAR, A. N., DAGDEVIREN, A. & BEKSAC, M. S. 1999. Vasculogenesis in early human placental villi: an ultrastructural study. *Ann Anat,* 181**,** 549-54.

ASHTON, S. V., WHITLEY, G. S., DASH, P. R., WAREING, M., CROCKER, I. P., BAKER, P. N. & CARTWRIGHT, J. E. 2005. Uterine spiral artery remodeling involves endothelial apoptosis induced by extravillous trophoblasts through Fas/FasL interactions. *Arterioscler Thromb Vasc Biol,* 25**,** 102-8.

AUSPRUNK, D. H. & FOLKMAN, J. 1977. Migration and proliferation of endothelial cells in preformed and newly formed blood vessels during tumor angiogenesis. *Microvasc Res,* 14**,** 53-65.

AVIGDOR, A., GOICHBERG, P., SHIVTIEL, S., DAR, A., PELED, A., SAMIRA, S., KOLLET, O., HERSHKOVIZ, R., ALON, R., HARDAN, I., BEN-HUR, H., NAOR, D., NAGLER, A. & LAPIDOT, T. 2004. CD44 and hyaluronic acid cooperate with SDF-1 in the trafficking of human CD34+ stem/progenitor cells to bone marrow. *Blood,* 103**,** 2981-9.

AYUZAWA, R., DOI, C., RACHAKATLA, R. S., PYLE, M. M., MAURYA, D. K., TROYER, D. & TAMURA, M. 2009. Naive human umbilical cord matrix derived stem cells significantly attenuate growth of human breast cancer cells in vitro and in vivo. *Cancer Lett,* 280**,** 31-7.

BACH, T. L., BARSIGIAN, C., YAEN, C. H. & MARTINEZ, J. 1998. Endothelial cell VE-cadherin functions as a receptor for the beta15-42 sequence of fibrin. *J Biol Chem,* 273**,** 30719-28.

BAINBRIDGE, S. A., ROBERTS, J. M., VON VERSEN-HOYNCK, F., KOCH, J., EDMUNDS, L. & HUBEL, C. A. 2009. Uric acid attenuates trophoblast invasion and integration into endothelial cell monolayers. *Am J Physiol Cell Physiol,* 297**,** C440-50.

BALL, E., BULMER, J. N., AYIS, S., LYALL, F. & ROBSON, S. C. 2006. Late sporadic miscarriage is associated with abnormalities in spiral artery transformation and trophoblast invasion. *J Pathol,* 208**,** 535-42.

BALLAS, C. B., ZIELSKE, S. P. & GERSON, S. L. 2002. Adult bone marrow stem cells for cell and gene therapies: implications for greater use. *J Cell Biochem Suppl,* 38**,** 20-8.

BARUT, F., BARUT, A., GUN, B. D., KANDEMIR, N. O., HARMA, M. I., HARMA, M., AKTUNC, E. & OZDAMAR, S. O. 2010. Intrauterine growth restriction and placental angiogenesis. *Diagn Pathol,* 5**,** 24.

BATES, D. O. 2010. Vascular endothelial growth factors and vascular permeability. *Cardiovasc Res,* 87**,** 262-71.

BAUTZ, F., RAFII, S., KANZ, L. & MOHLE, R. 2000. Expression and secretion of vascular endothelial growth factor-A by cytokine-stimulated hematopoietic progenitor cells. Possible role in the hematopoietic microenvironment. *Exp Hematol,* 28**,** 700-6.

BAZZONI, G. & DEJANA, E. 2004. Endothelial cell-to-cell junctions: molecular organization and role in vascular homeostasis. *Physiol Rev,* 84**,** 869-901.

BECK, L., JR. & D'AMORE, P. A. 1997. Vascular development: cellular and molecular regulation. *FASEB J,* 11**,** 365-73.

BECKERMANN, B. M., KALLIFATIDIS, G., GROTH, A., FROMMHOLD, D., APEL, A., MATTERN, J., SALNIKOV, A. V., MOLDENHAUER, G., WAGNER, W., DIEHLMANN, A., SAFFRICH, R., SCHUBERT, M., HO, A. D., GIESE, N., BUCHLER, M. W., FRIESS, H., BUCHLER, P. & HERR, I. 2008. VEGF expression by mesenchymal stem cells contributes to angiogenesis in pancreatic carcinoma. *Br J Cancer,* 99**,** 622-31.

BELTRAMI, A. P., BARLUCCHI, L., TORELLA, D., BAKER, M., LIMANA, F., CHIMENTI, S., KASAHARA, H., ROTA, M., MUSSO, E., URBANEK, K., LERI, A., KAJSTURA, J., NADAL-GINARD, B. & ANVERSA, P. 2003. Adult cardiac stem cells are multipotent and support myocardial regeneration. *Cell,* 114**,** 763-76.

BENJAMIN, L. E., HEMO, I. & KESHET, E. 1998. A plasticity window for blood vessel remodelling is defined by pericyte coverage of the preformed endothelial network and is regulated by PDGF-B and VEGF. *Development,* 125**,** 1591-8.

BENSINGER, W. I., BERENSON, R. J., ANDREWS, R. G., KALAMASZ, D. F., HILL, R. S., BERNSTEIN, I. D., LOPEZ, J. G., BUCKNER, C. D. & THOMAS, E. D. 1990. Positive selection of hematopoietic progenitors from marrow and peripheral blood for transplantation. *J Clin Apher,* 5**,** 74-6.

BIANCHI, D. W. 2004. Fetomaternal cell traffic, pregnancy-associated progenitor cells, and autoimmune disease. *Best Pract Res Clin Obstet Gynaecol,* 18**,** 959-75.

BONGSO, A., FONG, C. Y., NG, S. C. & RATNAM, S. 1994. Isolation and culture of inner cell mass cells from human blastocysts. *Hum Reprod,* 9**,** 2110-7.

BORLONGAN, C. V., GLOVER, L. E., TAJIRI, N., KANEKO, Y. & FREEMAN, T. B. 2011. The great migration of bone marrow-derived stem cells toward the ischemic brain: therapeutic implications for stroke and other neurological disorders. *Prog Neurobiol,* 95**,** 213-28.

BOYON, C., COLLINET, P., BOULANGER, L., RUBOD, C., LUCOT, J. P. & VINATIER, D. 2011. Fetal microchimerism: benevolence or malevolence for the mother? *Eur J Obstet Gynecol Reprod Biol,* 158**,** 148-52.

BRANCH, M. J., HASHMANI, K., DHILLON, P., JONES, D. R., DUA, H. S. & HOPKINSON, A. 2012. Mesenchymal stem cells in the human corneal limbal stroma. *Invest Ophthalmol Vis Sci,* 53**,** 5109-16.

BROWN, V. K., OGLE, E. W., BURKHARDT, A. L., ROWLEY, R. B., BOLEN, J. B. & JUSTEMENT, L. B. 1994. Multiple components of the B cell antigen receptor complex associate with the protein tyrosine phosphatase, CD45. *J Biol Chem,* 269**,** 17238-44.

BUDWORTH, R. A., ANDERSON, M., CLOTHIER, R. H. & LEACH, L. 1999. Histamine-induced Changes in the Actin Cytoskeleton of the Human Microvascular Endothelial Cell line HMEC-1. *Toxicol In Vitro,* 13**,** 789-95.

BULMER, J. N., INNES, B. A., LEVEY, J., ROBSON, S. C. & LASH, G. E. 2012. The role of vascular smooth muscle cell apoptosis and migration during uterine spiral artery remodeling in normal human pregnancy. *FASEB J,* 26**,** 2975-85.

BULMER, J. N., MORRISON, L., LONGFELLOW, M., RITSON, A. & PACE, D. 1991. Granulated lymphocytes in human endometrium: histochemical and immunohistochemical studies. *Hum Reprod,* 6**,** 791-8.

BURTON, G. J., JAUNIAUX, E. & WATSON, A. L. 1999. Maternal arterial connections to the placental intervillous space during the first trimester of human pregnancy: the Boyd collection revisited. *Am J Obstet Gynecol,* 181**,** 718-24.

BYRNE, A. M., BOUCHIER-HAYES, D. J. & HARMEY, J. H. 2005. Angiogenic and cell survival functions of vascular endothelial growth factor (VEGF). *J Cell Mol Med,* 9**,** 777-94.

CAI, C. L., MARTIN, J. C., SUN, Y., CUI, L., WANG, L., OUYANG, K., YANG, L., BU, L., LIANG, X., ZHANG, X., STALLCUP, W. B., DENTON, C. P., MCCULLOCH, A., CHEN, J. & EVANS, S. M. 2008. A myocardial lineage derives from Tbx18 epicardial cells. *Nature,* 454**,** 104-8.

CAI, L., JOHNSTONE, B. H., COOK, T. G., TAN, J., FISHBEIN, M. C., CHEN, P. S. & MARCH, K. L. 2009. IFATS collection: Human adipose tissue-derived stem cells induce angiogenesis and nerve sprouting following myocardial infarction, in conjunction with potent preservation of cardiac function. *Stem Cells,* 27**,** 230-7.

CAIN, R. J., VANHAESEBROECK, B. & RIDLEY, A. J. 2010. The PI3K p110alpha isoform regulates endothelial adherens junctions via Pyk2 and Rac1. *J Cell Biol,* 188**,** 863-76.

CALVI, L. M., ADAMS, G. B., WEIBRECHT, K. W., WEBER, J. M., OLSON, D. P., KNIGHT, M. C., MARTIN, R. P., SCHIPANI, E., DIVIETI, P., BRINGHURST, F. R., MILNER, L. A., KRONENBERG, H. M. & SCADDEN, D. T. 2003. Osteoblastic cells regulate the haematopoietic stem cell niche. *Nature,* 425**,** 841-6.

CAMPAGNOLO, P., CESSELLI, D., AL HAJ ZEN, A., BELTRAMI, A. P., KRANKEL, N., KATARE, R., ANGELINI, G., EMANUELI, C. & MADEDDU, P. 2010. Human adult vena saphena contains perivascular progenitor cells endowed with clonogenic and proangiogenic potential. *Circulation,* 121**,** 1735-45.

CAMPARD, D., LYSY, P. A., NAJIMI, M. & SOKAL, E. M. 2008. Native umbilical cord matrix stem cells express hepatic markers and differentiate into hepatocyte-like cells. *Gastroenterology,* 134**,** 833-48.

CAN, A. & KARAHUSEYINOGLU, S. 2007. Concise review: human umbilical cord stroma with regard to the source of fetus-derived stem cells. *Stem Cells,* 25**,** 2886-95.

CAPLAN, A. I. 1991. Mesenchymal stem cells. *J Orthop Res,* 9**,** 641-50.

CAPLAN, A. I. 2008. All MSCs are pericytes? *Cell Stem Cell,* 3**,** 229-30.

CARTWRIGHT, J. E., KENNY, L. C., DASH, P. R., CROCKER, I. P., APLIN, J. D., BAKER, P. N. & WHITLEY, G. S. 2002. Trophoblast invasion of spiral arteries: a novel in vitro model. *Placenta,* 23**,** 232-5.

CARVETH, H. J., BOHNSACK, J. F., MCINTYRE, T. M., BAGGIOLINI, M., PRESCOTT, S. M. & ZIMMERMAN, G. A. 1989. Neutrophil activating factor (NAF) induces polymorphonuclear leukocyte adherence to endothelial cells and to subendothelial matrix proteins. *Biochem Biophys Res Commun,* 162**,** 387-93.

CERDEIRA, A. S. & KARUMANCHI, S. A. 2012. Angiogenic factors in preeclampsia and related disorders. *Cold Spring Harb Perspect Med,* 2.

CHA, D., KHOSROTEHRANI, K., KIM, Y., STROH, H., BIANCHI, D. W. & JOHNSON, K. L. 2003. Cervical cancer and microchimerism. *Obstet Gynecol,* 102**,** 774-81.

CHARNOCK-JONES, D. S., KAUFMANN, P. & MAYHEW, T. M. 2004. Aspects of human fetoplacental vasculogenesis and angiogenesis. I. Molecular regulation. *Placenta,* 25**,** 103-13.

CHEN, C. P., LEE, M. Y., HUANG, J. P., APLIN, J. D., WU, Y. H., HU, C. S., CHEN, P. C., LI, H., HWANG, S. M., LIU, S. H. & YANG, Y. C. 2008. Trafficking of multipotent mesenchymal stromal cells from maternal circulation through the placenta involves vascular endothelial growth factor receptor-1 and integrins. *Stem Cells,* 26**,** 550-61.

CHERNYAVSKY, I. L., LEACH, L., DRYDEN, I. L. & JENSEN, O. E. 2011. Transport in the placenta: homogenizing haemodynamics in a disordered medium. *Philos Trans A Math Phys Eng Sci,* 369**,** 4162-82.

CHO, N. H., PARK, Y. K., KIM, Y. T., YANG, H. & KIM, S. K. 2004. Lifetime expression of stem cell markers in the uterine endometrium. *Fertil Steril,* 81**,** 403-7.

CHO, P. S., MESSINA, D. J., HIRSH, E. L., CHI, N., GOLDMAN, S. N., LO, D. P., HARRIS, I. R., POPMA, S. H., SACHS, D. H. & HUANG, C. A. 2008. Immunogenicity of umbilical cord tissue derived cells. *Blood,* 111**,** 430-8.

CHOI, M., LEE, H. S., NAIDANSAREN, P., KIM, H. K., O, E., CHA, J. H., AHN, H. Y., YANG, P. I., SHIN, J. C. & JOE, Y. A. 2013. Proangiogenic features of Wharton's jelly-derived mesenchymal stromal/stem cells and their ability to form functional vessels. *Int J Biochem Cell Biol,* 45**,** 560-70.

CHONG, J. J., CHANDRAKANTHAN, V., XAYMARDAN, M., ASLI, N. S., LI, J., AHMED, I., HEFFERNAN, C., MENON, M. K., SCARLETT, C. J., RASHIDIANFAR, A., BIBEN, C., ZOELLNER, H., COLVIN, E. K., PIMANDA, J. E., BIANKIN, A. V., ZHOU, B., PU, W. T., PRALL, O. W. & HARVEY, R. P. 2011. Adult cardiac-resident MSC-like stem cells with a proepicardial origin. *Cell Stem Cell,* 9**,** 527-40.

CHULAROJMONTRI, L. & WATTANAPITAYAKUL, S. K. 2009. Isolation and characterization of umbilical cord blood hematopoietic stem cells. *J Med Assoc Thai,* 92 Suppl 3**,** S88-94.

CONTRACTOR, S. F., BANKS, R. W., JONES, C. J. & FOX, H. 1977. A possible role for placental lysosomes in the formation of villous syncytiotrophoblast. *Cell Tissue Res,* 178**,** 411-9.

COOK-MILLS, J. M. & DEEM, T. L. 2005. Active participation of endothelial cells in inflammation. *J Leukoc Biol,* 77**,** 487-95.

CORADA, M., LIAO, F., LINDGREN, M., LAMPUGNANI, M. G., BREVIARIO, F., FRANK, R., MULLER, W. A., HICKLIN, D. J., BOHLEN, P. & DEJANA, E. 2001. Monoclonal antibodies directed to different regions of vascular endothelial cadherin extracellular domain affect adhesion and clustering of the protein and modulate endothelial permeability. *Blood,* 97**,** 1679-84.

CORADA, M., MARIOTTI, M., THURSTON, G., SMITH, K., KUNKEL, R., BROCKHAUS, M., LAMPUGNANI, M. G., MARTIN-PADURA, I., STOPPACCIARO, A., RUCO, L., MCDONALD, D. M., WARD, P. A. & DEJANA, E. 1999. Vascular endothelial-cadherin is an important determinant of microvascular integrity in vivo. *Proc Natl Acad Sci U S A,* 96**,** 9815-20.

CUVELIER, S. L. & PATEL, K. D. 2005. Studying leukocyte rolling and adhesion in vitro under flow conditions. *Methods Mol Biol,* 290**,** 331-42.

CUVELIER, S. L., PAUL, S., SHARIAT, N., COLARUSSO, P. & PATEL, K. D. 2005. Eosinophil adhesion under flow conditions activates mechanosensitive signaling pathways in human endothelial cells. *J Exp Med,* 202**,** 865-76.

DAHL, K. N., RIBEIRO, A. J. & LAMMERDING, J. 2008. Nuclear shape, mechanics, and mechanotransduction. *Circ Res,* 102**,** 1307-18.

DAHLIN, R. L., KINARD, L. A., LAM, J., NEEDHAM, C. J., LU, S., KASPER, F. K. & MIKOS, A. G. 2014. Articular chondrocytes and mesenchymal stem cells seeded on

biodegradable scaffolds for the repair of cartilage in a rat osteochondral defect model. *Biomaterials,* 35**,** 7460-9.

DAMSKY, C. H., LIBRACH, C., LIM, K. H., FITZGERALD, M. L., MCMASTER, M. T., JANATPOUR, M., ZHOU, Y., LOGAN, S. K. & FISHER, S. J. 1994. Integrin switching regulates normal trophoblast invasion. *Development,* 120**,** 3657-66.

DAWE, G. S., TAN, X. W. & XIAO, Z. C. 2007. Cell migration from baby to mother. *Cell Adh Migr,* 1**,** 19-27.

DE BRUYN, C., NAJAR, M., RAICEVIC, G., MEULEMAN, N., PIETERS, K., STAMATOPOULOS, B., DELFORGE, A., BRON, D. & LAGNEAUX, L. 2011. A rapid, simple, and reproducible method for the isolation of mesenchymal stromal cells from Wharton's jelly without enzymatic treatment. *Stem Cells Dev,* 20**,** 547-57.

DEJANA, E. 1996. Endothelial adherens junctions: implications in the control of vascular permeability and angiogenesis. *J Clin Invest,* 98**,** 1949-53.

DEJANA, E. 2004. Endothelial cell-cell junctions: happy together. *Nat Rev Mol Cell Biol,* 5**,** 261-70.

DEJANA, E., BAZZONI, G. & LAMPUGNANI, M. G. 1999. Vascular endothelial (VE)-cadherin: only an intercellular glue? *Exp Cell Res,* 252**,** 13-9.

DEJANA, E., CORADA, M. & LAMPUGNANI, M. G. 1995. Endothelial cell-to-cell junctions. *FASEB J,* 9**,** 910-8.

DEJANA, E., ORSENIGO, F. & LAMPUGNANI, M. G. 2008. The role of adherens junctions and VE-cadherin in the control of vascular permeability. *J Cell Sci,* 121**,** 2115-22.

DEJANA, E., ORSENIGO, F., MOLENDINI, C., BALUK, P. & MCDONALD, D. M. 2009. Organization and signaling of endothelial cell-to-cell junctions in various regions of the blood and lymphatic vascular trees. *Cell Tissue Res,* 335**,** 17-25.

DEL MASCHIO, A., ZANETTI, A., CORADA, M., RIVAL, Y., RUCO, L., LAMPUGNANI, M. G. & DEJANA, E. 1996. Polymorphonuclear leukocyte adhesion triggers the disorganization of endothelial cell-to-cell adherens junctions. *J Cell Biol,* 135**,** 497-510.

DELISSER, H. M., NEWMAN, P. J. & ALBELDA, S. M. 1994. Molecular and functional aspects of PECAM-1/CD31. *Immunol Today,* 15**,** 490-5.

DEMIR, R., KAUFMANN, P., CASTELLUCCI, M., ERBENGI, T. & KOTOWSKI, A. 1989. Fetal vasculogenesis and angiogenesis in human placental villi. *Acta Anat (Basel),* 136**,** 190-203.

DEMIR, R., KAYISLI, U. A., CELIK-OZENCI, C., KORGUN, E. T., DEMIR-WEUSTEN, A. Y. & ARICI, A. 2002. Structural differentiation of human uterine luminal and glandular epithelium during early pregnancy: an ultrastructural and immunohistochemical study. *Placenta,* 23**,** 672-84.

DEMIR, R., SEVAL, Y. & HUPPERTZ, B. 2007. Vasculogenesis and angiogenesis in the early human placenta. *Acta Histochem,* 109**,** 257-65.

DIAZ-FLORES, L., GUTIERREZ, R., MADRID, J. F., VARELA, H., VALLADARES, F., ACOSTA, E., MARTIN-VASALLO, P. & DIAZ-FLORES, L., JR. 2009. Pericytes. Morphofunction, interactions and pathology in a quiescent and activated mesenchymal cell niche. *Histol Histopathol,* 24**,** 909-69.

DIMITROFF, C. J., LEE, J. Y., RAFII, S., FUHLBRIGGE, R. C. & SACKSTEIN, R. 2001. CD44 is a major E-selectin ligand on human hematopoietic progenitor cells. *J Cell Biol,* 153**,** 1277-86.

DOMINICI, M., LE BLANC, K., MUELLER, I., SLAPER-CORTENBACH, I., MARINI, F., KRAUSE, D., DEANS, R., KEATING, A., PROCKOP, D. & HORWITZ, E.

2006. Minimal criteria for defining multipotent mesenchymal stromal cells. The International Society for Cellular Therapy position statement. *Cytotherapy,* 8**,** 315-7.

DOYLE, A. D., WANG, F. W., MATSUMOTO, K. & YAMADA, K. M. 2009. One-dimensional topography underlies three-dimensional fibrillar cell migration. *J Cell Biol,* 184**,** 481-90.

DUDEK, S. M. & GARCIA, J. G. 2001. Cytoskeletal regulation of pulmonary vascular permeability. *J Appl Physiol (1985),* 91**,** 1487-500.

DUNK, C., PETKOVIC, L., BACZYK, D., ROSSANT, J., WINTERHAGER, E. & LYE, S. 2003. A novel in vitro model of trophoblast-mediated decidual blood vessel remodeling. *Lab Invest,* 83**,** 1821-8.

DWYER, J., LE GUELTE, A., GALAN MOYA, E. M., SUMBAL, M., CARLOTTI, A., DOUGUET, L., GUTKIND, J. S., GRANGE, P. A., DUPIN, N. & GAVARD, J. 2011. Remodeling of VE-cadherin junctions by the human herpes virus 8 G-protein coupled receptor. *Oncogene,* 30**,** 190-200.

EBRAHIM, N. & LEACH, L. 2014. Temporal Studies into Attachment, Ve-Cadherin Perturbation and Paracellular Migration of Human Umbilical Mesenchymal Stem Cells across Umbilical Vein Endothelial Monolayers. *Stem Cells Dev*.

EBRAHIM, N. A. & LEACH, L. 2015. Temporal studies into attachment, VE-cadherin perturbation, and paracellular migration of human umbilical mesenchymal stem cells across umbilical vein endothelial monolayers. *Stem Cells Dev,* 24**,** 426-36.

EDWARDS, S. S., ZAVALA, G., PRIETO, C. P., ELLIOTT, M., MARTINEZ, S., EGANA, J. T., BONO, M. R. & PALMA, V. 2014. Functional analysis reveals angiogenic potential of human mesenchymal stem cells from Wharton's jelly in dermal regeneration. *Angiogenesis,* 17**,** 851-66.

ERBS, S., LINKE, A., ADAMS, V., LENK, K., THIELE, H., DIEDERICH, K. W., EMMRICH, F., KLUGE, R., KENDZIORRA, K., SABRI, O., SCHULER, G. & HAMBRECHT, R. 2005. Transplantation of blood-derived progenitor cells after recanalization of chronic coronary artery occlusion: first randomized and placebo-controlled study. *Circ Res,* 97**,** 756-62.

ERIKSSON, U. & ALITALO, K. 1999. Structure, expression and receptor-binding properties of novel vascular endothelial growth factors. *Curr Top Microbiol Immunol,* 237**,** 41-57.

ESSER, S., LAMPUGNANI, M. G., CORADA, M., DEJANA, E. & RISAU, W. 1998. Vascular endothelial growth factor induces VE-cadherin tyrosine phosphorylation in endothelial cells. *J Cell Sci,* 111 (Pt 13)**,** 1853-65.

FACKLER, O. T. & GROSSE, R. 2008. Cell motility through plasma membrane blebbing. *J Cell Biol,* 181**,** 879-84.

FAN, C. G., ZHANG, Q. J. & ZHOU, J. R. 2011. Therapeutic potentials of mesenchymal stem cells derived from human umbilical cord. *Stem Cell Rev,* 7**,** 195-207.

FAROOQUI, R. & FENTEANY, G. 2005. Multiple rows of cells behind an epithelial wound edge extend cryptic lamellipodia to collectively drive cell-sheet movement. *J Cell Sci,* 118**,** 51-63.

FIRTH, J. A. 2002. Endothelial barriers: from hypothetical pores to membrane proteins. *J Anat,* 200**,** 541-8.

FIRTH, J. A., BAUMAN, K. F. & SIBLEY, C. P. 1983. The intercellular junctions of guinea-pig placental capillaries: a possible structural basis for endothelial solute permeability. *J Ultrastruct Res,* 85**,** 45-57.

FONG, C. Y., GAUTHAMAN, K., CHEYYATRAIVENDRAN, S., LIN, H. D., BISWAS, A. & BONGSO, A. 2012. Human umbilical cord Wharton's jelly stem cells and its

conditioned medium support hematopoietic stem cell expansion ex vivo. *J Cell Biochem,* 113**,** 658-68.

FONG, C. Y., SUBRAMANIAN, A., BISWAS, A., GAUTHAMAN, K., SRIKANTH, P., HANDE, M. P. & BONGSO, A. 2010. Derivation efficiency, cell proliferation, freeze-thaw survival, stem-cell properties and differentiation of human Wharton's jelly stem cells. *Reprod Biomed Online,* 21**,** 391-401.

FRANK, M. & KEMLER, R. 2002. Protocadherins. *Curr Opin Cell Biol,* 14**,** 557-62.

FRIEDENSTEIN, A. J., GORSKAJA, J. F. & KULAGINA, N. N. 1976. Fibroblast precursors in normal and irradiated mouse hematopoietic organs. *Exp Hematol,* 4**,** 267-74.

FRIEDENSTEIN, A. J., PIATETZKY, S., II & PETRAKOVA, K. V. 1966. Osteogenesis in transplants of bone marrow cells. *J Embryol Exp Morphol,* 16**,** 381-90.

FRIEDL, P., BORGMANN, S. & BROCKER, E. B. 2001. Amoeboid leukocyte crawling through extracellular matrix: lessons from the Dictyostelium paradigm of cell movement. *J Leukoc Biol,* 70**,** 491-509.

FRIEDL, P. & GILMOUR, D. 2009. Collective cell migration in morphogenesis, regeneration and cancer. *Nat Rev Mol Cell Biol,* 10**,** 445-57.

FRIEDL, P. & WOLF, K. 2010. Plasticity of cell migration: a multiscale tuning model. *J Cell Biol,* 188**,** 11-9.

FRIEDL, P., ZANKER, K. S. & BROCKER, E. B. 1998. Cell migration strategies in 3-D extracellular matrix: differences in morphology, cell matrix interactions, and integrin function. *Microsc Res Tech,* 43**,** 369-78.

FU, J. R., LIU, W. L., ZHOU, J. F., SUN, H. Y., XU, H. Z., LUO, L., ZHANG, H. & ZHOU, Y. F. 2006. Sonic hedgehog protein promotes bone marrow-derived endothelial progenitor cell proliferation, migration and VEGF production via PI 3-kinase/Akt signaling pathways. *Acta Pharmacol Sin,* 27**,** 685-93.

FU, X., HAN, B., CAI, S., LEI, Y., SUN, T. & SHENG, Z. 2009. Migration of bone marrow-derived mesenchymal stem cells induced by tumor necrosis factor-alpha and its possible role in wound healing. *Wound Repair Regen,* 17**,** 185-91.

FUCHS, S., BAFFOUR, R., ZHOU, Y. F., SHOU, M., PIERRE, A., TIO, F. O., WEISSMAN, N. J., LEON, M. B., EPSTEIN, S. E. & KORNOWSKI, R. 2001. Transendocardial delivery of autologous bone marrow enhances collateral perfusion and regional function in pigs with chronic experimental myocardial ischemia. *J Am Coll Cardiol,* 37**,** 1726-32.

FUKUCHI, Y., NAKAJIMA, H., SUGIYAMA, D., HIROSE, I., KITAMURA, T. & TSUJI, K. 2004. Human placenta-derived cells have mesenchymal stem/progenitor cell potential. *Stem Cells,* 22**,** 649-58.

GAENGEL, K., NIAUDET, C., HAGIKURA, K., LAVINA, B., MUHL, L., HOFMANN, J. J., EBARASI, L., NYSTROM, S., RYMO, S., CHEN, L. L., PANG, M. F., JIN, Y., RASCHPERGER, E., ROSWALL, P., SCHULTE, D., BENEDITO, R., LARSSON, J., HELLSTROM, M., FUXE, J., UHLEN, P., ADAMS, R., JAKOBSSON, L., MAJUMDAR, A., VESTWEBER, D., UV, A. & BETSHOLTZ, C. 2012. The sphingosine-1-phosphate receptor S1PR1 restricts sprouting angiogenesis by regulating the interplay between VE-cadherin and VEGFR2. *Dev Cell,* 23**,** 587-99.

GALLI, R., BORELLO, U., GRITTI, A., MINASI, M. G., BJORNSON, C., COLETTA, M., MORA, M., DE ANGELIS, M. G., FIOCCO, R., COSSU, G. & VESCOVI, A. L. 2000. Skeletal myogenic potential of human and mouse neural stem cells. *Nat Neurosci,* 3**,** 986-91.

GALUSTIAN, C., DYE, J., LEACH, L., CLARK, P. & FIRTH, J. A. 1995. Actin cytoskeletal isoforms in human endothelial cells in vitro: alteration with cell passage. *In Vitro Cell Dev Biol Anim,* 31**,** 796-802.

GARZON, I., ALFONSO-RODRIGUEZ, C. A., MARTINEZ-GOMEZ, C., CARRIEL, V., MARTIN-PIEDRA, M. A., FERNANDEZ-VALADES, R., SANCHEZ-QUEVEDO, M. C. & ALAMINOS, M. 2014a. Expression of epithelial markers by human umbilical cord stem cells. A topographical analysis. *Placenta*.

GARZON, I., MARTIN-PIEDRA, M. A., ALFONSO-RODRIGUEZ, C., GONZALEZ-ANDRADES, M., CARRIEL, V., MARTINEZ-GOMEZ, C., CAMPOS, A. & ALAMINOS, M. 2014b. Generation of a biomimetic human artificial cornea model using Wharton's jelly mesenchymal stem cells. *Invest Ophthalmol Vis Sci,* 55**,** 4073-83.

GAUDRY, M., BREGERIE, O., ANDRIEU, V., EL BENNA, J., POCIDALO, M. A. & HAKIM, J. 1997. Intracellular pool of vascular endothelial growth factor in human neutrophils. *Blood,* 90**,** 4153-61.

GAVARD, J. & GUTKIND, J. S. 2006. VEGF controls endothelial-cell permeability by promoting the beta-arrestin-dependent endocytosis of VE-cadherin. *Nat Cell Biol,* 8**,** 1223-34.

GAVARD, J., HOU, X., QU, Y., MASEDUNSKAS, A., MARTIN, D., WEIGERT, R., LI, X. & GUTKIND, J. S. 2009. A role for a CXCR2/phosphatidylinositol 3-kinase gamma signaling axis in acute and chronic vascular permeability. *Mol Cell Biol,* 29**,** 2469-80.

GAVARD, J., PATEL, V. & GUTKIND, J. S. 2008. Angiopoietin-1 prevents VEGF-induced endothelial permeability by sequestering Src through mDia. *Dev Cell,* 14**,** 25-36.

GERHARDT, H. & BETSHOLTZ, C. 2003. Endothelial-pericyte interactions in angiogenesis. *Cell Tissue Res,* 314**,** 15-23.

GIANCOTTI, F. G. 2000. Complexity and specificity of integrin signalling. *Nat Cell Biol,* 2**,** E13-4.

GRAESSER, D., SOLOWIEJ, A., BRUCKNER, M., OSTERWEIL, E., JUEDES, A., DAVIS, S., RUDDLE, N. H., ENGELHARDT, B. & MADRI, J. A. 2002. Altered vascular permeability and early onset of experimental autoimmune encephalomyelitis in PECAM-1-deficient mice. *J Clin Invest,* 109**,** 383-92.

GRAZIA LAMPUGNANI, M., ZANETTI, A., CORADA, M., TAKAHASHI, T., BALCONI, G., BREVIARIO, F., ORSENIGO, F., CATTELINO, A., KEMLER, R., DANIEL, T. O. & DEJANA, E. 2003. Contact inhibition of VEGF-induced proliferation requires vascular endothelial cadherin, beta-catenin, and the phosphatase DEP-1/CD148. *J Cell Biol,* 161**,** 793-804.

GRONTHOS, S., MANKANI, M., BRAHIM, J., ROBEY, P. G. & SHI, S. 2000. Postnatal human dental pulp stem cells (DPSCs) in vitro and in vivo. *Proc Natl Acad Sci U S A,* 97**,** 13625-30.

GROSS, S., HELM, K., GRUNTMEIR, J. J., STILLMAN, W. S., PYATT, D. W. & IRONS, R. D. 1997. Characterization and phenotypic analysis of differentiating CD34+ human bone marrow cells in liquid culture. *Eur J Haematol,* 59**,** 318-26.

GUILLOT, P. V., GOTHERSTROM, C., CHAN, J., KURATA, H. & FISK, N. M. 2007. Human first-trimester fetal MSC express pluripotency markers and grow faster and have longer telomeres than adult MSC. *Stem Cells,* 25**,** 646-54.

GUMBINER, B. M. 2000. Regulation of cadherin adhesive activity. *J Cell Biol,* 148**,** 399-404.

GUNDERSEN, H. J. & JENSEN, E. B. 1987. The efficiency of systematic sampling in stereology and its prediction. *J Microsc,* 147**,** 229-63.

HAGMANN, S., MORADI, B., FRANK, S., DREHER, T., KAMMERER, P. W., RICHTER, W. & GOTTERBARM, T. 2013. Different culture media affect growth characteristics, surface marker distribution and chondrogenic differentiation of human bone marrow-derived mesenchymal stromal cells. *BMC Musculoskelet Disord,* 14**,** 223.

HALPER, J. & KJAER, M. 2014. Basic components of connective tissues and extracellular matrix: elastin, fibrillin, fibulins, fibrinogen, fibronectin, laminin, tenascins and thrombospondins. *Adv Exp Med Biol,* 802**,** 31-47.

HAMILTON, R. D. & LEACH, L. 2011. Isolation and properties of an in vitro human outer blood-retinal barrier model. *Methods Mol Biol,* 686**,** 401-16.

HAN, I., YUN, M., KIM, E. O., KIM, B., JUNG, M. H. & KIM, S. H. 2014. Umbilical cord tissue-derived mesenchymal stem cells induce apoptosis in PC-3 prostate cancer cells through activation of JNK and downregulation of PI3K/AKT signaling. *Stem Cell Res Ther,* 5**,** 54.

HANAHAN, D. 1997. Signaling vascular morphogenesis and maintenance. *Science,* 277**,** 48-50.

HARLEY, B. A., KIM, H. D., ZAMAN, M. H., YANNAS, I. V., LAUFFENBURGER, D. A. & GIBSON, L. J. 2008. Microarchitecture of three-dimensional scaffolds influences cell migration behavior via junction interactions. *Biophys J,* 95**,** 4013-24.

HARRIS, L. K., KEOGH, R. J., WAREING, M., BAKER, P. N., CARTWRIGHT, J. E., APLIN, J. D. & WHITLEY, G. S. 2006. Invasive trophoblasts stimulate vascular smooth muscle cell apoptosis by a fas ligand-dependent mechanism. *Am J Pathol,* 169**,** 1863-74.

HASTON, W. S., SHIELDS, J. M. & WILKINSON, P. C. 1982. Lymphocyte locomotion and attachment on two-dimensional surfaces and in three-dimensional matrices. *J Cell Biol,* 92**,** 747-52.

HAY, E. D. 1981. Extracellular matrix. *J Cell Biol,* 91**,** 205s-223s.

HAYWARD, C. J., FRADETTE, J., GALBRAITH, T., REMY, M., GUIGNARD, R., GAUVIN, R., GERMAIN, L. & AUGER, F. A. 2013. Harvesting the potential of the human umbilical cord: isolation and characterisation of four cell types for tissue engineering applications. *Cells Tissues Organs,* 197**,** 37-54.

HENDIJANI, F., SADEGHI-ALIABADI, H. & HAGHJOOY JAVANMARD, S. 2014. Comparison of human mesenchymal stem cells isolated by explant culture method from entire umbilical cord and Wharton's jelly matrix. *Cell Tissue Bank,* 15**,** 555-65.

HENNRICK, K. T., KEETON, A. G., NANUA, S., KIJEK, T. G., GOLDSMITH, A. M., SAJJAN, U. S., BENTLEY, J. K., LAMA, V. N., MOORE, B. B., SCHUMACHER, R. E., THANNICKAL, V. J. & HERSHENSON, M. B. 2007. Lung cells from neonates show a mesenchymal stem cell phenotype. *Am J Respir Crit Care Med,* 175**,** 1158-64.

HERREN, B., LEVKAU, B., RAINES, E. W. & ROSS, R. 1998. Cleavage of beta-catenin and plakoglobin and shedding of VE-cadherin during endothelial apoptosis: evidence for a role for caspases and metalloproteinases. *Mol Biol Cell,* 9**,** 1589-601.

HIRSCHI, K. K. & D'AMORE, P. A. 1996. Pericytes in the microvasculature. *Cardiovasc Res,* 32**,** 687-98.

HORDIJK, P. L., ANTHONY, E., MUL, F. P., RIENTSMA, R., OOMEN, L. C. & ROOS, D. 1999. Vascular-endothelial-cadherin modulates endothelial monolayer permeability. *J Cell Sci,* 112 (Pt 12)**,** 1915-23.

HORVATH, G., SERRU, V., CLAY, D., BILLARD, M., BOUCHEIX, C. & RUBINSTEIN, E. 1998. CD19 is linked to the integrin-associated tetraspans CD9, CD81, and CD82. *J Biol Chem,* 273**,** 30537-43.

HU, J., WANG, Y., WANG, F., WANG, L., YU, X., SUN, R., WANG, Z., GAO, H., FU, Z., ZHAO, W. & YAN, S. 2014. Effect and mechanisms of human Wharton's jelly-derived mesenchymal stem cells on type 1 diabetes in NOD model. *Endocrine*.

HU, J., WANG, Y., WANG, F., WANG, L., YU, X., SUN, R., WANG, Z., GAO, H., FU, Z., ZHAO, W. & YAN, S. 2015. Effect and mechanisms of human Wharton's jelly-derived mesenchymal stem cells on type 1 diabetes in NOD model. *Endocrine,* 48**,** 124-34.

HU, J., YU, X., WANG, Z., WANG, F., WANG, L., GAO, H., CHEN, Y., ZHAO, W., JIA, Z., YAN, S. & WANG, Y. 2013. Long term effects of the implantation of Wharton's jelly-derived mesenchymal stem cells from the umbilical cord for newly-onset type 1 diabetes mellitus. *Endocr J,* 60**,** 347-57.

HUTTENLOCHER, A. & HORWITZ, A. R. 2011. Integrins in cell migration. *Cold Spring Harb Perspect Biol,* 3**,** a005074.

INVERNICI, G., EMANUELI, C., MADEDDU, P., CRISTINI, S., GADAU, S., BENETTI, A., CIUSANI, E., STASSI, G., SIRAGUSA, M., NICOSIA, R., PESCHLE, C., FASCIO, U., COLOMBO, A., RIZZUTI, T., PARATI, E. & ALESSANDRI, G. 2007. Human fetal aorta contains vascular progenitor cells capable of inducing vasculogenesis, angiogenesis, and myogenesis in vitro and in a murine model of peripheral ischemia. *Am J Pathol,* 170**,** 1879-92.

ISNER, J. M. & ASAHARA, T. 1999. Angiogenesis and vasculogenesis as therapeutic strategies for postnatal neovascularization. *J Clin Invest,* 103**,** 1231-6.

ITO, K., OKAMOTO, I., ARAKI, N., KAWANO, Y., NAKAO, M., FUJIYAMA, S., TOMITA, K., MIMORI, T. & SAYA, H. 1999. Calcium influx triggers the sequential proteolysis of extracellular and cytoplasmic domains of E-cadherin, leading to loss of beta-catenin from cell-cell contacts. *Oncogene,* 18**,** 7080-90.

IVANOV, D., PHILIPPOVA, M., ANTROPOVA, J., GUBAEVA, F., ILJINSKAYA, O., TARARAK, E., BOCHKOV, V., ERNE, P., RESINK, T. & TKACHUK, V. 2001. Expression of cell adhesion molecule T-cadherin in the human vasculature. *Histochem Cell Biol,* 115**,** 231-42.

JAFFE, E. A., NACHMAN, R. L., BECKER, C. G. & MINICK, C. R. 1973. Culture of human endothelial cells derived from umbilical veins. Identification by morphologic and immunologic criteria. *J Clin Invest,* 52**,** 2745-56.

JARVENPAA, J., VUORISTO, J. T., SAVOLAINEN, E. R., UKKOLA, O., VASKIVUO, T. & RYYNANEN, M. 2007. Altered expression of angiogenesis-related placental genes in pre-eclampsia associated with intrauterine growth restriction. *Gynecol Endocrinol,* 23**,** 351-5.

JAUNIAUX, E., WATSON, A. L., HEMPSTOCK, J., BAO, Y. P., SKEPPER, J. N. & BURTON, G. J. 2000. Onset of maternal arterial blood flow and placental oxidative stress. A possible factor in human early pregnancy failure. *Am J Pathol,* 157**,** 2111-22.

JOHNSON-LEGER, C., AURRAND-LIONS, M. & IMHOF, B. A. 2000. The parting of the endothelium: miracle, or simply a junctional affair? *J Cell Sci,* 113 (Pt 6)**,** 921-33.

JOHNSON, F. L., LOOK, A. T., GOCKERMAN, J., RUGGIERO, M. R., DALLA-POZZA, L. & BILLINGS, F. T., 3RD 1984. Bone-marrow transplantation in a patient with sickle-cell anemia. *N Engl J Med,* 311**,** 780-3.

JOHNSON, F. L., SANDERS, J. E., RUGGIERO, M., CHARD, R. L., JR. & THOMAS, E. D. 1988. Bone marrow transplantation for the treatment of acute nonlymphoblastic leukemia in children aged less than 2 years. *Blood,* 71**,** 1277-80.

JONES, C. J. & FOX, H. 1991. Ultrastructure of the normal human placenta. *Electron Microsc Rev,* 4**,** 129-78.

KALKA, C., MASUDA, H., TAKAHASHI, T., KALKA-MOLL, W. M., SILVER, M., KEARNEY, M., LI, T., ISNER, J. M. & ASAHARA, T. 2000. Transplantation of ex vivo expanded endothelial progenitor cells for therapeutic neovascularization. *Proc Natl Acad Sci U S A,* 97**,** 3422-7.

KAM, E. P., GARDNER, L., LOKE, Y. W. & KING, A. 1999. The role of trophoblast in the physiological change in decidual spiral arteries. *Hum Reprod,* 14**,** 2131-8.

KARA, R. J., BOLLI, P., KARAKIKES, I., MATSUNAGA, I., TRIPODI, J., TANWEER, O., ALTMAN, P., SHACHTER, N. S., NAKANO, A., NAJFELD, V. & CHAUDHRY, H. W. 2012. Fetal cells traffic to injured maternal myocardium and undergo cardiac differentiation. *Circ Res,* 110**,** 82-93.

KASOW, K. A., SIMS-POSTON, L., ELDRIDGE, P. & HALE, G. A. 2007. CD34(+) hematopoietic progenitor cell selection of bone marrow grafts for autologous transplantation in pediatric patients. *Biol Blood Marrow Transplant,* 13**,** 608-14.

KASSIS, I., ZANGI, L., RIVKIN, R., LEVDANSKY, L., SAMUEL, S., MARX, G. & GORODETSKY, R. 2006. Isolation of mesenchymal stem cells from G-CSF-mobilized human peripheral blood using fibrin microbeads. *Bone Marrow Transplant,* 37**,** 967-76.

KATAYAMA, Y., HIDALGO, A., FURIE, B. C., VESTWEBER, D., FURIE, B. & FRENETTE, P. S. 2003. PSGL-1 participates in E-selectin-mediated progenitor homing to bone marrow: evidence for cooperation between E-selectin ligands and alpha4 integrin. *Blood,* 102**,** 2060-7.

KAUFMANN, P., BLACK, S. & HUPPERTZ, B. 2003. Endovascular trophoblast invasion: implications for the pathogenesis of intrauterine growth retardation and preeclampsia. *Biol Reprod,* 69**,** 1-7.

KAWADA, H., FUJITA, J., KINJO, K., MATSUZAKI, Y., TSUMA, M., MIYATAKE, H., MUGURUMA, Y., TSUBOI, K., ITABASHI, Y., IKEDA, Y., OGAWA, S., OKANO, H., HOTTA, T., ANDO, K. & FUKUDA, K. 2004. Nonhematopoietic mesenchymal stem cells can be mobilized and differentiate into cardiomyocytes after myocardial infarction. *Blood,* 104**,** 3581-7.

KAZAKOFF, P. W., MCGUIRE, T. R., HOIE, E. B., CANO, M. & IVERSEN, P. L. 1995. An in vitro model for endothelial permeability: assessment of monolayer integrity. *In Vitro Cell Dev Biol Anim,* 31**,** 846-52.

KECK, P. J., HAUSER, S. D., KRIVI, G., SANZO, K., WARREN, T., FEDER, J. & CONNOLLY, D. T. 1989. Vascular permeability factor, an endothelial cell mitogen related to PDGF. *Science,* 246**,** 1309-12.

KEREN, K., PINCUS, Z., ALLEN, G. M., BARNHART, E. L., MARRIOTT, G., MOGILNER, A. & THERIOT, J. A. 2008. Mechanism of shape determination in motile cells. *Nature,* 453**,** 475-80.

KIEL, M. J. & MORRISON, S. J. 2008. Uncertainty in the niches that maintain haematopoietic stem cells. *Nat Rev Immunol,* 8**,** 290-301.

KIM, D. S., KIM, J. H., LEE, J. K., CHOI, S. J., KIM, J. S., JEUN, S. S., OH, W., YANG, Y. S. & CHANG, J. W. 2009. Overexpression of CXC chemokine receptors is required for the superior glioma-tracking property of umbilical cord blood-derived mesenchymal stem cells. *Stem Cells Dev,* 18**,** 511-9.

KIM, M. J., SHIN, K. S., JEON, J. H., LEE, D. R., SHIM, S. H., KIM, J. K., CHA, D. H., YOON, T. K. & KIM, G. J. 2011. Human chorionic-plate-derived mesenchymal stem cells and Wharton's jelly-derived mesenchymal stem cells: a comparative analysis of their potential as placenta-derived stem cells. *Cell Tissue Res,* 346**,** 53-64.

KINNAIRD, T., STABILE, E., BURNETT, M. S., LEE, C. W., BARR, S., FUCHS, S. & EPSTEIN, S. E. 2004. Marrow-derived stromal cells express genes encoding a broad

spectrum of arteriogenic cytokines and promote in vitro and in vivo arteriogenesis through paracrine mechanisms. *Circ Res,* 94**,** 678-85.

KITA, K., GAUGLITZ, G. G., PHAN, T. T., HERNDON, D. N. & JESCHKE, M. G. 2010. Isolation and characterization of mesenchymal stem cells from the sub-amniotic human umbilical cord lining membrane. *Stem Cells Dev,* 19**,** 491-502.

KLEMKE, R. L., CAI, S., GIANNINI, A. L., GALLAGHER, P. J., DE LANEROLLE, P. & CHERESH, D. A. 1997. Regulation of cell motility by mitogen-activated protein kinase. *J Cell Biol,* 137**,** 481-92.

KLUGER, M. S. 2004. Vascular endothelial cell adhesion and signaling during leukocyte recruitment. *Adv Dermatol,* 20**,** 163-201.

KO, T. L., FU, Y. Y., SHIH, Y. H., LIN, Y. H., KO, M. H., FU, T. W., LIN, T. Y., HSIAO, H. S., CHU, P. M. & FU, Y. S. 2014. A High Efficiency Induction of Dopaminergic Cells from Human Umbilical Mesenchymal Stem Cells for the Treatment of Hemiparkinsonian Rats. *Cell Transplant*.

KOBAYASHI, K., KUBOTA, T. & ASO, T. 1998. Study on myofibroblast differentiation in the stromal cells of Wharton's jelly: expression and localization of alpha-smooth muscle actin. *Early Hum Dev,* 51**,** 223-33.

KOCH, T. G., HEERKENS, T., THOMSEN, P. D. & BETTS, D. H. 2007. Isolation of mesenchymal stem cells from equine umbilical cord blood. *BMC Biotechnol,* 7**,** 26.

KONIG, J., LANG, I., SIWETZ, M., FROHLICH, J. & HUPPERTZ, B. 2014. Amnion-derived mesenchymal stromal cells show a mesenchymal-epithelial phenotype in culture. *Cell Tissue Bank,* 15**,** 193-8.

KOPP, H. G., AVECILLA, S. T., HOOPER, A. T. & RAFII, S. 2005. The bone marrow vascular niche: home of HSC differentiation and mobilization. *Physiology (Bethesda),* 20**,** 349-56.

KRISTENSEN, J., VESTERGAARD, M., WISBORG, K., KESMODEL, U. & SECHER, N. J. 2005. Pre-pregnancy weight and the risk of stillbirth and neonatal death. *BJOG,* 112**,** 403-8.

LA ROCCA, G., ANZALONE, R., CORRAO, S., MAGNO, F., LORIA, T., LO IACONO, M., DI STEFANO, A., GIANNUZZI, P., MARASA, L., CAPPELLO, F., ZUMMO, G. & FARINA, F. 2009. Isolation and characterization of Oct-4+/HLA-G+ mesenchymal stem cells from human umbilical cord matrix: differentiation potential and detection of new markers. *Histochem Cell Biol,* 131**,** 267-82.

LAMMERDING, J., FONG, L. G., JI, J. Y., REUE, K., STEWART, C. L., YOUNG, S. G. & LEE, R. T. 2006. Lamins A and C but not lamin B1 regulate nuclear mechanics. *J Biol Chem,* 281**,** 25768-80.

LAMMERMANN, T. & SIXT, M. 2009. Mechanical modes of 'amoeboid' cell migration. *Curr Opin Cell Biol,* 21**,** 636-44.

LAMPUGNANI, M. G., CORADA, M., ANDRIOPOULOU, P., ESSER, S., RISAU, W. & DEJANA, E. 1997. Cell confluence regulates tyrosine phosphorylation of adherens junction components in endothelial cells. *J Cell Sci,* 110 (Pt 17)**,** 2065-77.

LAMPUGNANI, M. G., CORADA, M., CAVEDA, L., BREVIARIO, F., AYALON, O., GEIGER, B. & DEJANA, E. 1995. The molecular organization of endothelial cell to cell junctions: differential association of plakoglobin, beta-catenin, and alpha-catenin with vascular endothelial cadherin (VE-cadherin). *J Cell Biol,* 129**,** 203-17.

LAMPUGNANI, M. G. & DEJANA, E. 1997. Interendothelial junctions: structure, signalling and functional roles. *Curr Opin Cell Biol,* 9**,** 674-82.

LAMPUGNANI, M. G., ORSENIGO, F., GAGLIANI, M. C., TACCHETTI, C. & DEJANA, E. 2006. Vascular endothelial cadherin controls VEGFR-2 internalization and signaling from intracellular compartments. *J Cell Biol,* 174**,** 593-604.

LAMPUGNANI, M. G., RESNATI, M., DEJANA, E. & MARCHISIO, P. C. 1991. The role of integrins in the maintenance of endothelial monolayer integrity. *J Cell Biol,* 112**,** 479-90.

LAMPUGNANI, M. G., RESNATI, M., RAITERI, M., PIGOTT, R., PISACANE, A., HOUEN, G., RUCO, L. P. & DEJANA, E. 1992. A novel endothelial-specific membrane protein is a marker of cell-cell contacts. *J Cell Biol,* 118**,** 1511-22.

LASH, G. E., ROBSON, S. C. & BULMER, J. N. 2010. Review: Functional role of uterine natural killer (uNK) cells in human early pregnancy decidua. *Placenta,* 31 Suppl**,** S87-92.

LAUER, M. S. 2012. Advancing cardiovascular research. *Chest,* 141**,** 500-5.

LAVIOLA, L., ORLANDO, M. R., INCALZA, M. A., CACCIOPPOLI, C., MELCHIORRE, M., LEONARDINI, A., CIGNARELLI, A., TORTOSA, F., LABARBUTA, R., MARTEMUCCI, S., PACELLI, C., COCCO, T., PERRINI, S., NATALICCHIO, A. & GIORGINO, F. 2013. TNFalpha signals via p66(Shc) to induce E-Selectin, promote leukocyte transmigration and enhance permeability in human endothelial cells. *PLoS One,* 8**,** e81930.

LEACH, L., BABAWALE, M. O., ANDERSON, M. & LAMMIMAN, M. 2002. Vasculogenesis, angiogenesis and the molecular organisation of endothelial junctions in the early human placenta. *J Vasc Res,* 39**,** 246-59.

LEACH, L., CLARK, P., LAMPUGNANI, M. G., ARROYO, A. G., DEJANA, E. & FIRTH, J. A. 1993. Immunoelectron characterisation of the inter-endothelial junctions of human term placenta. *J Cell Sci,* 104 (Pt 4)**,** 1073-81.

LEACH, L., EATON, B. M., WESTCOTT, E. D. & FIRTH, J. A. 1995. Effect of histamine on endothelial permeability and structure and adhesion molecules of the paracellular junctions of perfused human placental microvessels. *Microvasc Res,* 50**,** 323-37.

LEACH, L. & FIRTH, J. A. 1992. Fine structure of the paracellular junctions of terminal villous capillaries in the perfused human placenta. *Cell Tissue Res,* 268**,** 447-52.

LEACH, L., GRAY, C., STATON, S., BABAWALE, M. O., GRUCHY, A., FOSTER, C., MAYHEW, T. M. & JAMES, D. K. 2004. Vascular endothelial cadherin and beta-catenin in human fetoplacental vessels of pregnancies complicated by Type 1 diabetes: associations with angiogenesis and perturbed barrier function. *Diabetologia,* 47**,** 695-709.

LEACH, L., HAMILTON, R. D. & FOSS, A. J. 2012. Phenotypic plasticity of human umbilical vein endothelial cells. *Br J Ophthalmol,* 96**,** 1152.

LEACH, L., LAMMIMAN, M. J., BABAWALE, M. O., HOBSON, S. A., BROMILOU, B., LOVAT, S. & SIMMONDS, M. J. 2000. Molecular organization of tight and adherens junctions in the human placental vascular tree. *Placenta,* 21**,** 547-57.

LEACH, L., TAYLOR, A. & SCIOTA, F. 2009. Vascular dysfunction in the diabetic placenta: causes and consequences. *J Anat,* 215**,** 69-76.

LEUNG, D. W., CACHIANES, G., KUANG, W. J., GOEDDEL, D. V. & FERRARA, N. 1989. Vascular endothelial growth factor is a secreted angiogenic mitogen. *Science,* 246**,** 1306-9.

LI, C. X. & POZNANSKY, M. J. 1990. Characterization of the ZO-1 protein in endothelial and other cell lines. *J Cell Sci,* 97 (Pt 2)**,** 231-7.

LI, P., ZHANG, J., LIU, J., MA, H., LIE, P., WANG, Y., LIU, G., ZENG, H., LI, Z. & WEI, X. 2014a. Promoting the Recovery of Injured Liver with Poly (3-Hydroxybutyrate-Co-3-Hydroxyvalerate-Co-3-Hydroxyhexanoate) Scaffolds Loaded with Umbilical Cord-Derived Mesenchymal Stem Cells. *Tissue Eng Part A.*

LI, P., ZHANG, R., SUN, H., CHEN, L., LIU, F., YAO, C., DU, M. & JIANG, X. 2013. PKH26 can transfer to host cells in vitro and vivo. *Stem Cells Dev,* 22**,** 340-4.

LI, R., REN, M., CHEN, N., LUO, M., ZHANG, Z. & WU, J. 2012. Vitronectin increases vascular permeability by promoting VE-cadherin internalization at cell junctions. *PLoS One,* 7**,** e37195.

LI, X., BAI, J., JI, X., LI, R., XUAN, Y. & WANG, Y. 2014b. Comprehensive characterization of four different populations of human mesenchymal stem cells as regards their immune properties, proliferation and differentiation. *Int J Mol Med,* 34**,** 695-704.

LILIEN, J. & BALSAMO, J. 2005. The regulation of cadherin-mediated adhesion by tyrosine phosphorylation/dephosphorylation of beta-catenin. *Curr Opin Cell Biol,* 17**,** 459-65.

LIN, M. N., SHANG, D. S., SUN, W., LI, B., XU, X., FANG, W. G., ZHAO, W. D., CAO, L. & CHEN, Y. H. 2013. Involvement of PI3K and ROCK signaling pathways in migration of bone marrow-derived mesenchymal stem cells through human brain microvascular endothelial cell monolayers. *Brain Res,* 1513**,** 1-8.

LIN, Y., LIN, L., WANG, Q., JIN, Y., ZHANG, Y., CAO, Y. & ZHENG, C. 2014. Transplantation of human umbilical mesenchymal stem cells attenuates dextran sulfate sodium-induced colitis in mice. *Clin Exp Pharmacol Physiol*.

LIU, L., YU, Y., HOU, Y., CHAI, J., DUAN, H., CHU, W., ZHANG, H., HU, Q. & DU, J. 2014. Human umbilical cord mesenchymal stem cells transplantation promotes cutaneous wound healing of severe burned rats. *PLoS One,* 9**,** e88348.

LIU, L. Y., CHAI, J. K., DUAN, H. J., HOU, Y. S., YIN, H. N., YU, Y. H., HU, Q., HAO, D. F., FENG, G., LI, T. & DU, J. D. 2013. [Comparison of different methods for the isolation of human umbilical cord mesenchymal stem cells]. *Zhonghua Yi Xue Za Zhi,* 93**,** 2592-6.

LUNN, D. P. 1993. A comparative review of human and equine leucocyte differentiation antigens. *Br Vet J,* 149**,** 31-49.

LV, F. J., TUAN, R. S., CHEUNG, K. M. & LEUNG, V. Y. 2014. The surface markers and identity of human mesenchymal stem cells. *Stem Cells*.

LYALL, F. 2002. The human placental bed revisited. *Placenta,* 23**,** 555-62.

MAASER, K., WOLF, K., KLEIN, C. E., NIGGEMANN, B., ZANKER, K. S., BROCKER, E. B. & FRIEDL, P. 1999. Functional hierarchy of simultaneously expressed adhesion receptors: integrin alpha2beta1 but not CD44 mediates MV3 melanoma cell migration and matrix reorganization within three-dimensional hyaluronan-containing collagen matrices. *Mol Biol Cell,* 10**,** 3067-79.

MARAMBAUD, P., SHIOI, J., SERBAN, G., GEORGAKOPOULOS, A., SARNER, S., NAGY, V., BAKI, L., WEN, P., EFTHIMIOPOULOS, S., SHAO, Z., WISNIEWSKI, T. & ROBAKIS, N. K. 2002. A presenilin-1/gamma-secretase cleavage releases the E-cadherin intracellular domain and regulates disassembly of adherens junctions. *EMBO J,* 21**,** 1948-56.

MARTIN, C., BURDON, P. C., BRIDGER, G., GUTIERREZ-RAMOS, J. C., WILLIAMS, T. J. & RANKIN, S. M. 2003. Chemokines acting via CXCR2 and CXCR4 control the release of neutrophils from the bone marrow and their return following senescence. *Immunity,* 19**,** 583-93.

MAYHEW, T. M. & SAMPSON, C. 2003. Maternal diabetes mellitus is associated with altered deposition of fibrin-type fibrinoid at the villous surface in term placentae. *Placenta,* 24**,** 524-31.

MCELREAVEY, K. D., IRVINE, A. I., ENNIS, K. T. & MCLEAN, W. H. 1991. Isolation, culture and characterisation of fibroblast-like cells derived from the Wharton's jelly portion of human umbilical cord. *Biochem Soc Trans,* 19**,** 29S.

MENGE, T., GERBER, M., WATAHA, K., REID, W., GUHA, S., COX, C. S., JR., DASH, P., REITZ, M. S., JR., KHAKOO, A. Y. & PATI, S. 2013. Human mesenchymal stem

cells inhibit endothelial proliferation and angiogenesis via cell-cell contact through modulation of the VE-Cadherin/beta-catenin signaling pathway. *Stem Cells Dev,* 22**,** 148-57.

MICHEL, C. C. 2012. Electron tomography of vesicles. *Microcirculation,* 19**,** 473-6.

MILLAUER, B., WIZIGMANN-VOOS, S., SCHNURCH, H., MARTINEZ, R., MOLLER, N. P., RISAU, W. & ULLRICH, A. 1993. High affinity VEGF binding and developmental expression suggest Flk-1 as a major regulator of vasculogenesis and angiogenesis. *Cell,* 72**,** 835-46.

MIRAVET, S., PIEDRA, J., CASTANO, J., RAURELL, I., FRANCI, C., DUNACH, M. & GARCIA DE HERREROS, A. 2003. Tyrosine phosphorylation of plakoglobin causes contrary effects on its association with desmosomes and adherens junction components and modulates beta-catenin-mediated transcription. *Mol Cell Biol,* 23**,** 7391-402.

MITCHELL, J. B., MCINTOSH, K., ZVONIC, S., GARRETT, S., FLOYD, Z. E., KLOSTER, A., DI HALVORSEN, Y., STORMS, R. W., GOH, B., KILROY, G., WU, X. & GIMBLE, J. M. 2006. Immunophenotype of human adipose-derived cells: temporal changes in stromal-associated and stem cell-associated markers. *Stem Cells,* 24**,** 376-85.

MITCHELL, K. E., WEISS, M. L., MITCHELL, B. M., MARTIN, P., DAVIS, D., MORALES, L., HELWIG, B., BEERENSTRAUCH, M., ABOU-EASA, K., HILDRETH, T., TROYER, D. & MEDICETTY, S. 2003. Matrix cells from Wharton's jelly form neurons and glia. *Stem Cells,* 21**,** 50-60.

MONTANUCCI, P., BASTA, G., PESCARA, T., PENNONI, I., DI GIOVANNI, F. & CALAFIORE, R. 2011. New simple and rapid method for purification of mesenchymal stem cells from the human umbilical cord Wharton jelly. *Tissue Eng Part A,* 17**,** 2651-61.

MOSER, G., ORENDI, K., GAUSTER, M., SIWETZ, M., HELIGE, C. & HUPPERTZ, B. 2011. The art of identification of extravillous trophoblast. *Placenta,* 32**,** 197-9.

MULLER, A., HOMEY, B., SOTO, H., GE, N., CATRON, D., BUCHANAN, M. E., MCCLANAHAN, T., MURPHY, E., YUAN, W., WAGNER, S. N., BARRERA, J. L., MOHAR, A., VERASTEGUI, E. & ZLOTNIK, A. 2001. Involvement of chemokine receptors in breast cancer metastasis. *Nature,* 410**,** 50-6.

MULLER, I., KORDOWICH, S., HOLZWARTH, C., SPANO, C., ISENSEE, G., STAIBER, A., VIEBAHN, S., GIESEKE, F., LANGER, H., GAWAZ, M. P., HORWITZ, E. M., CONTE, P., HANDGRETINGER, R. & DOMINICI, M. 2006. Animal serum-free culture conditions for isolation and expansion of multipotent mesenchymal stromal cells from human BM. *Cytotherapy,* 8**,** 437-44.

MULLER, W. A. 2002. Leukocyte-endothelial cell interactions in the inflammatory response. *Lab Invest,* 82**,** 521-33.

MULLER, W. A. 2003. Leukocyte-endothelial-cell interactions in leukocyte transmigration and the inflammatory response. *Trends Immunol,* 24**,** 327-34.

MUSIALEK, P., MAZUREK, A., JAROCHA, D., TEKIELI, L., SZOT, W., KOSTKIEWICZ, M., BANYS, R. P., URBANCZYK, M., KADZIELSKI, A., TRYSTULA, M., KIJOWSKI, J., ZMUDKA, K., PODOLEC, P. & MAJKA, M. 2015. Myocardial regeneration strategy using Wharton's jelly mesenchymal stem cells as an off-the-shelf 'unlimited' therapeutic agent: results from the Acute Myocardial Infarction First-in-Man Study. *Postepy Kardiol Interwencyjnej,* 11**,** 100-7.

NAGAMURA-INOUE, T. & HE, H. 2014. Umbilical cord-derived mesenchymal stem cells: Their advantages and potential clinical utility. *World J Stem Cells,* 6**,** 195-202.

NAKAJIMA, H., UCHIDA, K., GUERRERO, A. R., WATANABE, S., SUGITA, D., TAKEURA, N., YOSHIDA, A., LONG, G., WRIGHT, K. T., JOHNSON, W. E. & BABA, H. 2012. Transplantation of mesenchymal stem cells promotes an alternative pathway of macrophage activation and functional recovery after spinal cord injury. *J Neurotrauma,* 29**,** 1614-25.

NAMIKI, A., BROGI, E., KEARNEY, M., KIM, E. A., WU, T., COUFFINHAL, T., VARTICOVSKI, L. & ISNER, J. M. 1995. Hypoxia induces vascular endothelial growth factor in cultured human endothelial cells. *J Biol Chem,* 270**,** 31189-95.

NARTPRAYUT, K., Y, U. P., KHEOLAMAI, P., MANOCHANTR, S., CHAYOSUMRIT, M., ISSARAGRISIL, S. & SUPOKAWEJ, A. 2013. Cardiomyocyte differentiation of perinatallyderived mesenchymal stem cells. *Mol Med Rep,* 7**,** 1465-9.

NASDALA, I., WOLBURG-BUCHHOLZ, K., WOLBURG, H., KUHN, A., EBNET, K., BRACHTENDORF, G., SAMULOWITZ, U., KUSTER, B., ENGELHARDT, B., VESTWEBER, D. & BUTZ, S. 2002. A transmembrane tight junction protein selectively expressed on endothelial cells and platelets. *J Biol Chem,* 277**,** 16294-303.

NAUCK, M., ROTH, M., TAMM, M., EICKELBERG, O., WIELAND, H., STULZ, P. & PERRUCHOUD, A. P. 1997. Induction of vascular endothelial growth factor by platelet-activating factor and platelet-derived growth factor is downregulated by corticosteroids. *Am J Respir Cell Mol Biol,* 16**,** 398-406.

NAVARRO, P., CAVEDA, L., BREVIARIO, F., MANDOTEANU, I., LAMPUGNANI, M. G. & DEJANA, E. 1995. Catenin-dependent and -independent functions of vascular endothelial cadherin. *J Biol Chem,* 270**,** 30965-72.

NAVARRO, P., RUCO, L. & DEJANA, E. 1998. Differential localization of VE- and N-cadherins in human endothelial cells: VE-cadherin competes with N-cadherin for junctional localization. *J Cell Biol,* 140**,** 1475-84.

NAWROTH, R., POELL, G., RANFT, A., KLOEP, S., SAMULOWITZ, U., FACHINGER, G., GOLDING, M., SHIMA, D. T., DEUTSCH, U. & VESTWEBER, D. 2002. VE-PTP and VE-cadherin ectodomains interact to facilitate regulation of phosphorylation and cell contacts. *EMBO J,* 21**,** 4885-95.

NELSON, D. M. 1996. Apoptotic changes occur in syncytiotrophoblast of human placental villi where fibrin type fibrinoid is deposited at discontinuities in the villous trophoblast. *Placenta,* 17**,** 387-91.

NEUFELD, G., COHEN, T., GENGRINOVITCH, S. & POLTORAK, Z. 1999. Vascular endothelial growth factor (VEGF) and its receptors. *FASEB J,* 13**,** 9-22.

NEWMAN, P. J. 1997. The biology of PECAM-1. *J Clin Invest,* 100**,** S25-9.

NIAKAN, K. K. & EGGAN, K. 2013. Analysis of human embryos from zygote to blastocyst reveals distinct gene expression patterns relative to the mouse. *Dev Biol,* 375**,** 54-64.

NOE, V., FINGLETON, B., JACOBS, K., CRAWFORD, H. C., VERMEULEN, S., STEELANT, W., BRUYNEEL, E., MATRISIAN, L. M. & MAREEL, M. 2001. Release of an invasion promoter E-cadherin fragment by matrilysin and stromelysin-1. *J Cell Sci,* 114**,** 111-118.

NORMAN, L. L., BRUGUES, J., SENGUPTA, K., SENS, P. & ARANDA-ESPINOZA, H. 2010. Cell blebbing and membrane area homeostasis in spreading and retracting cells. *Biophys J,* 99**,** 1726-33.

O'DONOGHUE, K., CHOOLANI, M., CHAN, J., DE LA FUENTE, J., KUMAR, S., CAMPAGNOLI, C., BENNETT, P. R., ROBERTS, I. A. & FISK, N. M. 2003. Identification of fetal mesenchymal stem cells in maternal blood: implications for non-invasive prenatal diagnosis. *Mol Hum Reprod,* 9**,** 497-502.

ONAT, D., BRILLON, D., COLOMBO, P. C. & SCHMIDT, A. M. 2011. Human vascular endothelial cells: a model system for studying vascular inflammation in diabetes and atherosclerosis. *Curr Diab Rep,* 11**,** 193-202.

ORSENIGO, F., GIAMPIETRO, C., FERRARI, A., CORADA, M., GALAUP, A., SIGISMUND, S., RISTAGNO, G., MADDALUNO, L., KOH, G. Y., FRANCO, D., KURTCUOGLU, V., POULIKAKOS, D., BALUK, P., MCDONALD, D., GRAZIA LAMPUGNANI, M. & DEJANA, E. 2012. Phosphorylation of VE-cadherin is modulated by haemodynamic forces and contributes to the regulation of vascular permeability in vivo. *Nat Commun,* 3**,** 1208.

OWEN, M. 1988. Marrow stromal stem cells. *J Cell Sci Suppl,* 10**,** 63-76.

PAPAYANNOPOULOU, T. 2003. Bone marrow homing: the players, the playfield, and their evolving roles. *Curr Opin Hematol,* 10**,** 214-9.

PAPAYANNOPOULOU, T., PRIESTLEY, G. V., NAKAMOTO, B., ZAFIROPOULOS, V. & SCOTT, L. M. 2001. Molecular pathways in bone marrow homing: dominant role of alpha(4)beta(1) over beta(2)-integrins and selectins. *Blood,* 98**,** 2403-11.

PAPPA, K. I. & ANAGNOU, N. P. 2009. Novel sources of fetal stem cells: where do they fit on the developmental continuum? *Regen Med,* 4**,** 423-33.

PAQUET-FIFIELD, S., SCHLUTER, H., LI, A., AITKEN, T., GANGATIRKAR, P., BLASHKI, D., KOELMEYER, R., POULIOT, N., PALATSIDES, M., ELLIS, S., BROUARD, N., ZANNETTINO, A., SAUNDERS, N., THOMPSON, N., LI, J. & KAUR, P. 2009. A role for pericytes as microenvironmental regulators of human skin tissue regeneration. *J Clin Invest,* 119**,** 2795-806.

PARANT, O., DUBERNARD, G., CHALLIER, J. C., OSTER, M., UZAN, S., ARACTINGI, S. & KHOSROTEHRANI, K. 2009. CD34+ cells in maternal placental blood are mainly fetal in origin and express endothelial markers. *Lab Invest,* 89**,** 915-23.

PARDI, G., MARCONI, A. M. & CETIN, I. 2002. Placental-fetal interrelationship in IUGR fetuses--a review. *Placenta,* 23 Suppl A**,** S136-41.

PARK, H. J., ZHANG, Y., GEORGESCU, S. P., JOHNSON, K. L., KONG, D. & GALPER, J. B. 2006. Human umbilical vein endothelial cells and human dermal microvascular endothelial cells offer new insights into the relationship between lipid metabolism and angiogenesis. *Stem Cell Rev,* 2**,** 93-102.

PARK, S. A., RYU, C. H., KIM, S. M., LIM, J. Y., PARK, S. I., JEONG, C. H., JUN, J. A., OH, J. H., PARK, S. H., OH, W. & JEUN, S. S. 2011. CXCR4-transfected human umbilical cord blood-derived mesenchymal stem cells exhibit enhanced migratory capacity toward gliomas. *Int J Oncol,* 38**,** 97-103.

PARRY, E. W. 1970. Some electron microscope observations on the mesenchymal structures of full-term umbilical cord. *J Anat,* 107**,** 505-18.

PATI, S., KHAKOO, A. Y., ZHAO, J., JIMENEZ, F., GERBER, M. H., HARTING, M., REDELL, J. B., GRILL, R., MATSUO, Y., GUHA, S., COX, C. S., REITZ, M. S., HOLCOMB, J. B. & DASH, P. K. 2011. Human mesenchymal stem cells inhibit vascular permeability by modulating vascular endothelial cadherin/beta-catenin signaling. *Stem Cells Dev,* 20**,** 89-101.

PEREIRA, W. C., KHUSHNOOMA, I., MADKAIKAR, M. & GHOSH, K. 2008. Reproducible methodology for the isolation of mesenchymal stem cells from human umbilical cord and its potential for cardiomyocyte generation. *J Tissue Eng Regen Med,* 2**,** 394-9.

PIJNENBORG, R., ANTHONY, J., DAVEY, D. A., REES, A., TILTMAN, A., VERCRUYSSE, L. & VAN ASSCHE, A. 1991. Placental bed spiral arteries in the hypertensive disorders of pregnancy. *Br J Obstet Gynaecol,* 98**,** 648-55.

PIJNENBORG, R., BLAND, J. M., ROBERTSON, W. B. & BROSENS, I. 1983. Uteroplacental arterial changes related to interstitial trophoblast migration in early human pregnancy. *Placenta,* 4**,** 397-413.

PIJNENBORG, R., DIXON, G., ROBERTSON, W. B. & BROSENS, I. 1980. Trophoblastic invasion of human decidua from 8 to 18 weeks of pregnancy. *Placenta,* 1**,** 3-19.

PIJNENBORG, R., VERCRUYSSE, L. & BROSENS, I. 2011. Deep placentation. *Best Pract Res Clin Obstet Gynaecol,* 25**,** 273-85.

PIJNENBORG, R., VERCRUYSSE, L. & HANSSENS, M. 2006. The uterine spiral arteries in human pregnancy: facts and controversies. *Placenta,* 27**,** 939-58.

PINAR, H. & CARPENTER, M. 2010. Placenta and umbilical cord abnormalities seen with stillbirth. *Clin Obstet Gynecol,* 53**,** 656-72.

PITTENGER, M. F., MACKAY, A. M., BECK, S. C., JAISWAL, R. K., DOUGLAS, R., MOSCA, J. D., MOORMAN, M. A., SIMONETTI, D. W., CRAIG, S. & MARSHAK, D. R. 1999. Multilineage potential of adult human mesenchymal stem cells. *Science,* 284**,** 143-7.

POTTER, M. D., BARBERO, S. & CHERESH, D. A. 2005. Tyrosine phosphorylation of VE-cadherin prevents binding of p120- and beta-catenin and maintains the cellular mesenchymal state. *J Biol Chem,* 280**,** 31906-12.

RABIET, M. J., PLANTIER, J. L., RIVAL, Y., GENOUX, Y., LAMPUGNANI, M. G. & DEJANA, E. 1996. Thrombin-induced increase in endothelial permeability is associated with changes in cell-to-cell junction organization. *Arterioscler Thromb Vasc Biol,* 16**,** 488-96.

RADCLIFF, G. & JAROSZESKI, M. J. 1998. Basics of flow cytometry. *Methods Mol Biol,* 91**,** 1-24.

RESTA, R. & THOMPSON, L. F. 1997. T cell signalling through CD73. *Cell Signal,* 9**,** 131-9.

REYNOLDS, L. P. & REDMER, D. A. 1995. Utero-placental vascular development and placental function. *J Anim Sci,* 73**,** 1839-51.

RIBEIRO, J., PEREIRA, T., AMORIM, I., CASEIRO, A. R., LOPES, M. A., LIMA, J., GARTNER, A., SANTOS, J. D., BARTOLO, P. J., RODRIGUES, J. M., MAURICIO, A. C. & LUIS, A. L. 2014. Cell therapy with human MSCs isolated from the umbilical cord Wharton jelly associated to a PVA membrane in the treatment of chronic skin wounds. *Int J Med Sci,* 11**,** 979-87.

RICHARDSON, R. L., HAUSMAN, G. J. & CAMPION, D. R. 1982. Response of pericytes to thermal lesion in the inguinal fat pad of 10-day-old rats. *Acta Anat (Basel),* 114**,** 41-57.

RIDLEY, A. J., SCHWARTZ, M. A., BURRIDGE, K., FIRTEL, R. A., GINSBERG, M. H., BORISY, G., PARSONS, J. T. & HORWITZ, A. R. 2003. Cell migration: integrating signals from front to back. *Science,* 302**,** 1704-9.

RISAU, W. 1997. Mechanisms of angiogenesis. *Nature,* 386**,** 671-4.

ROBINSON, C. J. & STRINGER, S. E. 2001. The splice variants of vascular endothelial growth factor (VEGF) and their receptors. *J Cell Sci,* 114**,** 853-65.

ROBSON, A., HARRIS, L. K., INNES, B. A., LASH, G. E., ALJUNAIDY, M. M., APLIN, J. D., BAKER, P. N., ROBSON, S. C. & BULMER, J. N. 2012. Uterine natural killer cells initiate spiral artery remodeling in human pregnancy. *FASEB J,* 26**,** 4876-85.

ROGER, V. L., GO, A. S., LLOYD-JONES, D. M., BENJAMIN, E. J., BERRY, J. D., BORDEN, W. B., BRAVATA, D. M., DAI, S., FORD, E. S., FOX, C. S., FULLERTON, H. J., GILLESPIE, C., HAILPERN, S. M., HEIT, J. A., HOWARD, V. J., KISSELA, B. M., KITTNER, S. J., LACKLAND, D. T., LICHTMAN, J. H., LISABETH, L. D., MAKUC, D. M., MARCUS, G. M., MARELLI, A., MATCHAR,

D. B., MOY, C. S., MOZAFFARIAN, D., MUSSOLINO, M. E., NICHOL, G., PAYNTER, N. P., SOLIMAN, E. Z., SORLIE, P. D., SOTOODEHNIA, N., TURAN, T. N., VIRANI, S. S., WONG, N. D., WOO, D. & TURNER, M. B. 2012. Heart disease and stroke statistics--2012 update: a report from the American Heart Association. *Circulation,* 125**,** e2-e220.

ROMANOV, Y. A., SVINTSITSKAYA, V. A. & SMIRNOV, V. N. 2003. Searching for alternative sources of postnatal human mesenchymal stem cells: candidate MSC-like cells from umbilical cord. *Stem Cells,* 21**,** 105-10.

ROY, E., SEPPANEN, E., ELLIS, R., LEE, E. S., KHOSROTEHRANI, K., FISK, N. M. & BOU-GHARIOS, G. 2014. Biphasic recruitment of microchimeric fetal mesenchymal cells in fibrosis following acute kidney injury. *Kidney Int,* 85**,** 600-10.

RUBIN, L. L. 1992. Endothelial cells: adhesion and tight junctions. *Curr Opin Cell Biol,* 4**,** 830-3.

RUBIN, L. L. & STADDON, J. M. 1999. The cell biology of the blood-brain barrier. *Annu Rev Neurosci,* 22**,** 11-28.

SALEHINEJAD, P., ALITHEEN, N. B., ALI, A. M., OMAR, A. R., MOHIT, M., JANZAMIN, E., SAMANI, F. S., TORSHIZI, Z. & NEMATOLLAHI-MAHANI, S. N. 2012. Comparison of different methods for the isolation of mesenchymal stem cells from human umbilical cord Wharton's jelly. *In Vitro Cell Dev Biol Anim,* 48**,** 75-83.

SALOMON, C., RYAN, J., SOBREVIA, L., KOBAYASHI, M., ASHMAN, K., MITCHELL, M. & RICE, G. E. 2013. Exosomal signaling during hypoxia mediates microvascular endothelial cell migration and vasculogenesis. *PLoS One,* 8**,** e68451.

SALOMON, D., AYALON, O., PATEL-KING, R., HYNES, R. O. & GEIGER, B. 1992. Extrajunctional distribution of N-cadherin in cultured human endothelial cells. *J Cell Sci,* 102 (Pt 1)**,** 7-17.

SANTOS, J. M., BARCIA, R. N., SIMOES, S. I., GASPAR, M. M., CALADO, S., AGUA-DOCE, A., ALMEIDA, S. C., ALMEIDA, J., FILIPE, M., TEIXEIRA, M., MARTINS, J. P., GRACA, L., CRUZ, M. E., CRUZ, P. & CRUZ, H. 2013. The role of human umbilical cord tissue-derived mesenchymal stromal cells (UCX(R)) in the treatment of inflammatory arthritis. *J Transl Med,* 11**,** 18.

SANTOS NASCIMENTO, D., MOSQUEIRA, D., SOUSA, L. M., TEIXEIRA, M., FILIPE, M., RESENDE, T. P., ARAUJO, A. F., VALENTE, M., ALMEIDA, J., MARTINS, J. P., SANTOS, J. M., BARCIA, R. N., CRUZ, P., CRUZ, H. & PINTO-DO, O. P. 2014. Human umbilical cord tissue-derived mesenchymal stromal cells attenuate remodeling after myocardial infarction by proangiogenic, antiapoptotic, and endogenous cell-activation mechanisms. *Stem Cell Res Ther,* 5**,** 5.

SANZ-MORENO, V. & MARSHALL, C. J. 2009. Rho-GTPase signaling drives melanoma cell plasticity. *Cell Cycle,* 8**,** 1484-7.

SANZ-RODRIGUEZ, F., GUERRERO-ESTEO, M., BOTELLA, L. M., BANVILLE, D., VARY, C. P. & BERNABEU, C. 2004. Endoglin regulates cytoskeletal organization through binding to ZRP-1, a member of the Lim family of proteins. *J Biol Chem,* 279**,** 32858-68.

SCHALLMOSER, K., BARTMANN, C., ROHDE, E., REINISCH, A., KASHOFER, K., STADELMEYER, E., DREXLER, C., LANZER, G., LINKESCH, W. & STRUNK, D. 2007. Human platelet lysate can replace fetal bovine serum for clinical-scale expansion of functional mesenchymal stromal cells. *Transfusion,* 47**,** 1436-46.

SCHMELZ, M. & FRANKE, W. W. 1993. Complexus adhaerentes, a new group of desmoplakin-containing junctions in endothelial cells: the syndesmos connecting retothelial cells of lymph nodes. *Eur J Cell Biol,* 61**,** 274-89.

SCHMELZ, M., MOLL, R., KUHN, C. & FRANKE, W. W. 1994. Complexus adhaerentes, a new group of desmoplakin-containing junctions in endothelial cells: II. Different types of lymphatic vessels. *Differentiation,* 57**,** 97-117.

SCHMIDT, A., LADAGE, D., STEINGEN, C., BRIXIUS, K., SCHINKOTHE, T., KLINZ, F. J., SCHWINGER, R. H., MEHLHORN, U. & BLOCH, W. 2006. Mesenchymal stem cells transmigrate over the endothelial barrier. *Eur J Cell Biol,* 85**,** 1179-88.

SCHNITZER, J. E. 1993. Update on the cellular and molecular basis of capillary permeability. *Trends Cardiovasc Med,* 3**,** 124-30.

SCHULZE, C. & FIRTH, J. A. 1992. The interendothelial junction in myocardial capillaries: evidence for the existence of regularly spaced, cleft-spanning structures. *J Cell Sci,* 101 (Pt 3)**,** 647-55.

SECUNDA, R., VENNILA, R., MOHANASHANKAR, A. M., RAJASUNDARI, M., JESWANTH, S. & SURENDRAN, R. 2014. Isolation, expansion and characterisation of mesenchymal stem cells from human bone marrow, adipose tissue, umbilical cord blood and matrix: a comparative study. *Cytotechnology*.

SENGER, D. R., GALLI, S. J., DVORAK, A. M., PERRUZZI, C. A., HARVEY, V. S. & DVORAK, H. F. 1983. Tumor cells secrete a vascular permeability factor that promotes accumulation of ascites fluid. *Science,* 219**,** 983-5.

SEPPANEN, E., FISK, N. M. & KHOSROTEHRANI, K. 2013. Pregnancy-acquired fetal progenitor cells. *J Reprod Immunol,* 97**,** 27-35.

SEPPANEN, E. J., HODGSON, S. S., KHOSROTEHRANI, K., BOU-GHARIOS, G. & FISK, N. M. 2012. Fetal microchimeric cells in a fetus-treats-its-mother paradigm do not contribute to dystrophin production in serially parous mdx females. *Stem Cells Dev,* 21**,** 2809-16.

SHABBIR, A., COX, A., RODRIGUEZ-MENOCAL, L., SALGADO, M. & VAN BADIAVAS, E. 2015. Mesenchymal Stem Cell Exosomes Induce Proliferation and Migration of Normal and Chronic Wound Fibroblasts, and Enhance Angiogenesis In Vitro. *Stem Cells Dev,* 24**,** 1635-47.

SHARMA, P., TEMPLIN, T. & GRABHAM, P. 2013. Short term effects of gamma radiation on endothelial barrier function: uncoupling of PECAM-1. *Microvasc Res,* 86**,** 11-20.

SHI, S., JIA, S., LIU, J. & CHEN, G. 2014. Accelerated Regeneration of Skin Injury by Co-transplantation of Mesenchymal Stem Cells from Wharton's Jelly of the Human Umbilical Cord Mixed with Microparticles. *Cell Biochem Biophys*.

SHYU, W. C., LIN, S. Z., CHIANG, M. F., SU, C. Y. & LI, H. 2006. Intracerebral peripheral blood stem cell (CD34+) implantation induces neuroplasticity by enhancing beta1 integrin-mediated angiogenesis in chronic stroke rats. *J Neurosci,* 26**,** 3444-53.

SIDIBE, A. & IMHOF, B. A. 2014. VE-cadherin phosphorylation decides: vascular permeability or diapedesis. *Nat Immunol,* 15**,** 215-7.

SIMON, A. M. & GOODENOUGH, D. A. 1998. Diverse functions of vertebrate gap junctions. *Trends Cell Biol,* 8**,** 477-83.

SIMS, D. E. 1986. The pericyte--a review. *Tissue Cell,* 18**,** 153-74.

SIPOS, P. I., RENS, W., SCHLECHT, H., FAN, X., WAREING, M., HAYWARD, C., HUBEL, C. A., BOURQUE, S., BAKER, P. N., DAVIDGE, S. T., SIBLEY, C. P. & CROCKER, I. P. 2013. Uterine vasculature remodeling in human pregnancy involves functional macrochimerism by endothelial colony forming cells of fetal origin. *Stem Cells,* 31**,** 1363-70.

SMITH, L. A., ARANDA-ESPINOZA, H., HAUN, J. B., DEMBO, M. & HAMMER, D. A. 2007. Neutrophil traction stresses are concentrated in the uropod during migration. *Biophys J,* 92**,** L58-60.

SOBOLEWSKI, K., BANKOWSKI, E., CHYCZEWSKI, L. & JAWORSKI, S. 1997. Collagen and glycosaminoglycans of Wharton's jelly. *Biol Neonate,* 71**,** 11-21.

SOKOLOVA, I. B., ZIN'KOVA, N. N., SHVEDOVA, E. V., KRUGLYAKOV, P. V. & POLYNTSEV, D. G. 2007. Distribution of mesenchymal stem cells in the area of tissue inflammation after transplantation of the cell material via different routes. *Bull Exp Biol Med,* 143**,** 143-6.

SOUADKIA, N., BROWN, A., LEACH, L. & PRITCHARD, D. I. 2010. Hookworm (Necator americanus) larval enzymes disrupt human vascular endothelium. *Am J Trop Med Hyg,* 83**,** 549-58.

SPRADLING, A., DRUMMOND-BARBOSA, D. & KAI, T. 2001. Stem cells find their niche. *Nature,* 414**,** 98-104.

SPRING, K., CHABOT, C., LANGLOIS, S., LAPOINTE, L., TRINH, N. T., CARON, C., HEBDA, J. K., GAVARD, J., ELCHEBLY, M. & ROYAL, I. 2012. Tyrosine phosphorylation of DEP-1/CD148 as a mechanism controlling Src kinase activation, endothelial cell permeability, invasion, and capillary formation. *Blood,* 120**,** 2745-56.

SPRINGER, T. A. 1994. Traffic signals for lymphocyte recirculation and leukocyte emigration: the multistep paradigm. *Cell,* 76**,** 301-14.

STATKUTE, L., VERDA, L., OYAMA, Y., TRAYNOR, A., VILLA, M., SHOOK, T., CLIFTON, R., JOVANOVIC, B., SATKUS, J., LOH, Y., QUIGLEY, K., YAUNG, K., GONDA, E., KROSNJAR, N., SPAHOVIC, D. & BURT, R. K. 2007. Mobilization, harvesting and selection of peripheral blood stem cells in patients with autoimmune diseases undergoing autologous hematopoietic stem cell transplantation. *Bone Marrow Transplant,* 39**,** 317-29.

STEVENSON, B. R., SILICIANO, J. D., MOOSEKER, M. S. & GOODENOUGH, D. A. 1986. Identification of ZO-1: a high molecular weight polypeptide associated with the tight junction (zonula occludens) in a variety of epithelia. *J Cell Biol,* 103**,** 755-66.

STOCK, C. & RIETHMULLER, C. 2011. Endothelial activation drives lateral migration and diapedesis of leukocytes. *Cell Immunol,* 271**,** 180-3.

SUGISHITA, Y., TAKAHASHI, T., SHIMIZU, T., YAO, A., KINUGAWA, K., SUGISHITA, K., HARADA, K., MATSUI, H. & NAGAI, R. 2000. Expression of genes encoding vascular endothelial growth factor and its Flk-1 receptor in the chick embryonic heart. *J Mol Cell Cardiol,* 32**,** 1039-51.

SUN, Z., LI, X., MASSENA, S., KUTSCHERA, S., PADHAN, N., GUALANDI, L., SUNDVOLD-GJERSTAD, V., GUSTAFSSON, K., CHOY, W. W., ZANG, G., QUACH, M., JANSSON, L., PHILLIPSON, M., ABID, M. R., SPURKLAND, A. & CLAESSON-WELSH, L. 2012. VEGFR2 induces c-Src signaling and vascular permeability in vivo via the adaptor protein TSAd. *J Exp Med,* 209**,** 1363-77.

TAKECHI, K., KUWABARA, Y. & MIZUNO, M. 1993. Ultrastructural and immunohistochemical studies of Wharton's jelly umbilical cord cells. *Placenta,* 14**,** 235-45.

TANAKA, Y., ALBELDA, S. M., HORGAN, K. J., VAN SEVENTER, G. A., SHIMIZU, Y., NEWMAN, W., HALLAM, J., NEWMAN, P. J., BUCK, C. A. & SHAW, S. 1992. CD31 expressed on distinctive T cell subsets is a preferential amplifier of beta 1 integrin-mediated adhesion. *J Exp Med,* 176**,** 245-53.

TANG, J., WANG, J., KONG, X., YANG, J., GUO, L., ZHENG, F., ZHANG, L., HUANG, Y. & WAN, Y. 2009. Vascular endothelial growth factor promotes cardiac stem cell migration via the PI3K/Akt pathway. *Exp Cell Res,* 315**,** 3521-31.

TANTRAWATPAN, C., MANOCHANTR, S., KHEOLAMAI, P., Y, U. P., SUPOKAWEJ, A. & ISSARAGRISIL, S. 2013. Pluripotent gene expression in mesenchymal stem

cells from human umbilical cord Wharton's jelly and their differentiation potential to neural-like cells. *J Med Assoc Thai,* 96**,** 1208-17.

TELO, P., BREVIARIO, F., HUBER, P., PANZERI, C. & DEJANA, E. 1998. Identification of a novel cadherin (vascular endothelial cadherin-2) located at intercellular junctions in endothelial cells. *J Biol Chem,* 273**,** 17565-72.

TELUGU, B. P., ADACHI, K., SCHLITT, J. M., EZASHI, T., SCHUST, D. J., ROBERTS, R. M. & SCHULZ, L. C. 2013. Comparison of extravillous trophoblast cells derived from human embryonic stem cells and from first trimester human placentas. *Placenta,* 34**,** 536-43.

TEO, G. S., ANKRUM, J. A., MARTINELLI, R., BOETTO, S. E., SIMMS, K., SCIUTO, T. E., DVORAK, A. M., KARP, J. M. & CARMAN, C. V. 2012. Mesenchymal stem cells transmigrate between and directly through tumor necrosis factor-alpha-activated endothelial cells via both leukocyte-like and novel mechanisms. *Stem Cells,* 30**,** 2472-86.

THORESON, M. A., ANASTASIADIS, P. Z., DANIEL, J. M., IRETON, R. C., WHEELOCK, M. J., JOHNSON, K. R., HUMMINGBIRD, D. K. & REYNOLDS, A. B. 2000. Selective uncoupling of p120(ctn) from E-cadherin disrupts strong adhesion. *J Cell Biol,* 148**,** 189-202.

THURSTON, G. 2002. Complementary actions of VEGF and angiopoietin-1 on blood vessel growth and leakage. *J Anat,* 200**,** 575-80.

TODESCHI, M. R., EL BACKLY, R., CAPELLI, C., DAGA, A., PATRONE, E., INTRONA, M., CANCEDDA, R. & MASTROGIACOMO, M. 2015. Transplanted Umbilical Cord Mesenchymal Stem Cells Modify the In Vivo Microenvironment Enhancing Angiogenesis and Leading to Bone Regeneration. *Stem Cells Dev,* 24**,** 1570-81.

TOMA, J. G., AKHAVAN, M., FERNANDES, K. J., BARNABE-HEIDER, F., SADIKOT, A., KAPLAN, D. R. & MILLER, F. D. 2001. Isolation of multipotent adult stem cells from the dermis of mammalian skin. *Nat Cell Biol,* 3**,** 778-84.

TOMITA, S., LI, R. K., WEISEL, R. D., MICKLE, D. A., KIM, E. J., SAKAI, T. & JIA, Z. Q. 1999. Autologous transplantation of bone marrow cells improves damaged heart function. *Circulation,* 100**,** II247-56.

TORSNEY, E. & XU, Q. 2011. Resident vascular progenitor cells. *J Mol Cell Cardiol,* 50**,** 304-11.

TRIFFITT, J. T. 2002. Stem cells and the philosopher's stone. *J Cell Biochem Suppl,* 38**,** 13-9.

TSAGIAS, N., KOLIAKOS, I., KARAGIANNIS, V., ELEFTHERIADOU, M. & KOLIAKOS, G. G. 2011. Isolation of mesenchymal stem cells using the total length of umbilical cord for transplantation purposes. *Transfus Med,* 21**,** 253-61.

TSAI, P. J., WANG, H. S., LIN, G. J., CHOU, S. C., CHU, T. H., CHUAN, W. T., LU, Y. J., WENG, Z. C., SU, C. H., HSIEH, P. S., SYTWU, H. K., LIN, C. H., CHEN, T. H. & SHYU, J. F. 2014. Undifferentiated Wharton?s Jelly Mesenchymal Stem Cell Transplantation Induces Insulin-Producing Cell Differentiation and Suppression of T Cell-Mediated Autoimmunity in Non-Obese Diabetic Mice. *Cell Transplant.*

TSAI, P. J., WANG, H. S., LIN, G. J., CHOU, S. C., CHU, T. H., CHUAN, W. T., LU, Y. J., WENG, Z. C., SU, C. H., HSIEH, P. S., SYTWU, H. K., LIN, C. H., CHEN, T. H. & SHYU, J. F. 2015. Undifferentiated Wharton's Jelly Mesenchymal Stem Cell Transplantation Induces Insulin-Producing Cell Differentiation and Suppression of T-Cell-Mediated Autoimmunity in Nonobese Diabetic Mice. *Cell Transplant,* 24**,** 1555-70.

TUROWSKI, P., MARTINELLI, R., CRAWFORD, R., WATERIDGE, D., PAPAGEORGIOU, A. P., LAMPUGNANI, M. G., GAMP, A. C., VESTWEBER, D., ADAMSON, P., DEJANA, E. & GREENWOOD, J. 2008. Phosphorylation of vascular endothelial cadherin controls lymphocyte emigration. *J Cell Sci,* 121**,** 29-37.

UKROPEC, J. A., HOLLINGER, M. K., SALVA, S. M. & WOOLKALIS, M. J. 2000. SHP2 association with VE-cadherin complexes in human endothelial cells is regulated by thrombin. *J Biol Chem,* 275**,** 5983-6.

ULFMAN, L. H., JOOSTEN, D. P., VAN DER LINDEN, J. A., LAMMERS, J. W., ZWAGINGA, J. J. & KOENDERMAN, L. 2001. IL-8 induces a transient arrest of rolling eosinophils on human endothelial cells. *J Immunol,* 166**,** 588-95.

UNEK, G., OZMEN, A., MENDILCIOGLU, I., SIMSEK, M. & KORGUN, E. T. 2014. The expression of cell cycle related proteins PCNA, Ki67, p27 and p57 in normal and preeclamptic human placentas. *Tissue Cell,* 46**,** 198-205.

URBICH, C. & DIMMELER, S. 2004. Endothelial progenitor cells functional characterization. *Trends Cardiovasc Med,* 14**,** 318-22.

VAJKOCZY, P., BLUM, S., LAMPARTER, M., MAILHAMMER, R., ERBER, R., ENGELHARDT, B., VESTWEBER, D. & HATZOPOULOS, A. K. 2003. Multistep nature of microvascular recruitment of ex vivo-expanded embryonic endothelial progenitor cells during tumor angiogenesis. *J Exp Med,* 197**,** 1755-65.

VEIKKOLA, T., KARKKAINEN, M., CLAESSON-WELSH, L. & ALITALO, K. 2000. Regulation of angiogenesis via vascular endothelial growth factor receptors. *Cancer Res,* 60**,** 203-12.

VESTWEBER, D. 2000. Molecular mechanisms that control endothelial cell contacts. *J Pathol,* 190**,** 281-91.

VESTWEBER, D. & KEMLER, R. 1985. Identification of a putative cell adhesion domain of uvomorulin. *EMBO J,* 4**,** 3393-8.

VESTWEBER, D., WESSEL, F. & NOTTEBAUM, A. F. 2014. Similarities and differences in the regulation of leukocyte extravasation and vascular permeability. *Semin Immunopathol,* 36**,** 177-92.

VESTWEBER, D., WINDERLICH, M., CAGNA, G. & NOTTEBAUM, A. F. 2009. Cell adhesion dynamics at endothelial junctions: VE-cadherin as a major player. *Trends Cell Biol,* 19**,** 8-15.

WALLEZ, Y., CAND, F., CRUZALEGUI, F., WERNSTEDT, C., SOUCHELNYTSKYI, S., VILGRAIN, I. & HUBER, P. 2007. Src kinase phosphorylates vascular endothelial-cadherin in response to vascular endothelial growth factor: identification of tyrosine 685 as the unique target site. *Oncogene,* 26**,** 1067-77.

WANG, D., LI, J., ZHANG, Y., ZHANG, M., CHEN, J., LI, X., HU, X., JIANG, S., SHI, S. & SUN, L. 2014. Umbilical cord mesenchymal stem cell transplantation in active and refractory systemic lupus erythematosus: a multicenter clinical study. *Arthritis Res Ther,* 16**,** R79.

WANG, G. K., ZHU, J. Q., ZHANG, J. T., LI, Q., LI, Y., HE, J., QIN, Y. W. & JING, Q. 2010. Circulating microRNA: a novel potential biomarker for early diagnosis of acute myocardial infarction in humans. *Eur Heart J,* 31**,** 659-66.

WANG, H. S., HUNG, S. C., PENG, S. T., HUANG, C. C., WEI, H. M., GUO, Y. J., FU, Y. S., LAI, M. C. & CHEN, C. C. 2004. Mesenchymal stem cells in the Wharton's jelly of the human umbilical cord. *Stem Cells,* 22**,** 1330-7.

WARD, B. J., BAUMAN, K. F. & FIRTH, J. A. 1988. Interendothelial junctions of cardiac capillaries in rats: their structure and permeability properties. *Cell Tissue Res,* 252**,** 57-66.

WATT, F. M. & HOGAN, B. L. 2000. Out of Eden: stem cells and their niches. *Science,* 287**,** 1427-30.

WEGENER, J. & SEEBACH, J. 2014a. Experimental tools to monitor the dynamics of endothelial barrier function: a survey of in vitro approaches. *Cell Tissue Res*.

WEGENER, J. & SEEBACH, J. 2014b. Experimental tools to monitor the dynamics of endothelial barrier function: a survey of in vitro approaches. *Cell Tissue Res,* 355**,** 485-514.

WEIS, S. M. & CHERESH, D. A. 2005. Pathophysiological consequences of VEGF-induced vascular permeability. *Nature,* 437**,** 497-504.

WEIS, W. I. & NELSON, W. J. 2006. Re-solving the cadherin-catenin-actin conundrum. *J Biol Chem,* 281**,** 35593-7.

WESSEL, F., WINDERLICH, M., HOLM, M., FRYE, M., RIVERA-GALDOS, R., VOCKEL, M., LINNEPE, R., IPE, U., STADTMANN, A., ZARBOCK, A., NOTTEBAUM, A. F. & VESTWEBER, D. 2014. Leukocyte extravasation and vascular permeability are each controlled in vivo by different tyrosine residues of VE-cadherin. *Nat Immunol,* 15**,** 223-30.

WILLIAMS, J. T., SOUTHERLAND, S. S., SOUZA, J., CALCUTT, A. F. & CARTLEDGE, R. G. 1999. Cells isolated from adult human skeletal muscle capable of differentiating into multiple mesodermal phenotypes. *Am Surg,* 65**,** 22-6.

WITMER, A. N., VRENSEN, G. F., VAN NOORDEN, C. J. & SCHLINGEMANN, R. O. 2003. Vascular endothelial growth factors and angiogenesis in eye disease. *Prog Retin Eye Res,* 22**,** 1-29.

WOLBURG, H. & LIPPOLDT, A. 2002. Tight junctions of the blood-brain barrier: development, composition and regulation. *Vascul Pharmacol,* 38**,** 323-37.

WOLF, K., MAZO, I., LEUNG, H., ENGELKE, K., VON ANDRIAN, U. H., DERYUGINA, E. I., STRONGIN, A. Y., BROCKER, E. B. & FRIEDL, P. 2003. Compensation mechanism in tumor cell migration: mesenchymal-amoeboid transition after blocking of pericellular proteolysis. *J Cell Biol,* 160**,** 267-77.

WOLF, K., WU, Y. I., LIU, Y., GEIGER, J., TAM, E., OVERALL, C., STACK, M. S. & FRIEDL, P. 2007. Multi-step pericellular proteolysis controls the transition from individual to collective cancer cell invasion. *Nat Cell Biol,* 9**,** 893-904.

WRIGHT, T. J., LEACH, L., SHAW, P. E. & JONES, P. 2002. Dynamics of vascular endothelial-cadherin and beta-catenin localization by vascular endothelial growth factor-induced angiogenesis in human umbilical vein cells. *Exp Cell Res,* 280**,** 159-68.

WU, X., WANG, S., CHEN, B. & AN, X. 2010. Muscle-derived stem cells: isolation, characterization, differentiation, and application in cell and gene therapy. *Cell Tissue Res*, 340**,** 549-67.

XIAO, Q., WANG, S. K., TIAN, H., XIN, L., ZOU, Z. G., HU, Y. L., CHANG, C. M., WANG, X. Y., YIN, Q. S., ZHANG, X. H. & WANG, L. Y. 2012. TNF-alpha increases bone marrow mesenchymal stem cell migration to ischemic tissues. *Cell Biochem Biophys,* 62**,** 409-14.

XU, L., MENG, F., NI, M., LEE, Y. & LI, G. 2012. N-cadherin regulates osteogenesis and migration of bone marrow-derived mesenchymal stem cells. *Mol Biol Rep*.

YAMANE, A., SEETHARAM, L., YAMAGUCHI, S., GOTOH, N., TAKAHASHI, T., NEUFELD, G. & SHIBUYA, M. 1994. A new communication system between hepatocytes and sinusoidal endothelial cells in liver through vascular endothelial growth factor and Flt tyrosine kinase receptor family (Flt-1 and KDR/Flk-1). *Oncogene,* 9**,** 2683-90.

YAN, L., HAN, Y., WANG, J., LIU, J., HE, Y., WANG, H. & FAN, D. 2008. Peripheral blood monocytes from the decompensated liver cirrhosis could migrate into nude

mouse liver with human hepatocyte-markers expression. *Biochem Biophys Res Commun,* 371**,** 635-8.

YANCOPOULOS, G. D., DAVIS, S., GALE, N. W., RUDGE, J. S., WIEGAND, S. J. & HOLASH, J. 2000. Vascular-specific growth factors and blood vessel formation. *Nature,* 407**,** 242-8.

YANG, X., ZHANG, M., ZHANG, Y., LI, W. & YANG, B. 2011. Mesenchymal stem cells derived from Wharton jelly of the human umbilical cord ameliorate damage to human endometrial stromal cells. *Fertil Steril,* 96**,** 1029-36.

YAP, A. S., CRAMPTON, M. S. & HARDIN, J. 2007. Making and breaking contacts: the cellular biology of cadherin regulation. *Curr Opin Cell Biol,* 19**,** 508-14.

YAP, A. S., NIESSEN, C. M. & GUMBINER, B. M. 1998. The juxtamembrane region of the cadherin cytoplasmic tail supports lateral clustering, adhesive strengthening, and interaction with p120ctn. *J Cell Biol,* 141**,** 779-89.

YEH, E. T., ZHANG, S., WU, H. D., KORBLING, M., WILLERSON, J. T. & ESTROV, Z. 2003. Transdifferentiation of human peripheral blood CD34+-enriched cell population into cardiomyocytes, endothelial cells, and smooth muscle cells in vivo. *Circulation,* 108**,** 2070-3.

YOON, J., MIN, B. G., KIM, Y. H., SHIM, W. J., RO, Y. M. & LIM, D. S. 2005. Differentiation, engraftment and functional effects of pre-treated mesenchymal stem cells in a rat myocardial infarct model. *Acta Cardiol,* 60**,** 277-84.

YOSHIDA, K. & SOLDATI, T. 2006. Dissection of amoeboid movement into two mechanically distinct modes. *J Cell Sci,* 119**,** 3833-44.

YOSHIMURA, K., SHIGEURA, T., MATSUMOTO, D., SATO, T., TAKAKI, Y., AIBA-KOJIMA, E., SATO, K., INOUE, K., NAGASE, T., KOSHIMA, I. & GONDA, K. 2006. Characterization of freshly isolated and cultured cells derived from the fatty and fluid portions of liposuction aspirates. *J Cell Physiol,* 208**,** 64-76.

YOSHIOKA, K., YOSHIDA, K., CUI, H., WAKAYAMA, T., TAKUWA, N., OKAMOTO, Y., DU, W., QI, X., ASANUMA, K., SUGIHARA, K., AKI, S., MIYAZAWA, H., BISWAS, K., NAGAKURA, C., UENO, M., ISEKI, S., SCHWARTZ, R. J., OKAMOTO, H., SASAKI, T., MATSUI, O., ASANO, M., ADAMS, R. H., TAKAKURA, N. & TAKUWA, Y. 2012. Endothelial PI3K-C2alpha, a class II PI3K, has an essential role in angiogenesis and vascular barrier function. *Nat Med,* 18**,** 1560-9.

YUAN, D., XU, S. & HE, P. 2014. Enhanced permeability responses to inflammation in streptozotocin-induced diabetic rat venules: Rho-mediated alterations of actin cytoskeleton and VE-cadherin. *Am J Physiol Heart Circ Physiol,* 307**,** H44-53.

ZANNETTINO, A. C., PATON, S., ARTHUR, A., KHOR, F., ITESCU, S., GIMBLE, J. M. & GRONTHOS, S. 2008. Multipotential human adipose-derived stromal stem cells exhibit a perivascular phenotype in vitro and in vivo. *J Cell Physiol,* 214**,** 413-21.

ZENG, X. X., TAN, K. H., YEO, A., SASAJALA, P., TAN, X., XIAO, Z. C., DAWE, G. & UDOLPH, G. 2010. Pregnancy-associated progenitor cells differentiate and mature into neurons in the maternal brain. *Stem Cells Dev,* 19**,** 1819-30.

ZENGIN, E., CHALAJOUR, F., GEHLING, U. M., ITO, W. D., TREEDE, H., LAUKE, H., WEIL, J., REICHENSPURNER, H., KILIC, N. & ERGUN, S. 2006. Vascular wall resident progenitor cells: a source for postnatal vasculogenesis. *Development,* 133**,** 1543-51.

ZHANG, J., NIU, C., YE, L., HUANG, H., HE, X., TONG, W. G., ROSS, J., HAUG, J., JOHNSON, T., FENG, J. Q., HARRIS, S., WIEDEMANN, L. M., MISHINA, Y. & LI, L. 2003. Identification of the haematopoietic stem cell niche and control of the niche size. *Nature,* 425**,** 836-41.

ZHANG, W., LIU, X. C., YANG, L., ZHU, D. L., ZHANG, Y. D., CHEN, Y. & ZHANG, H. Y. 2013. Wharton's jelly-derived mesenchymal stem cells promote myocardial regeneration and cardiac repair after miniswine acute myocardial infarction. *Coron Artery Dis,* 24**,** 549-58.

ZHAO, X., DAS, A. V., THORESON, W. B., JAMES, J., WATTNEM, T. E., RODRIGUEZ-SIERRA, J. & AHMAD, I. 2002. Adult corneal limbal epithelium: a model for studying neural potential of non-neural stem cells/progenitors. *Dev Biol,* 250**,** 317-31.

ZHOU, B., MA, Q., RAJAGOPAL, S., WU, S. M., DOMIAN, I., RIVERA-FELICIANO, J., JIANG, D., VON GISE, A., IKEDA, S., CHIEN, K. R. & PU, W. T. 2008. Epicardial progenitors contribute to the cardiomyocyte lineage in the developing heart. *Nature,* 454**,** 109-13.

ZHOU, Y., DAMSKY, C. H. & FISHER, S. J. 1997a. Preeclampsia is associated with failure of human cytotrophoblasts to mimic a vascular adhesion phenotype. One cause of defective endovascular invasion in this syndrome? *J Clin Invest,* 99**,** 2152-64.

ZHOU, Y., FISHER, S. J., JANATPOUR, M., GENBACEV, O., DEJANA, E., WHEELOCK, M. & DAMSKY, C. H. 1997b. Human cytotrophoblasts adopt a vascular phenotype as they differentiate. A strategy for successful endovascular invasion? *J Clin Invest,* 99**,** 2139-51.

ZOLA, H., SWART, B., NICHOLSON, I., AASTED, B., BENSUSSAN, A., BOUMSELL, L., BUCKLEY, C., CLARK, G., DRBAL, K., ENGEL, P., HART, D., HOREJSI, V., ISACKE, C., MACARDLE, P., MALAVASI, F., MASON, D., OLIVE, D., SAALMUELLER, A., SCHLOSSMAN, S. F., SCHWARTZ-ALBIEZ, R., SIMMONS, P., TEDDER, T. F., UGUCCIONI, M. & WARREN, H. 2005. CD molecules 2005: human cell differentiation molecules. *Blood,* 106**,** 3123-6.

ZUK, P. A., ZHU, M., MIZUNO, H., HUANG, J., FUTRELL, J. W., KATZ, A. J., BENHAIM, P., LORENZ, H. P. & HEDRICK, M. H. 2001. Multilineage cells from human adipose tissue: implications for cell-based therapies. *Tissue Eng,* 7**,** 211-28.